Optimisation of the Handover Decision in Infrastructure Networks Using Realistic Simulation Environments

Von der Fakultät für Elektrotechnik, Informationstechnik, Physik
der Technischen Universität Carolo-Wilhelmina zu Braunschweig

zur Erlangung des Grades eines Doktors
der Ingenieurwissenschaften (Dr.-Ing.)

genehmigte Dissertation

von Dipl.-Ing. Thomas Jansen, M.Sc.

aus Papenburg

Eingereicht am: 09.04.2015

Mündliche Prüfung am: 07.10.2015

Prüfungsvorsitzender: Prof. Dr.-Ing. Ulrich Reimers
1. Referent: Prof. Dr.-Ing. Thomas Kürner
2. Referent: Prof.dr.ir. Erik R. Fledderus

Braunschweig, 2016

Mitteilungen aus dem Institut für Nachrichtentechnik der
Technischen Universität Braunschweig

Band 45

Thomas Jansen

Optimisation of the Handover Decision in Infrastructure Networks Using Realistic Simulation Environments

Shaker Verlag
Aachen 2016

Bibliographic information published by the Deutsche Nationalbibliothek
The Deutsche Nationalbibliothek lists this publication in the Deutsche Nationalbibliografie; detailed bibliographic data are available in the Internet at http://dnb.d-nb.de.

Zugl.: Braunschweig, Techn. Univ., Diss., 2015

Printed in Germany.

ISBN 978-3-8440-4516-1
ISSN 1865-2484

Shaker Verlag GmbH • P.O. BOX 101818 • D-52018 Aachen
Phone: 0049/2407/9596-0 • Telefax: 0049/2407/9596-9
Internet: www.shaker.de • e-mail: info@shaker.de

Vorwort

Diese Arbeit ist während meiner Zeit am Institut für Nachrichtentechnik der Technischen Universität Braunschweig entstanden. Auf dem Weg zur Promotion habe ich das wissenschaftliche und professionelle Umfeld am Institut sehr genossen. Darum möchte ich die Gelegenheit nutzen, um mich bei einigen Personen zu bedanken.

Einen besonderen Dank möchte ich meinem Doktorvater Prof. Thomas Kürner aussprechen. Die Zusammenarbeit mit Ihnen sowie der wissenschaftliche und fachliche Austausch waren mir immer eine große Freude und haben mich im Laufe der Dissertation immer wieder motiviert. Mein weiterer Dank gilt Prof. Erik Fledderus für die Rolle des zweiten Gutachters meiner Dissertationsschrift. Einen ganz herzlichen Dank möchte ich auch unserem Institutsleiter Prof. Ulrich Reimers für die Übernahme des Prüfungsvorsitzes aussprechen. Darüber hinaus danke ich Ihnen für die gemeinsamen wissenschaftlichen Projekte und Gutachten. Ihnen allen vielen Dank für Ihre Unterstützung und Ihren Rat.

Bedanken möchte ich mich bei den Mitarbeitern des IfN für die herzliche Atmosphäre, die vielen gemeinsamen sozialen Aktivitäten und die wissenschaftliche Zusammenarbeit, die das Insitut zu einem besonderen Ort machen. Mein spezieller Dank gilt Patrick Bauer, Johannes Baumgarten, Martin Jacob, Peter Neumann, Jörg Nuckelt, Piotr Palka, Dennis Rose, Moritz Schack, Marius Spika, Philipp Steckel und Peter Unger. Euch allen ein ganz herzlicher Dank für eine unvergessliche und schöne Zeit am IfN. Rudi Görke, Andreas Gudat und Peter Schlegel möchte ich für die Versorgung mit Büchern und IT ebenso danken wie Petra Beyer, Boguslawa Brandt, Jutta Nottbohm und Nina Andersen für die Organisation der vielen kleinen und großen Dinge und für die Ratschläge in Nachwuchsfragen.

Ein herzlicher Dank geht an meine Studenten Johannes Baumgarten, Sören Hahn, Markus Hübner, Ari Manik, Jaroslaw Sulak und Dennis Rose, die mit Ihren Abschlussarbeiten meine wissenschaftlichen Studien unterstützt haben.

In wissenschaftlichen Fragen habe ich mich häufig mit Dr. Andreas Eisenblätter und Dr. Ulrich Türke von atesio ausgetauscht, mit denen ich drei Jahre lang im internationalen

Forschungsprojekt SOCRATES zusammengearbeitet habe. Für die Unterstützung in der Promotionszeit möchte ich Euch ganz herzlich danken. Many thanks to the colleagues of the SOCRATES project for the interesting research and co-operation in the area of self-organising networks and intercultural exchange during the project meetings in many European cities.
Abschließend möchte ich mich noch ganz herzlich bei meiner Familie für die Unterstützung und den Rückhalt bedanken. Meinen Eltern Klara und Wilhelm Jansen danke ich für das Vertrauen und den Glauben an mich. Meinen Brüdern Marcus und Stefan Jansen für die fortwährende Motivation. Meinen Schwiegereltern Yvonne und Reiner Pertschy für so manche Kinderbetreuung. Ein ganz besonderer Dank gilt meiner Frau Sylvia, die mich immer bedingungslos unterstützt. Unsere Kinder Felix und Mats sorgen stets für Abwechslung und bereichern unser Leben. Euch allen ein ganz herzlicher Dank, dass alles so ist, wie es ist.

Bonn im Mai 2016 Thomas Jansen

Contents

List of Abbreviations

2D	Two Dimensional
3D	Three Dimensional
3GPP	3rd Generation Partnership Project
AAS	Adaptive Antenna Systems
App	Application
ARMA	Autoregressive Moving Average
BPSK	Binary Phase-Shift Keying
C-RNTI	Cell Radio Network Temporary Identifier
CBR	Constant Bit Rate
CCO	Coverage and Capacity Optimization
CQI	Channel Quality Indicator
DL	Downlink
DRX	Discontinuous Reception
DTX	Discontinuous Transmission
E3	End-to-End Efficiency
EC	European Commission
eNB	evolved Node B
EPC	Evolved Packet Core
EU	European Union
FDD	Frequency Division Duplex
FEC	Forward Error Correction
FIFO	First In First Out
GBR	Guaranteed Bit Rate
GSM	Global System for Mobile Communications
GPRS	General Packet Radio Service
HO	Handover
HOP	Handover Operating Point
HP-Pred-Opt	Handover Performance Prediction Optimization Algorithm

HPI	Handover Performance Indicator
HYS	Hysteresis
HYS-Off	Hysteresis Offset
HW	Hardware
ISD	Inter Side Distance
KS-Test	Kolmogorov Smirnov Test
LOS	Line-of-Sight
LTE	Long Term Evolution
LTE-A	LTE-Advanced
MCS	Modulation and Coding Scheme
MIMO	Multiple Input Multiple Output
MLB	Mobility Load Balancing
MME	Mobility Management Entity
MPM	Multi-Path Model
NGMN	Next Generation Mobile Networks
NHP-Opt	Neighbouring HOP Performance Handover Optimization Algorithm
NLOS	Non-Line-of-Sight
OFDM	Orthogonal Frequency Division Multiplex
OPEX	Operational Expenditure
OSM	OpenStreetMap
PCell	Primary Cell
PDSCH	Physical Downlink Shared Channel
PRB	Physical Resource Block
QAM	Quadrature Amplitude Modulation
QoS	Quality of Service
RACH	Random Access Channel
RAT	Radio Access Technology
RB	Resource Block
RF	Radio Frequency
RLF	Radio Link Failure
RRC	Radio Resource Control
RRM	Radio Resource Management
RSRP	Reference Signal Received Power
RSRQ	Reference Signal Received Quality
RSSI	Received Signal Strength Indicator

S1	S1-Interface
SCell	Serving Cell
SEMAFOUR	Self-Management for Unified Heterogeneous radio Access Networks
SeNB	Source evolved Node B
SIMONE	SImulation of MObile NEtworks
SINR	Signal to Interference plus Noise Ratio
SN	Sequence Number
SOCRATES	Self-Optimisation and self-ConfiguRATion in wirelEss networkS
SON	Self-Organising Network
STD	Standard Deviation
SUMO	Simulation of Urban MObility
TDD	Time Division Duplex
TeNB	Target evolved Node B
TNL	Transport Network Layer
TTT	Time-To-Trigger
UE	User Equipment
UL	Uplink
UMTS	Universal Mobile Telecommunications System
VPM	Vertical Plane Model
WCDMA	Wideband Code Division Multiple Access
WGS84	World Geodetic System 1984
WLAN	Wireless Local Area Network
X2	X2-Interface

Abstract

The development of mobile communication services and technologies in recent years boosts the importance and ubiquity of terminal equipments in our everyday life. The main drivers for this development are the reliability of the offered services and the user friendliness, allowing a huge variety of communication services with a single device. To assure a high communication quality and the usability of the services a seamless connectivity is beneficial or even mandatory, e.g. for voice calls, video streaming, gaming or safety-critical application based on car-to-car communication. Due to the cellular nature of infrastructure networks, mobile users will cross cell boundaries and need to switch the serving cell with the help of a handover procedure. The timing of the handover is essential to keep the mobile devices connected to the network.

The introduction of measurement based optimisation in the context of self-organising networks enables the optimisation of the handover decision. The key enabler for the optimisation are a cost function that incorporates the relevant handover performance indicators, a reasonable observation time to evaluate the performance and an optimisation algorithm that reliably improves the handover performance in various, ever-changing network conditions. In the recent years several handover optimisation algorithms have been investigated. Nevertheless, the influence of the target function on the optimisation, the dimensioning of the observation window and the impact of network condition changes have not been investigated so far.

In this dissertation a detailed analysis of the handover performance indicators is presented. Beyond that, additional system information or measurements are valued as potential candidates to allow further improvement of the handover performance. Particular attention is paid to the ability to adapt to changing network conditions since the introduction of new cell layers (small cells), new techniques like adaptive antenna systems or spectrum sharing or the introduction of new communication technologies like LTE-Advanced increases the complexity of future mobile communication networks. Finally, we develop an optimisation algorithm that reliably and quickly optimises the handover performance in various and fast-changing network conditions.

Kurzfassung

Mobile Endgeräte gewinnen in unserem täglichen Leben zunehmend an Bedeutung. Dieser Trend wird vorangetrieben durch die rasante Entwicklung der Mobilfunktechnologien und neu angebotene Dienste in den letzten Jahren. Immer mehr Dienstleistungen werden über ein einzelnes Endgerät bereitgestellt. Um eine hohe Übertragungsqualität zur Nutzung der Dienste sicherzustellen, ist eine nahtlose Verbindung zum Kommunikationsnetzwerk wünschenswert oder sogar obligatorisch, z.B. für Sprachverbindungen, Video-Streaming, Onlinespiele oder sicherheitsrelevante Anwendungen der Car-to-Car-Kommunikation. Bedingt durch die zellulare Struktur der Mobilfunknetze ist zur Aufrechterhaltung der Kommunikation ein Zellwechsel (Handover) im Randbereich des Versorgungsgebietes einer Zelle notwendig. Der genaue Zeitpunkt des Zellwechsels ist dabei von besonderer Bedeutung.
Die Einführung der messungsbasierten Selbst-Optimierung für Mobilfunknetze ermöglicht die Optimierung der Zellwechsel-Entscheidung. Die wesentlichen Voraussetzungen für eine Optimierung sind eine Optimierungszielfunktion auf Basis der Leistungsindikatoren, eine angemessene Beobachtungszeit sowie die Entwicklung eines möglichst allgemeingültigen Optimierungsverfahrens. In den letzten Jahren sind viele solcher Verfahren untersucht und veröffentlicht worden. Dennoch sind der Einfluss der Zielfunktion auf die Optimierung, die Dimensionierung des Beobachtungszeitraums und die Auswirkungen von Netzzustandsänderungen auf die Optimierung bisher weitgehend vernachlässigt worden. In dieser Arbeit wird eine detaillierte Analyse der Zellwechsel-Leistungsindikatoren in LTE durchgeführt. Darüber hinaus wird die Eignung zusätzlicher Systeminformationen oder Messungen zur weiteren Verbesserung der Zellwechsel-Entscheidung untersucht. Durch die Einführung neuer Zelltypen (z.B. Small Cells), moderner Übertragungstechniken wie adaptive Antennensysteme oder die Einführung neuer Technologien wie LTE-Advanced nimmt die Komplexität der zukünftigen Mobilfunknetze stetig zu. Das in dieser Arbeit entwickelte Optimierungsverfahren ermöglicht eine schnelle und zuverlässige Anpassung der Zellwechselparameter an die veränderlichen Bedingungen in den Mobilfunknetzen und kann daher auch in komplexeren Systemen eingesetzt werden.

Chapter 1

Introduction

One of the key features of mobile communication systems - the clue is in the name - is to support user mobility in combination with communication services. Internet connectivity and e-mail access is the number one sales argument, claimed to be the most important factor to buy a smartphone by eighty six percent of the interviewed persons in [GPRA11]. Even though these mentioned services could be realised via "normadic use", i.e. the User Equipment (UE) is stationary while in use, the survey result shows that the supported mobile services are the main drivers to sign a contract with a network operator. This conclusion is strengthened by the fact that the number of available Applications (Apps) is constantly growing in the recent decade and more than one million Apps are available in each of the two largest App stores (Google Play Store: 1.3 million Apps, Apple App Store: 1.2 million Apps [Statista14]). Depending on the type of service offered by the App and the implementation, continuous Internet connectivity is mandatory, e.g. for navigation, gaming, video streaming or audio guides. Moreover, future currently developed services like Voice over LTE or car-to-car applications require reliable continuous network connectivity as well. Due to the cellular structure of the mobile communication networks, mobile users will cross cell boundaries and need to switch the serving cell with the help of a handover procedure in connected mode. If the selected service requires continuous network connectivity, the timing for the handover is essential to keep up the service. Thus, the user satisfaction with the offered service depends on successful handovers. In addition, suboptimal handover triggering can lead to signal quality degradation and hence suboptimal radio resource usage and overloaded signalling channels which is undesired by the mobile network operators.

In order to ensure uninterrupted mobile network connectivity the communication network has to meet two main conditions: First, the neighbouring cells need overlapping coverage areas. This enables the users to enter a new cell area without loosing connection

to the network. Second, a handover procedure has to be provided that assures fast and reliable cell changes. The first condition is a matter of the network planning, whereas the second condition is handled by the Radio Resource Management (RRM). The key function of the handover procedure is the handover decision, since it defines the moment of the handover initiation. A big challenge making the optimal handover decision is that the future development of the signal strength and quality of potential serving cells is unknown at the moment of the handover decision. Moreover, many circumstances like the user speed, the user moving direction, the signal interference from surrounding cells, the temporary signal blocking from other moving obstacles, etc., influence the optimal handover decision.

In recent years, the complexity of the networks increased by the introduction of new Radio Access Technologies (RATs), cell layers and the objective to increase the system performance by optimisation algorithms in the context of Self-Organising Networks (SONs). However, not all these network enhancements influence the handover conditions but changes to the cell shape or the interference situation impact the location of mobile-assisted handovers and hence the handover performance. Small cells, which can be activated by the users to cover their homes or other indoor environments, and pico cells, which temporarily serve hot-spot areas, influence the cell shapes. Furthermore Coverage and Capacity Optimization (CCO) algorithms modify the orientation (tilt) of the transmit antennas and Adaptive Antenna Systems (AAS) change the antenna diagrams to improve the network performance, which impacts the cell shapes as well. Spectrum sharing temporarily affects the signal interference in the network. Reducing the energy consumption aims at a better carbon dioxide footprint and the reduction of the Operational Expenditure (OPEX). However, shutting down cells to save energy significantly impacts the cell layout and changes the conditions in the network. Mobility Load Balancing (MLB) algorithms even use the handover control parameters to shift the users from overloaded cells to neighbouring cells [Lobinger10].

In order to maintain good handover performance in ever-changing networks a reliable optimisation of the handover control parameters is essential. The introduction of SONs to mobile communication networks enables measurement based optimisation. The optimisation target cannot simply be formulated as a handover performance improvement since opposing trends for the Handover Performance Indicators, i.e. the handover failure events and ping-pong handovers, are observed in the networks. Thus handover optimisation will be a trade-off between acceptable levels of the individual performance indicators. In [3GPP11] it is stated that “the main objective of mobility robustness

optimisation should be reducing the number of Handover (HO)-related radio-link failures." This is because service interruption, which goes along with a radio-link failure, is noticed by the user and affects the satisfaction with the offered service much more than suboptimal service delivery. Another objective is the avoidance of unnecessary handovers (ping-pong handovers), which lead to additional signalling traffic. In the area of handover optimisation several concepts and algorithms have been designed that improve the handover performance from a selected starting condition. However, important research fields in handover optimisation are neglected in previous investigations: the impact of the network configuration and capacity utilisation (network load) on the handover condition and hence the identification and selection of a more optimal handover configuration is still unclear. The optimisation algorithms developed so far have not been assessed and compared to an "optimal" handover configuration, i.e. a configuration that has been identified as best performing solution by system simulations or theoretical approaches. An analysis of the necessary handover performance observation cycles, i.e. the time period in which the current handover performance is evaluated, and the impact of this observation cycle on the optimisation speed is still pending. The observation cycle mainly impacts the ability to adjust the handover configuration to temporary network conditions, which is important to define the application area of handover optimisation algorithms.

The objective of this dissertation is to examine the handover behaviour in Long Term Evolution (LTE) based on system-level simulations using realistic simulation environments. In order to deepen the understanding of the handover optimisation problem and to pave the way for successful handover optimisation solutions we analyse the Handover Performance Indicators (HPIs) in detail. We discuss the impact of the network configuration on the optimisation activities and evaluate the influence of the cells capacity utilisation in system-level simulations. As introduced before, one of the central questions in handover optimisation is the dimensioning of the observation cycle. This interval influences the accuracy of the ongoing performance observation and the achievable optimisation speed, since long observation intervals lead to long optimisation cycles. Hence, an analysis of the "optimal" observation interval is a central part of this dissertation. Based on these analyses, we develop and assess two optimisation algorithms in this dissertation: the first solution is an algorithm aiming at the successive adaptation of the handover control parameters in small steps. The algorithm was developed in the SOCRATES project and bases on the direct handover performance comparison of two handover configuration sets. A multitude of this kind of optimisation algorithms

has been suggested by the research community in recent years. The advantage of these algorithm is easy implementation since they base on performance indicators which are already used in the networks to monitor the handover performance. The second solution bases on the measurement based prediction of the handover events in all potential handover configuration sets. We develop this prediction based optimisation algorithm to enable the selection of a new handover configuration set based on a pre-assessment of the expected handover performance. The advantage of this solution is that local minima in the optimisation space are discovered and the algorithm allows large-scale handover configuration adaptations with limited risk to temporary degrade the handover performance. The main assessment criteria for the evaluation of the optimisation algorithms are: the overall handover performance improvement in the network; the reached handover performance compared to an "optimal" handover performance identified by system-level simulations; and the optimisation speed as well as the adaptation to changes in the network condition (network load).

This document is organised as follows: In Chapter 2, the LTE physical layer and the concept of self-organizing networks are introduced. The support of user mobility in mobile communication networks is described in Chapter 3. This includes the LTE handover procedure, the handover decision and control parameters, the Handover Performance Indicators and additional mobility related measurements used by one handover optimisation algorithm developed in this dissertation. Chapter 4 gives an overview of the research activities in handover optimisation in recent years and analyses the open issues that will be covered in this dissertation. The simulation environment comprises the geodetic data, the simulation models, the simulation database implemented as web service named SImulation of MObile NEtworks (SIMONE) and the simulation scenarios and is described in Chapter 5. Chapter 6 contains the analyses of the Handover Performance Indicators and the impact of the network configuration and capacity utilisation on the handover performance. The evaluations from this chapter lead to the identification of suitable observation intervals for the Handover Performance Indicators. Two handover optimisation algorithms are described and their performance is analysed in Chapter 7. A conclusion on the investigations in this dissertation and an outlook on future open research topics in the field of handover optimisation is given in Chapter 8.

Chapter 2

The Main LTE Features and SON Concept

The main features of the LTE physical layer and the general concept of SON are presented in this chapter. The first section (Section 2.1) focusses on the LTE physical layer and describes the fundamental LTE function which is the basis for the development of the simulation models and scenarios. The second section (Section 2.2) elaborates the concept of SONs which has been introduced in LTE to increase the system performance by continuous optimisation of the network configuration.

2.1 The LTE Physical layer

In this section, the LTE physical layer is introduced. The section starts with the LTE operating bands in Europe and the definition of a LTE resource block. Furthermore the Modulation and Coding Schemes (MCSs) and UE categories are described, which mainly impact the spectral efficiency of the LTE system. To give an idea of the maximum communication distance between a base station and a UE the coverage range of an LTE base station together with the link budget are exemplified at the end of the section.
The LTE operating bands allocated in Europe are listed in Table 2.1 [3GPP14a, Table 5.5-1]. In Europe the utilisation of the bands is not limited to one RAT, i.e. the licenses allow to operate several, specified mobile communication technologies in these bands. The usage of the bands is harmonised among the members of the European Union (EU) and the decisions of the European Commission (EC) are binding for the EU member countries. Examples for EC decisions on the usage of certain operating bands are: 2010/267/EU in the 790-862 MHz frequency band and 2014/276/EU in the 3400-3800 MHz frequency band, which can be assessed via [Office14]. Two duplex modes

Band Number	Duplex-Mode	Frequency Range [MHz]	
		Uplink	Downlink
1	FDD	1920 - 1980	2110 - 2170
3	FDD	1710 - 1785	1805 - 1880
7	FDD	2500 - 2570	2620 - 2690
8	FDD	880 - 915	925 - 960
20	FDD	832 - 862	791 - 821
33	TDD	1900 - 1920	
34	TDD	2010 - 2025	
38	TDD	2570 - 2620	
40	TDD	2300 - 2400	
42	TDD	3400 - 3600	
43	TDD	3600 - 3800	

Table 2.1: The duplex modes and LTE operating bands in Europe according to [3GPP14a, Table 5.5-1]

are defined in LTE, namely Frequency Division Duplex (FDD) and Time Division Duplex (TDD). The LTE operating bands overlap with bands of other communication technologies as shown in Figure 2.1. This enables network operators to re-farm frequency bands dedicated to other technologies and upgrade the network step-by-step to LTE. Another plus of the wide range of operating bands is that subject to the purpose of the cell the most appropriate frequency band can be chosen. This means cells in low

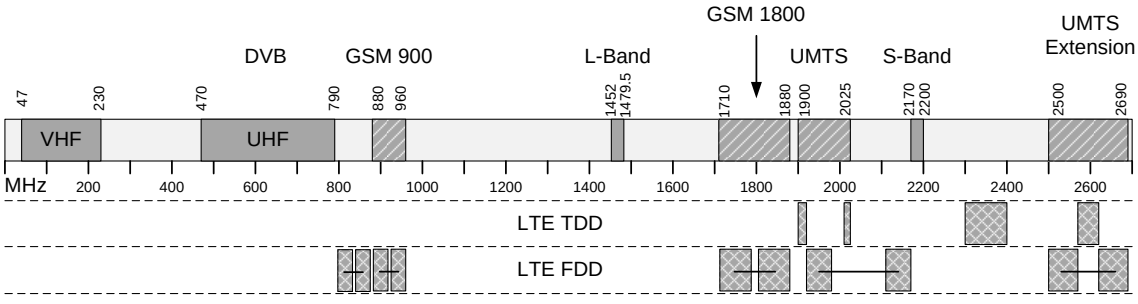

Figure 2.1: Location of the LTE operating bands and other radio technologies [Jansen10c]

density areas can operate on low frequencies and benefit from the wave propagation characteristics of these frequency bands that allow larger communication distances. Cells dedicated to serve a small hot-spot area can operate on higher frequencies. The requirement to utilize this advantage is that the network operator holds licenses in different operating bands.

Details on the physical resource elements and slot structure are specified in [3GPP13a, Section 5.1]. The transmission scheme in LTE is based on Orthogonal Frequency Division Multiplex (OFDM) using a cyclic prefix. Figure 2.2 shows two LTE resource block in the OFDM transmission scheme. The sub-carrier spacing is 15 kHz and a sub-frame lasts 1 ms. A sub-frame is further divided into two slots with seven OFDM-symbols each. A resource block consists of 12 consecutive sub-carriers and one slot. A resource block is the smallest amount of resources that can be assigned to a UE, i.e. seven OFDM symbols, for data transmission. Two cyclic prefix modes exist, i.e. normal cyclic prefix and extended cyclic prefix. In normal mode the length of the cyclic prefix for the first symbol is 5.2 μs the remaining symbols of one slot have a cyclic prefix of 4.68 μs. The extended mode uses a cyclic prefix of 16.67 μs for all symbols. A transmission scheme with reduced sub-carrier spacing of 7.5 kHz allows further extension of the cyclic prefix length.

The number of available resource blocks in the frequency domain depends on the channel bandwidth. Table 2.2 shows the channel bandwidths specified in LTE and the corresponding amount of resource blocks in one slot. The range of bandwidths allows to operate LTE in small band gaps as long as the interference to adjacent bands does not

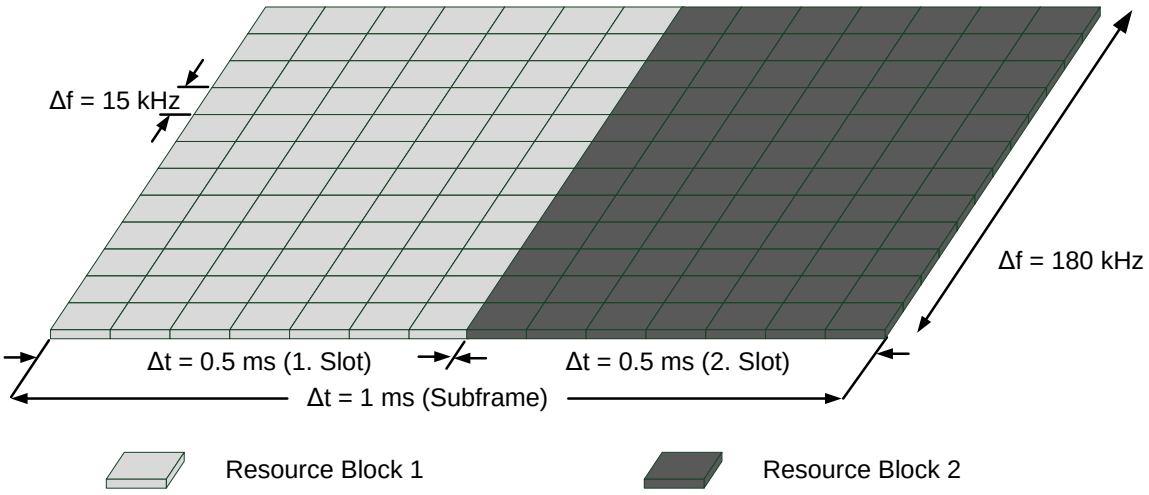

Figure 2.2: The LTE resource block [Jansen10c]

Channel Bandwidth [MHz]	1.4	3	5	10	15	20
Number of Resource Blocks	6	15	25	50	75	100

Table 2.2: The relation of the LTE channel bandwidth and number of resource blocks [3GPP14a, Table 5.6-1]

impair the operation of other technologies in these bands.

Five different modulation schemes are defined in LTE: Binary Phase-Shift Keying (BPSK) and M-Quadrature Amplitude Modulation (QAM) with $M = \{4, 16, 64, 256\}$ [3GPP14c]. The selection of the modulation scheme depends on the reception quality of the UE in the case of a transport channel and on the importance of the information

CQI Index	Modulation	Code Rate	Spectral Efficiency $[\frac{\frac{bit}{s}}{Hz}]$
1	QPSK	0.9239	0.142
2	QPSK	0.8829	0.219
3	QPSK	0.8116	0.352
4	QPSK	0.6993	0.561
5	QPSK	0.5616	0.818
6	QPSK	0.4122	1.097
7	16-QAM	0.6309	1.378
8	16-QAM	0.5215	1.786
9	16-QAM	0.3985	2.246
10	64-QAM	0.5645	2.439
11	64-QAM	0.4463	3.101
12	64-QAM	0.3497	3.642
13	64-QAM	0.2461	4.222
14	64-QAM	0.1475	4.774
15	64-QAM	0.0743	5.184

Table 2.3: Modulation and coding schemes plus spectral efficiencies in the PDSCH [3GPP14e, Table 7.2.3-1]

in the case of a control channel. For the transport channels like the Physical Downlink Shared Channel (PDSCH) a subset of modulation schemes is specified. Forward Error Correction (FEC) is realized by Turbo coding in the PDSCH. Based on the Channel Quality Indicator (CQI) the modulation and coding rate are defined in MCS. Table 2.3 shows the MCS for the PDSCH. The MCS for a transmission is selected by the network based on the channel quality reporting from the UE. Transport channels use two different coding schemes, namely Turbo coding and convolutional coding. More details on the coding schemes and transport channels can be found in [3GPP14d, Table 5.1.3-1].

In the case that the UE supports 256-QAM another MCS table is used specified in [3GPP14e, Table 7.2.3-2]. In the LTE control channels convolutional codes, block codes and the repetition code are used. More details on the coding schemes in control channels can be found in [3GPP14d, Table 5.1.3-2].

The specification of the UE capabilities in so-called UE categories is given in Table 2.4. The maximum data rates shown in the table are theoretical values that can not be interpreted as the user throughput in the network. In the latest releases new categories have been introduced that support a higher number of Multiple Input Multiple Output (MIMO) layers. The numbers neglect any kind of overhead introduced by signalling or higher layer information.

UE Category	Release	Max. Data Rate DL	Max. Data Rate UL	MIMO Layers
1	8	10.3 Mbit/s	5.2 Mbit/s	1
2	8	51.0 Mbit/s	25.5 Mbit/s	2
3	8	102.0 Mbit/s	51.0 Mbit/s	2
4	8	150.8 Mbit/s	51.0 Mbit/s	2
5	8	299.6 Mbit/s	75.4 Mbit/s	4
6	10	301.5 Mbit/s	51.0 Mbit/s	2 or 4
7	10	301.5 Mbit/s	102.0 Mbit/s	2 or 4
8	10	2998.6 Mbit/s	1497.8 Mbit/s	8
9	11	452.2 Mbit/s	51.0 Mbit/s	2 or 4
10	11	452.2 Mbit/s	102.0 Mbit/s	2 or 4

Table 2.4: UE categories specified by the 3GPP-Releases [3GPP14f, Table 4.1-1 & 4.1-2]

Calculation	Transmitter (eNodeB)	
a	Tx Power	46 dBm
b	Tx Antenna Gain	18 dBi
c	Cable Loss	2 dB
$d = a + b - c$	EIRP	62 dBm
Calculation	Receiver (UE)	
e	UE Noise Figure	7 dB
f	Thermal Noise	-104.5 dBm
g	Min. SINR	-9 dB
$h = e + f + g$	Receiver Sensitivity	-106.5 dBm
i	Interference Margin	4 dB
j	Control Channel Oeverhead	1 dB
$d - h - i - j$	Maximum Pathloss	163.5 dB

Table 2.5: Downlink link budget for a data rate of 1 Mbit/s [Holma09, Table 9.10]

Table 2.5 shows the link budget for a transmission with a data rate of 1 Mbit/s in the downlink. More details on the assumptions for the link budget can be found in [Holma09, Section 9.6]. The resulting maximum pathloss between the base station and the UE is 163.5 dB.

The coverage range of the LTE cells depends on the carrier frequency and maximum pathloss. Table 2.6 shows the coverage range and thus the maximum cell sizes using the maximum pathloss from Table 2.5. This means a minimum data rate of 1 Mbit/s is assumed for the transmission. The coverage ranges show that lower carrier frequencies are beneficial for areas with a low population density. The simulation scenarios described

Carrier Frequency [MHz]	800	900	1800	2000	2300	2600	3600
Coverage Range [km]	14.68	13.42	7.93	7.32	6.58	5.99	4.68

Table 2.6: Coverage range of LTE in urban environments for a minimum data rate of 1 Mbit/s

in Chapter 5 use carrier frequencies between 1800 - 2000 MHz. The chosen inter site distance of 500 m in one scenario and the typical inter site distance of less than 1 km in the dense-urban areas of the other scenario show that the communication is interference limited and not noise limited in the simulation scenarios. To calculate the coverage ranges, the Okumura-Hata propagation model for urban environments has been used. Details on the model can be found in [Lüders01, Section 7.3]. Further assumptions for the model are the base station height of 40 m and a UE height of 1.5 m. The model was originally defined for operation frequencies of up to 1500 MHz. Research results in [Baumgarten12] show that the model can be used for higher operation frequencies as well.

2.2 The Concept of Self-Organizing Networks

The concept of SONs follows the idea of a network deployment where the cells automatically tune the system parameters to get a basic configuration for system operation followed by the measurement based optimisation of the system parameters. Self-organization splits in three parts: self-configuration, self-optimisation and self-healing [Scully08, Section 1.1]. Figure 2.3 shows the interaction of the self-organization functions. The common basis for the SON-functions is the continuous measurement cycle that allows the evaluation of the current performance and the evaluation of the impact of system parameter changes by the SON-functions.

Self-configuration functions are active in the pre-operational state of newly deployed base stations. The objective of these SON-functions is to enable system operation by automatic tuning of the basic setup and initial radio configuration parameters. The pre-operational state is the phase between the power-on of a cell including backbone connectivity and the activation of the Radio Frequency (RF) transmitter. [3GPP13a, Section 22.1]

Self-optimisation functions are active in the operational state of the base stations. These functions aim at the improvement of the system performance by adaptation of the system parameters. The basis for the optimisation are the UE and system measurements. [3GPP13a, Section 22.1]

Self-healing functions are activated in the case of system failures of “non-intentional nature”. Examples are the failure of a cell or base station. The objective of these functions is to improve the coverage or capacity problems during the repair activities. Once the cell is back in operation the former system configuration is restored.

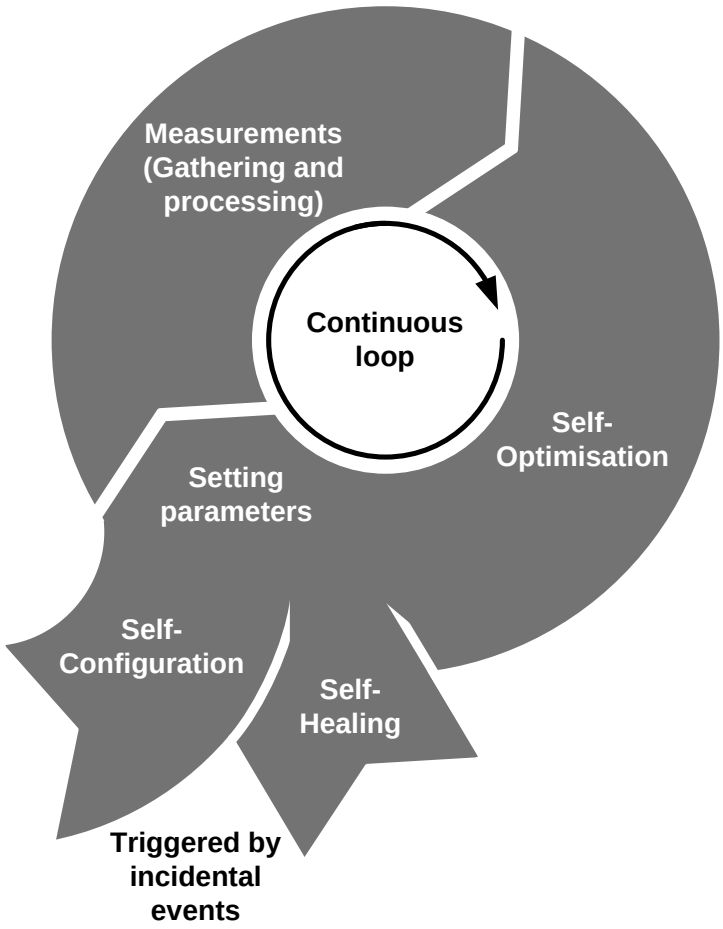

Figure 2.3: The Concept of Self-Organization in the SOCRATES Project [Scully08]

Several SON use cases have been defined by 3rd Generation Partnership Project (3GPP) [3GPP11], Self-Optimisation and self-ConfiguRATion in wirelEss networkS (SOCRATES) [Scully08] [Amirijoo08] or Next Generation Mobile Networks (NGMN) [NGMN08]. LTE includes supporting functions for a variety of SON functions standardised in [3GPP13a, Section 22].

Chapter 3

Support of User Mobility in Mobile Communication Networks

This chapter introduces the main features of the handover procedure in the 3GPP LTE including measurement setup, measurement triggering and signalling and data flow in Section 3.1. Furthermore, the handover decision and handover control parameters are introduced in Section 3.2. Section 3.3 is dedicated to handover performance indicators used as the basis for the handover optimisation and finally, additional mobility related measurements are described in Section 3.4. The additional mobility related measurements are unnecessary for the standard handover procedure in LTE. They are used as additional system information in one of the considered optimisation algorithm in Chapter 7.

3.1 The Handover Procedure in 3GPP LTE

The handover procedure in 3GPP LTE allows a UE to switch from the serving evolved Node B (eNB) to another eNB in the network without loss of connection. The final handover decision is made by the network, i.e. the eNB, and is based upon measurement reports of the UE. The reasons for the initiation of a handover procedure vary from decreasing service quality, decreasing signal strength of the serving cell or frequency layer switch due to user mobility, to load balancing activities. Based on predefined thresholds and conditions, the UE sends measurement reports to the network. These measurements are used to observe the service quality of the user and to evaluate the signal strength of neighbouring cells to identify a potential Target evolved Node B (TeNB) for a handover. If the service quality or signal strength of the serving cell decreases further than a predefined threshold, or another precondition for a handover initiation is met, a handover

to the cell with the highest signal strength is executed. In case that the service quality or signal strength degradation is temporary, the measurement reporting is disabled again. In case of a handover, the user data (communication content) is stored and transferred to the TeNB of the handover process, to ensure continuous service delivery.
The handover procedure can be subdivided in four parts:

1. Measurement report triggering
2. Handover decision by the network
3. Identification of the TeNB
4. Handover execution

The configuration of the measurements and hence the events that trigger the measurement reporting from the UE to the eNB are defined by the network and communicated to the UE. Once the entering condition for an event is met, i.e. the UE identifies a cell that is an offset stronger than the serving cell, the measurement reporting starts. A UE that is in the mode of transferring measurements to the network can be classified as a potential handover candidate. In any case this UE will be located close to the cell border of its serving cell and any neighbour cell in the same RAT and frequency layer or close to a coverage hole. In the inter-RAT case, only UEs located at the border of a cell qualify for a handover since these UEs may benefit from less interference and hence better service quality in a neighbour cell. Even in the case of a load balancing handover, the UEs located at the cell border will be selected to unload a cell since the probability that these UEs can be served from a neighbouring cell is higher than for cell centre UEs. Note that cell border does not necessarily mean that a UE is physically located in the middle between two cells. Fading effects may lead to a handover initiation for a UE that is located close to its serving cell. Hence the term “cell border” has to be interpreted in the sense of a potential increase in the UE service quality or network throughput by a serving cell change. The initiation of a handover to another cell layers on a different transmission frequency or other communication technology is not necessarily initiated by users located close to the inter-RAT cell border, since other reasons for the handover initiation like load balancing, the user speed class or the demanded service might necessitate the handover. Steps two and three, i.e. the handover decision and identification of the TeNB by the network, are based on the measurement reports. In the case of a quality based handover, the handover decision implies the identification of a TeNB

already. This means step two and three merge to one step in this case. In the case of a load balancing handover the detection of a highly loaded or overloaded cell initiates the identification of potential TeNBs. In this case the two steps are executed individually.
The steps one to three of the handover procedure rely upon cell signal strength measurements reported by the UE. This shows that the measurements are very important for a successful mobility support. Thus, the following subsections introduce the most important UE measurements, the measurement report triggering and the data flow between the LTE entities.

3.1.1 Measurements

To evaluate the connection quality to the network the UE continuously measures the Reference Signal Received Power (RSRP) and Reference Signal Received Quality (RSRQ) level of the serving cell and neighbour cells. One purpose of these continuous measurements is, to identify best server cell changes, which trigger the handover procedure or cell reselection. Hence, these measurements are the basis for successful user mobility support. The definition of the measurements elaborated below are taken from the LTE standard. The references to the relevant documents are given in the sections below.
In general, the measurement configuration differs for different states of a UE. For instance the current Radio Resource Control (RRC) state, i.e. RRC-IDLE and RRC-CONNECTED, influences the time period of the channel quality measurements. In some cases, the measurement configuration is influenced by the Discontinuous Transmission (DTX) and Discontinuous Reception (DRX) mode as well. The DTX and DRX are introduced in LTE to enable energy saving in RRC-IDLE and RRC-CONNECTED state. In the case of a low data rate service like a voice over IP call, discontinuous transmission and reception are used to power down the UE in pre-defined time slots. Depending on the data rate, the configuration of DTX and DRX can be adapted by the network. In RRC-IDLE state the UE can enter a UE sleep mode for a communicated time period. Since no data transmission or reception is possible in the time periods the UE is in sleep mode, the measurement configuration is adapted to the DRX cycle.

Reference Signal Received Power

The RSRP measurement is defined in [3GPP12a, P. 7] as “the linear average over the power contributions (in [W]) of the resource elements that carry cell-specific reference signals within the considered measurement frequency bandwidth”. 3GPP leaves some

implementation details up to the UE manufacturers as long as the measurement accuracy requirements are guaranteed. This means that the number of resource elements that are used to determine the RSRP are not standardised and left up to the UE implementation. The reference point for the RSRP is the antenna connector of the UE.

Reference Signal Received Quality

In [3GPP12a, P. 8] the RSRQ is defined as:

$$RSRQ = \frac{N \times RSRP}{RSSI} \tag{3.1}$$

where N is the number of Resource Blocks (RBs) considered for the measurements, $RSRP$ is the reference signal received power introduced before and $RSSI$ is the Received Signal Strength Indicator. The RSSI is defined as "the linear average of the total received power (in [W]) observed only in OFDM symbols containing reference symbols for antenna port 0, in the measurement bandwidth, over N number of resource blocks by the UE from all sources, including co-channel serving and non-serving cells, adjacent channel interference, thermal noise etc." in [3GPP12a, P. 8]. The individual measurements for the terms in the numerator and denominator have to be done over the same set of RBs. Again the reference point for the RSRQ is the antenna connector of the UE.

Measurement Period and Measurement Reporting Period

In RRC-IDLE state the RSRP and RSRQ level of the serving cell are measured at least every DRX cycle. Table 3.1 shows the DRX cycle lengths and the corresponding serving cell evaluation period N_{serv}, which is the time period in which a UE checks for

DRX Cycle length [s]	N_{serv} [Number of DRX Cycles]
0.32	4
0.62	4
1.28	2
2.56	2

Table 3.1: Interdependency of the DRX cycles and the serving cell evaluation cycle [3GPP14b, P. 32]

DRX Cycle length [s]	T_{detect} [s] (Number of DRX Cycles)	$T_{measure}$ [s] (Number of DRX Cycles)
0.32	11.52 (36)	1.28 (4)
0.62	17.92 (28)	1.28 (2)
1.28	32 (25)	1.28 (1)
2.56	58.88 (23)	2.56 (1)

Table 3.2: Measurement periods for E-UTRAN intra cells subject to the DRX cycle length [3GPP14b, P. 33]

a better serving cell. If the serving cell evaluation identifies a better serving cell, the cell reselection is triggered by the UE. The ranking of the cells is influenced by the cell selection criterion that defines signal strength offsets between the serving cell and other cells, i.e. the network can influence the UE serving cell selection by the cell selection criterion. [3GPP14b, P. 32]
In the cell reselection mode, the UE continuously measures the RSRP and RSRQ level of the intra-frequency cells. The identification of new intra-frequency cells is done autonomously by the UE and the cell reselection criteria, similar to the cell selection criterion, for new cells is evaluated at least every T_{detect} as given in Table 3.2. Cells that fulfil the reselection criteria are measured every $T_{measure}$. The UE reselects a new serving cell if the reselection criteria for that cell is met for a defined time period. [3GPP14b, P. 33]
From this it follows that the RSRP and RSRQ level of the intra-frequency cells are measured depending on the DRX cycle at least every 2.56 seconds in RRC-IDLE state. In RRC-CONNECTED state the measurement period for the RSRP and RSRQ level of the intra-frequency cells is 200 ms. This means that new RSRP and RSRQ values are available every 200 ms and can potentially be reported every 200 ms to the network. [3GPP14b, P. 66]
For all RSRP and RSRQ measurements a minimum filtering condition is specified that ensures that at least the average of two measurement values is evaluated in a measurement period.

3.1.2 Measurement Report Triggering

Measurement reports are triggered by the network through the measurement configuration. Usually the triggering reason is that the user approaches a “cell border” and hence

sooner or later runs the risk of losing the connection to the network. As introduced before, "cell border" has to be interpreted as the chance to increase the service quality in another cell, layer or RAT. The triggering of measurement reports is the first step to initiate the handover procedure. The measurement report triggering is defined in [3GPP13b, Section 5.5.4] and distinguishes between six different cases for intra RAT (Event A) triggering events and two additional cases for inter RAT (Event B) triggering events. All events are evaluated for the RSRP and RSRQ measurements. The defined events are:

- Event A1: Serving becomes better than threshold
- Event A2: Serving becomes worse than threshold
- Event A3: Neighbour becomes offset better than Primary Cell (PCell)
- Event A4: Neighbour becomes better than threshold
- Event A5: PCell becomes worse than threshold1 and neighbour becomes better than threshold2
- Event A6: Neighbour becomes offset better than Serving Cell (SCell)
- Event B1: Inter RAT neighbour becomes better than threshold
- Event B2: PCell becomes worse than threshold1 and inter RAT neighbour becomes better than threshold2

The term PCell stands for the primary cell in the case of carrier aggregation in LTE-Advanced (LTE-A) and SCell terms the serving cell in one of the frequency layers. In the case of carrier aggregation a user might be served by more than one cell. Nevertheless, one cell (PCell) is defined as the main connected cell and the other cells are termed Serving Cells. Since we focus the investigations in this dissertation on intra RAT HO optimisation in LTE, the most important measurement report triggering events are the intra RAT events. Hence, the inter RAT events B1 and B2 are of less importance. Triggering events A1, A2, A4 and A5 define certain thresholds for the serving or neighbour cell measurement triggering. Event A3 and Event A6 specify an offset between the signal strength or quality measurements of the serving and neighbour cells. The difference between Event A3 and Event A6 is minor, i.e. the first event includes frequency offsets used in the case of carrier aggregation for LTE-A. Due to the focus on LTE, the most

important triggering event is Event A6 and no frequency offsets are needed since one frequency layer is considered. The event A6 is described in detail below:

Event A6 - Neighbour becomes offset better than SCell

The definition of this event is taken from [3GPP13b]. The term entering conditions means that an Event A6 is detected if the specified condition is fulfilled. The leaving condition specifies the condition that terminates the Event A6.
Entering condition:

$$M_n + O_{cn} - \mathrm{HYS}_{trig} > M_s + O_{cs} + \mathrm{Off} \tag{3.2}$$

Leaving condition:

$$M_n + O_{cn} + \mathrm{HYS}_{trig} < M_s + O_{cs} + \mathrm{Off} \tag{3.3}$$

where the variables are defined as:

- M_n is the measurement result of the neighbouring cell, not taking into account any offsets
- O_{cn} is the cell specific offset of the neighbour cell to the SCell and set to zero if not configured for the neighbour cell
- M_s is the measurement result of the SCell, not taking into account any offsets
- O_{cs} is the cell specific offset of the SCell to the neighbour cell and is set to zero if not configured for the SCell
- HYS_{trig} is the hysteresis parameter for this event
- Off is the offset parameter for this event
- M_n, M_s are expressed in dBm in case of RSRP, or in dB in case of RSRQ
- $O_{cn}, O_{cs}, \mathrm{HYS}_{trig}$ and Off are expressed in dB

In our investigations, i.e. system-level simulations in LTE, the signal strength and quality conditions are known in every time step for every UE. If the offset values $O_{cn}, O_{cs}, \mathrm{HYS}_{trig}$ and Off are set to zero in a real network, the RSRP measurements are reported, when a neighbour cell becomes stronger than the serving cell. This leads to

heavy signalling traffic in the network. Thus, the offset values are used to trigger the measurement reporting subject to the handover control parameters to avoid unnecessary measurement report transmission. In the case that a high Hysteresis (HYS) value is defined in a cell, it is needless to send measurements report, when the neighbouring cell becomes stronger by only 0.5 dB.

3.1.3 Signalling and Data Flow

The handover procedure in 3GPP LTE involves signalling between the UE, Source evolved Node B (SeNB) and TeNB. SeNB terms the connected cell when the handover is initiated and TeNB terms the strongest cell at the UE location, which is the potential target for the handover. The individual steps in the procedure are illustrated in Figure 3.1. The following description is taken from [3GPP13a] and reduced to the main features to give an overview of the signalling and data flow. A more detailed description of the handover procedure can be found in [3GPP13a, Setcion 10.1.2.1].

1. The SeNB sends the measurement configuration to the UE including the area restriction information, i.e. information on cell access and frequency restrictions.

2. According to the measurement report triggering in Section 3.1.2 measurement reports are send to the SeNB.

3. The SeNB makes a handover decision based on the measurement reports and RRM information (HYS, Time-To-Trigger (TTT)) and selects a TeNB.

4. The SeNB issues a “handover request” message to the TeNB. The request message includes information for Radio Link Failure (RLF) recovery and enables the TeNB to address the SeNB and the Evolved Packet Core (EPC).

5. Admission Control may be performed by the TeNB depending on the received Quality of Service (QoS) information to increase the likelihood of a successful HO, if the resources can be granted by the TeNB. The TeNB configures the required resources according to the received QoS information and reserves a Cell Radio Network Temporary Identifier (C-RNTI) and optionally a Random Access Channel (RACH) preamble.

6. The TeNB prepares the HO and sends the “handover request acknowledgement” to the SeNB. The message includes handover information dedicated to the UE that

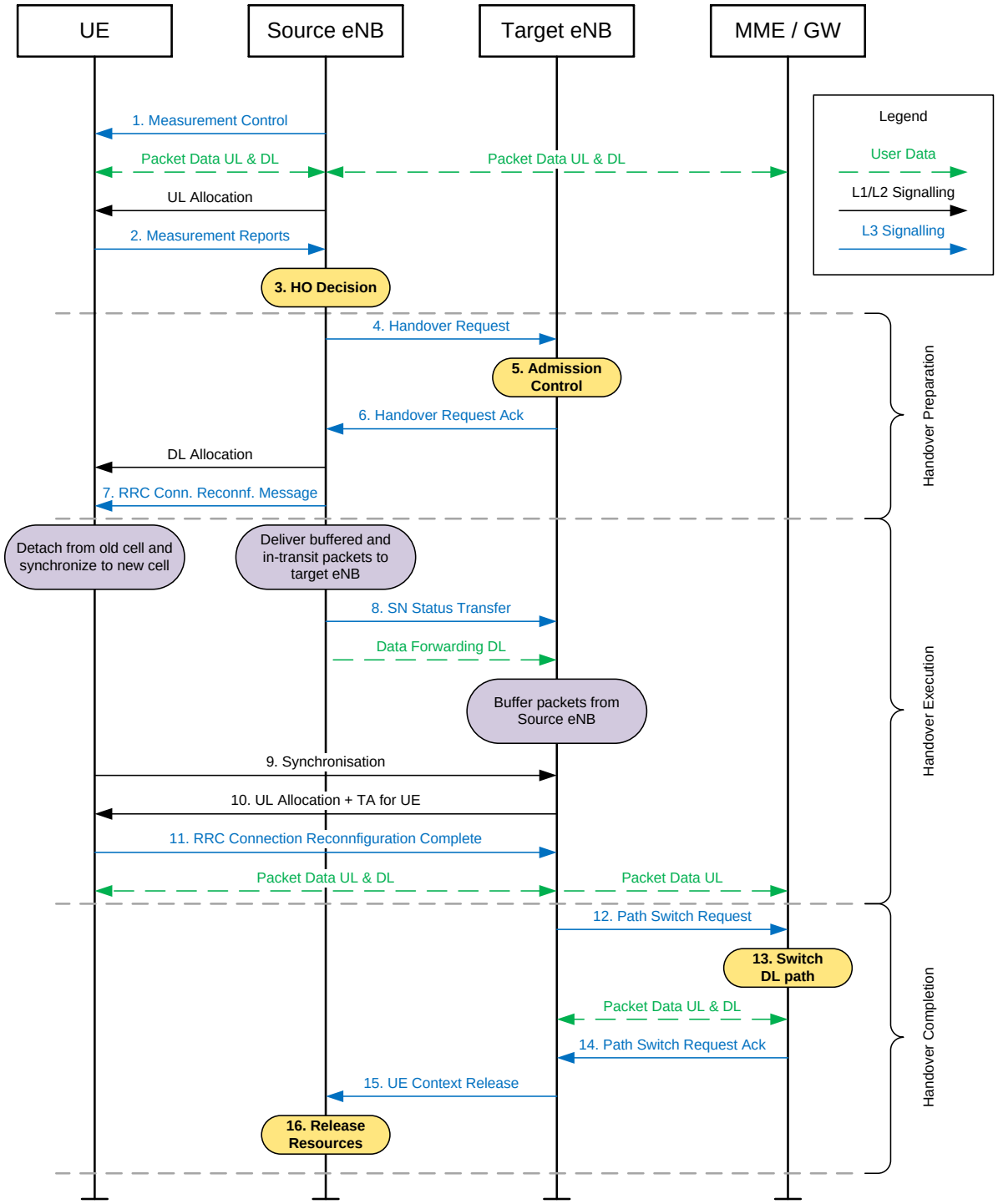

Figure 3.1: Flowchart of the 3GPP LTE handover procedure [3GPP13a]

eases the connection procedure to the TeNB. As soon as the SeNB receives the handover request acknowledgement, or the transmission of the handover command is initiated in the downlink, data forwarding from the SeNB to the TeNB may be initiated.

7. The RRC message to perform the handover, i.e "RRC Connection Reconfiguration" message, is sent towards the UE. The UE receives the message and is commanded to perform the HO by the SeNB.

8. The SeNB sends the "Sequence Number (SN) status transfer" message to the TeNB to convey the uplink receiver status and the downlink transmitter status.

9. After receiving the "RRC Connection Reconfiguration" message the UE performs synchronisation to the TeNB and accesses the TeNB via the RACH.

10. The TeNB responds with Uplink (UL) allocation and timing advance.

11. When the UE has successfully accessed the TeNB, the UE sends the "RRC Connection Reconfiguration Complete" message to the TeNB to indicate that the handover procedure is completed for the UE. The TeNB verifies the message and can now begin sending data to the UE.

12. The TeNB sends a "path switch request" message to the Mobility Management Entity (MME) to inform that the UE has changed the eNB.

13. The Serving Gateway switches the downlink data path to the TeNB.

14. The MME confirms the "path switch request" message with the "path switch request acknowledge" message.

15. By sending the "UE context release" message, the TeNB informs success of the HO to the SeNB and triggers the release of resources by the SeNB. The TeNB sends this message after the "path switch request acknowledge" message is received from the MME.

16. Upon reception of the "UE context release" message, the SeNB can release the resources associated to the UE. Any ongoing data forwarding may continue.

3.2 Handover Decision and Control Parameters

The HO decision in LTE networks introduced in the last Section 3.1.3 is influenced by a number of control parameters, i.e. the HYS, Hysteresis Offset (HYS-Off) and TTT standardised by 3GPP in [3GPP13b]. The HO decision starts the handover preparation phase as shown in Figure 3.1. The decision is based on UE measurements that are triggered by the event A6 as introduced before. The standardised handover control parameters define the exact moment the HO decision is made. Assuming that the offset values $O_{cn}, O_{cs}, \mathrm{HYS}_{trig}$ and Off introduced in Section 3.1.2 are set to zero, the UE measurements are triggered if the RSRP or RSRQ of a neighbour cell becomes stronger than the RSRP or RSRQ of the connected cell.

For clarification, an exemplary set of two RSRP courses (Cell A and Cell B) is depicted in Figure 3.2. In the beginning, the user is connected to Cell B. Event A marks the point in time when the signal strength of Cell A becomes stronger than the signal strength of Cell B. The event A6 triggers the measurement reports that the user henceforth transmits to Cell B (under the above assumption that the offset values are set to zero). Once the HYS condition set by the serving cell B is fulfilled, Cell A qualifies as handover candidate. If that condition holds for a duration longer than the time defined by TTT, the handover decision is made. If the signal strength of cell A falls below the offset defined by the HYS again, cell A has to re-qualify by better RSRP values to fulfil the HYS condition. Likewise, the TTT condition has to be met in that case after the HYS condition is fulfilled. The HO decision implicitly includes the selection of the TeNB for the handover, i.e. the cell that fulfils the HYS and TTT condition.

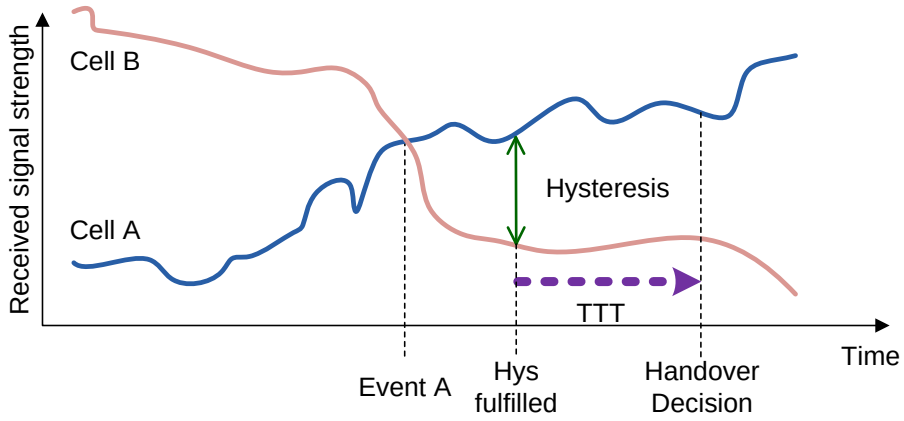

Figure 3.2: The handover decision based on HYS and TTT

The example shows that the handover control parameters define the exact moment for the handover decision of a UE. Moreover, it becomes clear that minor changes in the course of the signal strength of Cell A and B lead to a different handover decision (in time and location). These changes can be caused by many temporary interferences with the transmission channel, like obstacles that interfere with the signal reception or even changes in orientation of the body or head of the user. In addition, the handover control parameters impact the user cell assignment as shown in Figure 3.3. In the upper case a smaller HYS value has been defined as indicated by the smaller HYS arrows in the schematic diagram. The intersection area between the two cells gives the area where users connected to any of the two cells could be located without fulfilling the HYS condition. Once a user connected to the SeNB leaves the intersection area towards the TeNB, the HYS condition is fulfilled. The TTT defines the time a user stays connected to the SeNB before the handover is initiated. Hence, it depends on the user speed how far a user can enter the area of the TeNB before the handover decision is made. This

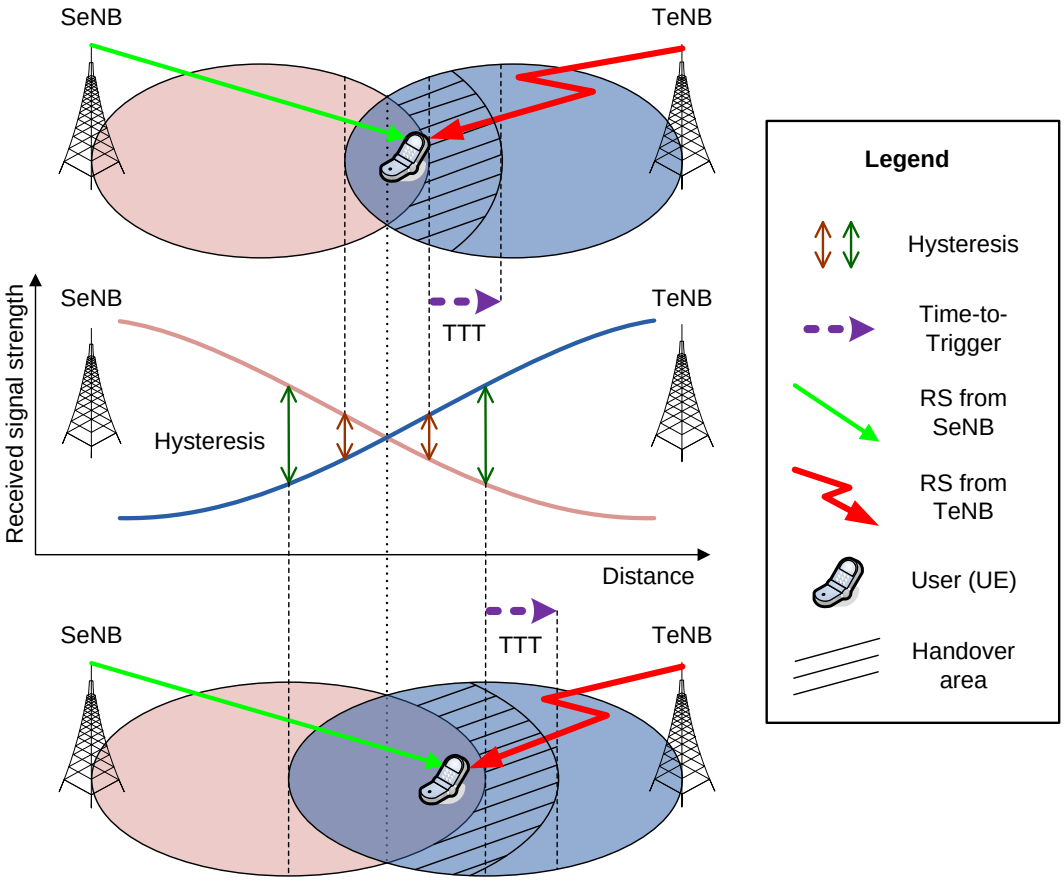

Figure 3.3: Impact of the handover control parameters on the user cell assignment

indicates that defining different handover parameters for user speed classes makes sense. In the lower case a higher HYS value has been defined for a SeNB. Consequentially the intersection area of the two cells is larger in this case. The underlying assumption for this example is that the HYS has been adapted in both cells in equal measure. Otherwise the intersection area would shift towards one cell. The higher HYS value causes a larger area in which users of any of the two cells could be located. This will probably lead to worse signal quality conditions for the users located at the cell border in the intersection area between the cells. Nevertheless, higher HYS settings make sense to avoid frequent cell changes of cell edge users between neighbouring cells. As mentioned before, this causes undesired backhaul traffic. In reality the cell areas are not circular as in the example nor coherent in any case. One reason for this are obstacles like buildings and vegetation that influence the wave propagation. Moreover, the user movement is not mandatory directed from one cell to a neighbouring cell but might follow the cell border. Therefore, an optimisation of the handover control parameters to cope with the variety of user needs and environmental impacts is needed.

3GPP specifies value ranges for the handover control parameters in [3GPP13b]. The corresponding value ranges are listed below.

Hysteresis

The HYS is defined as the minimum difference between the signal strength of the SeNB and the TeNB in dB, given that the signal of the TeNB is stronger. The HYS is defined for every eNB and is taken into account for every UE that leaves the SeNB to any TeNB. 3GPP defines HYS values between 0 dB and 15 dB with a step size of 0.5 dB for LTE [3GPP13b, P. 247]. Due to high computing time, the number of considered HYS values has to be reduced for the system simulations. In the controllability and observability studies in the SOCRATES project [SOCRATES08] we showed that the system performance for high HYS values is dominated by high radio-link failure ratios with unacceptable performance. Hence, the value range is limited to 10 dB with a step size of 1 dB for the simulations in this work. Thus a value set of 11 HYS values is taken into account:

Values specified in 3GPP:

$$\begin{aligned}\mathrm{HYS} \in \{&0, 0.5, 1, 1.5, 2, 2.5, 3, 3.5, 4, 4.5, 5, 5.5, 6, 6.5, 7, 7.5, 8, 8.5,\\ &9, 9.5, 10, 10.5, 11, 11.5, 12, 12.5, 13, 13.5, 14, 14.5, 15\}\end{aligned}$$

Values used in this work:

$$\text{HYS} \in \{0, 1, 2, 3, 4, 5, 6, 7, 8, 9, 10\}$$

Hysteresis Offset

The HYS-Off or Q-OffsetRange (as named in 3GPP [3GPP13b, P. 243]) parameter is an additional HYS value that can be used to set cell individual HYS-Offs. The offsets are used to account for differences in the mobility between cell pairs. For example an eNB that serves an area at the border of a city could see UEs that leave the city (and hence the cell) with high speed on a road into the countryside towards cell A. On the other side of the cell area (towards the city) pedestrians could walk into the city on a side-walk towards cell B. In this case, it might make sense to treat the UEs that leave the city with high speed differently than the UEs that walk into the city. In contrast to the HYS, the HYS-Off can be defined differently for UEs travelling from the SeNB towards cell A or cell B. Hence, the individual situation of the UEs can be accounted for. The HYS-Off is defined in dB as well and allows values between -24 dB and 24 dB. The step size varies between 1 dB and 2 dB. The specified values are:

$$\begin{aligned}\text{HYS-Off} \in \{&-24, -22, -20, -18, -16, -14, -12, -10, -8, -6, -5, -4,\\ &-3, -2, -1, 0, 1, 2, 3, 4, 5, 6, 8, 10, 12, 14, 16, 18, 20, 22, 24\}\end{aligned}$$

Time-To-Trigger

The TTT is defined in ms and allows values between 0 ms and 5120 ms [3GPP13b, P. 263]. The exact values defined in the 3GPP specification are listed below. Since the time resolution in the used simulation environment is limited to 100 ms, the TTT values that are taken into account for the simulations are adapted to the values listed below. Hence, a value set of 11 TTT values is considered:

Values specified in 3GPP:

$$TTT \in \{0, 40, 64, 80, 100, 128, 160, 256, 320, 480, 512, 640, 1024, 1280, 2560, 5120\}$$

Values used in this work:

$$TTT \in \{0, 100, 200, 300, 400, 500, 600, 1000, 1200, 2500, 5100\}$$

Handover Operating Points

A combination of a HYS and TTT value will from now on be referred to as a Handover Operating Point (HOP). Given that a set of 11 HYS and 11 TTT values has been defined for the simulations in this work a total number of 121 HOPs are investigated.

3.3 Handover Performance Indicators

The assessment of the handover performance of a cell or network is based on reports of handover related events. The term handover related events indicates that not only successful handovers and handover failures, which clearly are handover related events, have to be considered. Radio-link failures, which might happen before a handover is initiated, can be caused by suboptimal handover settings as well, e.g. the handover control parameters have high values that cause the UE to loose the connection to the network before the handover procedure is initiated. This section gives an overview of the relevant handover related events and the HPIs that are used in this dissertation. The definitions of the HPIs have been taken from the SOCRATES project in which the author participated and slightly adapted to recent findings [Kürner11]. The major difference is that the same denominator is used for the calculation of all HPIs ratios, i.e. the number of handover related events. This eases the identification of the most significant HPI and increases the comparability between the HPIs.
The detection of handover related events in a real network involves data exchange between the eNBs. In [3GPP11, Section 4.5.2] 3GPP lists the required functionalities for the detection of three different kinds of radio-link failures, i.e. too late handovers, too early handovers and handovers to the wrong cell. In case of a too late handover, the UE will re-establish the connection to the network in a different cell than the SeNB. This RLF can either be detected by the SeNB or by the eNB the UE re-establishes the connection to. In the second case, the new serving eNB informs the old SeNB that the UE is now served by it. RLFs caused by too early handovers happen shortly after a UE has connected to the TeNB. The UE re-establishes the connection to the SeNB in this case and hence the SeNB can detect this error itself. If a handover was performed to a wrong cell, the UE loses connection to the network in the TeNB and re-establishes the

connection to a third eNB. In this case, the SeNB and TeNB should be informed by the third eNB. In any case a radio-link failure leads to temporary interruption of the data stream.

Successful Handovers

A successful handover HO_{succ} is defined as a completed handover of a UE from a SeNB to a TeNB without interruption of the communication to the network. Since the handover control parameters of the SeNB define the exact moment of the handover decision, the successful handovers are counted in the SeNB. The number of successful handovers N_{succ} is used to determine the handover performance of a cell. It is defined as the sum of successful handovers over a time span Δt or a fixed number of handover related events N_{hr_events}:

$$N_{succ} = \sum_{\Delta t} HO_{succ}(t) \qquad \text{or} \qquad N_{succ} = \sum_{N_{hr\_events}} HO_{succ}(t) \tag{3.4}$$

The number of successful handovers can be split up in the number of ping-pong handovers N_{pp} and the number of successful handovers without ping-pong N_{npp} as follows:

$$N_{succ} = N_{pp} + N_{npp} \tag{3.5}$$

Ping-Pong Handovers

A ping-pong handover HO_{pp} is a successful handover of a user from a SeNB to a TeNB followed by another successful handover back from the TeNB to the SeNB within the time span $T_{crit-pp}$. $T_{crit-pp}$ is defined as:

$$T_{crit-pp} = 2 * (TTT + t_{min}) \tag{3.6}$$

with TTT as time to trigger of the SeNB and t_{min} as the minimum time span a user should be connected to a cell. t_{min} has been defined by the SOCRATES project in an internal deliverable [Balan09] and is set to a value between two and five seconds.
The number of ping-pong handovers N_{pp} is defined as a subset of the number of successful handovers N_{succ}. Equivalent to the number of successful handovers the number of ping-pong handovers is calculated as the sum of ping-pong handovers over a time span Δt or a fixed number of handover related events N_{hr_events}.

$$N_{pp} = \sum_{\Delta t} HO_{pp}(t) \qquad \text{or} \qquad N_{pp} = \sum_{N_{hr\_events}} HO_{pp}(t) \tag{3.7}$$

Handover Failures

A handover failure HO_{fail} is defined as a radio-link failure of the link to the SeNB or TeNB in the handover process, i.e. the handover preparation and handover execution phase as introduced in Figure 3.1. A connection loss is detected when the Signal to Interference plus Noise Ratio (SINR) of the user falls below the minimum threshold $SINR_{min}$ for the time span $T_{crit-hof}$. $SINR_{min}$ is usually set to -6.5 dB [3GPP12c, Section A2] and $T_{crit-hof}$ to 100 ms (due to the simulation step size of 100 ms) in our system-level simulations. In the case that the radio-link to the TeNB fails, it can be attempted to hand the UE back to the SeNB. If the attempt is successful, the UE does not lose connection to the network. For the analysis of the handover performance, the number of handover failures N_{fail} is calculated as the sum of handover failures over a time span Δt or a fixed number of handover related events N_{hr_events}:

$$N_{fail} = \sum_{\Delta t} HO_{fail}(t) \qquad \text{or} \qquad N_{fail} = \sum_{N_{hr\_events}} HO_{fail}(t) \tag{3.8}$$

Radio-Link Failures

A radio-link failure HO_{rlf} is defined as the connection loss of a UE from the network. As for the handover failures, a connection loss is detected when the SINR of a user falls below the minimum threshold $SINR_{min}$ for the time span $T_{crit-rlf}$. $T_{crit-rlf}$ is usually set to 5 s in system-level simulations[1]. It should be noted that a radio-link failure may be caused by suboptimal handover parameter settings but could also be caused by coverage holes in the network. For the analysis of the handover performance the number of radio-link failures N_{rlf} is calculated as the sum of radio-link failures over a time span Δt or a fixed number of handover related events N_{hr_events}:

$$N_{rlf} = \sum_{\Delta t} HO_{rlf}(t) \qquad \text{or} \qquad N_{rlf} = \sum_{N_{hr\_events}} HO_{rlf}(t) \tag{3.9}$$

[1] This value has been discussed in the SOCRATES project and defined to 5 s. The value represents the time a user waits for a service to recover from a link failure.

Handover Related Events

The number of handover related events N_{hr_events} terms the sum of all handover events. It provides the basis for the calculation of the handover performance ratios that are used as input statistics for the optimisation algorithms. N_{hr_events} is defined as:

$$N_{hr\_events} = N_{succ} + N_{fail} + N_{rlf} = N_{pp} + N_{npp} + N_{fail} + N_{rlf} \tag{3.10}$$

Negative Handover Events

The number of negative handover events N_{neg_events} terms the sum of ping-pong handovers HO_{pp}, handover failures HO_{fail} and radio-link failures HO_{rlf} over a time span Δt or a fixed number of handover related events N_{hr_events}. It is a subset of N_{hr_events} and used as assessment criteria for the evaluation of the optimisation algorithms. N_{neg_events} is defined as:

$$N_{neg\_events} = N_{pp} + N_{fail} + N_{rlf} \tag{3.11}$$

Failure Events

The number of failure events N_{fail_events} terms the sum of handover failures HO_{fail} and radio-link failures HO_{rlf} over a time span Δt or a fixed number of handover related events N_{hr_events}. It is a subset of N_{hr_events} and used as assessment criteria for the evaluation of the optimisation algorithms. N_{fail_events} is defined as:

$$N_{fail\_events} = N_{fail} + N_{rlf} \tag{3.12}$$

For clarification the different sets of HPIs are visualised in Figure 3.4.

Handover Success Ratio

The handover success ratio is the ratio of the number of successful handovers N_{succ} to the number of handover related events N_{hr_events}. As introduced before N_{succ} and N_{hr_events} are calculated over a time span Δt or a fixed number of handover related events N_{hr_events}. The handover success ratio is one of the key HPIs and will further be labelled HPI_{succ}, i.e. HPI successful handovers. HPI_{succ} is defined as:

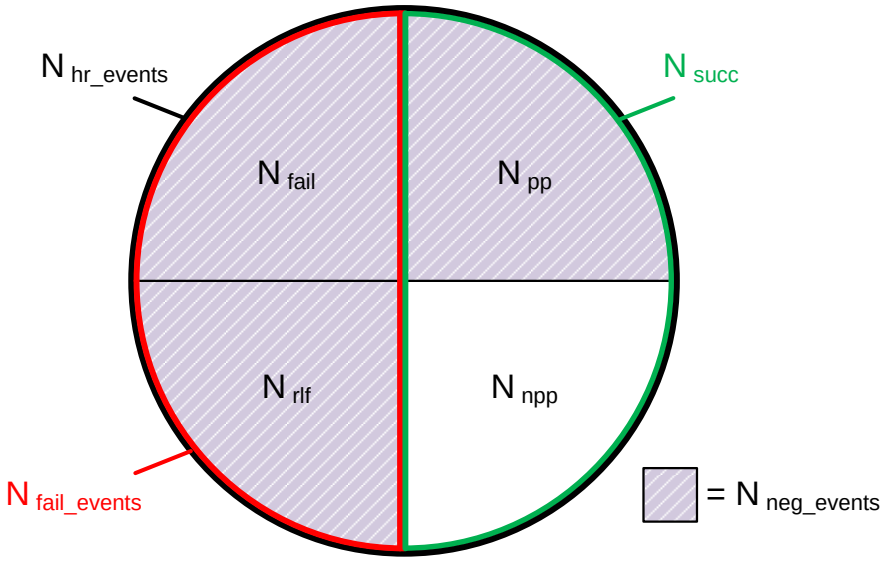

Figure 3.4: Different sets of Handover Performance Indicators introduced in this section

$$HPI_{succ} = \frac{N_{succ}}{N_{hr\_events}} \tag{3.13}$$

Ping-Pong Handover Ratio

The ping-pong handover ratio is the ratio of the number of ping-pong handovers N_{pp} to the number of handover related events N_{hr_events}. As introduced before N_{pp} and N_{hr_events} are calculated over a time span Δt or a fixed number of handover related events N_{hr_events}. The ping-pong handover ratio is one of the key HPIs and will further be labelled HPI_{pp}, i.e. HPI ping-pong handovers. HPI_{pp} is defined as:

$$HPI_{pp} = \frac{N_{pp}}{N_{hr\_events}} \tag{3.14}$$

Handover Failure Ratio

The handover failure ratio is the ratio of the number of handover failures N_{fail} to the number of handover related events N_{hr_events}. As introduced before, N_{fail} and N_{hr_events} are calculated over a time span Δt or a fixed number of handover related events N_{hr_events}. The handover failure ratio is one of the key HPIs and will further be labelled HPI_{fail}, i.e. HPI handovers failures. HPI_{fail} is defined as:

$$HPI_{fail} = \frac{N_{fail}}{N_{hr\_events}} \tag{3.15}$$

Radio-Link Failure Ratio

The radio-link failure ratio is the ratio of the number of radio-link failures N_{rlf} to the number of handover related events N_{hr_events}. As introduced before, N_{rlf} and N_{hr_events} are calculated over a time span Δt or a fixed number of handover related events N_{hr_events}. The radio-link failure ratio is one of the key HPIs and will further be labelled HPI_{rlf}, i.e. HPI radio-link failure. HPI_{rlf} is defined as:

$$HPI_{rlf} = \frac{N_{rlf}}{N_{hr\_events}} \tag{3.16}$$

Failure Event Ratio

The failure event ratio HPI_{fail_event} is the ratio of the number of radio-link failures N_{rlf} and the ratio of the number of handover failures N_{fail} to the number of handover related events N_{hr_events}. As introduced before, N_{rlf}, N_{fail} and N_{hr_events} are calculated over a time span Δt or a fixed number of handover related events N_{hr_events}. HPI_{fail_event} is defined as:

$$HPI_{fail\_event} = \frac{N_{rlf} + N_{fail}}{N_{hr\_events}} \tag{3.17}$$

3.4 Additional Mobility Related Measurements

In this section further LTE measurements or information exchange related to user mobility is described.

Load Reporting

The load reporting function specified in [3GPP13a, P. 179] enables neighbouring cells to exchange load information. In the intra-RAT case the information is exchanged via the X2-Interface (X2) and in the inter-RAT case via the S1-Interface (S1). The load information consists of:

- Radio Resource Usage
  - Total Physical Resource Block (PRB) usage
  - Guaranteed Bit Rate (GBR) PRB usage
  - Non-GBR PRB usage

- Hardware (HW) Load (low, mid, high, overload)
- Transport Network Layer (TNL) Load (low, mid, high, overload)
- Capacity value (available capacity for load balancing as percentage of total cell capacity)
- (Optionally) Cell Capacity Class value (relative capacity indicator)

The load information is reported for the Uplink (UL) and Downlink (DL) in any of the cases. The load information radio resource usage is further specified in [3GPP12b, P. 6] as:

$$M(T) = \lfloor \frac{M1(T)}{P(T)} \times 100 \rfloor \tag{3.18}$$

with $M(T)$ as the total PRB usage in percent of PRBs in use averaged over the measurement time period T, $M1(T)$ as the count of full PRBs, $P(T)$ as the total number of PRBs available during time period T. It is left up to the hardware manufacturers to define $P(T)$, i.e. which resources are defined as available in a cell.
If an eNB desires load reporting from any neighbour cell, the reporting needs to be initiated from the eNB by the "Resource Status Reporting Initiation" defined in [3GPP14g, P. 26]. The reporting period is defined in [3GPP14g, P. 44] as "Reporting Periodicity" and can take values from the open interval $[1000\,\text{ms}, 2000\,\text{ms}, 5000\,\text{ms}, 10000\,\text{ms}, ...)$.
Initially load reporting was introduced in LTE as support for the load balancing functionality that bases on three main elements, i.e. load reporting, load balancing action and amending handovers [Holma11, P. 245]. Nevertheless, the load information can be used to support other SON functions as well and might be helpful for the optimisation of the handover control parameters. A limiting factor for the load reporting function is the "processing resources available in the eNB for performance measurement and statistical tasks" [Kreher10, Section 4.2.3]. As this statement is from the year 2010 and the eNBs are further developed to support a variety of SON functions, the processing power should be adapted by the hardware manufacturers, if it is shown that the gain by SON functions using the load indicator is high. Thus, and because of the fact that LTE hardware is not available for measurements in this dissertation, we will neglect the limitations and assume that the load reporting works as standardized.

Chapter 4

Research Activities in Handover Optimisation

4.1 State of the Art

The optimisation of the handover performance by adaptation of the handover control parameters is not solely investigated in LTE. In [Flanagan02], [Werner07] and [Tseng10] the authors introduce optimisation algorithms for Wideband Code Division Multiple Access (WCDMA) systems. In WCDMA the handover control parameters are very similar to the LTE parameters. Thus the algorithms can be adapted to LTE.
In [Dimou09] and [Legg10] the authors analyse the handover behaviour in LTE. The handover metrics (performance indicators) are introduced and simulations on the impact of the UE speed on the handover delay are performed [Dimou09]. The result is that even for high speed users (up to 200 km/h), the handover delay is smaller than 100 ms. The impact of the user speed on the handover failure rate is evaluated in [Legg10]. The authors identify the interrelation of the handover failures in the case of too late handovers and the ping-pong handovers in the case of too early handovers. An analysis on the handover behaviour with different speed classes and variation of the handover parameter settings is given in [Zetterberg13]. The results show that the development of the handover failures caused by too early handovers, too late handovers and handovers to the wrong cell correspond to the overall handover failure and ping-pong handover development. This means that the number of handover failures caused by too early handovers or handovers to the wrong cell decreases for higher HYS and TTT settings similar to the behaviour of ping-pong handovers. Handover failures caused by too late handover triggering increase with higher handover control parameter settings which is the same behaviour observed for the overall number of handover failures. The authors

of [Lee10] examine the impact of TTT changes on the handover performance and take different user speed classes into account as well. The observed effects are similar to the findings in the other papers.

A successive optimisation of the handover control parameters is suggested by the authors of [Schröder08]. Their algorithms base on the optimisation algorithm developed for WCDMA in [Flanagan02] which is a control theory based approach. The authors identified an impact of the optimisation activities on the performance of the neighbouring cells. The optimisation algorithm presented in [Jansen11] was developed in the SOCRATES project [SOCRATES08]. The basis for the evaluation of the current handover performance is a weighted sum of the handover indicators ping-pong handover ratio, handover failure ratio and radio-link failure ratio. In the optimisation the adaptation of the HYS or TTT is alternated and the performance is compared to the last settings. In the case of a performance improvement the optimisation is continued in the same direction. Otherwise the optimisation direction (increasing or decreasing the handover control parameters) is changed. A similar definition of the weighting function for the handover performance indicators as in [Jansen11] is selected for the handover optimisation algorithm in [Mwanje12]. The algorithm evaluates the handover performance for a given handover parameter settings and adapts one handover control parameter, i.e. the TTT or HYS. By comparing the performance for changes of one handover control parameter the best performing operating point for this parameter is identified. The optimisation algorithm then switches to the optimisation of the second control parameter. In [Kitagawa11] an optimisation algorithm based the observed handover related event categories (too early, too late, HO to wrong cell, ping-pong handover) is suggested. If the handover events for a certain category cross a pre-defined threshold, a fixed set of rules defines how the handover control parameters are adapted.

Successive optimisation of the cell handover control parameters and the cell-pair individual offsets is suggested by the authors of [Ewe11]. In a first step the TTT and HYS are optimized by comparison of the handover performance with "neighbouring" handover operating points. This contains all combinations of one step lower and higher control parameter settings. For every performance evaluation 1000 handover events are observed. The evaluation of the performance bases on a weighted sum of the handover performance indicators as in [Jansen11]. In a second step the cell individual offsets are tuned if 1000 handover events per cell-pair are available. The simulation scenario bases on OpenStreetMap (OSM) data and users with different speed classes are considered.

A handover optimisation algorithm based on control theory is proposed in [Beletchi13].

The algorithm uses the weighted handover performance function and handover performance indicators defined in [Jansen11]. The controller uses the relative number of ping-pong handover events and failure events as feedback information. The handover performance of neighbouring handover operating points is evaluated and fed into a gradient approximation function. Based on this evaluation the next handover operating point is selected. The authors in [Buenestado13] use a fuzzy logic controller to optimize the handover performance. The most important parameters for this algorithm are the fuzzy logic controller rules derived form observations in earlier simulations. As input parameters the number of handovers and the radio-link failure ratio are considered. The algorithm adapts the handover control parameters in two increments (small or large) to allow fast adaptation of the parameters. A similar approach based on a fuzzy logic controller from the same department is one of the main topics in the doctoral thesis [Luengo14].

The authors of [Mwanje14] propose an optimisation dedicated to a variety of UE speed classes based on a Q-learning algorithm. The requirement is that the user speed is known or can be measured by the network. The idea is that the optimisation can be accelerated by a joint optimisation of a single Q-Table from the handover activities of several cells.

The handover oscillation algorithm described in [Bergman12] is evaluated using field trials in an LTE network. The drawback is that the interference in the network was low due to a low user density. The authors show that the ping-pong handover ratio can be reduced significantly by the introduction of additional constraints after a cell change. The handover margin is increased for handover requests of users that changed the connected cell within a defined time span. Unfortunately the impact on the radio-link failure ratio could only be estimated for low load in the network. The optimisation algorithm introduced in [Khan14] aims at the reduction of ping-pong handover only. The algorithm follows the concept of the algorithm in [Jansen11] and uses the same weighted handover performance function. The difference is that the authors suggest a linear or exponential averaging of the handover performance indicators over longer time frames as basis for the optimisation decision. This will significantly delay the handover optimisation.

An optimisation algorithm dedicated to the cell individual offsets defined for every cell-pair is described in [Watanabe13]. Based on the analysis of the ping-pong handover rate and the handover failure rate and the comparison with target performance levels and maximum performance levels the cell individual offsets are adapted. The optimisation assumption is that increasing the offsets reduces the ping-pong handovers and vice versa.

The authors in [Viering11] analyse the impact of the user mobility modelling on the handover performance indicators. They discover that it is important to model the user mobility with respect to the street and side-way paths. User mobility concentrates on streets and side-ways since the movement of the users is aim-oriented. Thus the developing of the signal quality of the strongest cells in these positions is more important than in locations with lower user density. The authors analyse how fast the signal quality changes at the cell border and evaluated the signal strength difference between the strongest and second strongest cell. The outcome is that in some locations on the border of two cells the signal degradation is steep and in others flat. Thus the user path selection has a major impact on the handover performance in the network.

Inter-RAT handover control parameter optimisation is a hot topic in the recent past as well. Several algorithms have been suggested in [Awada11], [Awada13], [Song09] and the doctoral thesis [Awada14].

Research on automatic (self-)optimisation has been a topic in international research projects for several years and is still covered by running projects. The GANDALF project (2005-2007) [GANDALF05] investigated automatic optimisation in Global System for Mobile Communications (GSM), General Packet Radio Service (GPRS), Universal Mobile Telecommunications System (UMTS) and Wireless Local Area Network (WLAN). The End-to-End Efficiency (E3) project (2008-2009) [E308] was dedicated to improve the efficiency of the system management and introduced self-organization capabilities into the LTE architecture. The SOCRATES project (2008-2011) [SOCRATES08] [Kürner11] [Jansen09] focussed on self-organization functions for LTE, i.e. self-configuration, self-optimisation and self-healing capability, and developed a variety of optimisation algorithms. One use case was dedicated to the optimisation of the handover performance. The optimisation algorithm developed in this project is part of this thesis. The Self-Management for Unified Heterogeneous radio Access Networks (SEMAFOUR) project (2012-2015) [SEMAFOUR12] is the follow-up project of the SOCRATES project and aims at the development of a unified solution for an integrated SON management. The project considers different radio access technologies and network layers and develops new concepts, methods and algorithms for a selected set of SON functions.

4.2 Open Issues

In this section the state of the art in research on handover optimisation is analysed and uncovered research topics are identified. The research topics, uncovered at the beginning

of the research for this thesis or still uncovered, are listed below and will be the central topics for this work on handover optimisation in LTE.

1. For the evaluation of the handover performance, "stable" network conditions are assumed by many designers of handover optimisation algorithms. Nevertheless, it is unclear what "stable" conditions in the context of the evaluation of the handover performance means. Thus, we discuss the "influencing factors" on the evaluation of the handover performance and analyse the impact of load changes in the network. (Addressed in Section 6.1 and 6.4)

2. State of the art handover optimisation algorithms base on the same handover performance indicators, namely the ping-pong handovers, the handover failures and radio-link failures. In some cases the failure events are subdivided into the classes too early handover, too late handover and handover to a wrong cell. Nevertheless, previous research on handover optimisation lacks a detailed analysis of the interaction of the handover performance indicators, i.e. the impact of different handover parameter configurations on the shift between the negative handover events. (Addressed in Section 6.2)

3. In many optimisation approaches a weighted sum of the handover performance indicators is used as target function. In most cases the simulation results are given for only one set of weighting parameters in the publications. Thus, the influence of weighting parameter changes and the possibilities for manipulation of the optimisation target by the network operators is not analysed so far. (Addressed in Section 6.3)

4. The performance of the developed optimisation algorithms is usually evaluated in one simulation environment by the researchers. Therefore it is still unclear how the simulation assumptions and environment influences the simulation results and performance evaluation of the optimisation approaches. The analysis in [Viering11] shows that detailed modelling of the user mobility is necessary for research in the area of handover optimisation. Therefore, we investigate the handover performance in two simulation environments and compare the behaviour of the target function for different weighting parameter settings. (Addressed in Section 6.3)

5. The evaluation of the performance gain, using a specific optimisation algorithm, usually bases on the performance comparison of a fixed handover control parameter setting in the complete network and the suggested optimisation algorithm. In

some cases the results of other optimisation approaches are compared as well. The recent research lacks an examination of the possible "best" handover performance in the network and the question how close the suggested algorithms get. In this dissertation the "best" fixed handover configuration is evaluated by system-level simulations and used as assessment criteria for the optimisation algorithms in Chapter 7.

6. The observation cycle for the evaluation of the current handover performance is one of the key parameters in handover optimisation. It influences the optimisation speed and the reliability of the optimisation actions. The identification of the optimal window size and the question whether the window should be defined in the time or event domain is not investigated up to the present. (Addressed in Section 6.6 and 6.7)

7. The handover optimisation algorithms developed and suggested so far lack the ability to estimate the handover performance for other handover configurations. The result for the optimisation decisions is to select handover configurations with small parameter variations in promising direction. The analysis of the handover performance for different handover control parameter settings in this work shows that even the performance degradation for small control parameter changes can be severe (Section 6.2). The acceptance to rely on automatic tuning of the handover control parameters by the operators will be low for algorithms that might temporarily worsen the network performance. Thus, we develop an optimisation concept that allows the selection of handover configurations based on estimated handover performance. (Addressed in Chapter 7)

8. Changing the handover configuration in a cell can impact the handover performance of adjacent cells, which complicates the evaluation of the optimisation actions in the cells. This impact has not been quantified by the research community so far. In this work we will analyse the interaction of handover configuration changes on the handover performance in the cells. This interaction and the global handover performance are important assessment criteria for the evaluation of the optimisation success. (Addressed in Section 7.2)

Chapter 5

The Simulation Environment

The main objective for the development of the simulation environment for this work is to emulate the user network experience to evaluate the performance of the suggested handover optimisation algorithms. State-of-the-art system-level simulations for mobile communication networks base on hexagonal network layouts, empiric propagation models and random walk models for the user mobility. The reasons to select these models range from low computation times, easy implementation in simulation environments to sufficient quality of the simulation results to justify further extensive research. In this work new simulation approaches based on realistic network layouts, a ray-tracing propagation model and realistic user mobility models are conducted. The aim of these is to evaluate whether more realistic modelling of the simulation environment changes the simulation results and thus impacts the development of the optimisation algorithms. Hence, two simulation scenarios with different levels of detail in the selected simulation models are prepared and selected for this work.
In this chapter the data sources for the used models are presented in Section 5.1. The simulation models are described in detail in Section 5.2. The in-house developed database and simulation tool SIMONE is introduced in Section 5.3. Section 5.4 gives an overview of the used simulation scenarios.

5.1 Geodetic Data

Geodetic data is the most important basis for the generation of a realistic simulation environment since the objective is to model the reality. In this section the data sources and usage are described in detail. The presented simulation environment partially bases on freely available data sources. In recent years, the dedication of free cartographers lead to a large pool of detailed freely available open source data bases of geodetic data.

This geodetic information eases the compilation of simulation scenarios and allows a high level of detail in the system simulations as well.

5.1.1 Building Shapes of the City of Hanover

The building shapes originate from commercially available data, i.e. shape files with Two Dimensional (2D) building shapes and height information for the buildings. We refer to the combination of a 2D building shape and height information as 2.5D building information as only one height information is available per building part. As a result, all buildings have flat roofs in the simulation environment, which is not realistic since the majority of the buildings in the city of Hanover have pitched roofs. Nevertheless, the buildings' dimensions deliver important information used in the modelling of the simulation environment and the generation of simulation models. The available data comprises of 74058 building parts in an area of 192 km^2.

Figure 5.1 shows a cut-out of the building shapes in the city of Hanover. The building shapes are used for ray-optical pathloss predictions, the generation of indoor mobility and the pedestrian and bicycle mobility model.

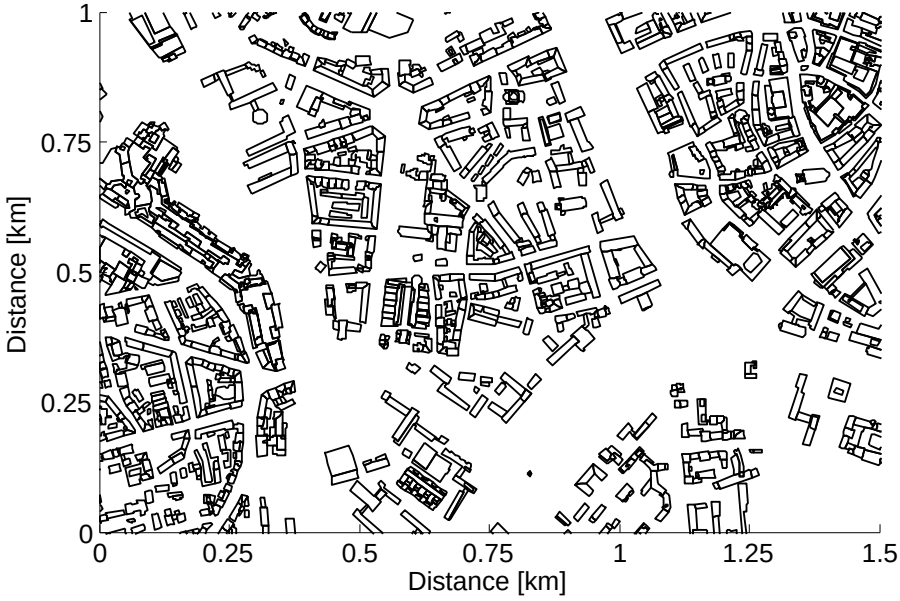

Figure 5.1: Cut-out of the 2D building shapes in the city of Hanover

5.1.2 Geodetic Data from the OpenStreetMap Project

OpenStreetMap (OSM) is a worldwide project aiming at the generation of a freely available geodetic map of the world [OSM14a]. The project started in the year 2004 and relies on free cartographers that add geodetic data to the project maps. In the last ten years the amount and granularity of the data increased rapidly. Besides streets, building shapes, railway tracks, park areas, rivers and seas the database nowadays includes restaurants, bars, right of way rules, traffic lights, park paths, traffic signs and in some areas even single trees. It is the declared goal of the project to ease research and teaching by freely providing the data [e.V.14]. Moreover everybody can join the project and add or change the data.
All OSM maps consist of a limited number of basic elements, i.e. *nodes*, *ways*, *relations* and *tags*. The fifth basic element, named *area*, is a special form of the element *way* since it is a closed *way* with special *tags*. *Nodes* describe points of interest in a map. Line elements like streets, rivers, borders, etc. are marked by *ways*. *Areas* describe forests, buildings, lakes, etc. *Relations* allow to connect basic elements and *tags* add information about the element. This means that besides the geodetic information on the location of the object the most important information is stored in the *tags* associated with the element. *Tags* allow detailed descriptions of the geodetic objects and enable manifold fields of application for the maps. The following data has been extracted from the OSM data base as geodetic source data for the compilation of the simulation environment:

- Street vectors
- Number of lanes per driving direction
- Position of traffic lights
- One-way roads
- Course of rivers
- Dimension of lakes
- Building areas (Residential, Commercial, Public, ...)
- Land-use information

The street vectors are used for the vehicular, pedestrian and bicycle mobility models as well as the land-use maps. The number of lanes, position of traffic lights and one-way

roads are necessary input data for the vehicular mobility model whereas the course of rivers, dimension of lakes and building information are needed to generate the pedestrian and bicycle mobility. The land-use maps are used in this work to visualize the simulation scenario, but could be used as data source for other models (propagation models) as well. An application of the OSM data in the area of channel modelling for vehicular to vehicular or infrastructure communication is given in [Nuckelt13].
To extract the data from the OSM database the desired information needs to be filtered. For this purpose a variety of open source tools is available [OSM14b]. Nevertheless, we implemented an own data converter to serve the needs of our simulation environment. The OSM shapes are stored in World Geodetic System 1984 (WGS84) format which can be transferred in every desired geodetic data format. More details on the used data formats can be found in Section 5.3.

5.1.3 Land-Use Maps

The land-use maps are generated from the OSM maps introduced in the last section. The elements of the OSM maps are described by tags which assign them to a group of map elements. A tag consists of a *key* and a *value*, e.g. the *key* is 'waterway' and a corresponding *value* is 'riverbank' or the *key* is 'leisure' and the corresponding *value* is 'garden'. The OSM project provides a long list of more than 1000 tags on their wiki page [OSM14b]. It is recommended to use existing tags to extend the maps to ease the usability of the data for other users. Nevertheless, it is possible to create own tags for every user.
For the generation of the land-use maps the most important and commonly used tags

Value	Land-Use Class	Value	Land-Use Class
1	Undefined	7	Commercial
2	Sealed Surface	8	Industrial
3	Roads	9	Wasteland
4	Railway Track	10	Forest
5	Small Building	11	Green Space
6	Building	12	Water

Table 5.1: List of Land-Use Classes

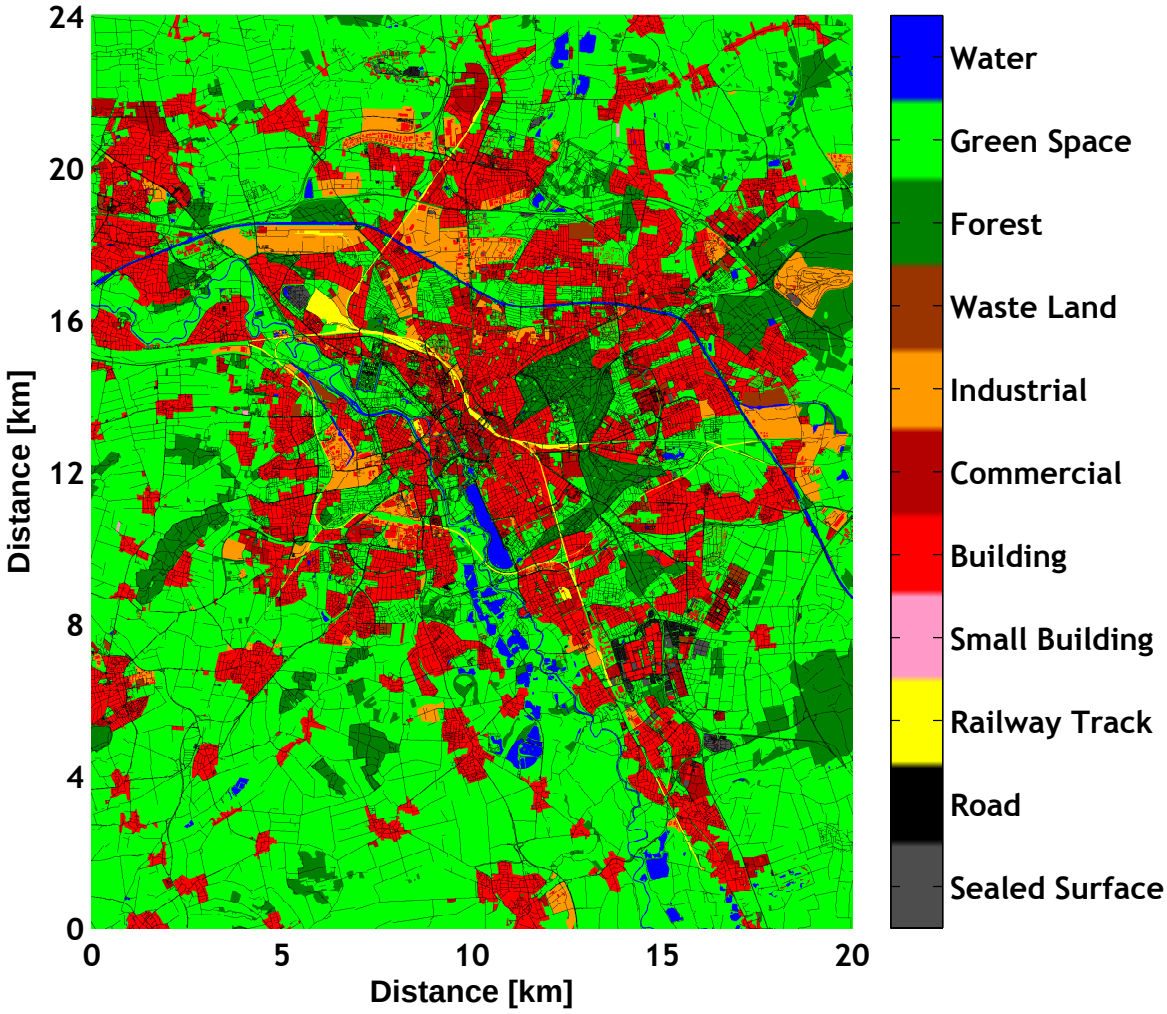

Figure 5.2: Land-use map of Hanover generated from the OSM database

have been taken into account and converted to the 12 land-use classes listed in Table 5.1. In the process the individual tags (more than 1000) have been linked to the best fitting land-use class. The resulting land-use map is shown in Figure 5.2. Since the geodetic information is modified by many cartographers, the OSM data base contains different tag versions describing the same element group and sometimes contradictory information for the same element. To handle these variations, priorities are defined to allow the generation of the land-use map.

5.2 Modelling the Wireless Communication System

In this section the models used in the system-level simulations are described in detail. In Section 5.2.1 the propagation models are described. Section 5.2.2 introduces the user mobility models followed by the description of the shadow fading model in Section 5.2.1. Subsequently the user data traffic model is addressed in Section 5.2.3. The calculation methods for the user SINR and cell load are given in Sections 5.2.4 and 5.2.5 respectively.

5.2.1 Propagation Models

In this section the propagation models used for the compilation of the two simulation scenarios are described. An empirical propagation model is used for the reference simulation scenario which is a state of the art scenario suggested by 3GPP. The availability of building shapes (2.5D building information) enables the application of a ray-optical pathloss predictor for the second simulation scenario, which is an in-house development used for the prediction of the signal propagation in a variety of research projects. While empirical models are easy to implement and have a low computation time for large scale simulations, the ray-optical model incorporates a higher level of detail of the environment. The pros and cons of the models in the context of system-level simulations for handover optimisation algorithms will be discussed in the results section of this work. More details on empirical, semi-empirical and ray-optical prediction models can be found in [Kürner12] and [Lostanlen12].

Ray-Optical Propagation Model

The ray-tracer, i.e. the central part of the ray-optical propagation model, searches the paths between the transmitter and receiver antenna in the simulation environment. The model is used for the predictions of the outdoor coverage in the Hanover scenario. Since the computation time for the model is high, the pathloss is predicted for a fixed raster of 10 m by 10 m in the simulation scenario. The model follows the concept of subdividing the contributions to the signal strength on the receiver side in sub-models as described in [Kürner99] and [Kürner02]. The ray tracer uses two sub-models, i.e. a Vertical Plane Model (VPM) and a Multi-Path Model (MPM).
The VPM differentiates between the Line-of-Sight (LOS) and the Non-Line-of-Sight (NLOS) case:

- In the LOS case the pathloss is calculated according to the distance of the re-

ceiver from the transmitter. Up to 200 m distance the free-space propagation loss is assumed, above 500 m distance the Okumura-Hata model with sub-urban correction factor is used and between 200 m and 500 m a transition model is applied. [Rose12b]

- In the NLOS case the direct path is replaced by a path over the roof-tops of the buildings. The total pathloss is then calculated as sum of the distance dependent pathloss taken from the LOS case and an additional diffraction component pathloss calculated with the Deygout model [Deygout66].

The MPM follows the approach described in [Kürner10] and incorporates the following type of paths:

- Reflections on the surfaces of the buildings are considered up to the second order, i.e. paths from the transmitter to the receiver are reflected on two building surfaces. Including third or fourth order reflections significantly increases the amount of paths and the computation time for the pathloss prediction and has limited impact on the final signal strength because of the attenuation on the wall. The maximum image source distance [Lostanlen12] is set to a value of 1000 m (see [Kürner02] for more details).

- Scattering on the building surfaces is included for a maximum distance of 500 m between the transmitter and receiver. According to the findings in [Kürner02] building surfaces up to a distance of 550 m around the base station are checked as potential scattering obstacles.

To calculate the signal strength of the different cells in a location (point raster), a masking process is started after the individual paths are found. In the masking process the transmit power of the cells and Three Dimensional (3D) antenna diagrams are taken into account to calculate the power contribution of the paths. The final signal strength is derived from the sum of the complex signal power contributions of the paths, i.e. the angular phase shift (depending on the delay) of the paths is taken into account, weighted with the antenna pattern.

3GPP Macro-Cell Model

The 3GPP propagation model belongs to a macro-cell simulation scenario specified by 3GPP in different standard documents. The model consists of a distance dependant

loss model, a vertical and horizontal antenna model and a penetration loss for indoor users. The distant dependant loss model is taken from [3GPP12c, Section 4.5.2] and is optimized for urban areas:

$$L = 128.1 + 37.6 \log_{10}(R) \tag{5.1}$$

where R is the separation between the base station and the UE in kilometres. The propagation model assumes a carrier frequency of 2000 MHz and a base station height of 15 m above the average rooftop level.

The antenna model is split in three parts, i.e. the vertical and horizontal antenna pattern and a combining method. The model is described in [3GPP10, Table A.2.1.1-2]. The formula for the vertical antenna pattern is:

$$A_v(\Theta) = -min\left[12 \cdot \left(\frac{\Theta - \Theta_{etilt}}{10}\right)^2, 20\right] \tag{5.2}$$

The horizontal antenna model is given by:

$$A_h(\varphi) = -min\left[12 \cdot \left(\frac{\varphi}{70}\right)^2, 25\right] \tag{5.3}$$

The combining method into a 3D antenna pattern is calculated as:

$$A(\varphi, \Theta) = -min\left[-(A_v(\Theta) + A_h(\varphi)), 25\right] \tag{5.4}$$

The remaining simulation parameters like indoor pathloss, inter-cell distance, carrier frequency and system bandwidth are given in [3GPP10, Table A.2.1.1-1] and will be listed in Section 5.4.

Outdoor-to-Indoor Propagation Model

The used outdoor-to-indoor propagation model is an in-house development. The model calculates the indoor propagation based on the existing outdoor predictions around the buildings. In addition the story height, the distance to the nearest outdoor point that has a signal strength prediction and the indoor environment are taken into account. For more details see [Rose12a].

Shadow Fading Maps

The shadow fading maps are used in combination with the ray-optical propagation model or the 3GPP propagation model. As mentioned before, the ray-tracer has the disadvantage of long computation times for the signal propagation. This is why the resolution of the ray-tracer predictions are limited to 10 m by 10 m in the considered scenario. The shadow fading maps have a resolution of 1 m by 1 m, a zero mean, a Standard Deviation (STD) of 3 dB and assure signal variation in a finer grid compared to the resolution of the ray-optical model. Moreover, buildings are the only shadow fading obstacles considered in the ray-tracer. The fading effects on other obstacles like cars, humans or vegetation are neglected. This is compensated by the use of the shadow fading maps as well. The 3GPP model does not include shadow fading by definition. Thus, we use shadow fading maps with a resolution of 1 m by 1 m, a zero mean but a STD of 9 dB for the empiric propagation model in this case based on the same shadow fading model described below. The correlation distance is 50 m.

Figure 5.3 shows a fading map generated with the model. The fading map has a zero mean and a STD of 9 dB. The figure shows that the signal fading is correlated in x- and

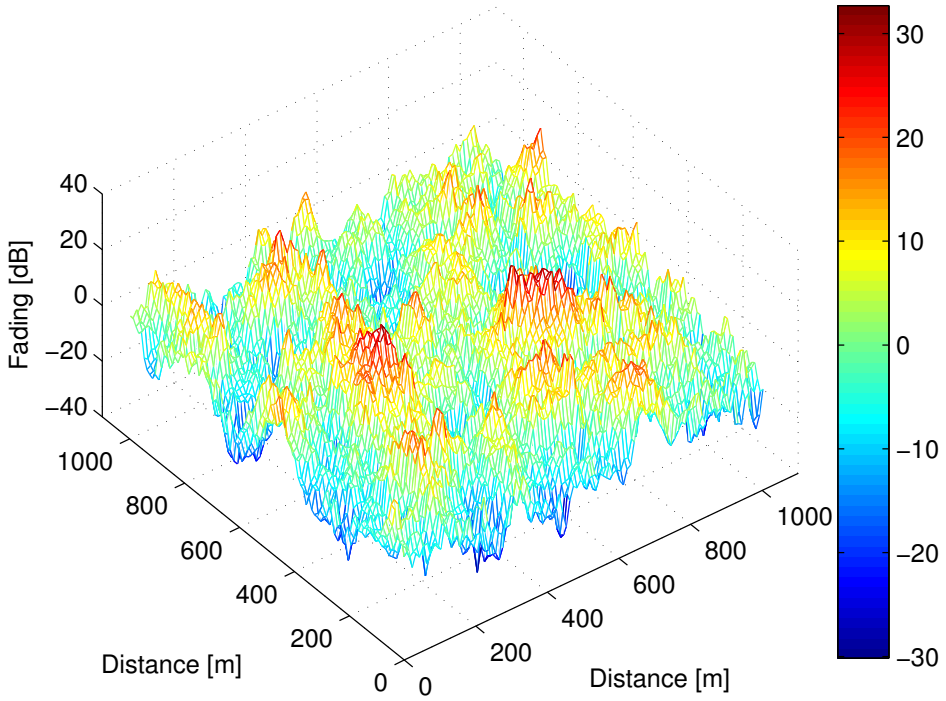

Figure 5.3: Shadow fading map with cross-correlation in x- and y-direction

y-dimension, i.e. cross-correlated in two dimensions. This means that a user that moves through the simulation environment experiences continuous signal variation without frequent signal jumps. If a base station serves more than one sector with identical antenna position, the same fading map is used for every antenna, i.e. the correlation factor between the sectors of one site is 1. The correlation between signals that arrive at a UE position from similar direction but from different antennas and base stations is not included in this model.

The first step in the generation process of the cross-correlated fading maps is the generation of correlated fading vectors along one axis. The vectors are generated using the Autoregressive Moving Average (ARMA) model. In the second step the vectors with correlation in one direction are correlated in the second dimension using the Cholesky decomposition and the covariance matrix. To ensure that the Cholesky decomposition works the covariance matrix must be positive definite. Since this is usually not the case the covariance matrix is changed using the alternating projection method to find a similar matrix that is positive definite. This matrix is used to compute the shadow fading maps. More details on this model can be found in [Monserrat07] and [Monserrat08].

5.2.2 User Mobility Models

The user mobility has a major impact on the network performance and consequently on the user network experience and satisfaction. The same amount of users located at the cell edge or at the cell centre of the base stations can lead to significant differences in service quality if the total user traffic demand is high. Moreover, the user movement permanently changes the reception quality of the UEs and thus changes the resource consumption of the UE. This leads to changes in the interference situation for all users, i.e. mobile and static, in a network. This shows that user mobility and the impact on the network performance or stochastic emulation of the user impact on the network performance is important in system-level simulations.

The simulation environment is designed to enable system-level simulations in the area of handover optimisation, i.e. the used models are selected with the objective to introduce a higher level of detail in the parts important for the handover behaviour. Since handovers are initiated when users leave a cell area and enter a neighbouring cell the user mobility is even more important in these system simulations. That is why a variety of user mobility models has been designed at the Institut fÃ¼r Nachrichtentechnik and selected for this work. The different mobility models are described below.

Indoor Mobility Model

The indoor mobility model was designed in a master thesis [Hahn12] that contains the creation of indoor building layouts, i.e. modelling multi-storey buildings [Rose14], the placing of walls [Hahn14], windows and doors and the logical definition of room roles like living-room, corridor, kitchen or bedroom and is published in [Rose13a]. Three building types are considered for the generation of the indoor layouts which are private apartments, office buildings and factory buildings. Based on the building types the indoor layout is generated and a set of rooms is defined as logical unit, i.e. private apartment in a multi-apartment building, office area of a company in a large office building, etc. The indoor layouts, logical room roles and logical units are then used to create the indoor user mobility in the buildings. The building shapes described in Section 5.1.1 are used as outside boundary of the buildings for the generation process of the indoor layouts.

The mobility model includes several forms of user mobility, i.e. aim-oriented user movement and "spontaneous" user movement. In the case of planned movement the user selects a certain target location like the kitchen or the bedroom, moves to the target location following pre-defined routes and stays at the target location. In the second case of spontaneous movement the model defines four sub-models: perambulate mobility, round-trip mobility, permanent change of position in a room and in office buildings visiting a team mate in his office. The selection of the different mobility forms is de-

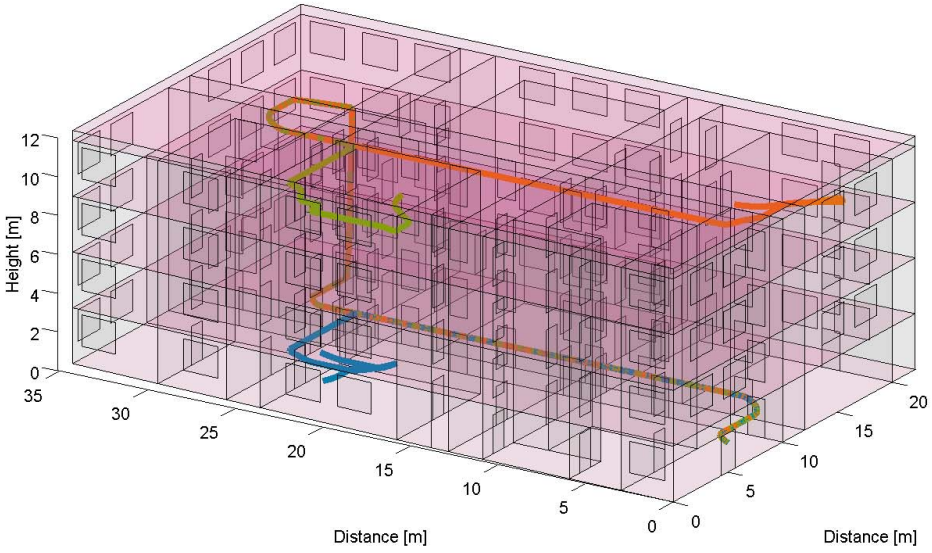

Figure 5.4: Indoor mobility model: User traces in a private apartment building

pendent on the building type and time of day. This means that for example some users will leave their private apartments in the morning or arrive at the office buildings. Some users stay in the apartment buildings and move between the rooms. The user speed is drawn from an equal distribution in the interval $[0.5, 2.5]\frac{m}{s}$ for every movement action. The model has been used in a variety of projects and is evaluated in [Rose13a].
Figure 5.4 shows three user mobility traces in a private apartment building. The users move inside their apartments in spontaneous movement before they leave the building. This user behaviour is typical in the morning hours when the people prepare to leave their homes to travel to their offices. The huge number of doors and windows illustrates the complexity of the used indoor building layouts.

Pedestrian and Bicycle Mobility Model

The pedestrian and bicycle mobility model was developed in a master thesis [Sulak12] as well. The model supports directed user mobility from a starting position to a target location. This means the user selects a movement target and travels along pre-defined routes towards the target location on the shortest path. The model is subdivided in mobility islands with inner user mobility and the connection network between the islands. An island is surrounded by streets and can include several buildings, areas with open space or a park area. Possible starting positions or target locations for the mobility are entrances of the buildings or locations in the park areas. The definition of the entrance locations can be handed over to the model in a file or is generated by the model based on the size of the buildings.
A mobility island is shown in Figure 5.5. Buildings are represented as yellow blocks in this case. The black, red and blue lines mark the routes a user can take to walk through the mobility island. The red crosses mark the entrances to the buildings. The outer black line marks the side-walk around the mobility island and is generated in the middle of the space between the buildings and the street. The inner black lines are generated using a Voronoi diagram to identify the routes in the middle of the space between the buildings. The red lines connect paths without any connection to the inner network on the shortest way to allow movement from one side of the path graph to the other. The blue lines connect the entrances of the buildings to the resulting path graph using the shortest path.
The connection path graph between the mobility islands is generated based on routes along the streets, rivers, lakes and other impassable obstacles. Open space and park areas are filled with side walks as well. To interconnect the routes of the connection

network cross-walks over the streets and bridges over the rivers are added at cross-ways or in random positions. In a final step the connection path graph and the mobility islands are connected in positions with short distance between the path graphs.
The generation of the users works as follows: Pedestrian and bicycle users are generated at a random starting position on the network and travel on the path graph to the target location with constant speed drawn form a user speed distribution based on the user type. For the pedestrian user a Gaussian distribution with a mean value of $1.3\,\frac{\mathrm{m}}{\mathrm{s}}$ and for the bicycle users a Gaussian distribution with a mean value of $4\,\frac{\mathrm{m}}{\mathrm{s}}$ is chosen. Starting in a mobility island the user moves to a connection point to the outer path graph, moves to the target mobility island on the shortest way and enters to target island to travel to the movement destination. After the user reached the target location he disappears from the mobility model.

Vehicular Mobility Model

The vehicular mobility model is based on a realistic vehicular mobility tool called Simulation of Urban MObility (SUMO). "SUMO is an open source, highly portable, microscopic and continuous road traffic simulation package designed to handle large road networks. It is mainly developed by employees of the Institute of Transportation Systems at the German Aerospace Center." [DLR14]

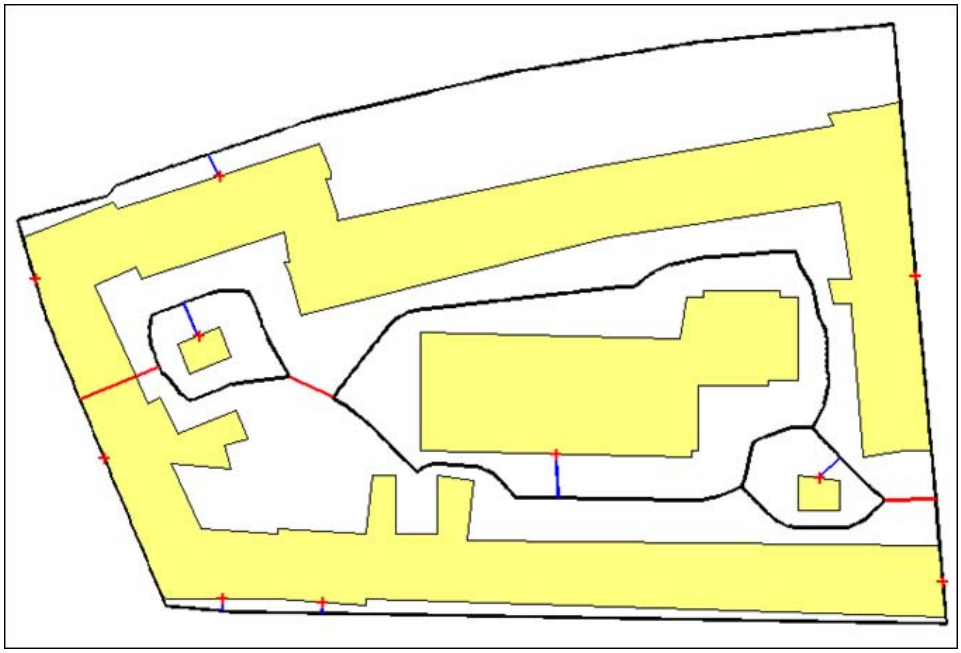

Figure 5.5: Path graph of the pedestrian and bicycle mobility model [Rose13b]

The road traffic simulator is used in a number of research projects dealing with vehicular communication, dynamic navigation or the evaluation of traffic surveillance systems [Krajzewicz12]. The simulation package includes a number of tools to generate or import road networks, define the vehicle movement flows, visualize the simulation results or to impact or to control the simulation on-line via different interfaces [Behrisch11]. One of the tools allows to import the road network from OSM which is one of the simulation data sources introduced before.

The level of detail supported by SUMO is high. The vehicles follow the street vectors on defined driving lanes. Vehicle lane changes, traffic light control, vehicle acceleration and braking, overtaking on the different lanes, queuing in front of traffic lights, and right-of-way rules are included. This leads to a realistic user behaviour and allows the simulation of the user network experience in a vehicle. The user speed is dependent on the maximum speed of the road the vehicle moves on. The maximum speed is extracted from OSM as well and imported to SUMO. In some areas of the road network in Hanover the maximum speed is limited to 30 $\frac{km}{h}$ (residential areas) in other areas the maximum speed is 50 $\frac{km}{h}$ (inner-city main roads). The vehicle interaction model used in SUMO allows the vehicles to exceed the maximum speed limit a little, i.e. real behaviour of car drivers is modelled.

A first implementation of the vehicular mobility model for system-level simulation of mobile communication networks has been done for the C3-World project [Schack12]. The mobility model has been designed in a diploma thesis [Jansen08] and used in the SOCRATES project [SOCRATES08] [Scully09]. The vehicular mobility area is limited to 1.5 km by 1.5 km in this model. The road network was generated based on data from a navigation system and the vehicle flows were calibrated by traffic counting in the real city of Braunschweig.

The limited simulation area and information on the road network necessitated a second implementation in a larger city. The new mobility model was designed in a diploma thesis [Baumgarten11] and is used in many research projects, e.g. the SEMAOUR project [SEMAFOUR12] which is the follow-up project of the SOCRATES project. The vehicular mobility area in this model is 5 km by 7 km large and is located in the city of Hanover in the north of Germany. The road network is based on OSM data and imported to SUMO and the vehicle flows are calibrated by traffic volume maps form the regional authorities in Hanover. The junction turning ratios for both implementations are set based on the mobility scenarios specified in the MOMENTUM project [MOMENTUM01] [Ferreira02]. Figure 5.6 shows a small part of the road network and

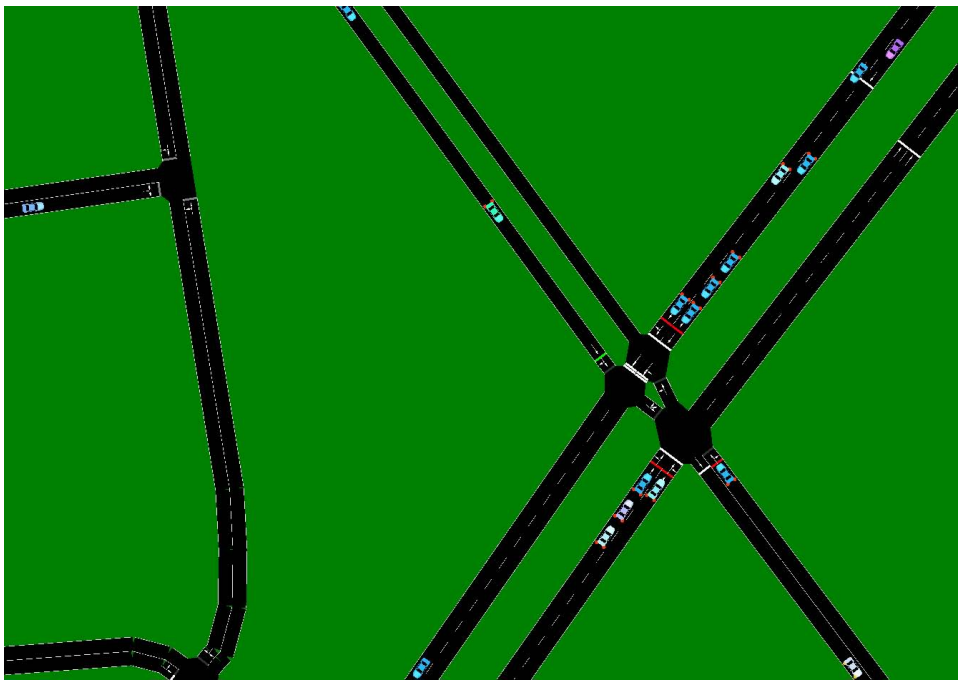

Figure 5.6: Road network and moving vehicles generated with the vehicular mobility model in Hanover [Jansen12]

some vehicles moving on the streets. The picture is generated with GUISIM - a visualization tool delivered with the SUMO package. The vehicles queue in front of the traffic light depicted as small red lines and overtake each other on the different lanes of a road.

Random-Walk Model

In the random walk model, the users move with a constant speed of 5 $\frac{km}{h}$, 15 $\frac{km}{h}$ or 50 $\frac{km}{h}$. The starting position of the users is randomly selected in the simulation area. The mobility traces are generated for a simulation step size of 100 ms. This means the moving direction of the users is randomly selected from 0 to 360 ° and the user moves along in this direction for 100 ms. Afterwards, a new moving direction is selected and the user moves in this direction for the next simulation step. If a user leaves the simulation area, he is not considered for the evaluations any more until he re-enters the scenario.

5.2.3 User Data Traffic Model

The user data traffic is realised as Constant Bit Rate (CBR) traffic varying from 16 $\frac{kbit}{s}$ to 512 $\frac{kbit}{s}$ for low, medium and high data traffic. “Low” data traffic (16 $\frac{kbit}{s}$) corresponds to a voice call, “medium” data traffic (100 - 128 $\frac{kbit}{s}$) to audio streaming and “high” data

traffic ($512\,\frac{kbit}{s}$) to video streaming. The implementation of more detailed user traffic models and the impact on the handover optimisation and system performance is not part of this thesis. Nevertheless, the variation of the user CBR traffic in combination with the detailed user mobility models presented in Section 5.2.2 leads to load variation in the cells and allows the evaluation of the handover optimisation algorithms in unstable load conditions.

The user data traffic model impacts the system performance since the data demand of the UEs defines the load of the serving cell. Furthermore, the cell load mainly influences the connection quality of the UEs since the higher the cell load the higher the interference from the corresponding cell. The simulation environment allows to influence the average cell load by a load multiplication factor that linearly increases the user data traffic demand. Thus it is possible to evaluate the developed algorithms in high and low load condition without loosing cell load variation over time.

5.2.4 Signal to Interference plus Noise Ratio

The SINR is calculated from the RSRPs of the serving cell and the n strongest interferes as:

$$SINR[dB] = RSRP_{Serv}[dBm] - 10\log_{10}((\sum_{int=1}^{n} L_{int} \cdot RSRP_{int}[mW]) + N_{therm}[mW]) \tag{5.5}$$

with L_{int} as the load factor of the interfering cell and N_{therm} as the thermal noise, which depends on the considered system bandwidth. The units foe the individual values are given in the brackets. The load factor L_{int} has a minimum value of 0.1 and can be set to a fixed value of 1 for full interference simulations, cell-wise to any value for static load scenarios or to the real cell load caused by the users currently connected to the cells.

5.2.5 Cell Load

The cell load is calculated based on the resource consumption of the UEs connected to the cell. In a first step the user throughput is calculated as:

$$Thr_{ue} = \begin{cases} 0 & \text{for } SINR_{ue} < SINR_{min} \\ \alpha \cdot \log_2(1 + SINR_{ue}) & \text{for } SINR_{min} <= SINR_{ue} <= SINR_{max} \\ Thr_{max} & \text{for } SINR_{ue} > SINR_{max} \end{cases} \quad (5.6)$$

with $\alpha = 0.6$, $SINR_{min} = -6.5\,\text{dB}$, $SINR_{max} = 22.05\,\text{dB}$ and $Thr_{max} = 4.4\,\frac{\frac{\text{bit}}{\text{s}}}{\text{Hz}}$. This equation is known as the Shannon approximation or truncated Shannon and standardized in [3GPP12c, Chapter A2]. The values are taken from the same standard document as well and adapted to the simulation assumptions.
The resource consumption R_{ue} of one UE has the measurement unit Hz and is computed as:

$$R_{ue} = \frac{CBR_{ue}}{Thr_{ue}} \quad (5.7)$$

with the user data demand CBR_{ue} realised as CBR traffic as introduced before and the user throughput Thr_{ue}. The cell load L_{cell} is then calculated as:

$$L_{cell} = \frac{\sum_{ue=1}^{k} R_{ue}}{BW_{cell}} \quad (5.8)$$

with BW_{cell} as the frequency bandwidth allocated to the cell. The resource consumption of all users connected to the cell is taken into account. The cell load is limited to a value of 1 in the system-level simulations. The cell load is used for the calculation of the SINR. The SINR is needed to calculate the resource consumption which results in the cell load and the cell load is needed to calculate the SINR in the case that the real load values are considered. In this case the SINR and cell load values are calculated in a loop until the variation of the values between two calculation steps is small enough. The maximum load variation is set to 0.01 % in the simulations. If the cell load and SINR calculation needs more than 30 iterations, the calculation is terminated and the mean load of the last 10 iterations is selected as the cell load and used for a final SINR calculation.

5.3 SIMONE - SImulation of MObile NEtworks

SIMONE is an in-house developed simulation environment that can be accessed either directly or via a web interface. SIMONE holds all the data in a database that has been introduced in this section, e.g. the signal propagation, the user traces of all mo-

bility models, the fading maps, the land-use maps and different network configurations including cell positions, antenna types, frequency bands and transmission technologies like LTE, UMTS or GSM. Interfaces to SIMONE allow to add new data to the environment and to define new simulation scenarios from existing data in the database. The simulation environment allows macro-simulations with large scenarios using data traffic maps changing over the day that are dedicated to simulations over larger time spans. Micro-simulations that include the mobility traces are possible as well. Even the combination of macro- and micro-simulations to simulate a large network but limit the detailed evaluations to a shorter time scale are possible.
The simulation capabilities of SIMONE are constantly growing and comprise RSRP, SINR and cell load calculations as well as the handover procedure. Moreover, SIMONE has a perception of time. This means simulations can be started at a certain time of day and SIMONE delivers the network state including all active users and cells. Stepwise, the next network states can be requested from SIMONE that include changes in the user positions (based on the mobility traces) or network, i.e. cells might be added to the scenario or be deactivated or reconfigured by a SON-function. Nevertheless, the simulation is controlled by the user side realised in a MATLAB program. All calculations can be done on the MATLAB side, if necessary, or requested from SIMONE if available which is a matter of processing speed.
SIMONE computes the RSRP values for the simulations as follows:

$$RSRP_{ue} = TP_{cell} - PL_{ue} + FAD \tag{5.9}$$

with TP_{cell} the transmit power of the cell, PL_{ue} the pathloss to the UE calculated by the propagation model and FAD the additional fading introduced by the shadow fading maps. As the pathloss and fading maps are calculated as point maps the values are bi-linearly interpolated in 2D to the real position of the UE.

5.4 Simulation Scenarios

The service areas of a mobile communication network can generally be divided into rural areas with small villages, small streets and a limited number of cars and urban or dense urban areas with cities, large buildings and a dense street network. The aim of the network planning for rural areas is to ensure seamless service for the users with acceptable service quality. Due to the low user density a single cell in the middle of an inhabited area might provide good service quality already. The user mobility in rural

areas is mainly street based since the car is the favourable means of transport. In urban or dense urban areas the network planning is far more complex. Besides cars and bikes the users travel by public transport or walk by foot which results in a huge variety of user speeds and path selection. Moreover, the user location is dependent on the time of day. Since at day time the users travel to work and back and visit public areas and commercial centres, the user location is mainly limited to private buildings in the evening and at night time. Hence, the network planning has to adapt to the day-to-day routine of the users. The result is a huge number of cells with different sizes and objectives as delivering service to users in a commercial centre, stadium, park, office building or in the road. The large number of cells leads to a challenging interference situation in the network and hence to challenging optimisation of the handover control parameters.
Because of the large number of cells the requirement to ensure overlapping cell areas can easily be met in urban areas since the usual cell sizes are far below the maximum possible cell sizes as given in Section 2.1. Consequential LTE networks in urban environments are interference limited and users can sense many different cells in urban areas. We focus on urban environments for the research on handover optimisation algorithms since the possibilities and potential of wrong decisions that significantly impact the network performance are manifold here. In rural areas only few cells are potential candidates for successful handovers and the user mobility is more predictable.
In the following, the simulation scenarios used in this work are specified. All scenarios represent urban environments, i.e. the typical inter cell distance is around 1 km.

5.4.1 The Hanover Scenario

The Hanover scenario is a simulation scenario located in the city of Hanover lying in northern Germany. The development target of the scenario is to emulate the user behaviour and user network experience with a higher level of detail compared to conventional hexagonal simulation scenarios [Rose12]. For this purpose the ray-tracer and the realistic user mobility models are selected. The main configuration and simulation parameters are given in Table 5.2. This scenario will henceforth be referred to as “Hanover” scenario. The 65 base stations span over an area of 20 km by 24 km around the city of Hanover. Each base station has three sectors and thus a total number of 195 cells is available. The evaluation area, i.e. the area considered for the evaluation of the simulation results, has a size of 3 km by 5 km. The user mobility models consider an area of 5 km by 7 km to assure a realistic network load in the surrounding cells of the evaluation area. The antenna heights are a result of the network planning that followed the concept of placing antennas

Parameter	Configuration
Number of Base Stations	65
Sectors per Base Station	3
Number of Cells	195
Evaluation Area	3 km · 5 km
Antenna Height	7 - 61 m
Antenna Diagram	Kathrein 742212
Mechanical Tilt	4 °
Cell Transmit Power	46 dBm
Frequency Bandwidth	10 MHz
Carrier Frequency	1800 MHz
Outdoor Propagation Model	Ray-Tracer (Section 5.2.1)
Indoor Propagation Model	Outdoor-to-Indoor Model (Section 5.2.1)
Additional Shadow Fading Maps	STD 3 dB, Correlation Distance 50 m
Total Number of Mobile Users	2526
Vehicular Mobility Users	1109
Pedestrian Mobility Users	791
Indoor Mobility Users	626
Vehic. & Ped. User Antenna Height	1.5 m
Indoor User Antenna Height	1 - 48.3 m

Table 5.2: Configuration and simulation parameters of the Hanover scenario

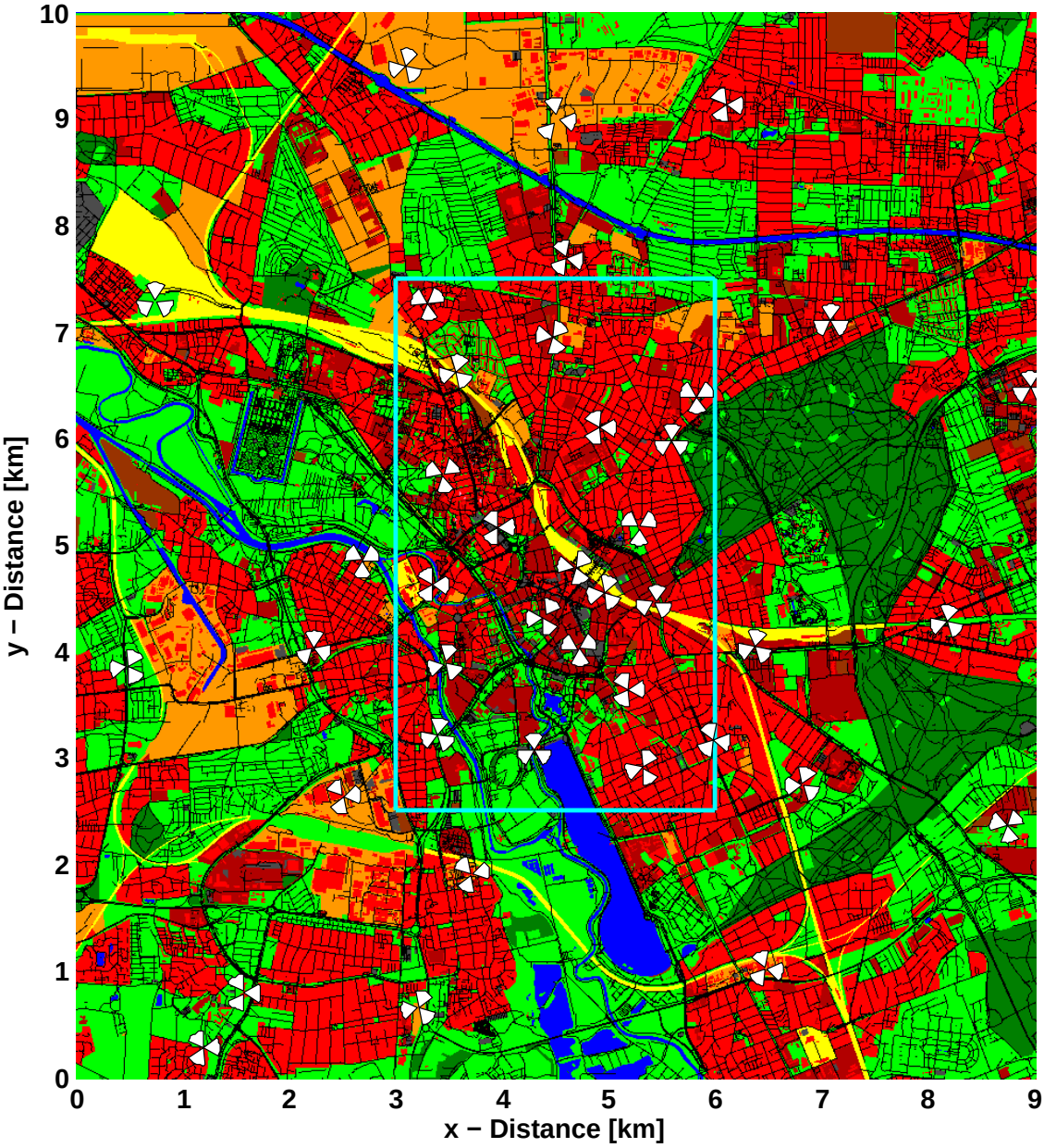

Figure 5.7: The Hanover scenario: base stations locations and sector orientation

on top of the largest buildings in the simulation scenario. Moreover, local knowledge of the real antenna locations of different network operators influenced the planning process. The signal propagation is calculated using the ray-tracer for outdoor predictions, the outdoor-to-indoor model for indoor predictions and the additional shadow fading maps to assure signal fading in a finer grid. Different realistic user mobility models are used. The user antenna heights for the indoor users depend on the height of the story the user are located in.

The location of the base stations and orientation (white sectors of a circle) of the sector antennas are visualized in Figure 5.7. The evaluation area is marked by the cyan rectangle in the middle of the figure. The cells outside the rectangle are considered as interference sources in the simulations. The position of the evaluation area has been selected to cover the dense urban areas of the city and some open spaces or green areas like the area around the lake and football stadium in the south or parts of the large forest "Eilenriede" in the mid-east.

The best-server RSRP-map is given in Figure 5.8. Best-server RSRP-map means that in each point of the map (grid: 10 m by 10 m) the RSRP value of the best serving cell is shown. The building shapes used in the ray-tracer to predict the signal propagation, the streets and open areas can easily be identified in the figure. The signal conditions vary because of the irregular positions of the base stations which can be discovered as the lightest yellow spots. In the north-east area of the map the RSRP values are low since the distance to the next base station is large. In the south next to the football stadium the cell is located in an open area which results in strong signal conditions in that area.

Figure 5.9 shows the best-server map of the Hanover scenario. The arrows give the orientation of the sector antennas. Dependent on the cell density the size of the coverage area of the individual cells changes. In the area around 2000 m in x- and y-direction the cell density is the highest resulting in the smallest cell coverage areas. The large cyan cell in the north covers a street passing the red and ochre cells to the south. This coverage behaviour is a special case of the Hanover scenario. As introduced before the other propagation models neglect the building shapes. Thus the case that the main beam of an antenna directs in the course of a street surrounded by buildings and, therefore, is the best server for that street can only be emulated by the Hanover scenario.

The SINR-histogram of the scenario is calculated under the assumption of full interference from the RSRP values of the 10 strongest cells in all points in the scenario (grid: 10 m by 10 m). If the SINR value of a UE falls below -6.5 dB, the condition for a con-

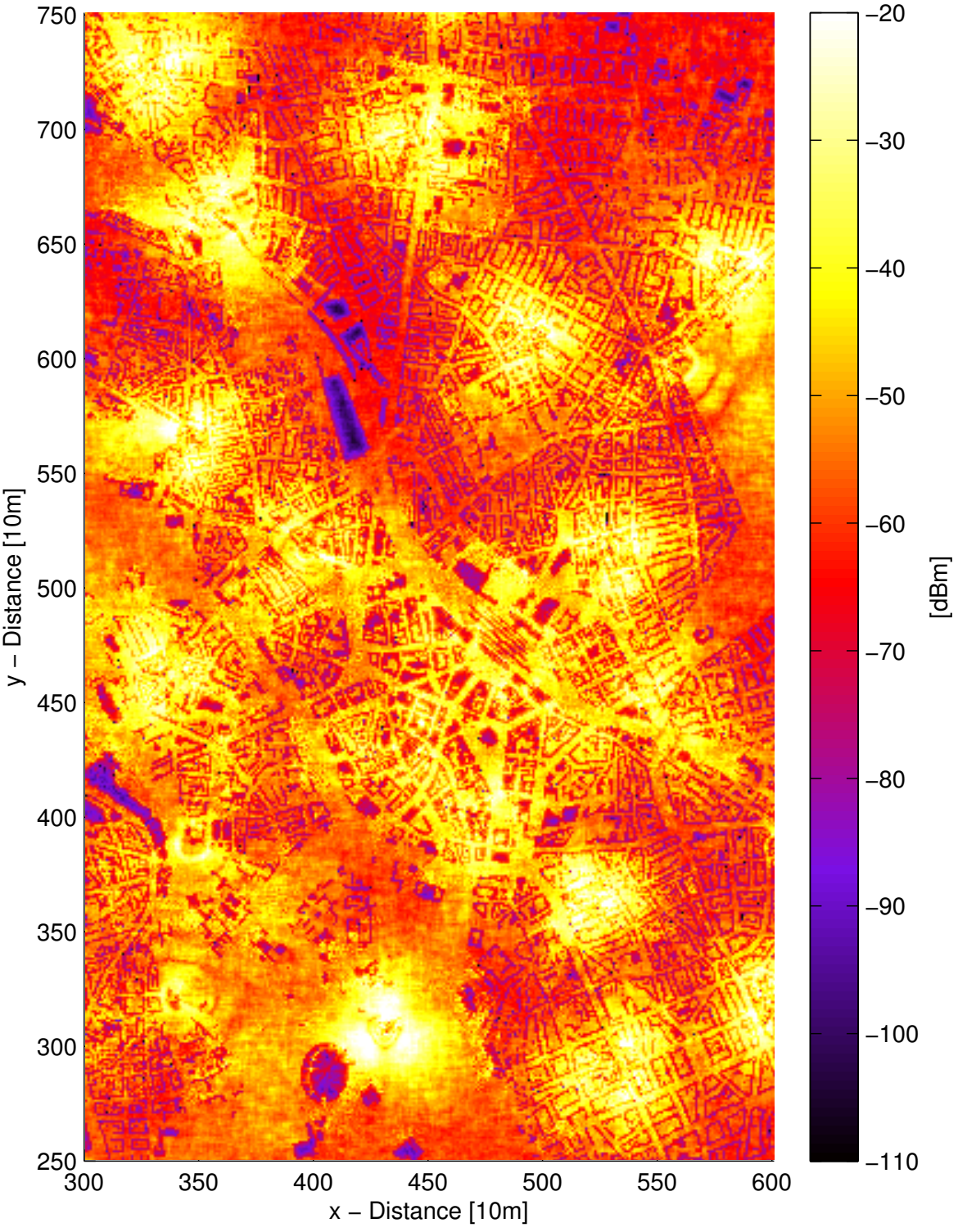

Figure 5.8: The Hanover scenario: best-server RSRP map

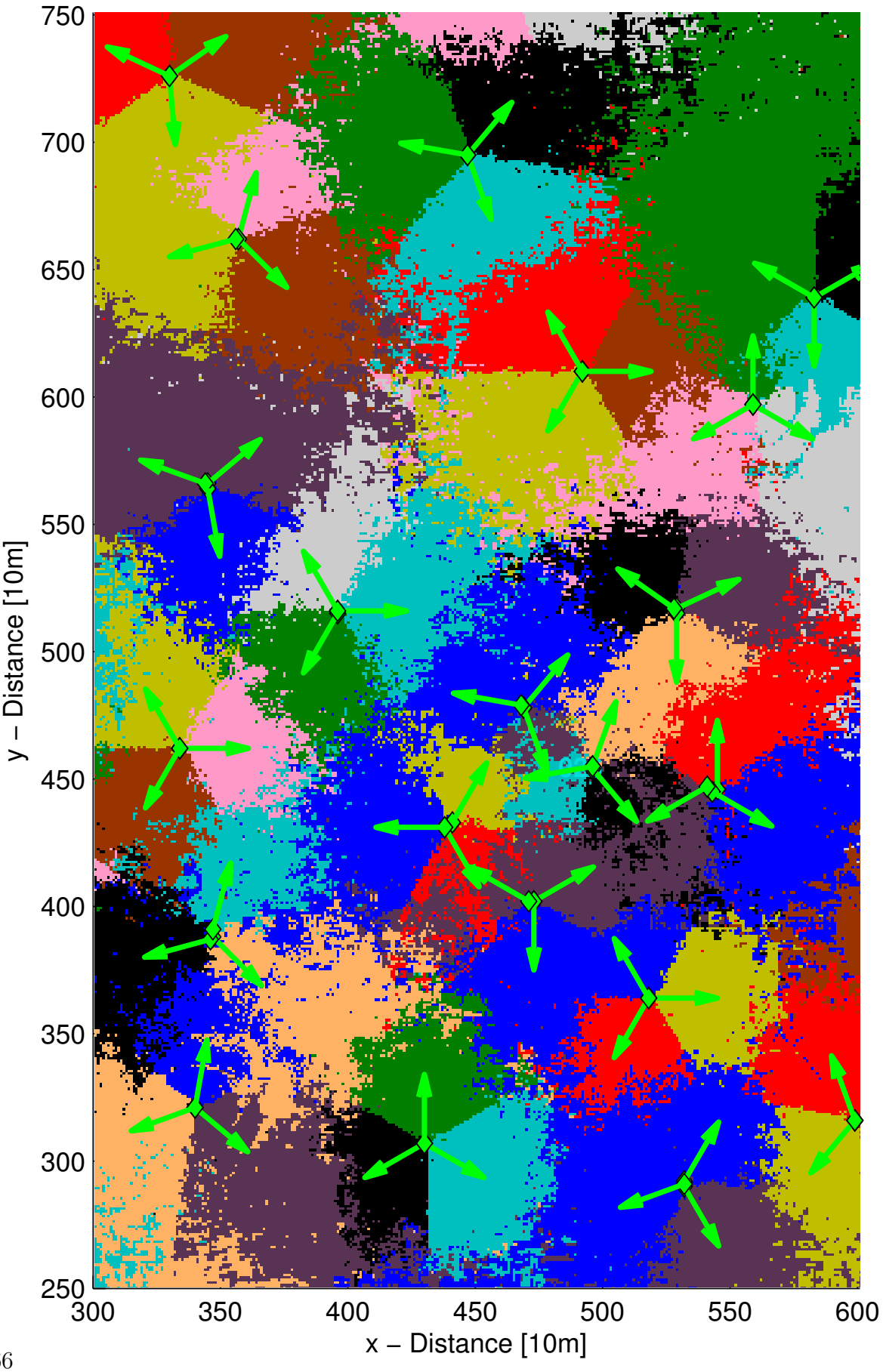

Figure 5.9: The Hanover scenario: best-server map

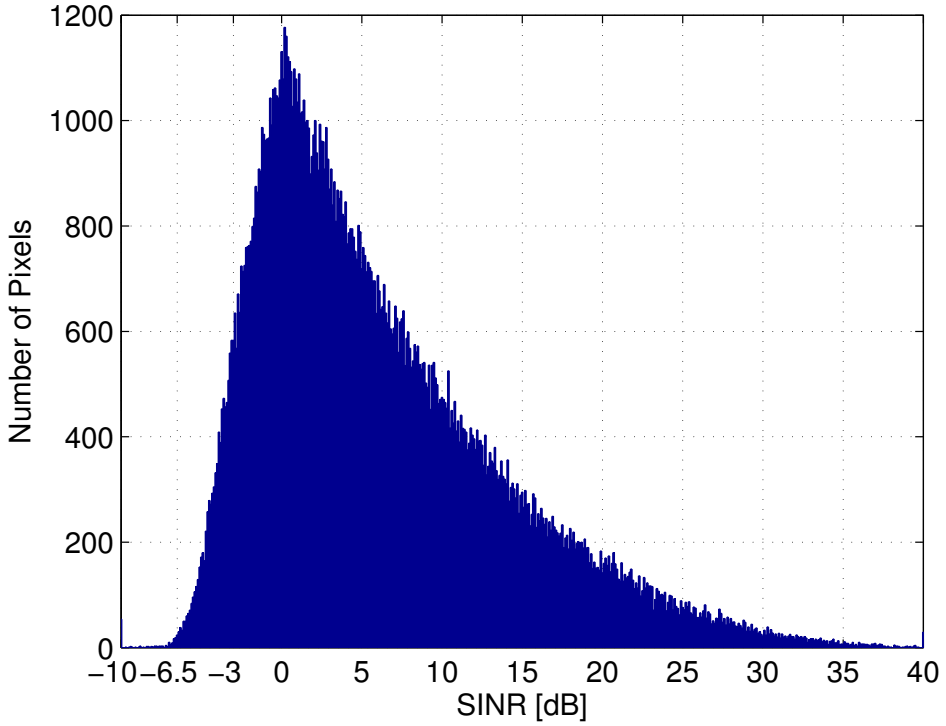

Figure 5.10: The Hanover scenario: SINR-histogram under the assumption of full interference and connection to the strongest serving cell

nection loss is fulfilled is the system simulations. The histogram in Figure 5.10 shows that the SINR value of almost no point in the scenario falls below this value even if the network is fully loaded. Therefore no coverage holes exist.
In Figure 5.11(a) the land-use map and in Figure 5.11(b) the mobility traces are depicted. The blue traces belong to the vehicular users travelling on the roads, the red traces are from the pedestrian and bicycle user and the white traces (small white dots in Figure 5.11(b)) show the movements of the indoor users. To increase the visibility the traces are cut to the first 100 s simulation time. The comparison of the mobility traces and the land-use map shows that the vehicular users mainly follow the main roads in the city whereas the pedestrian and bicycle users are generated at the entrance to a building or in the open spaces and move towards the road network.

5.4.2 The 3GPP Simulation Scenario

The 3GPP simulation scenario is specified in [3GPP10, Section A.2]. The scenario and recommended models are easy to implement and have low processing times. This

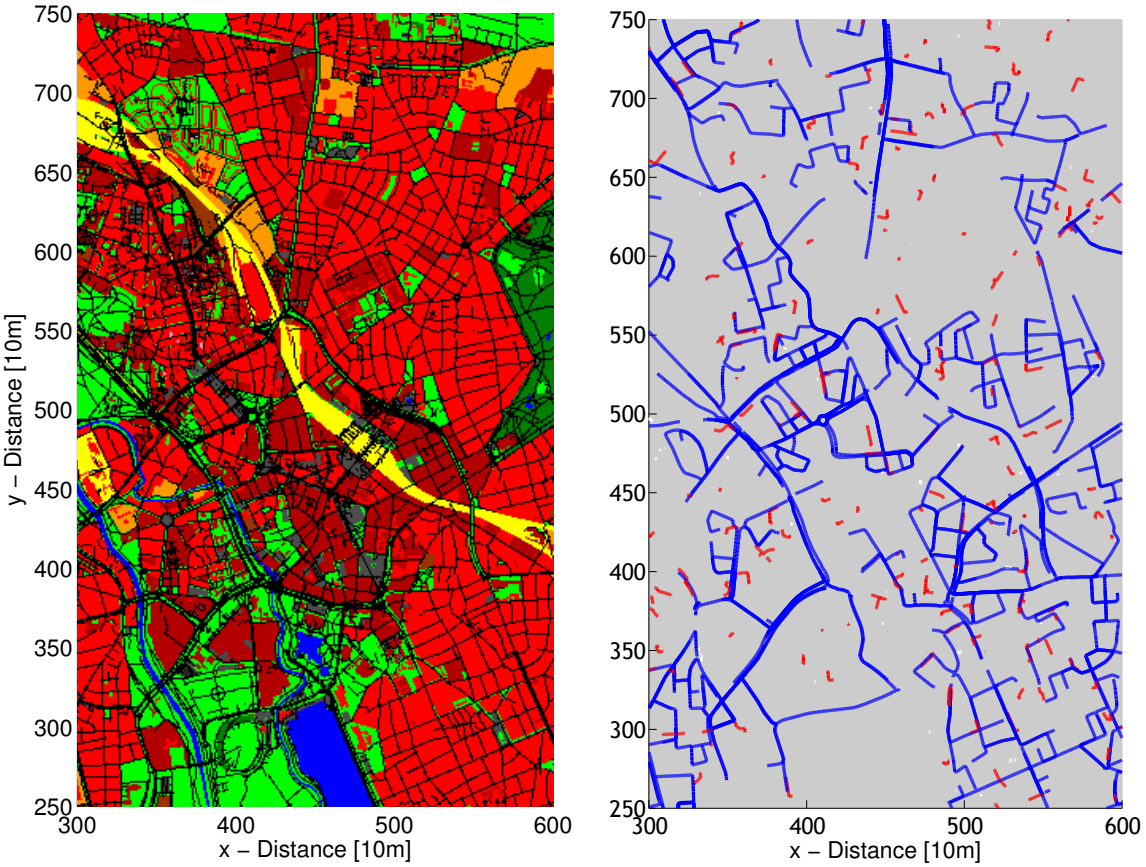

(a) Land-Use Map (b) User Mobility Traces

Figure 5.11: The Hanover scenario: land-use map and user mobility traces

means the system simulations take less time and due to the short implementation time, researchers get the simulation results quickly. This simulation scenario is chosen to compare the results of the more complex simulation scenarios to a common model. The main configuration and simulation parameters are given in Table 5.3. This scenario will henceforth be referred to as “3GPP” scenario.

The 61 base stations are arranged in rings in a hexagonal grid. Each base station serves three sectors resulting in a total number of 183 base stations. An Inter Side Distance (ISD) of 500 m is selected for the scenario. The evaluation area is limited to the coverage area of the inner 19 cells. According to the configuration specifications of the 3GPP propagation model in [3GPP10, Table A.2.1.1-1 and A.2.1.1-2] the antenna height, antenna diagram and mechanical tilt are set. The cell transmit power and frequency bandwidth are selected like in the Hanover scenario. The 3GPP propagation

Parameter	Configuration
Number of Base Stations	61
Sectors per Base Station	3
Number of Cells	183
Inter Side Distance (ISD)	500 m
Evaluation Area	Inner 19 Cells
Antenna Height	32 m
Antenna Diagram	3GPP-Model (Section 5.2.1)
Mechanical Tilt	15 °
Cell Transmit Power	46 dBm
Frequency Bandwidth	10 MHz
Carrier Frequency	2000 MHz
Outdoor Propagation Model	3GPP-Model (Section 5.2.1)
Indoor Propagation Model	No Indoor Areas
Additional Shadow Fading	Shadow Fading Maps with 9 dB STD
Total Number of Mobile Users	3000
Random Walk Users (5 $\frac{\text{km}}{\text{h}}$)	1000
Random Walk Users (15 $\frac{\text{km}}{\text{h}}$)	1000
Random Walk Users (50 $\frac{\text{km}}{\text{h}}$)	1000
User Antenna Height	1.5 m

Table 5.3: Configuration and simulation parameters of the 3GPP scenario

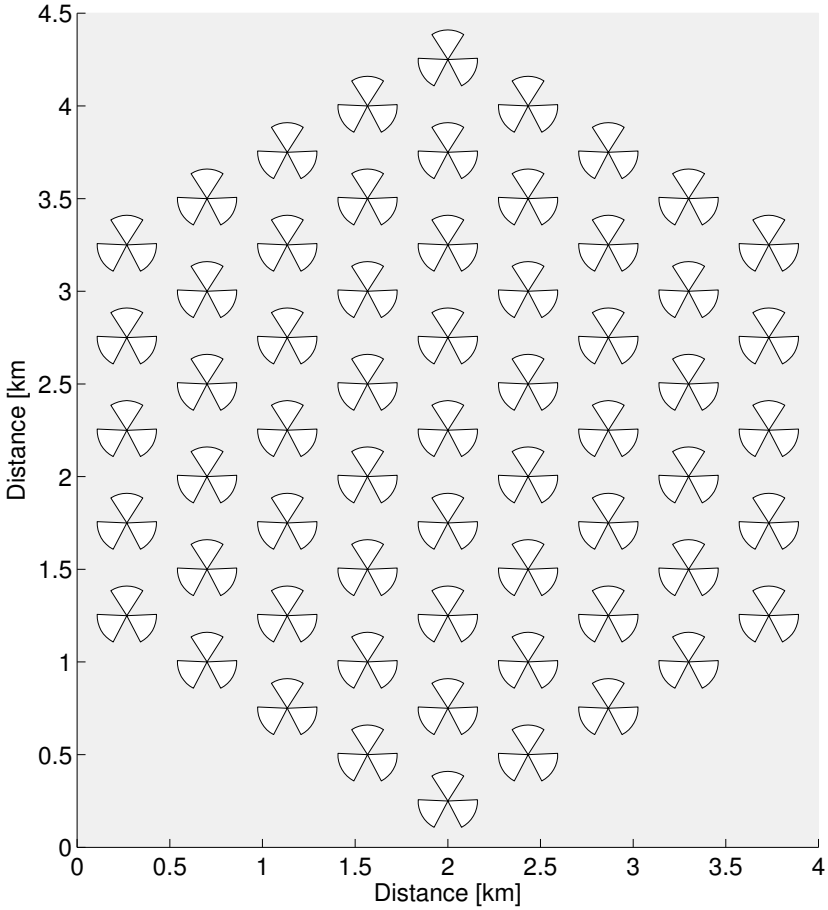

Figure 5.12: The 3GPP scenario: base stations locations and sector orientation

model is used for the outdoor propagation. No indoor areas are specified in the scenario. The additional shadow fading maps use a STD of 9 dB. A random walk model is used to introduce user mobility to the scenario.

The arrangement of the base stations is shown in Figure 5.12. The inner 19 cells used for the evaluation of the simulation results are surrounded by 2 rings of base station as interference sources.

In the best-server RSRP-map (Figure 5.13) the cell arrangement is still visible. Due to the higher antenna tilt of 15 ° the main beam of the antennas are directed to an area closer to the cell antenna location. The result is that the signal strength condition is improved close to the antenna and hence the influence of the shadow fading map is minor. In a scenario with an ISD of only 500 m these antenna tilts need to be directed to area close to the antenna location to reduce the interference to the remaining cells.

The best-server map given in Figure 5.14 shows that the coverage area of all cells is similar. The arrows depict the orientation of the sector antennas.

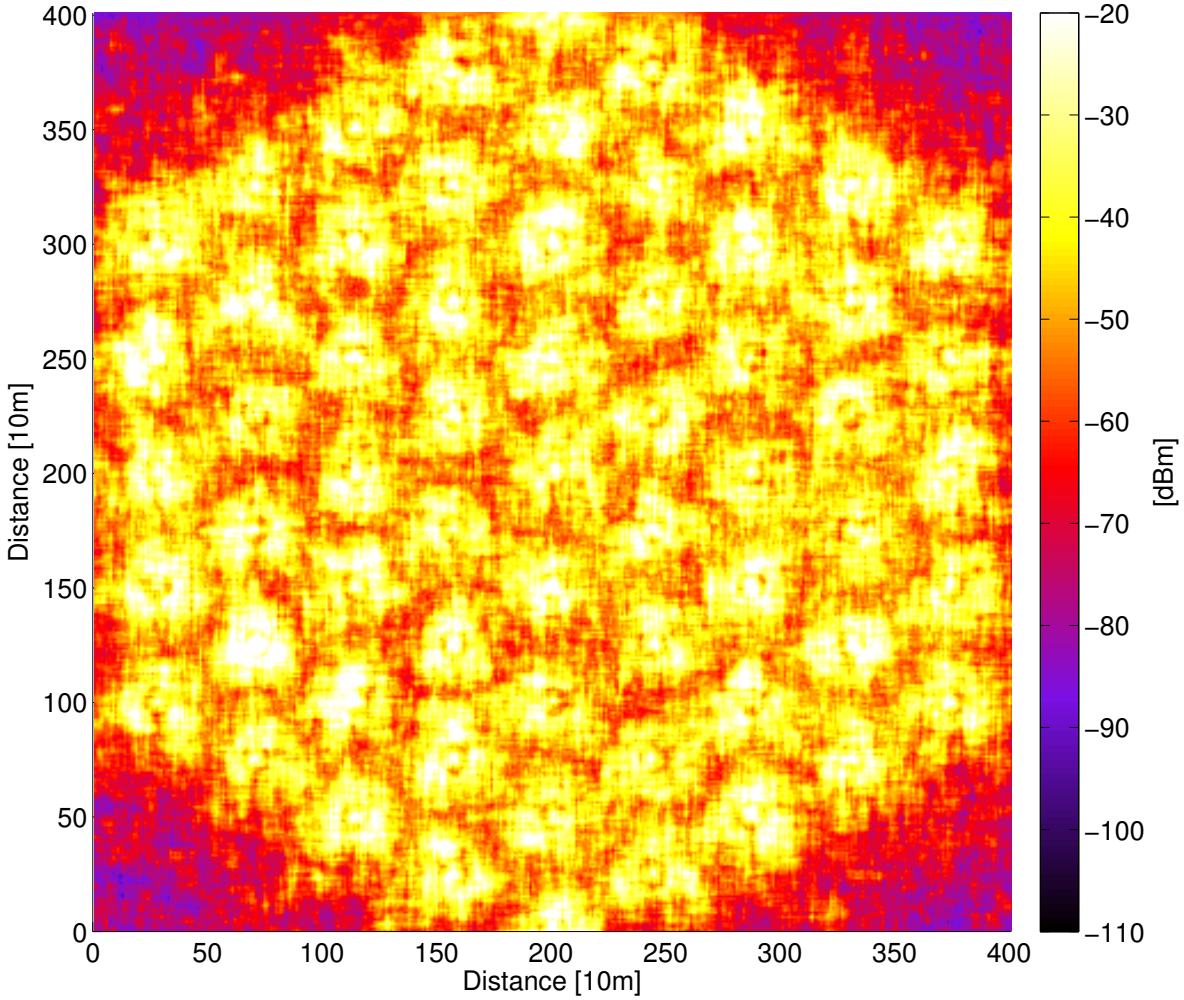

Figure 5.13: The 3GPP scenario: best-server RSRP map

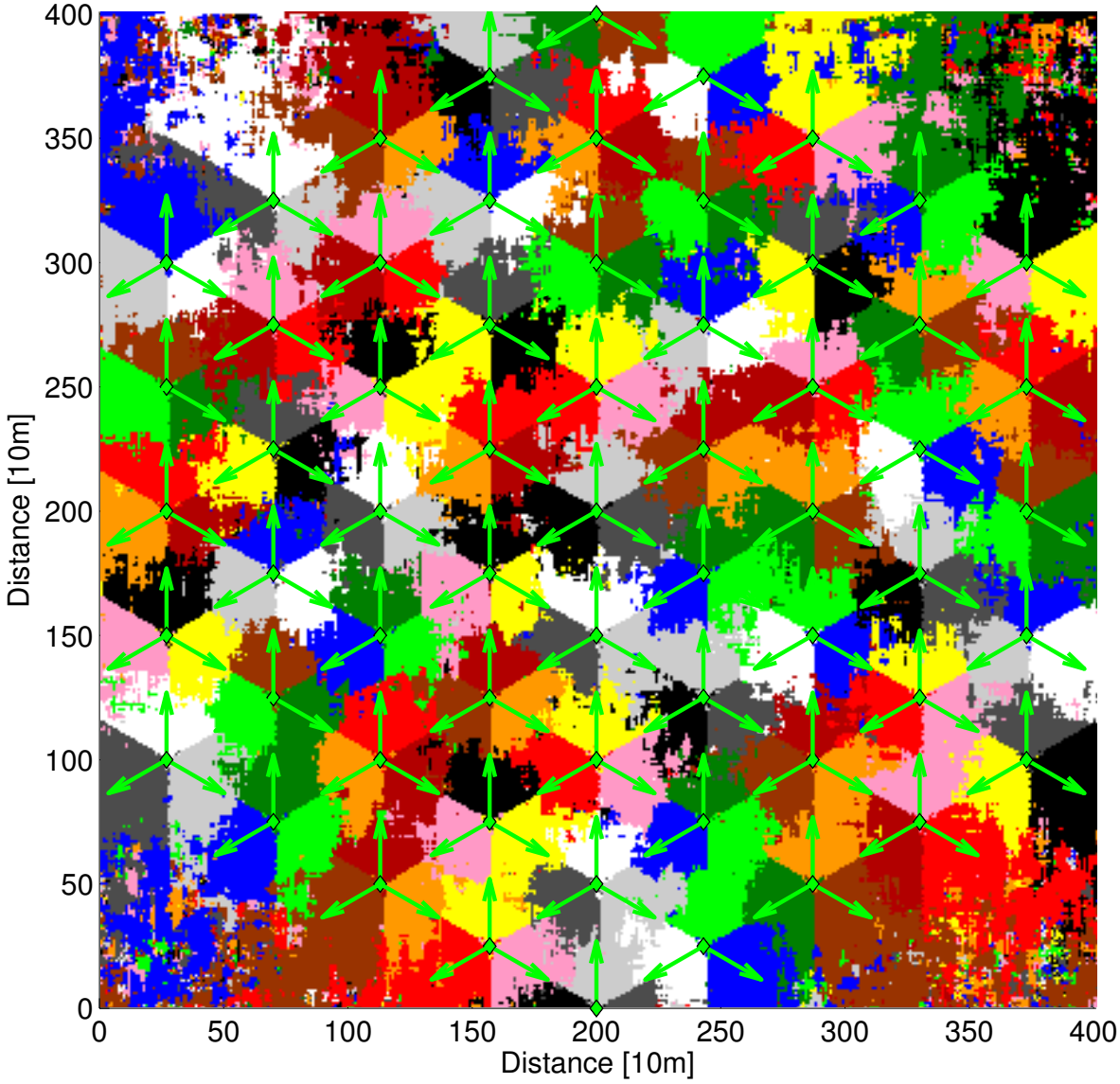

Figure 5.14: The 3GPP scenario: best-server map

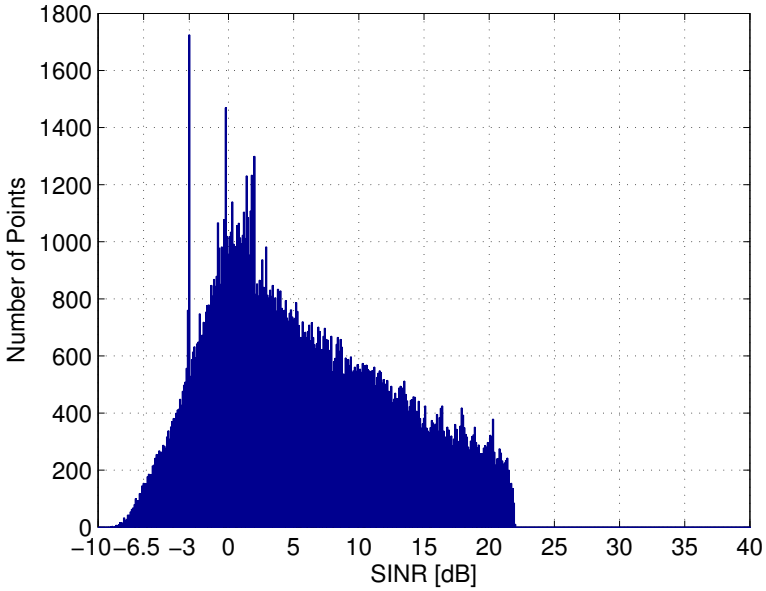

Figure 5.15: The 3GPP scenario: SINR-histogram under the assumption of full interference and connection to the strongest serving cell

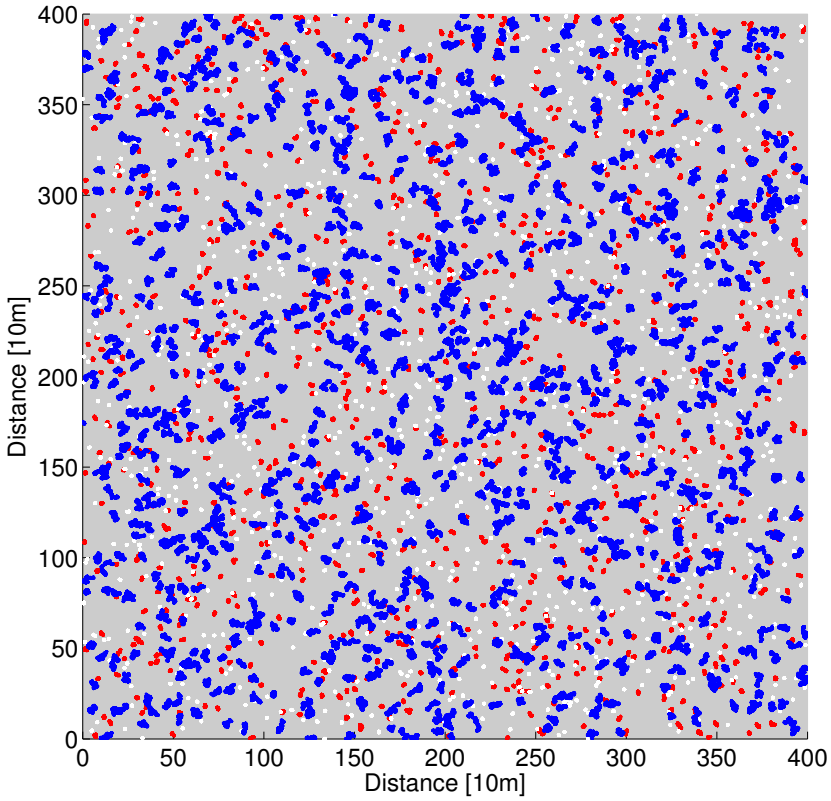

Figure 5.16: The 3GPP scenario: user mobility traces

The SINR-histogram significantly differs from the histogram of the other simulation scenarios. The reason for this is that the antenna diagram of the 3GPP propagation model specifies areas where the signal loss is limited to 25 dB. The peak at a value of -3 dB can be explained by this limitation. In an area close to the base station the signals from the three sectors of that base station are the strongest. Due to the signal loss limitation the power contribution of all three cells is the same in this area resulting in a SINR of -3 dB. The quick drop-off of the SINR values above 20 dB is caused by the antenna diagram as well. The strong power contribution to the interference from the sectors of the same base station limit the maximal SINR value.
Figure 5.16 shows the user mobility in the simulation scenario. The blue traces belong to the random walk users with a speed of 50 $\frac{km}{h}$, the red traces to the users with a speed of 15 $\frac{km}{h}$ and the white traces to the users with a speed of 5 $\frac{km}{h}$. More details on the random mobility model can be found in Section 5.2.2. The traces are cut to the first 100 s simulation time again to increase the visibility in the figure.

Chapter 6

Evaluation of the Handover Performance

The first step towards the optimisation of handovers in a mobile communication network is to determine the current handover performance of the network. The questions that arise for the determination of the handover performance are twofold:

- What requirements have to be met by the network to allow the determination of the current handover performance?
- How to evaluate the current handover performance to enable handover optimisation?

These are the two central questions that will be addressed in this chapter. The subsequent question on how to use the observations on the current handover performance for the optimisation purpose is subject to the next Chapter 7.
To answer the first question on the requirements that have to be met by the network, it is necessary to discuss how the configuration and current status of the network impacts the UE handover behaviour. If network configuration or status changes impact the handover behaviour, an ongoing handover performance evaluation needs to be repeated. Otherwise the performance evaluation represents an outdated network status. The second question on the evaluation of the handover performance deals with the characteristics of the performance indicators that are used to determine the handover performance. The general idea of the optimisation of the handover performance in this work is to observe the current performance of a cell for a certain time span and then adapt the handover control parameters according to the observations. This is visualized in Figure 6.1. In an optimisation interval the current handover performance is evaluated and results in the

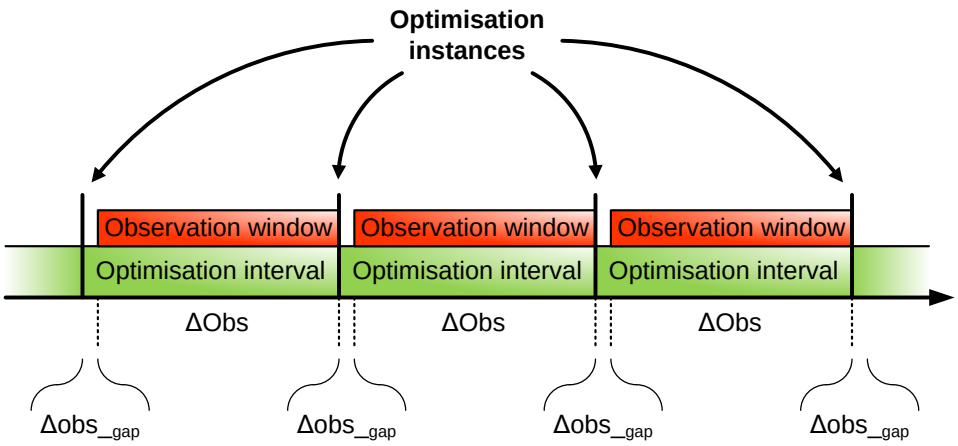

Figure 6.1: Optimisation Interval and Handover Performance Observation Window

optimisation instance. If the observation result shows the need to adapt the handover control parameters, the changes are executed in the optimisation instance. The observation gap after an optimisation instance ensures that the changes are accepted by the cells and communicated to the UEs if necessary. Thereafter, the next observation of the HPIs begins. The most important parameter for the evaluation of the handover performance is ΔObs, i.e the size of the observation window. This parameter influences the minimal optimisation interval and hence the reaction time to changes in the network that impact the handover performance. A small ΔObs allows short optimisation intervals leading to the ability to adapt to short-time temporary changes in the network. Nevertheless, the reliability of the observation result declines as well as the importance of single handover events increases for small ΔObs. Large observation windows increase the optimisation interval, which leads to slower adaptation to network condition changes. The selection of ΔObs will be a trade-off between the reliability of the performance evaluation and the chance to adapt to short-time network condition changes.

The network requirements are discussed in Section 6.1. Since the basis for the evaluation of the current handover performance are the HPIs, their characteristics are addressed in the next section of this chapter (Section 6.2). The handover control parameters are defined per cell in LTE. Hence, the handover performance has to be evaluated for every cell individually and the optimisation should be carried out in each individual cell as well. Section 6.3 defines an optimisation target function that allows influencing the optimisation target by introducing a set of weighting parameters for the individual HPIs. A detailed analysis of the statistical properties of the HPIs is given in Section 6.5. The evaluation of the impact of the HPI observation time on the estimation of the

current handover performance is the main topic of Section 6.6. Section 6.7 is dedicated to the deduction of the minimal observation window to enable handover optimisation. The conclusions from this chapter are summarised in Section 6.8.

6.1 Network Requirements to Enable the Evaluation of the Handover Performance

The introduction and description of the handover control parameters in Section 3.2 showed that the cell border plays an important role in the handover procedure. This is because the signal strength of a cell, other than the serving cell, is stronger than the signal strength of the serving cell when a UE crosses the cell border. The first necessary condition for a potential initiation of a handover is fulfilled in this case. It depends on the further developing of the signal strengths of the two cells and other neighbouring cells when a handover becomes necessary or is beneficial for the UE and the network. This development of the signal strengths is dependent on the positions of the base stations relative to the UE, the user mobility type and the environment of the UE, i.e. urban area with large buildings, open space, indoor environment, etc.
Therefore, the shape of the cell border has an impact on the handover behaviour of the UEs. Consequentially the handover optimisation can only target an adaptation of the handover control parameters to the current network situation. Changes in the network configuration or changes in the environment might impact the handover behaviour and justify to restart the evaluation of the handover performance and thus the handover optimisation.
In the following different categories of "influencing factors" on the handover behaviour are introduced and their level of influence is discussed.

Network Optimisation by Configuration Changes

This category of influencing factors includes the network configuration changes typically addressed by optimisation algorithms in the context of SON that impact the shape of the cell border. The most important configuration parameters in this sense are:

- Cell transmit power (interference mitigation)
- Electrical antenna tilt (Coverage and Capacity Optimization (CCO))
- Antenna azimuth and mechanical tilt (off-line CCO (no SON case))

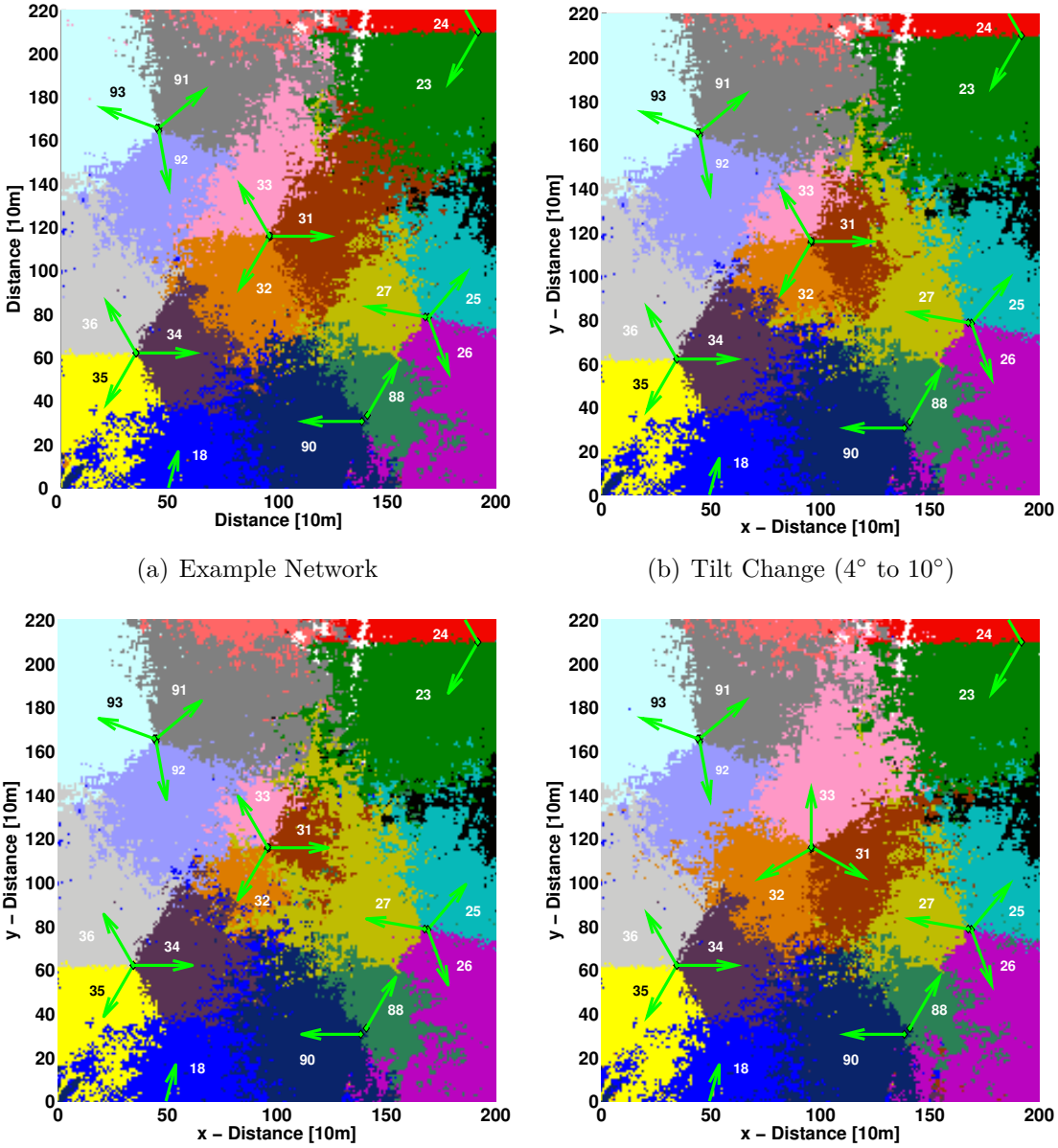

(a) Example Network

(b) Tilt Change (4° to 10°)

(c) Transmit Power Change (40 dBm to 30 dBm)

(d) Azimuth Change (Rotation by 30°)

Figure 6.2: Impact of network configuration changes at cell 31, 32 and 33 on the cell borders. The example network uses a tilt of 4° and a transmit power of 40 dBm. In cases b, c and d only the parameter given in the subtitle is changed compared to the example network.

Figure 6.2 shows an example network, i.e. a small cut-out from the Hanover scenario (Section 5.4.1). The best-server-map of the original unchanged network is shown in Figure 6.2(a). In the cell border areas, small best-sever islands of several cells can be observed. This shows that a cell border cannot be understood as a line that clearly separates the serving areas of two neighbouring cells. In the cell border area of cell 18, 32, 34 and 90 (the cell IDs are shown as numbers close to the arrows indicating the orientation of the cell antenna) best-server islands of all four cells extend deeply into the region of other neighbouring cells, i.e. if a cell region is defined as the area with the shortest distance to the cell antenna location. This is caused by the shadow fading of the buildings in the Hanover scenario. Hence, the cell border area is not a connected line between the serving areas of two neighbouring cells but the sum of smaller and larger areas lying next to best server areas of neighbouring cells.
The implication of a tilt change in cells 31, 32 and 33 from 4 ° to 10 ° is depicted in Figure 6.2(b). Besides the expectable effect of a smaller best-server area the location of the cell border changes significantly by the tilt change in the cells. Moreover, the configuration change impacts the cell neighbourship as cells 31 had a large common border to the dark green cell in the north-east of the example network. After the tilt change the cell border area of these cells significantly shrinks, i.e. due to the smaller cell border and resulting fewer handover events the handovers between the two cells become less important for the overall handover performance of the cells. The same holds for cells 31, 32 and 33 an other neighbouring cells.
The impact of transmit power changes is shown in Figure 6.2(c). In this example the transmit power is changed from 40 dBm to 30 dBm. The cell borders alter in a similar way as in the case of a tilt change. Hence, the impact on the cell borders and cell neighbourship is comparable.
The consequence of azimuth changes of 30 ° in cells 31, 32 and 33 is visualized in Figure 6.2(d). Here the cell border area between cell 33 and the dark green cell in the north-east of the example network significantly increases. Moreover, the shape and location of the best server-areas of the three cells takes the largest transformation. In contrast to the other configuration changes the azimuth change causes a shift of the cell border between the three sectors of the base station as well.

Network Roll-Out and Maintenance

Continuous network roll-out and improvement of existing infrastructure is the second influencing factor on the handover behaviour. Network extension aims at service quality

and coverage improvements and is realized by the roll-out of new base stations in different network layers, i.e. macro, micro, pico or femto layer. The improvement of an existing network can be realized by technology changes, carrier frequency adaptation, transmit antenna replacement or the upgrade of outdated infrastructure. The impact of these network changes on the cell borders between cells is severe as new cells can be added or existing cells vanish from a frequency layer. Furthermore cell borders and neighbouring cells as potential handover targets are introduced or vanish.

Temporary Operation of Cells

In certain areas of a city temporary gathering of people leads to a congestion of the mobile communication network. Typical examples for these hot spot areas are railway stations, airports, shopping malls, sport stadiums or pedestrian zones. To ensure the operation of the network additional micro, pico or femto cells are installed. These cells are only started up if the traffic situation in the network requires additional capacity. Nevertheless, these cells impact the cell borders in a network. Another hot topic in the optimisation of modern communication networks is the introduction of energy saving strategies. In energy saving unneeded cells are temporarily powered down if the current traffic can be handled by other cells or technologies. Moreover, the introduction of femto cells, i.e. small cells installed inside buildings by the customers [Rose11], transfers the operation of cells to the customer. This means the customer can power up and down the cell and change the location according to his own needs. The consequences for the network are unexpected coverage changes that influence the location of the cell borders.

Changes in the Network Environment

As discussed before the signal shadow fading has a major impact on the signal propagation. Consequential changes in the network environment and hence on the shadow fading objects like construction works, landscape changes or temporary installations like folk festivals or farmers markets impact the cell borders as well. The construction of streets in formerly uninhabited areas shifts the service users to new areas in the cells. This might result in cell changes in different locations and hence to new handover statistics as well. In this case the cell border is not impacted by the changes in the network environment. Nevertheless, the evaluation of the handover performance will be manipulated by these changes.

Network Load Variation

The load of the network, i.e. the distribution of the users in the network, has no impact on the cell borders between the cells. But the user distribution influences the cell load and thus the interference generated by a cell. The interference affects the virtual cell border, i.e. the border where the SINR of a cell gets to low to keep up the service. This means a user can advance deeper into the best-server area of a neighbouring cell in low load condition than in high load condition. The impact of the network load on the handover performance is further analysed in Section 6.4.

Conclusion

The evaluation of the handover performance is impacted by many temporary or long-term changes in the network. It depends on the handover performance observation interval how strong this impact is. If the time period of the change in the network is in the order of the observation interval, the conclusions from the observation might lead to a sub-optimal parameter configuration. In the case of long-term changes it depends on the exact moment of the network adaptation if the impact on the handover performance evaluation is strong enough to be regarded for the next optimisation step. Nevertheless, the importance of the network changes depends on the observation interval itself. If the interval is small, i.e. the handover performance can be evaluated several times a minute, the impact of sub-optimal parameter settings on the handover performance in the long-run is minor. For larger observation intervals it becomes more important that "stable" network conditions exist in the evaluation cycle, i.e. the shape of the cell borders and load condition is not significantly changed during the performance evaluation.

In Table 6.1 the main influencing factors for the evaluation of the handover performance, introduced above, are listed. The "occurrence", "duration" and "impact" on the handover evaluation are valued. The "occurrence" refers to how often changes on the influencing factor appear. "Duration" relates to the time period the change lasts before another adaptation is performed. The last column values the potential impact on the handover behaviour in the network, which means the impact on the cell shape and thus, a shift in the handover area of a cell. For the "cell transmit power" changes, the optimisation of cell power masks in the context of interference mitigation is considered. That means the total transmit power is the same as before but the distribution on the sub-carriers is varied to increase the signal quality for users located close to the border of a cell. For the "network roll-out" and "maintenance" the occurrence probability in a

Influencing Factor	Occurrence	Duration	Impact
Cell transmit power	seldom	long-term	severe
Electrical antenna tilt	seldom	long-term	severe
Mechanical antenna tilt	very seldom	long-term	severe
Antenna azimuth	very seldom	long-term	severe
Network roll-out	permanent	long-term	severe
Maintenance	permanent	temporary	severe
Temporary hot spot cells	medium	short-term (hours)	severe
Energy Saving	often (daily)	medium (half a day)	medium
Small cells	often (daily)	?	severe
Environment	seldom	long-term	minor
Network load	often (daily)	short-term (hours)	severe

Table 6.1: The occurrence, duration and degree of impact of network configuration or condition changes for the evaluation of the handover performance

certain area of the network is low. Though the assessment "permanent" for the "occurrence" refers to the high probability for activity somewhere in the network. Nevertheless, the case that the handover performance evaluation is disturbed by this influencing factor is low. The case maintenance refers to the replacement of hardware, which leads to temporary cell shut-down. Since the small cells are operated by the users the duration (time of operation) depends on the users wishes. Changes to the environment like the construction of buildings and streets evolve slowly which leads to a minor impact on the handover behaviour. The table shows that many configuration changes in the network affect the handover behaviour but only a few happen often and have a major impact. One of the most important influencing factors is the network load variation, which will be considered for the assessment of the optimisation algorithms.

As discussed before, the dimensioning of the observation interval is a trade-off between the reliability of the observations and the ability to quickly adapt to new network conditions. Independent of the necessary observation interval that will be examined in this dissertation, the identification of more optimal handover control parameter settings should be possible within few handover performance evaluations. This is a matter of the optimisation algorithm design and enables fast handover parameter adaptation.

Moreover, it is desirable to design an algorithm that is able to adapt quickly to new network configurations. This is especially important due to the high probability for more frequent network configuration changes in future networks caused by other SON-functions like energy saving or coverage and capacity optimisation or the temporary start-up of small cells in private buildings or hot spot areas. In the optimal case the algorithm gets a notification on major network changes.

6.2 Characteristics of the Handover Performance Indicators

For the evaluation of the current handover performance the ping-pong handover ratio (HPI_{pp}), the handover failure ratio (HPI_{fail}) and the radio-link failure ratio (HPI_{rlf}) are used as performance indicators. The sequence of two successful handovers from a SeNB to a TeNB and back is called a ping-pong handover as introduced in Section 3.3. Ping-pong handovers are usually caused by too early handovers to cells that temporarily offer the best service quality for a user or by handovers to a wrong cell that turns out to offer a too low service quality to keep up the demanded service. In this case the user is handed back to the source eNB after a short time. Handover failures and radio-link failures are usually caused by too late handovers or handovers to a wrong cell. In the first case the radio-link fails before the handover is finished and hence the user looses the connection to the network. The definition of a handover to a wrong cell is that the TeNB cannot serve the user and the user looses the connection. If the SeNB still offers sufficient service quality, the user can try to hand back to the SeNB in the case of a handover to the wrong cell. Another possibility for a handover to a wrong cell is that the TeNB hands the user back to the SeNB, which results in a ping-pong handover.
The evaluation of the HPIs characteristics in this section is based on system-level simulations using the simulation environment as introduced in Chapter 5. The section aims at introducing the HPIs and showing how the handover performance is affected by the handover control parameter settings. Further, the simulation results are used to depict the course of the HPIs for exemplary cells. Most simulation results presented in this section are from cell 31. The reason is that cell 31 serves the most users in the selected simulation scenario. Hence, more handover related events can be observed in the simulation time which allows the evaluation of small and large observation window sizes. Figure 6.3 shows the ping-pong handover ratio of cell 31 in the Hanover scenario (Section 5.4.1) for four sets of handover control parameter settings and 5 observation window sizes.

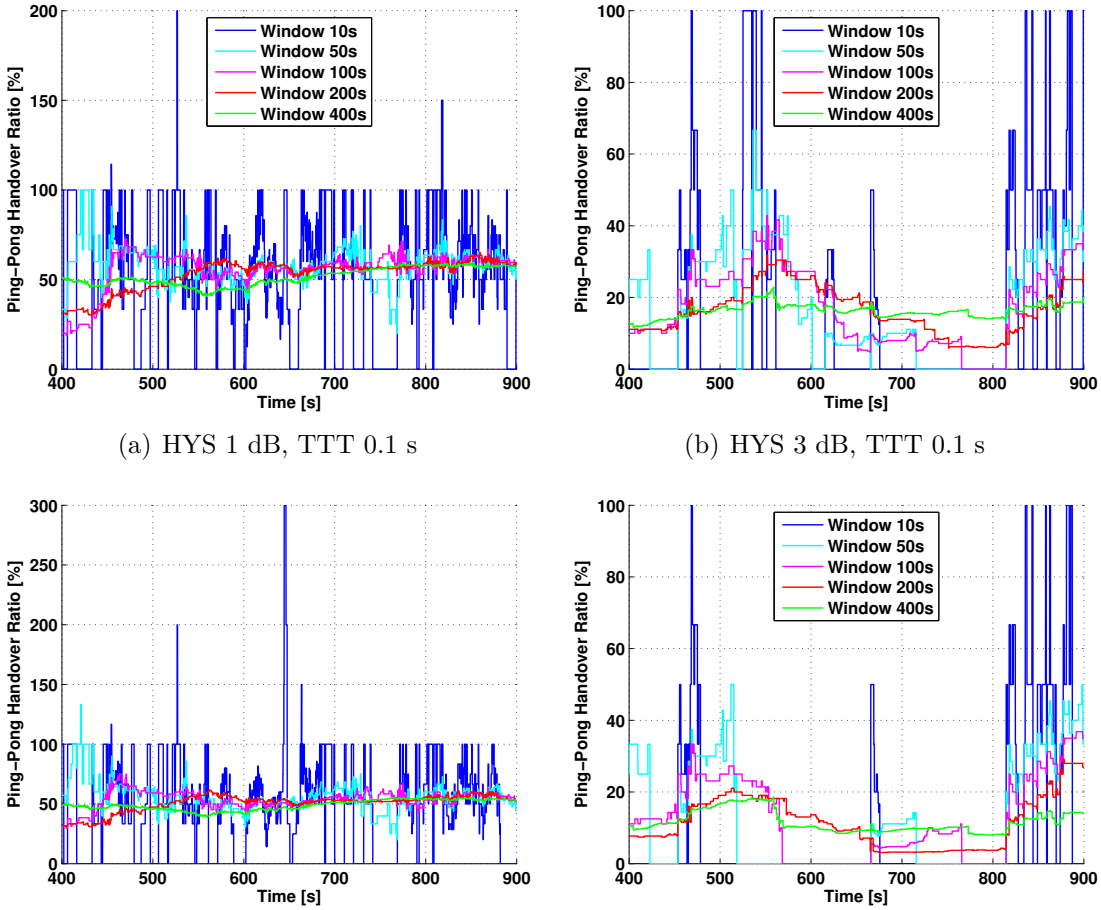

(a) HYS 1 dB, TTT 0.1 s

(b) HYS 3 dB, TTT 0.1 s

(c) HYS 1 dB, TTT 0.3 s

(d) HYS 3 dB, TTT 0.3 s

Figure 6.3: The ping-pong handover performance of cell 31 for different HOPs and observation window sizes

A set of handover control parameter settings, i.e. a combination of a HYS and TTT value will henceforth be named Handover Operating Point (HOP). The curves show the moving average of the ping-pong handover ratio for the corresponding window size. 400 s simulation time have passed before the values visualized in the plots have been calculated to get comparable results, i.e. for the 400 s observation window no values are available before the window size has been reached. For a HYS of 1 dB and a TTT of 0.1 s (Figure 6.3(a)) the variance of the ping-pong handover ratio decreases rapidly with higher observation window size. The ping-pong handover ratio for an observation window of 200 s has almost the same statistical properties as for a window size of 400 s between 700 s and 900 s simulation time (200 s: STD 2.14, Mean 58.15; 400 s: STD 1.50, Mean 56.91). A small STD of the HPIs is desirable for the evaluation of the current

handover performance to increase the representativeness of the performance observation of a single HOP. Increasing the TTT to a value of 0.3 s does not significantly change the characteristics (6.3(c)). Figures 6.3(b) and 6.3(d) indicate that the behaviour changes for other HOPs with higher HYS values. Besides the fact that lower ping-pong handover ratios can be observed in these cases the drop-off of the STD for higher observation windows decreases. Hence, longer observation times are needed to analyse the ping-pong handover performance for HOPs with higher HYS values.

The fact that longer observation times are needed to evaluate the ping-pong handover performance for HOPs with higher HYS values coincides with the lower amount of ping-pong handovers in these HOPs. Figure 6.4(b) depicts the number of ping-pong handovers for all 121 HOPs as specified in Section 3.2. The number of detected ping-pong handovers decreases significantly for HOPs with higher HYS and TTT values. The amount of successful handovers in the HOPs of cell 31 is illustrated in Figure 6.4(a) and shows that almost one handover per second is executed for a HYS of 0 dB and a TTT of 0 s. Other HOPs with low HYS and TTT values, hereafter named Low_{HOP}, still show a significant amount of executed handovers. This results in high signalling traffic which is an undesired effect for network operators and might lead to a system break-down. Consequentially, network operators will preferably avoid the selection of a Low_{HOP}. A comparison of Figure 6.4(a) and 6.4(b) shows that the majority of the additional handovers in $\text{Low}_{HOP}s$ are detected as ping-pong handovers.

To sum up, $\text{Low}_{HOP}s$ show a significant number of ping-pong events and successful handovers. Thus the evaluation of the ping-pong handover performance is possible for small observation windows and shows low STD values. But network operators try to avoid a high number of ping-pong handovers due to the risk of a system break-down. For higher handover control parameter values (HYS and/or TTT) the number of ping-pong events and successful handover events decreases significantly. This means these HOPs qualify from the network operator point of view. The drawback is that longer observation windows will be necessary to evaluate the ping-pong handover performance.

The number of radio-link failures is depicted in Figure 6.4(d). Note that Figures 6.4(d) and (c) use a different labelling on the x- and y-axes, i.e. the figures are turned horizontally by 180 °, to increase the visibility. As expected, the number of radio-link failures increases with higher HYS and TTT values. This indicates the interaction of the unnecessary ping-pong handovers on the one side and the radio-link failures caused by too late handover triggering on the other side. As introduced before, the users of mobile services are satisfied when the handovers are initiated timely (Low_{HOP}) but the network

operators aim at reducing the signalling traffic caused by the additional handovers. High handover control parameters lead to a significant increase in radio-link failures which leads to unsatisfied service users and hence network operators since the users could decide to switch the mobile network operator. A trade-off between these two extremes has to be found that leads to an acceptable handover performance and satisfies the service users and network operators.

Figure 6.4(c) depicts the number of handover failures that mainly occur in the transition region to the radio-link failure dominated area in the HOP-plane. Handover failures can be treated as a special form of radio-link failures where a certain chance of radio-link recovery exists. Nevertheless, the impact on the evaluation of the handover performance is the same as for radio-link failures since the handover decision was too late. Hence, the handover failures extend the area of too late handover triggering in the HOP-plane.

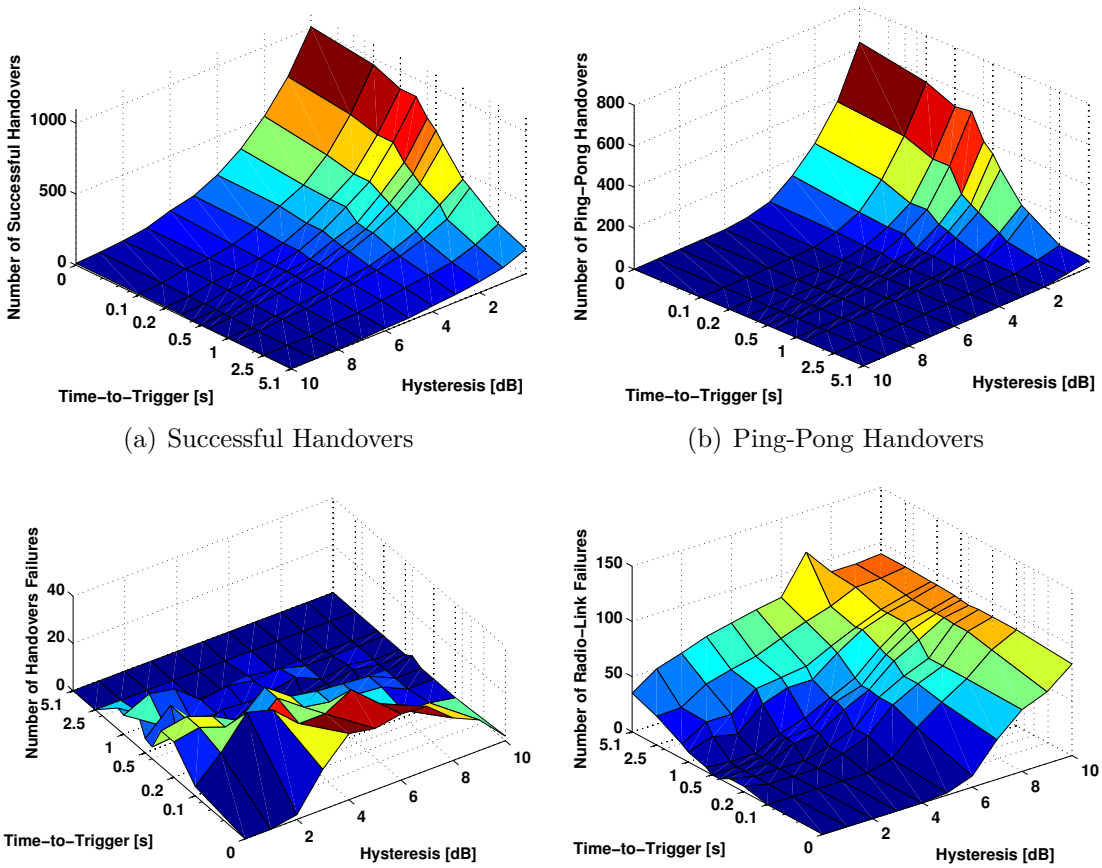

(a) Successful Handovers

(b) Ping-Pong Handovers

(c) Handover Failures

(d) Radio-Link Failures

Figure 6.4: Number of handover related events in all HOPs of cell 31 (Simulation Time: 1000 s)

Due to the fact that the handover failures are caused by too late handover triggering like the radio-link failures and the similar impact on the evaluation of the handover performance the handover failures will not be investigated separately in this section. The corresponding figure can be found in Appendix B.

The HPI radio-link failure ratio is shown in Figure 6.5 for four HOPs. Different HOPs have been selected for this HPI since the HOPs that have been used for the analysis of the ping-pong handover ratio showed no radio-link failures. Since the number of radio-link failures increases for higher HOPs (6.4(d)) the statistical properties of the radio-link failure ratio get more significant for these HOPs as well. In Figure 6.5(a) a small number of radio-link failure events occurs. Hence, the variation of the performance indicator is high as well especially for small observation windows. Due to the even distribution of

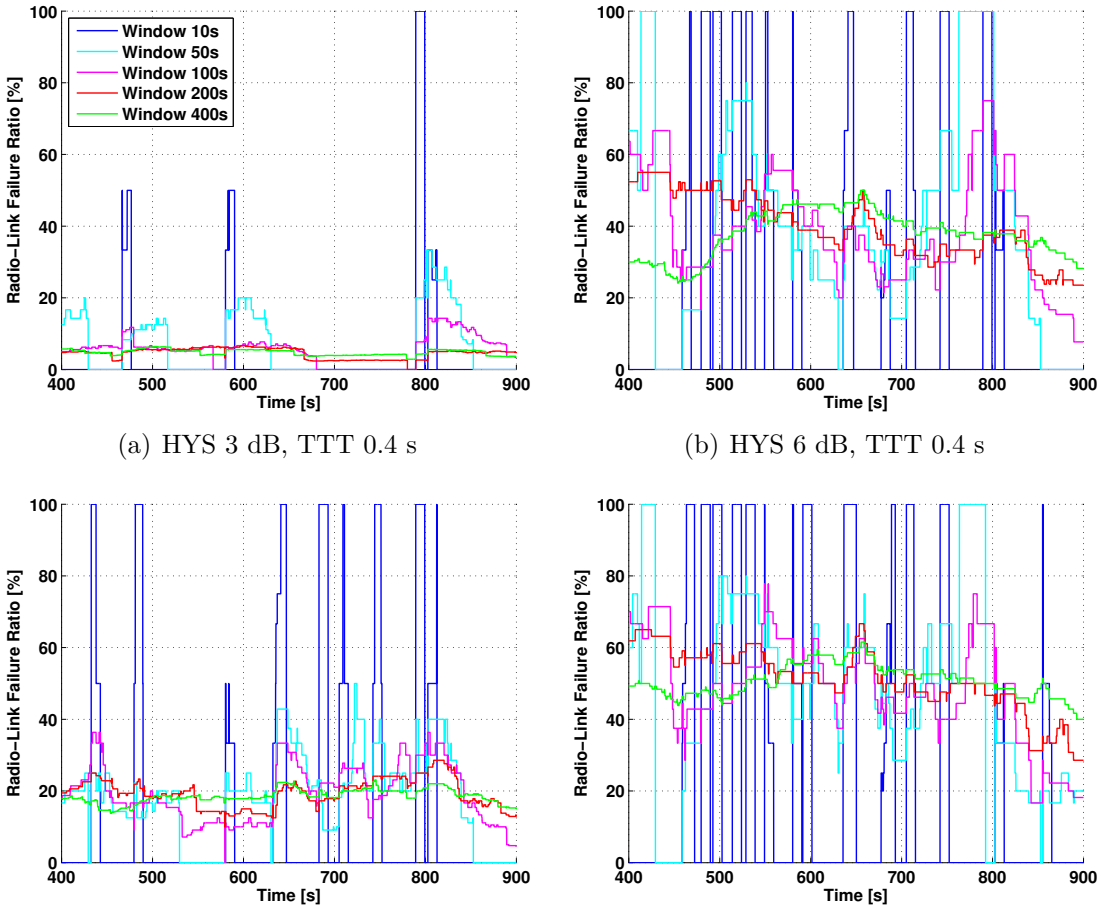

(a) HYS 3 dB, TTT 0.4 s

(b) HYS 6 dB, TTT 0.4 s

(c) HYS 3 dB, TTT 1.0 s

(d) HYS 6 dB, TTT 1.0 s

Figure 6.5: The radio-link failure performance of cell 31 for different HOPs and observation window sizes

the radio-link failures indicated by the curve of the HPI for an observation window of 10 s in Figure 6.5(a) the STD is low for larger observation window sizes. Increasing the TTT value to 1 s (6.5(c)) leads to an increase in the mean radio-link failure ratio from about 5 % to about 20 %. The different distribution of the events leads to an increasing variance of the performance indicator for larger window sizes. Figures 6.5(b) and (d) show the radio-link failure performance for a HYS of 6 dB. The number of radio-link failures significantly increases for higher HYS values. The outcome of this is that the statistical properties of the ping-pong handover ratio and the radio-link failure ratio show opposing trends for lower and higher HOPs. The arising question is how to evaluate the performance of a HOP given the opposing behaviour of the HPIs and interconnected with this question what statistical properties should be targeted to enable handover

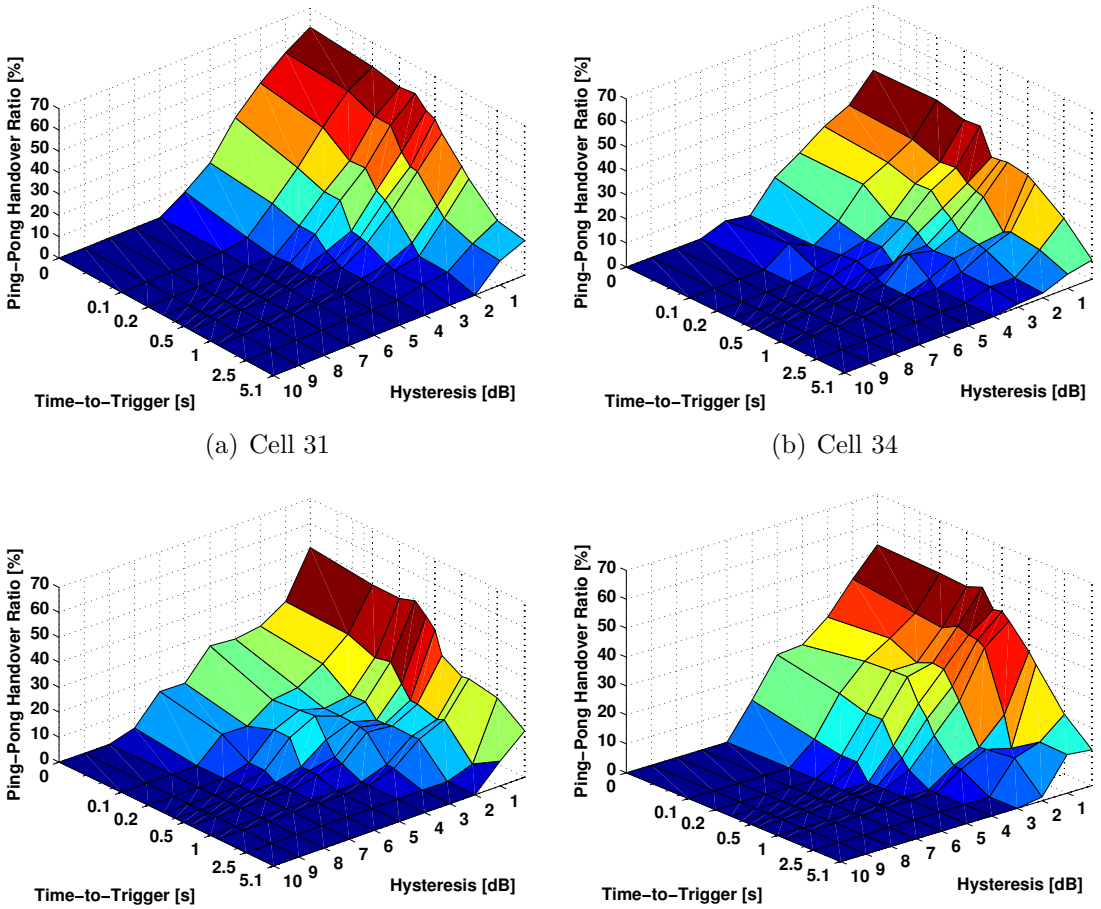

(a) Cell 31 (b) Cell 34

(c) Cell 36 (d) Cell 90

Figure 6.6: Comparison of ping-pong handover ratios in the HOP-plane for different cells (Simulation Time: 1000 s)

optimisation? This question is addressed in Sections 6.5, 6.6 and 6.7.
In addition to the evaluation of the handover performance the HPIs give information about the feasibility of performance improvement by handover optimisation. It has to be investigated how and if cells benefit from different handover control parameter settings. An indication for optimisation potential is the identification of performance differences of cells using the same handover control parameter settings. From this follows that adapting the control parameters to the cell individual situation is beneficial for the network performance. A comparison of ping-pong handover ratios from four cells in the network is shown in Figure 6.6. It can be observed that the overall trend of ping-pong handover events is the same in all four cases. Nevertheless, the ping-pong handover ratio goes up to 6o % in cell 31 and only reaches values close to 40 % in cell 34. For a HYS of 3 dB and a TTT of 0 s cells 34 and 36 show a ping-pong handover ratio of about 20 % whereas the other 2 cells have a ratio of about 30 %. But a deeper analysis of these

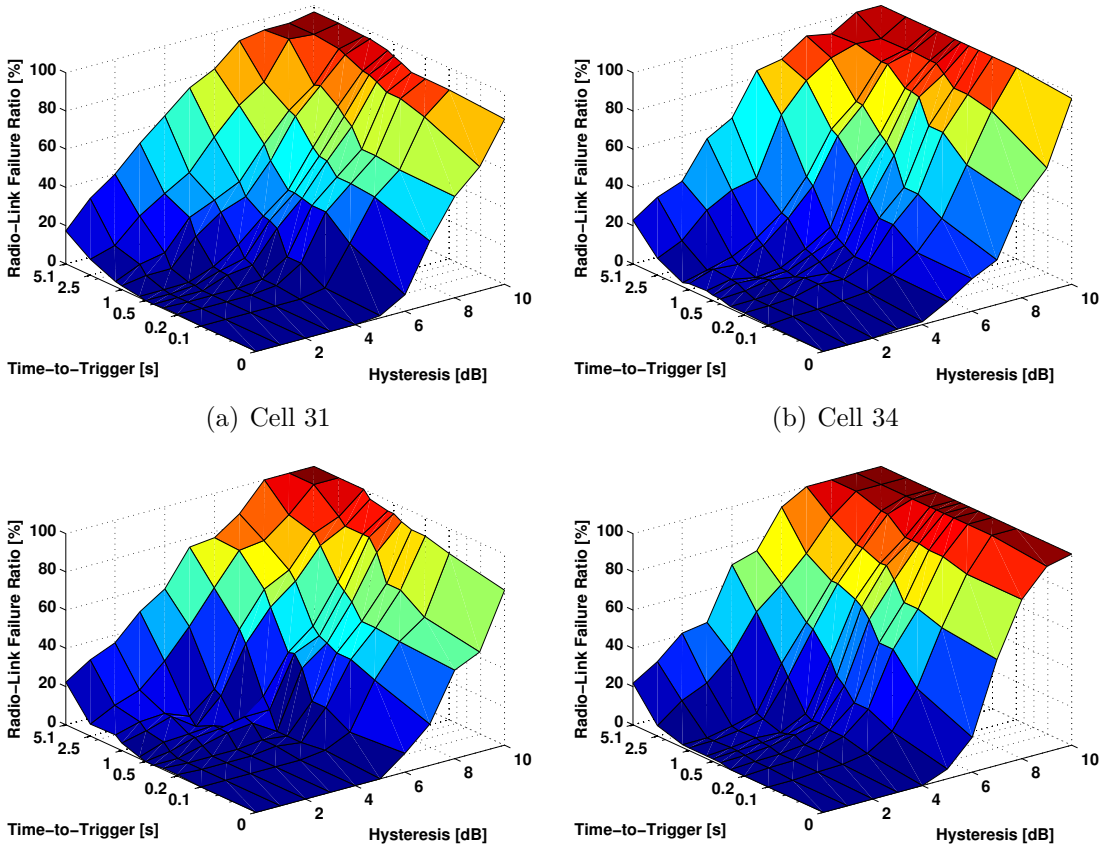

(a) Cell 31 (b) Cell 34

(c) Cell 36 (d) Cell 90

Figure 6.7: Comparison of radio-link failure ratios in the HOP-plane for different Cells (Simulation Time: 1000 s)

performance differences has to discover whether the performance gain is high enough to justify handover optimisation.
The radio-link failures ratio in the same four cells is visualized in Figure 6.7. It can clearly be observed that the radio-link failure performance for high HYS values is bad in all four cases. Better performance can be observed for lower HOPs. For a HYS of 5 dB and a TTT of 0 s the radio-link failure ratio in cell 31 and 36 is already zero while it lies around 10 % for the other two cells. Again a deeper analysis has to show how this differences can be used to improve the handover performance.
To sum up, the HPIs show different behaviour in the cells depending on the handover control parameter settings. This enables handover performance gain by handover optimisation on cell level. In the following sections the optimisation potential and performance gain will be analysed in detail.

6.3 Introduction of a Target Function for the Optimisation of the Handover Control Parameters

For the optimisation of the handover performance a target function is needed. The requirement for the definition of the target function is that it has to base on the HPIs and allows the adjustment of the optimisation target subject to the network operator requirements. Equation 6.1 gives a target function for the optimisation of the handover performance as a linear combination of the three HPIs introduced by the SOCRATES project ([Kürner11]).

$$HPI_{sum} = w_{pp}HPI_{pp} + w_{fail}HPI_{fail} + w_{rlf}HPI_{rlf} \tag{6.1}$$

The weighting parameters w_{pp}, w_{fail} and w_{rlf} allow the modification of the optimisation target. Higher weighting parameter values increase the importance of the individual HPI and lead to a favouring of HOPs with better performance for that indicator. Minimizing the target function and hence changing the HOP for the best HPI_{sum} value leads to the lowest amount of negative handover events according to the weighting parameter settings. This means the same weighting parameter settings for all HPI values will not necessarily lead to levelled HPI values if a HOP shows the lowest amount of negative handover only caused by e.g. radio-link failures, this HOP is identified by the target function. Thus additional constraints that limit certain HPIs to an overall maximum value have to be defined to avoid high HPI values.

Combining the HPIs to one target function permits the identification of the best performing HOPs for a set of weighting parameters. The weighting parameters can be defined by the network operators to influence the optimisation target according to their policy. The handover performance ratios of Cell 31 are depicted in Figure 6.8. Figures 6.8 a-c show the areas in the HOP plane where the individual HPIs are dominant. The ping-pong handover ratio increases for small handover control parameter settings and the radio-link failure ratio for high control parameter values. The handover failures mainly happen when small TTT and medium HYS values are selected. The reason behind this is that the handovers are initiated in time but the users SINRs are close to the minimum communication threshold of -6.5 dB already and reach SINRs lower than this threshold before the handover is completed. This means the users travelled to far into the coverage area of the target cell to complete a successful handover to that cell. The linear combination of the HPIs to the HPI_{sum} with weighting parameters set to one is

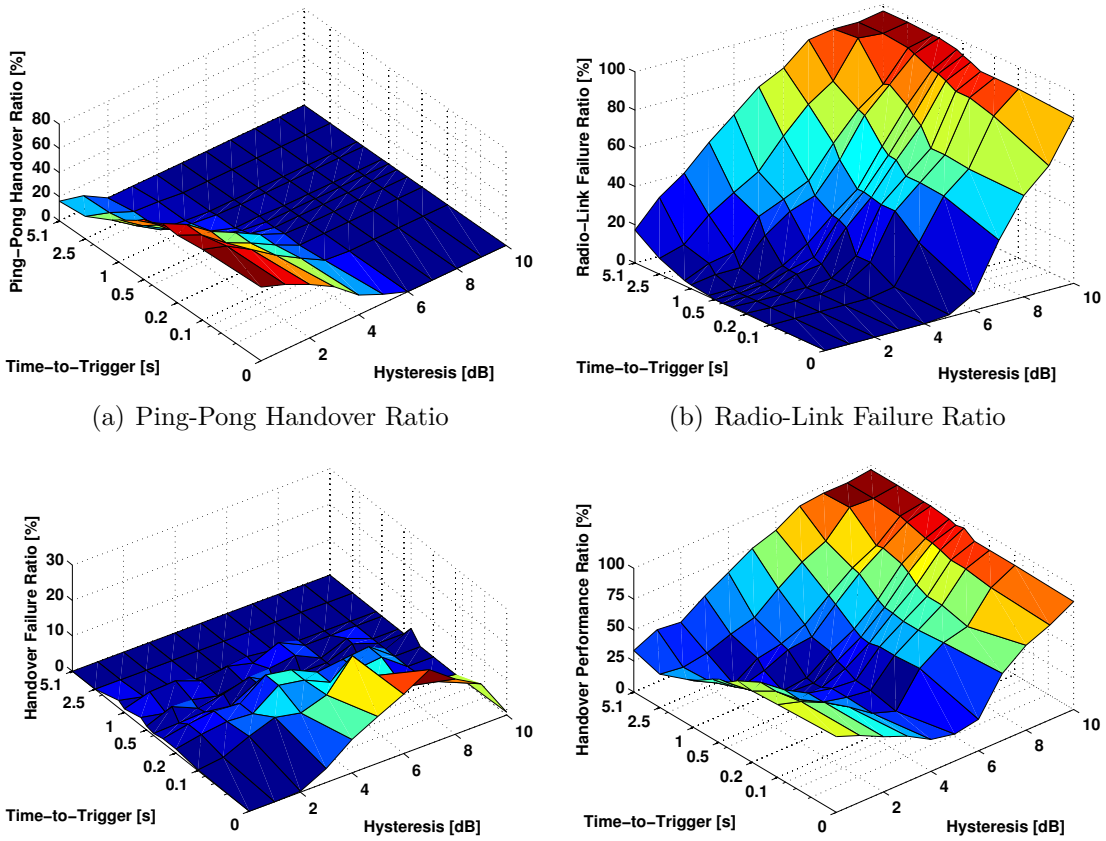

(a) Ping-Pong Handover Ratio

(b) Radio-Link Failure Ratio

(c) Handover Failure Ratio

(d) $HPI_{sum}(w_{pp} = 1, w_{fail} = 1, w_{rlf} = 1)$

Figure 6.8: Mean HPI ratios in all HOPs of cell 31 (Simulation Time: 1000 s)

shown in Figure 6.8(d). An area of better handover performance reaches from medium HYS values combined with small TTT values to smaller HYS values combined with high TTT values (larger than 1 s). This is the area in which the lowest amount of negative handover events take place. The best mean performance for the complete simulation time can be observed in the HOP with a HYS of 2 dB and a TTT of 1.2 s. In this HOP a mean ping-pong handover ratio of almost 4 %, a mean handover failure ratio of about 0 % and a mean radio-link failure ratio of approximately 3.2 % is reached.

For the evaluation of the handover performance it is important to analyse how the HPI weighting parameters influence the HPI_{sum} and the identification of the best HOP. The impact of the weighting parameters on the HPI_{sum} is visualized in Figure 6.9. An exemplary set of weighting parameters has been selected to illustrate the change in the handover performance evaluation for cell 34. The figure shows that varying the weighting parameters mainly shifts the area of better handover performance along the

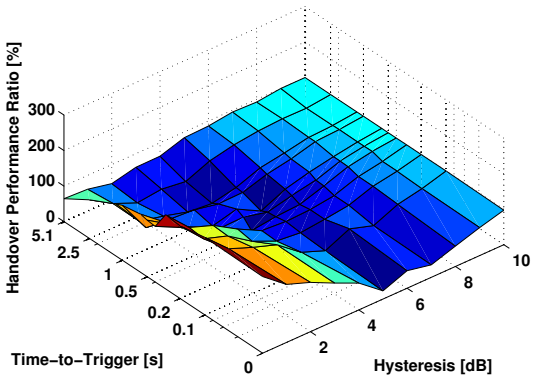

(a) Set 2 ($w_{pp} = 5, w_{fail} = w_{rlf} = 1$)

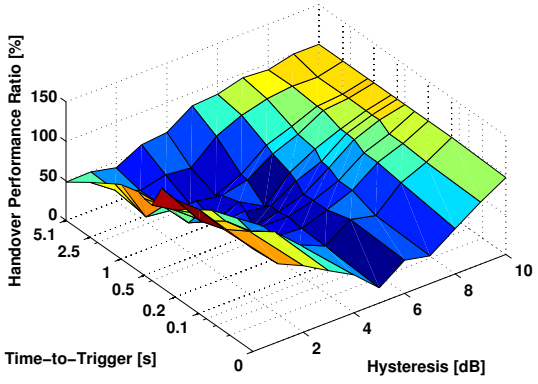

(b) Set 3 ($w_{pp} = 3, w_{fail} = w_{rlf} = 1$)

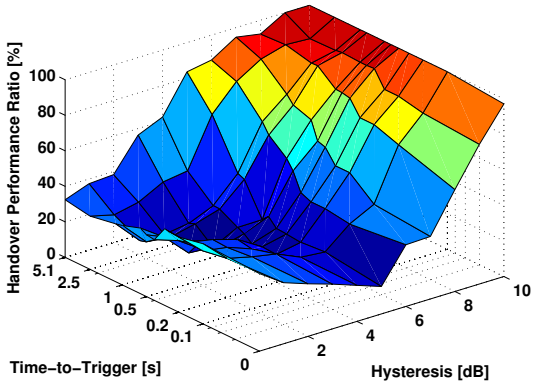

(c) Set 4 ($w_{pp} = 1, w_{fail} = w_{rlf} = 1$)

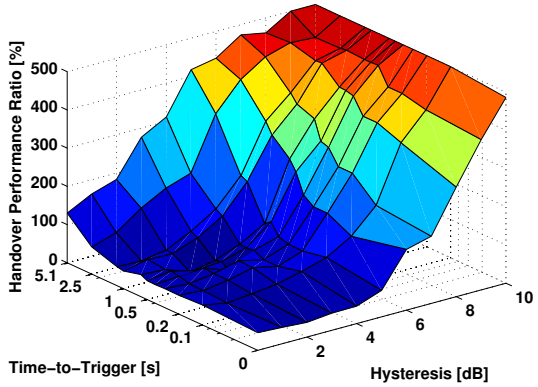

(d) Set 6 ($w_{pp} = 1, w_{fail} = w_{rlf} = 5$)

Figure 6.9: Impact of for HPI_{sum} weighting factor sets on the HOP performance of cell 34 (Simulation Time: 1000 s)

x-axis corresponding to the HYS values in this example. The HOP giving the best performance in the case that the weighting parameters are set to one (Figure 6.9(c)) uses a HYS of 3 dB and a TTT of 0.6 s resulting in a mean ping-pong handover ratio of 6.43 %, a mean handover failure ratio of 2.04 % and a mean radio-link failure ratio of 5.07 %. In this example the share of the ping-pong events (6.43 %) and failure events (7.11 %) is in the same order.

Increasing the weighting parameter for one HPI reduces the ratio of this handover related events. But this performance improvement is achieved at the expense of the remaining handover related events. The HOPs giving the best performance for other weighting parameter settings are listed in Table 6.2. Changing the weighting parameter settings from Set 4 to Set 5 (Table 6.2), i.e. increasing the weighting factors for the HPI_{fail} and the HPI_{rlf} to three, reduces the handover failure ratio from 2.04 % to 0 % and the radio-link failure ratio from 5.07 % to 3.56 %. The ping-pong handover ratio significantly increases in this example from 6.43 % to 10.99 %.

The weighting parameter sets 6 and 7 (Table 6.2) show that increasing the weighting parameters for the HPI_{fail} and the HPI_{rlf} to five and ten leads to the same best HOP and lacks further improvement of the failure event ratios. The reason behind this is that the ping-pong handover ratio is large in the HOPs that show better failure event performance. Increasing the weighting factor for the HPI_{pp} (Set 3 - 1) reduces the ping-

Parameter	Set 1	Set 2	Set 3	Set 4	Set 5	Set 6	Set 7
w_{pp}	10	5	3	1	1	1	1
w_{fail}	1	1	1	1	3	5	10
w_{rlf}	1	1	1	1	3	5	10
HYS	5 dB	5 dB	4 dB	3 dB	2 dB	2 dB	2 dB
TTT	0.6 s	0.6 s	0.4 s	0.6 s	0.6 s	0.6 s	0.6 s
HPI_{pp}	0 %	0 %	1.95 %	6.43 %	10.99 %	10.99 %	10.99 %
HPI_{fail}	1.31 %	1.31 %	5.15 %	2.04 %	0 %	0 %	0 %
HPI_{rlf}	19.40 %	19.40 %	8.03 %	5.07 %	3.56 %	3.56 %	3.56 %
HPI_{sum_min}	20.71	20.71	19.04	13.54	21.66	28.78	46.57

Table 6.2: Performance of the best HOP (lowest HPI_{sum} value) according to the weighting parameter settings in cell 34

pong handover ratio as expected. A weighting parameter value of five leads to a ratio of 0 % already. Thus, higher weighting parameter values show no further improvement. The corresponding figures and tables for other cells can be found in Appendix C.
The findings from the example of the handover performance of cell 34 are that influencing the weighting parameters leads to the desired shift between ping-pong handovers on the one hand and handover and radio-link failures on the other hand. This enables changing the optimisation target and the HOP selection for the cells. But the impact of the weighting parameter settings may be different for the cells in the network depending on the individual environment and user mobility. To explore the impact of the weighting parameters w_{pp}, w_{fail} and w_{rlf} on the handover performance of all cells in the network, we conduct a system-level simulation using the parameters given in Table 6.3. Due to the similar influence of handover and radio-link failures on the system performance and the visibility in the figures the weighting parameters w_{fail} and w_{rlf} are set to the same value in this analysis. The course of action for the analysis is as follows:

1. Execution of system-level simulations with fixed HOPs in every cell
2. Compilation of a considered cell list for the evaluation (minimum user activity required)
3. Calculation of the HPI statistics for every time step and considered cell
4. Generation of the HPI_{sum} for different weighting parameter settings for all cells
5. Identification of the best performing HOP for each weighting parameter setting and cell
6. Analysis of the handover performance for the selected HOP

In the first step system-level simulations are performed for every HOP that was defined in Section 3.2. This means the analysis is based on perfect knowledge of the handover performance for fixed HOP settings in all cells and thus all handover related events in the simulation scenario. Hereafter "fixed HOP settings" refers to the case that all cells use the same HOP for the complete simulation time (no optimisation). A list of considered cells for the evaluation of the impact of the weighting parameters is generated

[1]The requirement for a cell to be considered in the performance evaluation is that at least ten UEs are connected to the cell in any time step during the simulation. Cells in the outlying area are simulated as interference sources but not considered for the evaluation of the handover optimisation algorithm.

Parameter	Value	Description
Simulation Scenario	Hanover	-
Simulation Time	1000 s	-
Simulation Step Size	100 ms	-
Interference Model	Full Interference	-
w_{pp}	1-5	Step Size: 1
$w_{fail} = w_{rlf}$	1-10	Step Size: 1
Observation-Window-Size	400 s	For HPI-Values
Total Number of Users	2526 Users	Vehicular, Pedestrian and Indoor
Minimum Number of Users	10 Users per Cell	To be Considered for Evaluation
Considered Cells	65 Cells	Full-fill the Requirements[1]
HOPs	121	As defined in Section 3.2
HOP-Selection	Best Performance	In complete simulation time

Table 6.3: Simulation parameters for the analysis of the weighting parameter impact on the handover performance

by the minimum requirement of ten simultaneously connected users to consider only cells that have user traffic in the evaluation. In step three the HPI-ratios are calculated with regard to the observation window size listed in Table 6.3. The resulting HPI_{sum}-values are generated from the HPI-ratios for all weighting parameter combinations in step four. Note that the first HPI_{sum}-value is calculated when the first HPI-ratios are available which is after 400 s, i.e. the observation window size. From the definition of the HPI_{sum} in Equation 6.1 it is clear that lower HPI_{sum}-values represent better handover performance for the same weighting parameter settings. Hence, in step five the best performing HOPs are identified by the lowest mean HPI_{sum}-values for each weighting parameter setting and cell. The analysis of the handover performance for every cell and selected HOP is taken from the 121 system-level simulations that have been executed in step 1. Finally, the results of the analysis are discussed below.

The presupposition for the analysis of the impact of the weighting parameters on the handover performance in the network is that it is possible to identify the best performing HOP in a cell for a given set of weighting parameters. Consequently, the analysis shows

how the weighting parameters would change the network performance given that an optimisation algorithm exists that finds the best performing HOP for each cell. Nevertheless, only one HOP is selected for a set of weighting parameters and cell, i.e. the HOP showing the best performance over the complete simulation time for that cell. There might still be room for further improvement by changing the HOPs of a cell during the simulation. This is neglected for this analysis. It will be discussed later in this work how fast and reliable the optimisation of the handover parameters can be.

Figure 6.10 shows the results of the analysis in the Hanover-scenario. The ratio of ping-pong handovers to the sum of negative handover events, i.e. the sum of ping-pong handovers, handover failures and radio-link failures, is shown in Figure 6.10(a). The graph shows that increasing the weighting parameters w_{fail} and w_{rlf} leads to an increase in the ping-pong handover to negative event ratio. This is a desired effect since increasing the weighting parameters for the failure events should lead to a reduction of failure events in the network and an increase in ping-pong handovers. On the other hand an accentuation of the weighting parameter w_{pp} leads to a reduction of ping-pong handovers which is the opposite case and desired as well. Having a closer look at the weighting parameter combination of $w_{fail} = w_{rlf} = 10$ and $w_{pp} = 1$ discloses that roughly 62 % of all negative handover events in the network are ping-pong handovers and the remaining 38 % are failure events. Even though the weighting parameter for the failure events is set to a high value more than a third of all negative events are still failure events. This is caused by the fact that significantly more ping-pong handover events are observed for Low_{HOPs} compared to failure events (more than ten time more ping-pong handovers, see Figure 6.4), which leads to a HOP selection with failure events. The vertical bars in the figure indicate the standard deviation of the ping-pong handover to negative event ratio. The standard deviation is larger than 20 % for many weighting parameter settings. This shows that the simulation scenario is heterogeneous resulting in a deviation of the impact of weighting parameter settings of the individual cell performance.

The ratio of the failure events to the total number of handover related events is visualized in Figure 6.10(b). The graph points out that increasing the weighting parameters w_{fail} and w_{rlf} up to a value of ten fails in reducing the amount of failure events in the network significantly. This can again be explained by the significantly higher amount of ping-pong handover events for small handover control parameter settings. Increasing the weighting parameter for the ping-pong handovers leads to a rising number of failure events up to more than a third of all handover related events in the network. While this behaviour is as expected, the high ratio of failure events can be explained by the assumption of a

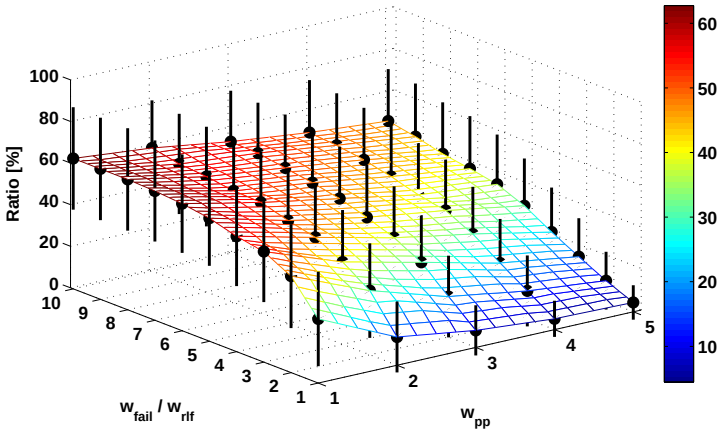

(a) Ping-pong handover (N_{pp}) to negative event (N_{neg_events}) ratio

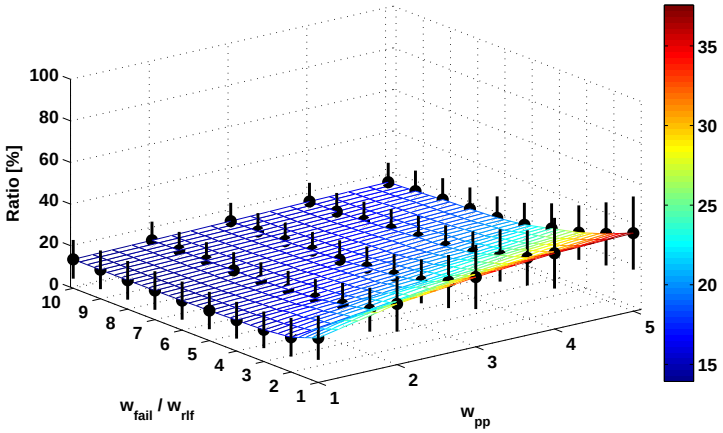

(b) Failure event (N_{fail_events}) to handover related event ratio

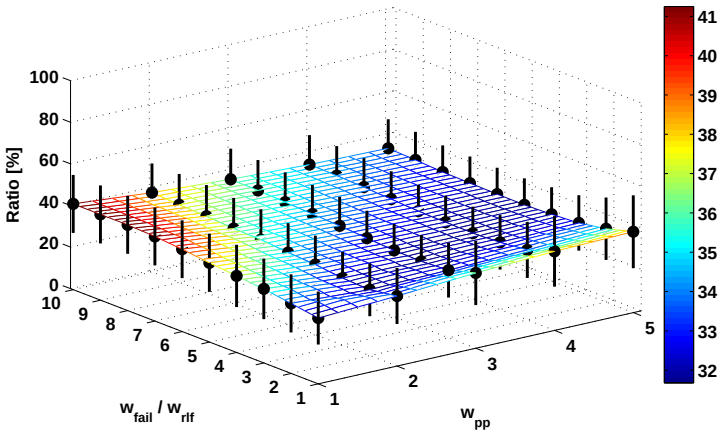

(c) Negative event to handover related event (N_{hr_events}) ratio

Figure 6.10: Impact of the weighting parameter settings on the handover performance in the Hanover scenario

fully loaded network (full-interference) leading to high interference from all cells. Peering the negative handover event to a handover related event ratio, given in Figure 6.10(c), reveals one fundamental characteristic of the HPI_{sum}-based handover optimisation, i.e. the minimum number of negative handover events in the network is observed for equal settings of the handover weighting parameters w_{pp}, w_{fail} and w_{rlf}. As described before the increase of negative events for higher failure weighting parameters is caused by additional ping-pong handovers and the increase in negative events for higher ping-pong weighting parameters by additional radio-link failures. To understand this connection between the ping-pong handovers and failure events is essential for the definition of the optimisation target and the definition of the weighting parameter settings. Once the HOP with the lowest amount of negative handovers is identified (equal weighting parameter settings), better performance of one HPI can only be achieved by worse performance of another HPI.

A closer look at the HOP selection of the individual cells subject to the weighting parameter settings is shown in Figure 6.11. The bar diagrams 6.11(a) and 6.11(b) show a TTT range of 0.1 s to 1 s and a HYS range of 0 dB to 5 dB for the HOP selection in the individual cells with accentuation of the ping-pong handover weighting parameter ($w_{pp} = 5$ and $w_{pp} = 3$). While the range of TTT and HYS parameters maintains for other weighting parameter settings (Figures 6.11(d) to (f)), a trend towards only two best performing HOPs for the majority of the cells can be observed. Nevertheless, the bar diagrams clearly underline the need for handover parameter optimisation in the network by the huge span of selected HOPs for varying weighting parameter settings.

One of the important questions for simulations in the area of SON is the impact of the simulation scenario as well as the used system models on the simulation results and evaluation of the optimisation algorithms. A first indication is given by a comparison of the weighting parameter impact on the system performance between the Hanover scenario and the 3GPP-Scenario. The results for the analysis of the weighting parameter impact on the system performance in the 3GPP-Scenario are depicted in Figure 6.12 and 6.13. The ping-pong handover to failure event ratio shown in Figure 6.12(a) confirms the trends of the analysis of the Hanover scenario. The difference is that weighting parameter settings, allowing for handover operating points with roughly 5 % failure events or roughly 1 % ping-pong handover events in the network, exist. Consequential it is possible to tune the handover parameter settings to match the requirements of a network operator in this scenario. Figure 6.12(b) reveals that the failure event ratio increases almost linearly with increasing ping-pong handover parameter settings. The share of

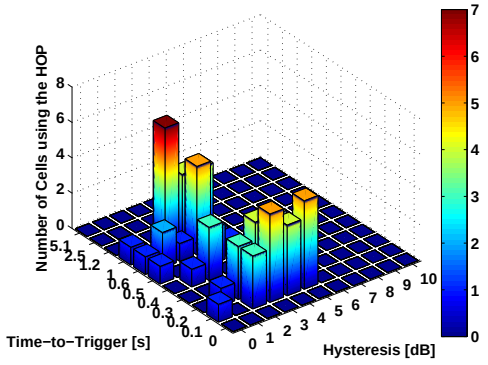

(a) Set 2 ($w_{pp} = 5, w_{fail} = w_{rlf} = 1$)

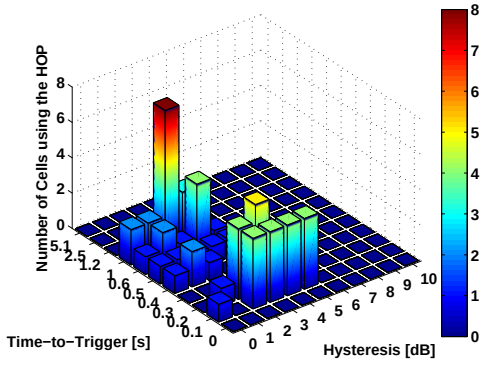

(b) Set 3 ($w_{pp} = 3, w_{fail} = w_{rlf} = 1$)

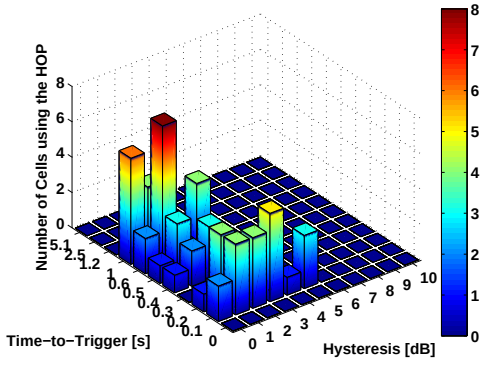

(c) Set 4 ($w_{pp} = 1, w_{fail} = w_{rlf} = 1$)

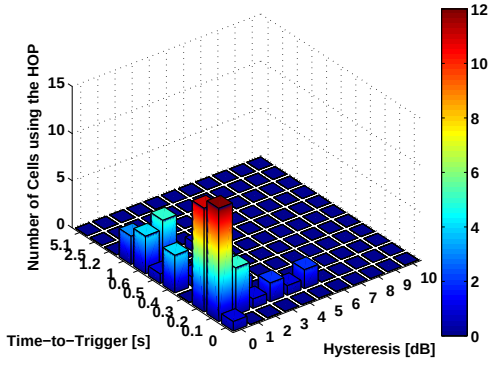

(d) Set 5 ($w_{pp} = 1, w_{fail} = w_{rlf} = 3$)

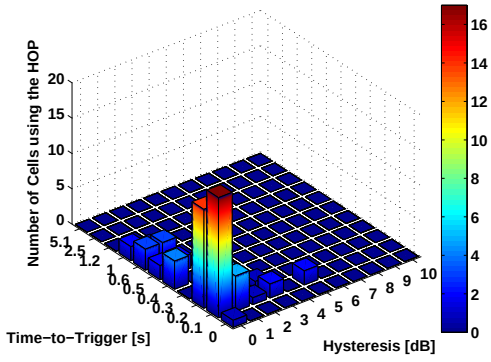

(e) Set 6 ($w_{pp} = 1, w_{fail} = w_{rlf} = 5$)

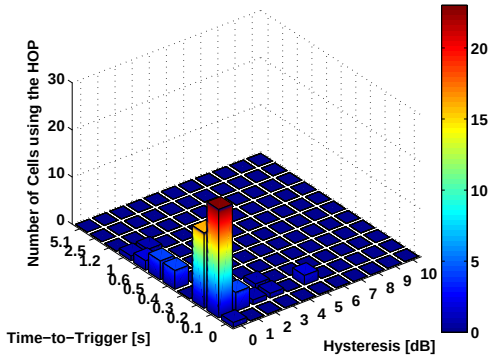

(f) Set 7 ($w_{pp} = 1, w_{fail} = w_{rlf} = 10$)

Figure 6.11: HOP selection subject to the weighting parameter settings in the Hanover scenario

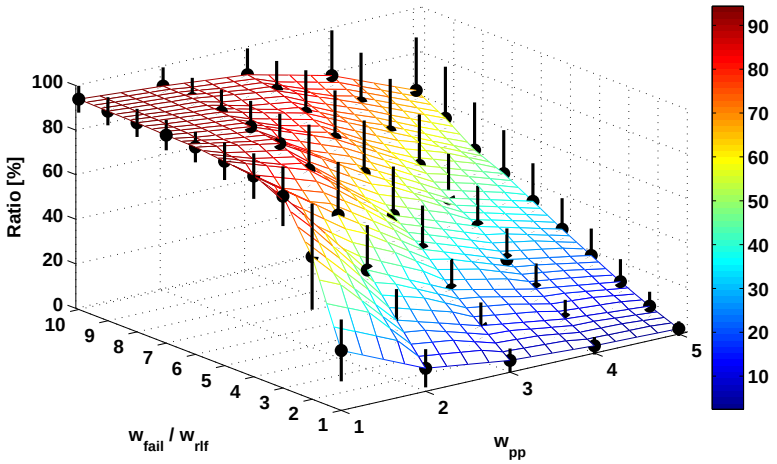

(a) Ping-pong handover to failure event ratio

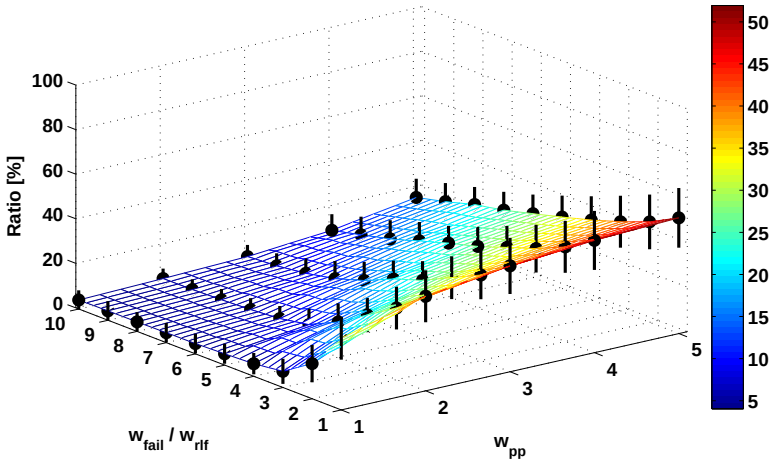

(b) Failure event to handover related event ratio

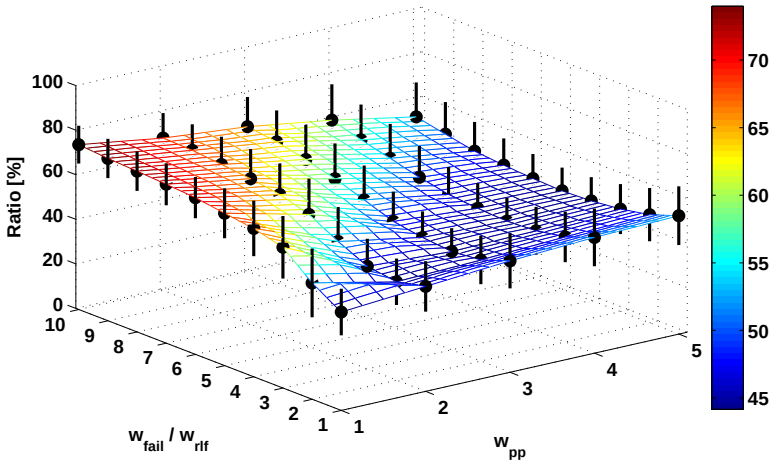

(c) Negative event to handover related event ratio

Figure 6.12: Impact of the weighting parameter settings on the handover performance in the 3GPP scenario

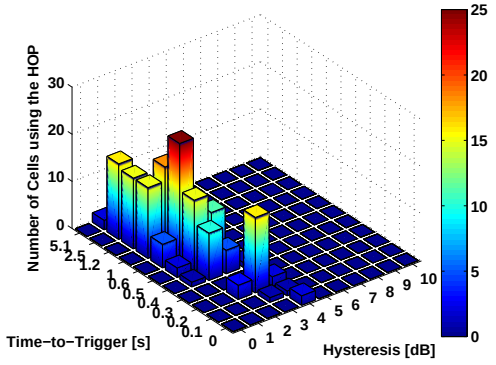

(a) Set 2 ($w_{pp} = 5, w_{fail} = w_{rlf} = 1$)

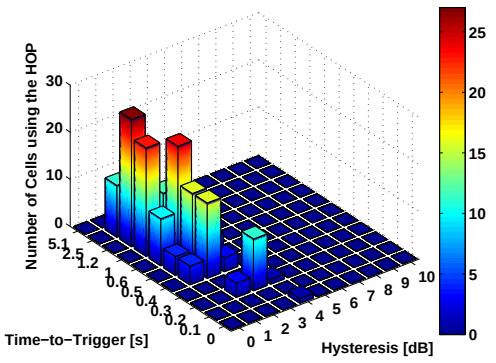

(b) Set 3 ($w_{pp} = 3, w_{fail} = w_{rlf} = 1$)

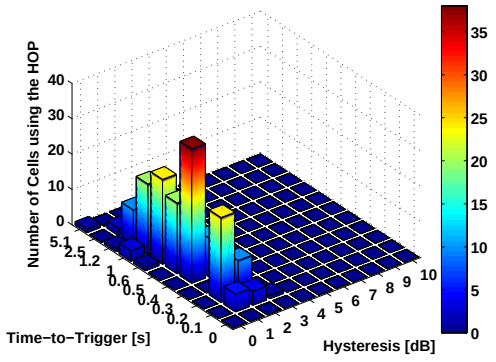

(c) Set 4 ($w_{pp} = 1, w_{fail} = w_{rlf} = 1$)

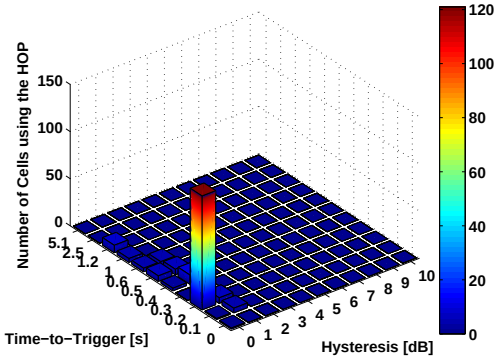

(d) Set 5 ($w_{pp} = 1, w_{fail} = w_{rlf} = 3$)

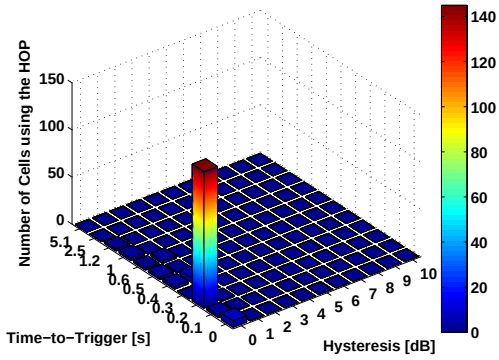

(e) Set 6 ($w_{pp} = 1, w_{fail} = w_{rlf} = 5$)

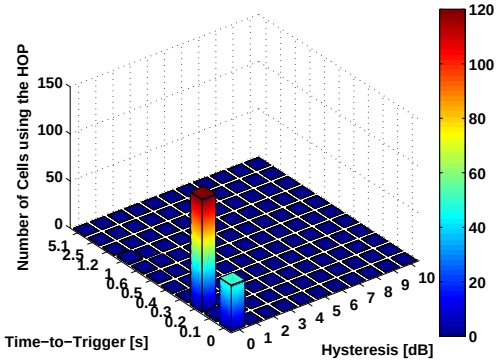

(f) Set 7 ($w_{pp} = 1, w_{fail} = w_{rlf} = 10$)

Figure 6.13: HOP selection subject to the weighting parameter settings in the 3GPP scenario

negative handover events in all handover related events is above 40 % for all weighting parameter settings as depicted in Figure 6.12(c). Again equal weighting parameter settings lead to the lowest total amount of negative handover events as expected but avoiding failure events by $w_{fail} = w_{rlf} = 10$ and $w_{pp} = 1$ causes a ping-pong handover ratio of about 70 %. The impact on the signalling traffic in the network would be severe for this handover parameter configuration.
The assessment of the HOP selection in the 3GPP-Scenario is given in Figure 6.13. In the case that the optimisation target is the avoidance of ping-pong handovers (Figure 6.13(a) and (b)) the range of HYS values for the selected HOPs is limited to 1 dB to 4 dB. The importance of the optimisation of the TTT value is escalated in this case as the values range from 0 s to 5.1 s. However, the prevention of failure events is the more likely case. Figures 6.13(d) to (f) reveal that the optimisation of the handover parameters is marginal in this case since the HOP using a HYS of 0 dB and a TTT of 0.2 s clearly shows the best performance in almost all cells in the network. This fact might lead to a conclusion of no need for optimisation of the handover parameters. This comparison highlights the importance of the simulation scenario and system models for the analysis of the performance and the need for handover optimisation algorithms.

6.4 Impact of the Network Load on the Handover Performance

In Section 6.1 the impact of the network configuration and load situation on the handover performance was identified as potential disturber with a successful evaluation of the handover performance. While the impact of network configuration changes on the cell borders and best server areas is obvious, the impact of network load changes is more difficult to rate. This is because load changes do not influence the RSRP measurements and thus have no impact on the cell borders and best server areas. But load changes do have a major impact on the RSRQ measurements and UE SINRs as the interference originated from resource blocks used in surrounding cells is influenced by the resource block occupation in these cells. The impact of the network load on the SINR calculation in our system-level simulations was introduced in Equation 5.5, i.e the cell load linearly increases the interference from the cells. In reality, the SINR estimation is complicated by the scheduling algorithms which are not standardized and left to the network operators. The scheduling algorithms decide which resource is used to transmit or receive data to or from a UE. Therefore, SINR estimation models are used for the scheduling algorithms to

identify a good resource distribution on the UEs. Nevertheless, the load dependent SINR calculation used in our system-level simulations allows modelling the general impact of load condition changes.

The influence of the UE SINRs on the handover performance of a cell is that in the case of lower interference power (low network load) the UEs can deeply penetrate the best serving area of a neighbouring cell without loosing the connection to the SeNB. Hence, higher HYS and TTT values can be selected as handover control parameters. This minimises the risk for ping-pong handovers and leads to better handover performance in the cells. In high load situations it is necessary to hand over the UEs timely to the TeNBs to avoid radio-link failures. Thus lower handover control parameters should be selected. However, it needs to be investigated how strong the load impact on the handover performance is.

To evaluate the network load impact on the handover performance, system-level simulations in the Hanover scenario are conducted. For the calculation of the UE SINRs the interference power is not calculated from the cell load caused by the connected users in this case. As introduced in Equation 5.5, the SINR calculation model allows to set the cell load used for the SINR calculation to fixed values. This enables system-level simulations in stable load conditions. Ten simulation runs with a fixed cell load varying from 10 % to 100 % are conducted, e.g. in one simulation run the cell load considered for the SINR calculation is set to 10 % in every cell in the simulation scenario. A cell load of 0 % is not considered as a completely empty network is fairly unrealistic and an optimisation to the conditions in an empty network is unnecessary. As before, for all 65 cells considered in the evaluation the best performing HOP for the complete simulation time is identified. Especially for low load situations several HOPs show the same performance. This is why the total number of selected HOPs is larger than 65 in the following performance assessment.

Figures 6.14 and 6.15 show the HOP selection of the cells dependant on the network load. In low load situations (Figures 6.14(a) and (b)) good handover performance is observed for the majority of the HOPs. The only exception are a HYS value of 0 dB and a combination of high HYS and TTT values. The results points out that in low load situation HYS values higher than 10 dB can be useful as standardized by 3GPP (Section 3.2). Moreover, it can be concluded that higher HYS values (5-10 dB) in combination with a TTT value of 0 s show the best performance in almost all cells. This clarifies that in low load situations the probability for a successful handover increases if the UE deeply penetrates the serving area of the TeNB.

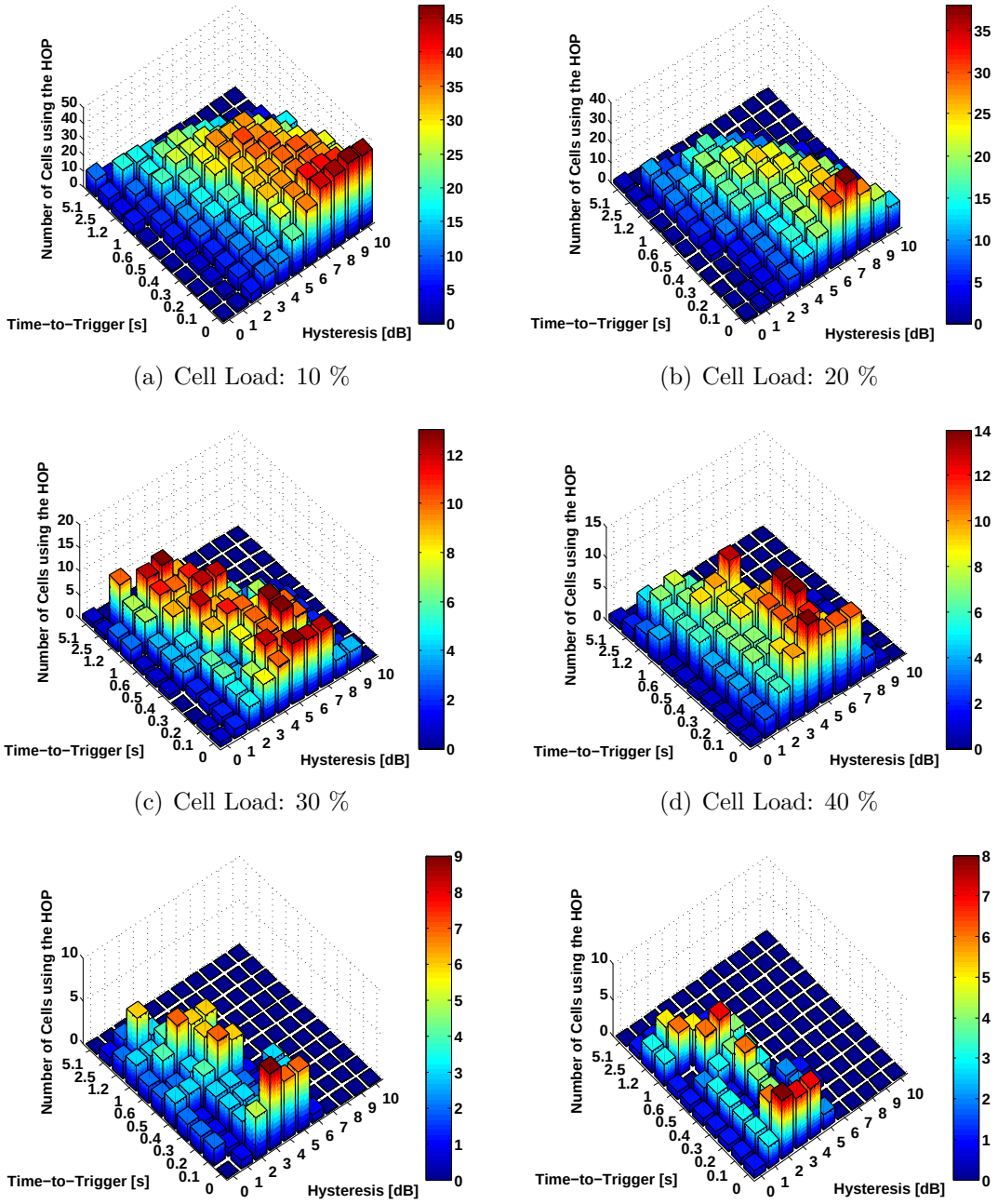

(a) Cell Load: 10 %

(b) Cell Load: 20 %

(c) Cell Load: 30 %

(d) Cell Load: 40 %

(e) Cell Load: 50 %

(f) Cell Load: 60 %

Figure 6.14: Network load dependant best HOP selection of the cells in the Hanover scenario

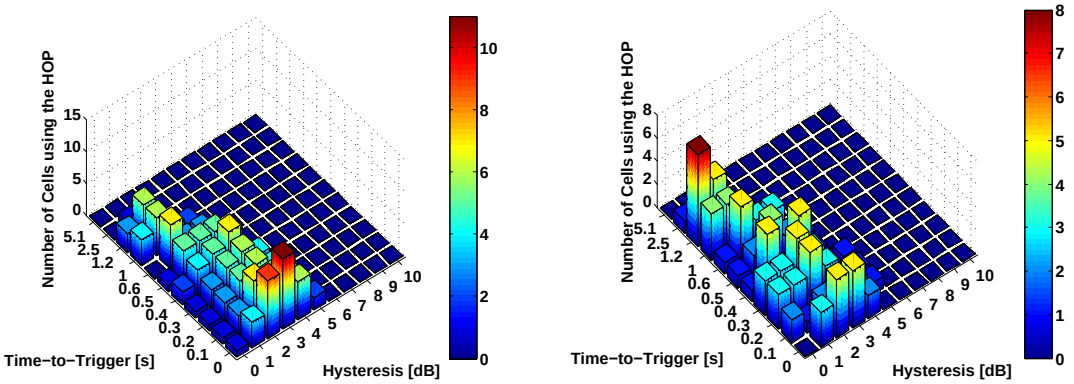

(a) Cell Load: 70 %

(b) Cell Load: 80 %

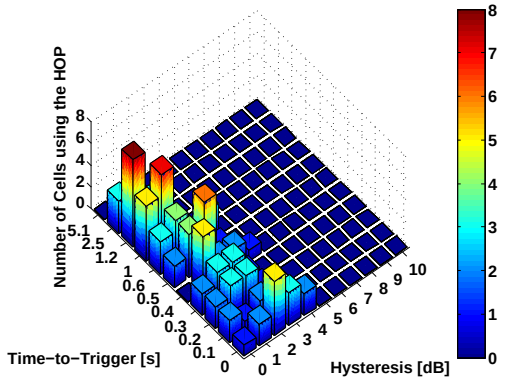

(c) Cell Load: 90 %

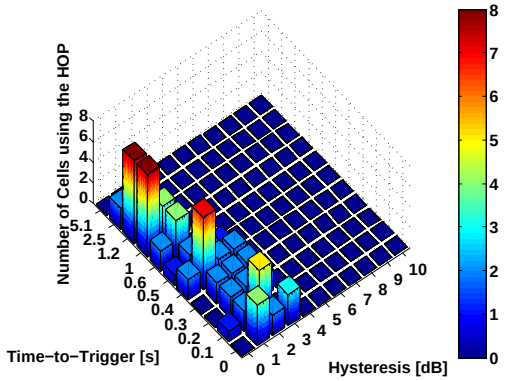

(d) Cell Load: 100 %

Figure 6.15: Network load dependant best HOP selection of the cells in the Hanover scenario

A special HOP selection behaviour can be observed in the case of a network load of 30 % (Figure 6.14(c)). It is not possible to identify a clear winner among the HOPs as a huge number of HOPs is selected in similar incidence as best performing HOP in the individual cells. As one HOP is seen as best performing HOP by only 13 cells in this simulation, it becomes clear that the selection of one handover control parameter set for all cells will not lead to optimal handover performance in the network. Increasing the network load to values from 40 % to 70 % (Figure 6.14(d) to Figure 6.15(a)) leads to best performing HOPs with 0 s TTT and HYS values between 2 dB and 5 dB. However, for some cells it is beneficial to select lower HYS values in combination with higher TTT values. This indicates that in medium load situations it is hard to predict if a combination of medium HYS values with very low TTT values or lower HYS values with higher TTT values will lead to better handover performance. The optimisation algorithm needs to identify the area of better performance.

In high load situations (Figures 6.15(b) to (d)) the trend of better handover performance changes to smaller HYS values in combination with higher TTT values. The conclusion from this result is that in the case of high interference from neighbouring cells it is necessary to switch to the TeNB in the cell border area. To avoid ping-pong handovers the better signal strength of the TeNB has to be ensured by high TTT values. Still even in the case of a fully loaded network some cells benefit from HYS values of 1 dB to 3 dB in combination with TTT values of 0 s or 0.1 s. HYS values higher than 3 dB are not selected as handover control parameter in any cell in the case of a network load of 100 %.

The results illustrated in Figures 6.14 and 6.15 demonstrate that the network load impacts the HOP selection in the cells. Though it is still unclear, how intense the impact on the handover performance is. Thus we further process the results of the system-level simulations in Table 6.4. It shows the results of a deeper analysis in two sets given in the first and last three rows of the table. The same tables for the individual HPIs can be found in Appendix D. The first row of a set, called "Optimised", gives the mean handover performance (HPI_{sum}) of all 65 cells evaluated in the network in the case that the best HOPs subject to the load situation are selected. Note that the weighting parameters for the HPI_{sum} are set to one in this analysis, i.e. the numbers reflect the negative handover rate in the network. The results of the optimised case show that the handover performance is much better in the case of a low network load (0.22 % negative handover rate in the case of 10 % network load) than in higher load situations (14.97 % negative handover rate in the case of 100 % network load). The negative handover rate constantly increases for higher network load except for a load of 70 % where the handover performance slightly increases.

The second row of a set gives the handover performance for the case that the cells select the best HOP identified for a network load of 70 % for every considered load condition. A network load of 70 % is considered since the real networks are usually designed for a daily busy hour load of 70 %. The performance degradation between the optimized case and the optimal configuration for 70 % load is listed in row three of set one. In the case that the system load is 70 % as well, the performance degradation is zero per definition. A load variation in the network by 10 % (to 60 % or 80 % network load) leads to a performance degradation of 3.37 % or 4.89 % already. For the case that the traffic further increases a maximum performance degradation of 11.15 % is observed for a network load of 100 %. For lower load situations the performance degradation is smaller. For a network load of 30 % a peak value of 6.97 % performance degradation is observed. The implication of the analysis is that a handover control parameter configuration, optimised for a certain

	Cell Load								
	10%	30%	40%	50%	60%	70%	80%	90%	100%
Optimised	0.22	2.21	3.19	5.60	7.35	7.33	11.07	12.73	14.97
Optimised (Load 70%)	6.77	9.18	7.97	9.95	10.72	7.33	15.96	21.32	26.12
Performance Degradation	6.55	6.97	4.78	4.35	3.37	0	4.89	8.60	11.15
Optimised	0.22	2.21	3.19	5.60	7.35	7.33	11.07	12.73	14.97
Optimised (Load 100%)	11.11	12.67	12.59	13.85	14.30	12.19	15.13	14.93	14.97
Performance Degradation	10.89	10.46	9.40	8.24	6.95	4.85	4.06	2.20	0

Table 6.4: Mean handover performance (HPI_{sum}) as a function of the cell load. Optimised performance to the current cell load, optimised for a fixed cell load and the performance degradation.

load level, leads to a significant performance degradation in other load conditions. Thus an optimisation to the load condition is desirable.

The second set of values listed in the last three rows of the table is dedicated to the case that the handover control parameter settings optimal for a network load of 100 % are used in the network. Row four is a copy of row one to ease the comparability of the configuration changes. The handover performance for a load level of 100 % is given in row five while row six shows the performance degradation between the optimized case and the optimal settings for a load level of 100 %. In this case the performance drops by 2.20 % to 4.06 % for a load level of 90 % or 80 % respectively. Lower load levels lead to a maximum performance degradation of 10.89 %. These results fortify that the load level in the network has to be regarded by the handover optimisation even if the performance degradation for small load changes in the network is lower in this case.

It seems odd to select the optimal settings for a fully loaded network in an analysis like this. But this case is relevant since some handover optimisation approaches primarily rely on the RSRP measurements to identify the optimal handover control parameters. As mentioned before the RSRP measurements are not influenced by the load level in the network. Hence, it is impossible to identify the optimal configuration for the load level in the network.

The conclusion from the evaluation of the load impact on the handover performance is that the network load has a severe impact on the handover performance and thus the HOP selection for optimal handover performance in the cells. This fact has to be regarded for the design of the handover optimisation algorithms.

6.5 Statistical Analysis of the Handover Performance Indicators

The handover performance indicators are the basis for the identification of the best handover operating point and hence the handover parameters for the cells in a mobile communication system. A pending question for the optimisation is the necessary observation time for the handover performance in a selected HOP to get reliable input data for the optimisation algorithms. The HPI observation time has significant impact on the handover optimisation. On the one hand it influences the adaptation speed of the handover parameters to a new configuration in the network which will usually be a multiple of the observation time. On the other hand it limits the noticeability of temporary handover effects and hence the chance for any optimisation of the handover parameters for short-time effects. Additionally it depends on the design of the optimisation algorithm how many observation cycles are needed to identify a more optimal handover configuration. We will elaborate on the impact of the algorithm design in Chapter 7.
Another important question that needs to be answered is whether the HPI observation time should be a parameter in the time domain, i.e. a fixed observation window given in seconds, or a parameter in the event domain, i.e. a fixed number of handover related events taken into account for the compilation of the HPI values, hereafter named time domain observation window or event domain observation window, respectively. In the case of a time domain observation window the amount of handover related events regarded for the compilation of the HPIs varies over time. This influences the HPIs in manifold manner. First, the accuracy of the HPIs becomes dependent on the current load situation of the cell, assuming that a higher cell load increases the amount of handover related events as well. As a consequence, the impact of a single negative handover event on the HPIs is dependent on the cell load and hence the traffic situation in the cell. This effect is negligible for high cell load since the HPIs typify the relative performance of incidences to all handover related events and get more precise in this case. Problems arise for low load situations. In this case, a single negative event could significantly increase a HPI and trigger an optimisation action. It is questionable if this

single negative event represents the handover performance of the HOP and justifies the optimisation of the handover control parameters.

Furthermore, a time domain observation window even impacts the comparability of the handover performance of two HOPs in the same cell. Given the results of Section 6.2 and assuming that the handover performance of a Low_{HOP} is compared to any other HOP with higher handover control parameters of the same cell, it is presumable that a higher amount of ping-pong handovers will be observed in the Low_{HOP}. Let us further assume that the total number of failure events (see Section 3.3) is the same for both HOPs. In the case of the Low_{HOP}, the higher amount of successful handovers, caused by the additional ping-pong handovers, lead to a lower failure event ratio for the Low_{HOP} and hence to the assumption that less failure events occured. In the case of additional constraints for the optimisation target that limit the failure event ratio, the Low_{HOP} could be identified as the better HOP leading to a communication overhead due to the additional handovers.

If the HPI observation time is defined in the event domain, every handover related event has the same impact on the HPIs of a HOP. In this case the observation time window is variable and dependent on the traffic conditions of a cell. For high load conditions the observation time window will be smaller since the fixed number of handover events is reached faster than for low load conditions. Consequently, the HPIs represent rather 'short-time' effects for high load situations and rather 'long-time' effects for low load situations. If the observed cell is in a high load condition and many handovers are initiated, setting the HPI observation window in the event domain limits the accuracy of the HPIs even though a larger observation window would be acceptable. Incidentally, the accuracy of the HPIs is defined by the number of handover related events directly, i.e. setting the HPI observation time to 100 handover related events leads to an accuracy of 1% for the HPIs. For low load conditions handover related events that took place hours ago could still be included for the compilation of the HPIs. This queries optimisation of the handover parameters in very low load situations, e.g. at night time.

The following statistical analysis of the HPIs aims at the definition of the minimum observation time to ensure a successful optimisation of the handover control parameters. Part of this analysis will be the investigation of the two options for the observation time definition in the time or event domain. Moreover, the analysis will focus on the characteristics of the HPIs to answer the question how different the indicators have to be in order to allow the identification of more optimal handover control parameters and on the gain and loss of handover performance for sub-optimal settings if the identification fails.

The outcome of this analysis is used for the development of the handover optimisation algorithms in Section 7.1 and 7.2.

The development of the HPI_{sum} for different observation window sizes is given in Figure 6.16. Each of the six figures shows the HPI_{sum} for one HOP and five exemplary observation windows ranging from 10 s to 400 s. The results are taken from the same simulations that have been executed for the analysis of the impact of the weighting parameter values on the performance of the network in Section 6.3 (see Table 6.3 for simulation parameter details). All weighting parameters have been set to one in this case ($w_{pp} = 1, w_{fail} = 1, w_{rlf} = 1$). Every curve gives the progression of the HPI_{sum} value, which is based on the observation window size, taking into account all handover related events in the observation time. Hence, the values are based on moving observation windows of the last seconds. The figures show values for 600 s simulation. The first 400 s of the complete simulation time of 1000 s have been cut off since the observation time is too short for the largest observation window resulting in zero values and increased visibility.

The HPI_{sum} values for the HOP with a HYS of 2 dB and a TTT of 1 s are displayed in Figure 6.16(a). For this HOP the HPI_{sum} values heavily fluctuate for small observation window sizes like 10 s. The fluctuations reduce significantly for larger observation windows. This expectable trend is confirmed by the other figures representing the handover performance of different HOPs of the same cell. In order to clarify the importance of this behaviour for the later optimisation task let us get back to the meaning of one single HPI_{sum} value. This value represents the handover performance of the last e.g. 400 s in the network taking into account all handover related events in this time frame. To compare the performance of this HOP with any other HOP in the same cell, the handover control parameters have to be changed to the settings for the new HOP. After the observation time for the second HOP passed, another HPI_{sum} value representing the handover performance of this HOP is available and a comparison of these two HOPs is possible. This means a single value of the curves, representing the observation window size 400 s, is taken into account for the comparison of the two different HOPs. If the fluctuations of the HPI_{sum} values are large, the comparison of the handover performance of two HOPs implies a high risk of misinterpretation and slows down or prevents the optimisation. Hence, assuming that the traffic conditions in a cell stay constant for the observation time of the two HOPs, the fluctuations of the HPI_{sum} values should be small enough to enable a comparison of the handover performance of the HOPs.

The HPI_{sum} values shown on the y-axis of Figures 6.16(a) to (f) give the negative

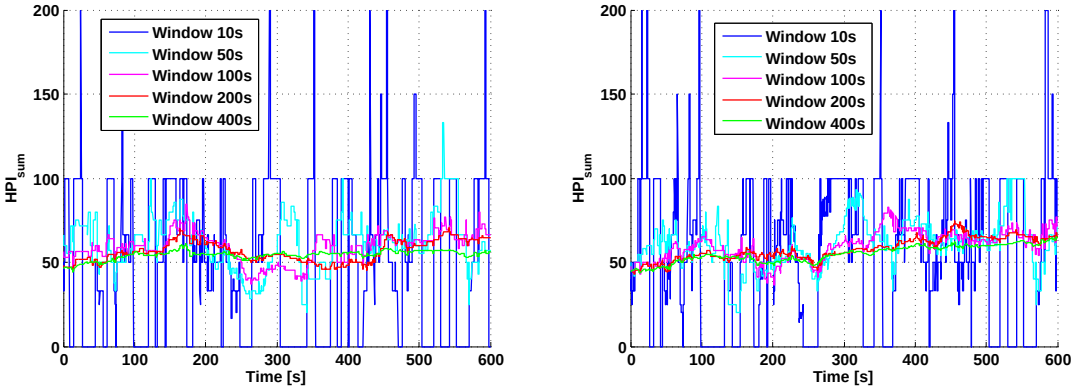

(a) $HYS = 2dB, TTT = 1s$ (b) $HYS = 1dB, TTT = 0.6s$

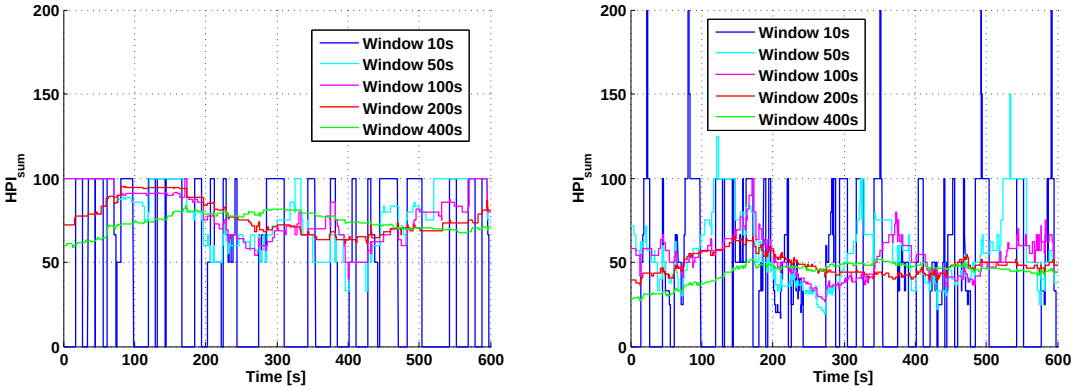

(c) $HYS = 5dB, TTT = 0.1s$ (d) $HYS = 3dB, TTT = 0.2s$

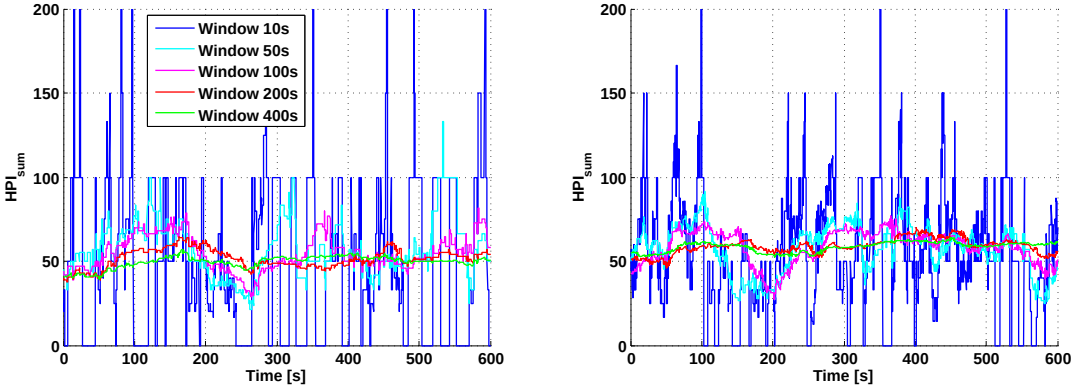

(e) $HYS = 2dB, TTT = 0.4s$ (f) $HYS = 0dB, TTT = 0.1s$

Figure 6.16: Handover performance (HPI_{sum}) of cell 31 for different HOPs and time domain observation window sizes

handover event ratio for the individual HOP and observation window. This is because the selected weighting parameter set used for the compilation of the HPI_{sum} values is $w_{pp} = 1, w_{fail} = 1$ and $w_{rlf} = 1$. In this case the individual negative handover event ratios, i.e. ping-pong handover ratio, handover failure ratio and radio-link failure ratio, are summed without any special weighting and hence give information about the total amount of negative handover events. For any other weighting parameter set this is not the case. Nevertheless, the HPI_{sum} values exceed the awaited maximum value of 100 % in Figures 6.16(a), (b), (d), (e) and (f) for small observation window sizes. This is caused by the timing for the detection of a ping-pong handover. If a user is handed over to a target cell and returns within the time span $T_{crit-pp}$ (defined in Section 3.3), a ping-pong handover is detected. The ping-pong handover is added to the handover statistics instantly in this case. The successful handover of that user to the selected target eNB happened earlier and therefore is regarded in the handover statistics earlier as well. Resulting from that the ping-pong handover is still regarded in the handover statistics when the successful handover of that user already passed the observation window. For short observation window sizes the observation time sometimes includes only a few handover events. If only one successful handover event later detected as a ping-pong handover and the ping-pong handover detection of an earlier handover are left in the handover statistics for the observation time, a HPI_{sum} value of 200 % is calculated. This behaviour could be avoided by deleting the detected ping-pong handover and the earlier successful handover event simultaneously from the handover statistics. The drawback of this solution would be that the ping-pong handover events are regarded for the compilation of the HPI_{sum} values for a shorter time frame as the positive (successful) handover events. Moreover, this time frame would be dependent on the current detection time span for ping-pong handover events $T_{crit-pp}$ which itself is dependent on the current TTT settings. This would handicap the comparability of the HPI_{sum} values and make HOPs with a higher ping-pong handover ratio more attractive for the selection of the best HOP in the optimisation task. Therefore, the ping-pong handovers are left in the handover statistics for the same time span as there corresponding successful handover events.

On closer inspection of Figures 6.16(d) and (f) a significant difference between the curves for the observation window size of 10 s leaps to the eye. In Figure 6.16(d) the blue curve jumps up and down on a limit number of HPI_{sum} values and holds individual values for periods of up to 10 s. In Figure 6.16(f) the curve assumes an increased number of HPI_{sum} values and holds one value for a shorter time span. The reason for this

behaviour is the difference in handover related events that can be observed in the corresponding HOPs of the figures. In the HOP represented by Figure 6.16(f) the HYS and TTT values are very low resulting in a high number of executed handovers in the cell. Hence, the calculations of the HPI_{sum} values base on more handover events which increases the significance of the values. The results for an observation window size of 400 s confirm the increased significance since the HPI_{sum} values vary between 30 % and above 50 % in Figure 6.16(d) and only between 50 % and above 50 % in Figure 6.16(f). These figures verify the assumption that the number of handover related events taken into account for the compilation of the HPI_{sum} values impact the significance of these values. Moreover, the significance varies between HOPs of the same cell for time domain observation windows.

The development of the HPI_{sum} for different event domain observation windows is given in Figure 6.17. Each of the six figures shows the HPI_{sum} for the same HOPs as used in Figure 6.16 and five exemplary numbers of handover related events ranging from 5 to 100 . Again, the results are taken from the simulations that have been executed before in Section 6.3 (see Table 6.3 for simulation parameter details). As for the time domain observation windows all weighting parameters have been set to '1' for the evaluation ($w_{pp} = 1, w_{fail} = 1, w_{rlf} = 1$). The compilation of the HPI_{sum} values is based on a handover related event history that is implemented as a list of a fixed length, i.e. the number of handover related events considered. The list works as a shift register with First In First Out (FIFO) logic. This means if a new handover related event is added to a list that reached the desired number of handover related events already, the oldest event is deleted from the list. In this case, the HPI_{sum} values are calculated from a moving window with a fixed number of events but variable in time. The figures show values for the complete simulation time (1000 s). As the first HPI_{sum} value is calculated when the desired number of handover related events is reached the curves start at different times depending on the HOP.

The first eye-catching difference is that for a fixed number of handover events the HPI_{sum} values are rarely larger than 100 % even when looking at the curves for five handover related events. It should be remembered that this happened for the time domain observation windows only in the case that few handover related events laid in the considered time span. In the case of an event domain observation window the minimum number of events is fixed and not dependent on the current traffic conditions in the cell. Hence, the impact of these undesired misinterpretations of the current handover performance is reduced due to the fixed number of considered handover events. Furthermore the curves

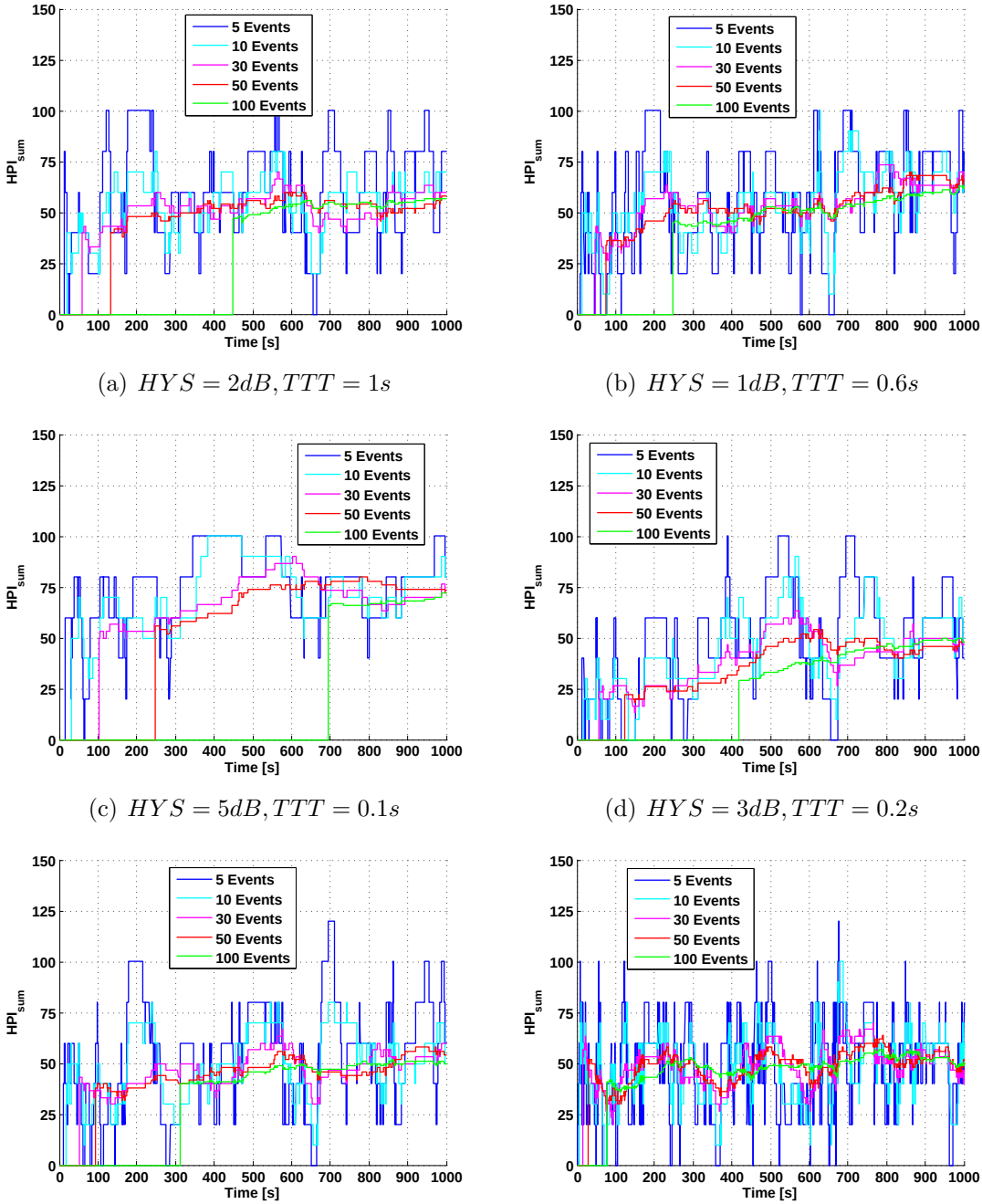

(a) $HYS = 2dB, TTT = 1s$

(b) $HYS = 1dB, TTT = 0.6s$

(c) $HYS = 5dB, TTT = 0.1s$

(d) $HYS = 3dB, TTT = 0.2s$

(e) $HYS = 2dB, TTT = 0.4s$

(f) $HYS = 0dB, TTT = 0.1s$

Figure 6.17: Handover performance (HPI_{sum}) of cell 31 for different HOPs and event domain observation window sizes

for the same number of handover related events show similar characteristics for different HOPs. As pointed out before, the HPI_{sum} values are limited to a fixed number due to the fixed denominator in Equations 3.14, 3.15 and 3.16. This can easily be observed for the curves with five handover related events where the HPI_{sum} takes the values {0, 20, 40, 60, 80, 100, 120, ...}. The variance of the HPI_{sum} seems to be similar for curves with the same number of handover related events as well. The main difference between the curves is the stretching along the x-axis that is influenced by the number of handover related events in a certain time frame of a HOP. The comparison of the curves for five handover related events in Figures 6.17(d) and 6.17(f) reveals this effect. The HPI_{sum} values in the first figure keep the same value for longer time spans than in the second figure. Again the reason for this lies in the higher number of handover related events in the HOP for the last curve.
The analysis in this section gives a first indication to the advantages of events domain observation windows. This will further be analysed in the next two sections.

6.6 Identification of the Required Observation Time for the Evaluation of the Handover Performance

In order to use the HPI_{sum} values for the optimization of the handover performance in a communication network, the values need to represent the current handover behaviour. The unanswered question is which quality of HPI_{sum} values is needed and how this quality can be defined. To approach this problem we will analyse the standard deviation of the HPI_{sum} values of all HOPs for different observation windows. The hypothesis is that the standard deviation of the HPI_{sum} values can serve as a quality attribute, i.e. if the standard deviation is low, we can assume the HPI_{sum} value represents the current handover performance. For the analysis we will examine the distribution functions of the HPI_{sum} values for different observation windows. We will show the impact of the observation window on the distribution functions and investigate the probability for a successful identification of the best HOP for a cell. Finally, we will deduce the needed observation window to gain reliable input data for the optimisation of the handover control parameters. The general assumption for this analysis is that the traffic conditions in the cells of the network are stable during the evaluation time. If this is not the case, the identification of a better HOP might fail due to the traffic dependency of the handover optimisation problem.
The HPI_{sum} values for every HOP and observation window are the input random vari-

ables for the calculation of the standard deviation, leading to the problem that these values are per definition not statistically independent. This is because they are generated as a moving average of the handover performance over a certain time (observation window). For clarification the following example is given in which the following conditions are assumed: a simulation step size of 100 ms; a simulation time of 1000 s ;and a observation window size of 10 s. The HPI_{sum} values are calculated every 100 ms starting from the simulation time 10 s up to the end of the simulation. Hence, 9900 HPI_{sum} values are calculated each representing the handover performance aggregated over the last 100 simulation steps. The difference between two subsequent values is only the handover related events of one simulation step, i.e. the statistics for the remaining 99 simulation steps are identical. Thus, the question is whether the standard deviation of the statistically dependent HPI_{sum} values can be calculated in the same way. To answer this question, we will compare the distribution functions of all 9900 values from the example with the 100 disjunct and statistically independent HPI_{sum} values generated every 10 s in the simulation. Disjunct means that no handover related events are used for the compilation of more than one HPI_{sum} value and hence the observation windows do not overlap. If the distribution functions for these two cases are equal or at least very similar, we can use all HPI_{sum} values for the analysis and assume they represent the distribution of the statistically independent values. This is helpful for longer observation windows for which only a few disjunct HPI_{sum} values can be calculated due to the limited simulation time.

To check if the HPI_{sum} values and the disjunct subset of statistically independent HPI_{sum} values follow the same probability distribution, we use the Kolmogorov Smirnov Test (KS-Test) [Stuart08]. The null hypothesis of the KS-Test is that the samples, e.g. sample set N with n observations and sample set M with m observations, are drawn from the same distribution. The test is based on the evaluation of the distance between the two empirical distribution function of the samples. Hence, the null hypothesis H_0 is:

$$H_0 : \quad F_n(x) = F_m(x) \tag{6.2}$$

with $F_n(x)$ the empirical distribution function of sample n and $F_m(x)$ the empirical distribution function of sample m. The alternative hypothesis is that the samples do not follow the same distribution:

$$H_1 : \quad F_n(x) \neq F_m(x) \tag{6.3}$$

To check the distance between the empirical distribution functions of two samples the following test statistic $D_{n,m}$ is used to get the supremum of the distance:

$$D_{n,m} = \sup_x |F_n(x) - F_m(x)| \tag{6.4}$$

The null hypothesis is rejected at significance level α if:

$$D_{n,m} > c(\alpha)\sqrt{\frac{n+m}{nm}} \tag{6.5}$$

where the coefficient $c(\alpha)$ is given in Table 6.5 as a function of the significance level α. The significance level α describes the accuracy of the KS-Test result. For a significance level of 0.05 (5 %) and if the result of the KS-Test is that the null hypothesis is rejected, the probability that the two samples do not follow the same distribution is 95 %. If the null hypothesis cannot be rejected by the KS-Test, it can be seen as a strong indication for the samples following the same distribution. In addition, we perform a visual inspection of the distribution functions to double check the result from the KS-Test.

α	0.10	0.05	0.025	0.01	0.005	0.001
$c(\alpha)$	1.22	1.36	1.48	1.63	1.73	1.95

Table 6.5: Coefficients $c(\alpha)$ for different significance levels α

The result of the KS-Test for different observation windows is shown in Figure 6.18. The figure shows the p-values for different observation windows which is the test result of the KS-Test. The p-value is an equivalent of the test statistic $D_{n,m}$. If the p-value is lower than the significance level α, the conclusion is that the distribution function are not equal. The larger the p-value, the higher is the possibility that the two value sets follow the same distribution. The curves illustrate that the p-values are significantly larger than the significance level in the majority of the cases. The larger the observation window, the lower the p-value gets in a few cases. Nevertheless, the p-value is always larger than the significance level, which translates to a minimum probability of 95 % that the values follow the same distribution. The decrease of the p-values for larger observation windows can be explained by the lower amount of samples that are available for the KS-Test. For an observation window of 100 s only 10 samples generated from disjunct observation windows can be used for the test. A distribution function generated from a very small amount of samples like this can hardly reflect the accuracy of a distribution function based on 9000 samples.

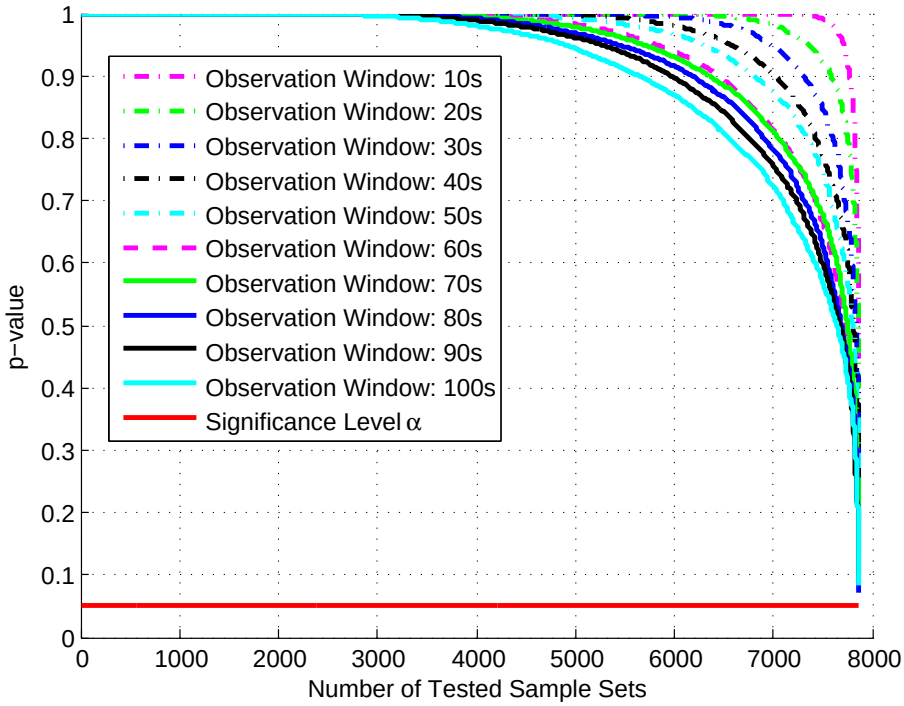

Figure 6.18: KS-Test results for different time domain observation windows

Nevertheless, we will finally check the distributions of some exemplary HPI_{sum} value sets by visual inspection. To assure the universal validity of the KS-Test result, we select the distribution functions of the observation windows from 10 s to 60 s with the lowest p-values. The histograms of the HPI_{sum} values are shown in Figure 6.19. The histogram bars generated from all HPI_{sum} values are plotted next to the histogram bars generated from the disjunct observation windows only. To increase the visibility, the distance between the bars is set to 0.1. The number of values for the disjunct observation windows decreases with increasing observation window size. For the observation window 10 s (Figure 6.19(a)) 100 samples are available resulting in a maximal granularity of 0.01 on the y-axis, i.e. one sample makes one percent of the total samples for the histogram. Only 20 samples are available for the observation window 50 s which causes the impact of 0.05 on the relative frequency.

Except for a few cases the HPI_{sum} values found in the histogram of all values are represented by the disjunct windows as well. The exceptional cases are limited to a low impact on the relative frequency, e.g. values 1.2 and 1.3 in Figure 6.19(a), value 0.8 and 1 in Figure 6.19(b), values 0.2 and 0.9 in Figure 6.19(d) and value 0.6 in Figures 6.19(e) and (f). This can be explained by the limited number of values for the disjunct windows as the probability of getting a value with low relative frequency is low as well. The only

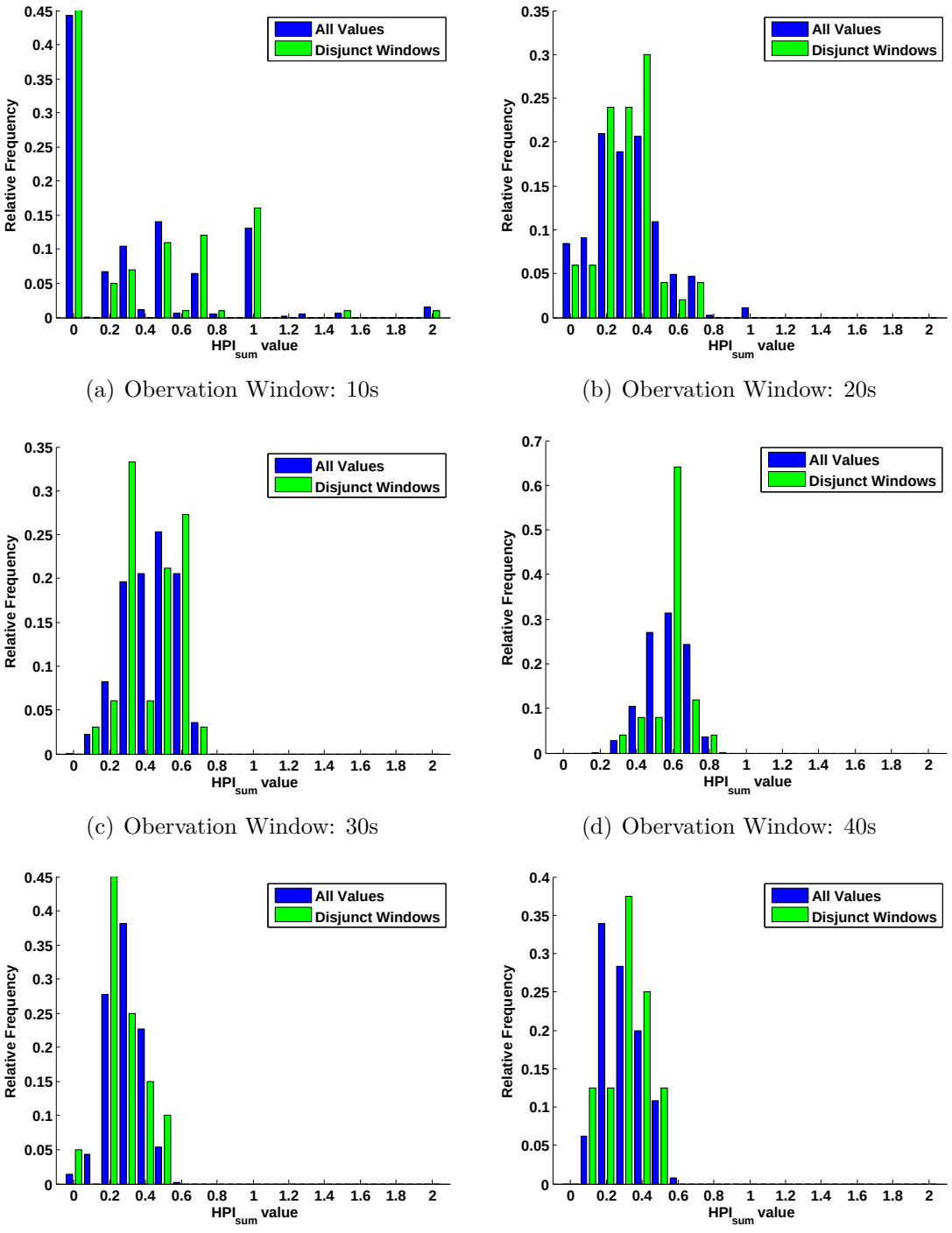

(a) Obervation Window: 10s

(b) Obervation Window: 20s

(c) Obervation Window: 30s

(d) Obervation Window: 40s

(e) Obervation Window: 50s

(f) Obervation Window: 60s

Figure 6.19: Histograms of the HPI_{sum} values for different time domain observation windows (smallest p-value)

example with a slightly higher relative frequency is value 0.1 in Figure 6.19(e). But in this case the impact of one value in the disjunct window histogram is 0.05 which is higher than the relative frequency of value 0.1. Hence, this is not an indication for a different distribution of the HPI_{sum} values. Evidence for a different distribution of the HPI_{sum} values would be a value with significant relative frequency in the middle range of the HPI_{sum} values that is not present in the disjunct window distribution. In that case the observation window, used to generate the HPI_{sum} values, could produce compensation values between extreme cases in the disjunct window case. This behaviour cannot be confirmed by the visual inspection of the histograms. Thus, the conclusion of the result of the KS-Test and the visual inspection of the distributions of the HPI_{sum} values generated by moving observation windows and disjunct windows is that the values come from similar distributions. Consequentially, the assumption for the further work is that all HPI_{sum} values can be used for the statistical analysis of the handover performance indicators.

As a next step we analyse the statistical properties of the HPI_{sum} values and their impact on the comparability of the handover performance in different HOPs. Based on the same simulation results used before, we calculate the standard deviation of the HPI_{sum} values for different observation windows. Since 65 cells are selected for the analysis and the HPI_{sum} values are generated for each of the 121 HOPs, a total amount of 7865 HPI_{sum} value sets is considered. The statistical properties are analysed for time domain observation windows and event domain observation windows. The standard deviations are depicted in Figure 6.20. The sizes of the time domain observation windows $Window_{Time}$ in seconds are:

$$Window_{Time} \in \{10, 20, 30, 40, 50, 60, 70, 80, 90, 100, 120, 140, \\ 160, 180, 200, 250, 300, 350, 400, 500, 600\}$$

The time domain observation windows are limited to a maximum size of 600 s for a simulation time of 1000 s to assure a reasonable amount of HPI_{sum} values for the analysis of the standard deviation.

Figure 6.21 shows the cumulative distribution of the number of handover related events in the 121 HOPs of the 65 considered cells in the network. For roughly 15 % of the HOPs more than 200 handover related events are observed in the simulation time. In only 8 % of the HOPs more than 300 handover related events take place. In order to analyse

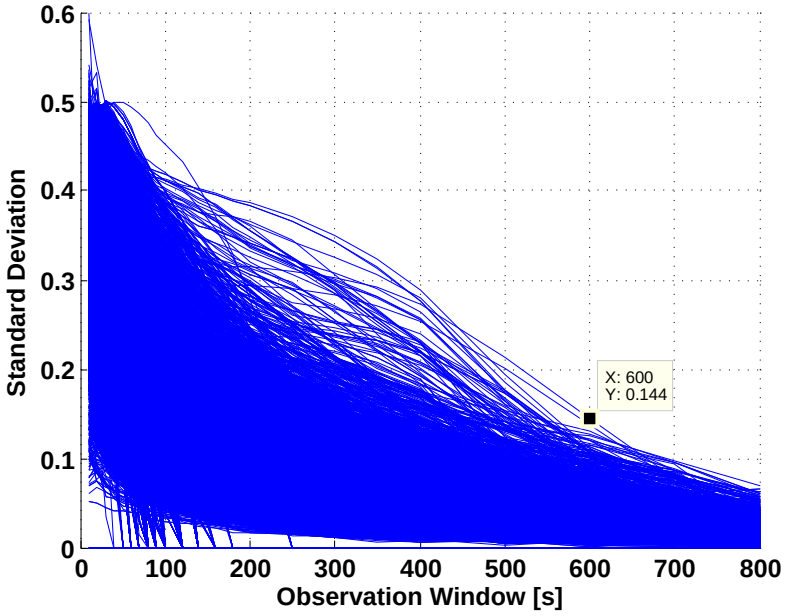

(a) Observation windows defined in the time domain

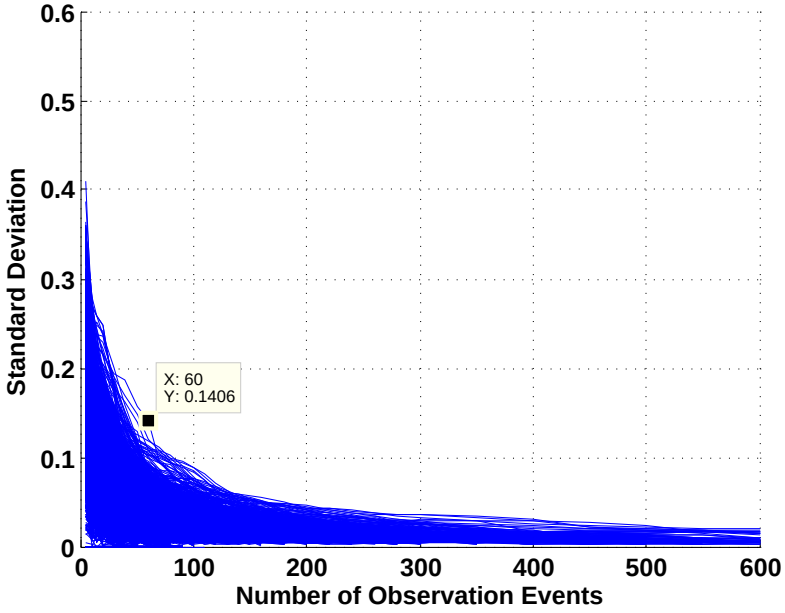

(b) Observation windows defined in the event domain

Figure 6.20: Standard deviations of the HPI_{sum} values for different time and event domain observation windows

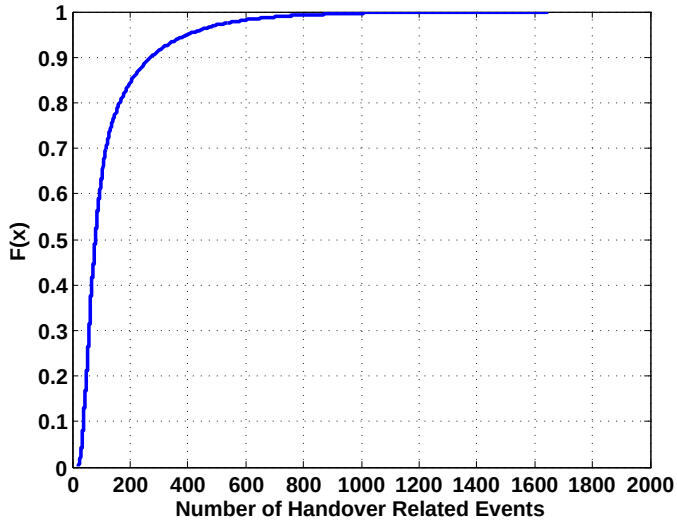

Figure 6.21: CDF of the number of handover related events in all HOPs of all 65 cells

the standard deviation of the HPI_{sum} values based on 200 handover related events, a larger number of events have to take place in the HOPs because the HPI_{sum} values are generated starting from the simulation step in which 200 events have been observed. As for the time domain handover observation windows a reasonable amount of values is needed to avoid boundary effects. Moreover, the analysis needs to cover a reasonable set of HPI_{sum} values to allow generalization of the behaviour of the HPI_{sum} values. Hence, the time event observation windows are defined as:

$$Window_{Event} \in \{5, 10, 15, 20, 30, 40, 50, 60, 70, 80, 90, 100, 110, 120, 130, 140, 150, \\ 160, 180, 200, 220, 240, 260, 280, 300, 350, 400, 450, 500, 550, 600\}$$

The standard deviations for the time domain observation windows in Figure 6.20(a) are generated as follows. For every HOP in the considered cells the HPI_{sum} values are calculated for the observation windows $Window_{Time}$. The first value is calculated when the observation time has passed, i.e. for an observation window of 400s the calculation starts in simulation time step 4000 (400 s). Due to the fixed time span the number of HPI_{sum} values is equal in every HOP for the same observation window. Nevertheless, on the one hand it is possible that no handover related event happened in the observation window and the handover performance drops to zero representing an error free mobility in the network. On the other hand one negative handover event, e.g. a radio-link failure, results in a handover performance of one representing a 100 % negative handover event

probability. Thus, the standard deviation of the HPI_{sum} values for small observation windows is higher. For larger observation windows the standard deviation slowly decreases reaching a maximum level of ~ 0.145 for 600 s observation time. This means that standard deviation of the handover performance indicator is still in the range of 14.5 %. This deviation is far to large to allow an optimisation of the handover control parameters since in real mobile communication networks the acceptable order of negative handover events is a few percent. Note that the standard deviations have only been calculated for the given observation windows and plotted as lines for clarity.

In the case of the event based observation windows (Figure 6.20(b)) the HPI_{sum} values are generated after the minimum number of handover related events is reached in a HOP. Therefore, the number of HPI_{sum} values varies for the same observation window in the HOPs. The advantage of the event domain observation windows is that single negative events or no handover related events in the last time cannot lead to extreme HPI_{sum} values since the same number of events is considered. The drawback is that depending on the HOP it might take more time to evaluate the handover performance because the minimum number of observation events has to be reached. For the analysis of the standard deviation of the HPI_{sum} values it is important to consider a reasonable set of values. To assure this, a minimum number of 2000 HPI_{sum} values has to be available. This amount of values is selected to match the minimum number of values in the time domain analysis of 200 s (2000 HPI_{sum} values). The reason behind this is again the boundary effect of the analysis. The standard deviations in Figure 6.20(b) are plotted only for the number of handover related events reached in the HOPs, given that the minimum number of HPI_{sum} values is available for the analysis. In contrast to the evaluation of the time domain observation windows not all HOPs are included in the analysis for the higher observation windows. By definition the observation time (number of handover related events) is not reached in these HOPs and hence no compilation of HPI_{sum} values is initiated. The impact of the lower amount of considered HOPs on the evaluation result on the standard deviation is minor since the HOPs with only a few handover related events use high handover control parameter settings, i.e. the standard deviation for these HOPs is low due to the high probability of failure events in these HOPs. Moreover, these HOPs are discarded as operating points due to the high amount of handover failures. The figure shows that the maximal standard deviation ($\sim 14.5\,\%$) for the time domain observation windows of 600 s is undercut with the event based observation windows of 60 handover related events already ($\sim 14\,\%$). Further, fewer outliers can be observed for higher observation windows. An observation window of 200

handover related events leads to a maximum standard deviation of $\sim 5\,\%$.

The conclusions from the analysis of the HPI_{sum}, which has been conducted so far, is twofold. Firstly, it is quite obvious that event domain observation windows should be used for the compilation of the HPI_{sum} since the standard deviation of the values reaches smaller values faster than in the time domain case. Secondly, the maximum standard deviation observed in the case of an event domain observation window with 200 handover related events is 0.05. As mentioned before, in the case that all weighting parameters are set to one (as for the complete analysis) this translates to a standard deviation of the negative handover event ratio of 5%. Given that an acceptable level of negative handover events in a network lies in the order of a few percent, the standard deviation of the handover performance indicator should lie far below this level. Hence, longer observation intervals are necessary to allow for the identification of the current handover performance and thus, for the optimisation of the handover control parameters. The two remaining questions are how large the observation windows should be and in what way incorrect optimization decisions based on shorter observation windows impact the handover performance..

To approach an answer to the first question, the noticeability of changes in the handover performance by the HPIs plays an important role. As mentioned before, the level of negative handover events usually lies in the order of a few percent at most. In the majority of the cases, it falls below one percent. Especially the ratio of radio-link failures should lie below one percent in a well designed network. This means that the noticeability of changes in the HPIs should be in that range as well, i.e. the noticeability of changes in the order of 0.001 ($0.1\,\%$) is desirable. The outcome of this is that the standard deviation of the HPIs should be lower than 0.001. Since the denominator of the HPI ratios, that are used for the calculation of the HPI_{sum} values as well, is the number of handover related events in the case of an event domain observation window, the maximum granularity of the HPI_{sum} values can easily be calculated. As an example for the observation window using 100 handover related events the granularity calculates to 0.01 ($1\,\%$) as every event represents one percent of the total events observed.

Tables 6.6 and 6.7 give the maximum granularity of the HPI_{sum} values named as HPI_{sum} resolution (HPI_{res}) for some exemplary observation windows ($Window_{Event}$) taken from the simulation results. The maximum standard deviation (STD_{max}) of the HPI_{sum} values observed in the simulation is listed in the subsequent row. The last row gives the difference between the granularity and the observed standard deviation as a multiplication factor (MF) calculated from:

$Window_{Event}$	50	100	150	200	240	300
HPI_{res}	0.020	0.010	0.0066	0.005	0.0041	0.0033
STD_{max}	0.1567	0.0887	0.0568	0.0469	0.0417	0.0365
MF	7,8333	8,8767	8,5257	9,3697	10,0167	10,9363

Table 6.6: Properties of the standard deviation for different event domain observation windows I

$Window_{Event}$	350	400	450	500	550	600
HPI_{res}	0.0028	0.0025	0.0022	0.002	0.0018	0.0016
STD_{max}	0.0334	0.0303	0.0266	0.0231	0.0197	0.0194
MF	11,7019	12,1108	11,9601	11,5727	10,8237	11,6314

Table 6.7: Properties of the standard deviation for different event domain observation windows II

$$MF(w) = \frac{STD_{max}(w)}{HPI_{res}(w)} \tag{6.6}$$

Above an observation window size of 200 handover related events the multiplication factor takes a value around 10. This translates to the maximum standard deviation of the HPI_{sum} values being approximately 10 times higher than the granularity of the HPI_{sum} values. Thus, in order to achieve a standard deviation of 0.001 the granularity of the HPI_{sum} values needs to be 0.0001 assuming a linear behaviour for larger observation windows. This means the observation window size should be 10000 handover related events to assure the noticeablility of handover performance changes in the network.

For the verification of the needed observation window size we further analyse the maximum standard deviation of the observation window sizes. Figure 6.22 shows the standard deviations for the event domain windows. The course of the maximum standard deviations is alike an exponential function with a negative exponent. Hence, we use the fitting toolbox from MATLAB to find a best-fit line for the maximum values of the standard deviation. The result is shown in Figure 6.22. The curve underestimates the maximum standard deviation for small window sizes (50 - 150 events) and for the largest observation window of 600 events. Except of these areas the curve fits the ob-

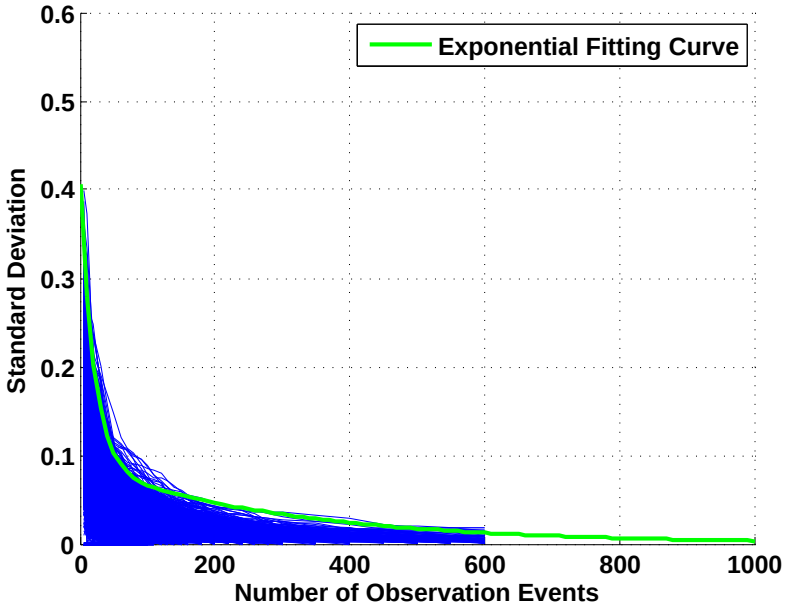

Figure 6.22: Exponential fitting curve for the standard deviations of the HPI_{sum} values

served course of the maximum standard deviation. Nevertheless, the fact that the fitting curve underestimates the standard deviation for the largest observation window reveals that the fitting can only be seen as the lower bound of the maximum standard deviation. This is enforced by the observation of the fitting results for a smaller set of observation windows (0 - 200 events) where the gradient of the curve was higher resulting in smaller estimates of the maximum standard deviation for higher observation windows.

The equation of the best-fit curve ($F_c(x)$) for the maximum standard deviation of the HPI_{sum} values is given here:

$$F_c(x) = a \cdot e^{b \cdot x} + c \cdot e^{d \cdot x} \tag{6.7}$$

with $a = 0.3173$, $b = -0.04898$, $c = 0.08866$ and $d = -0.003246$.

To evaluate the required observation window size the estimates for the maximum standard deviation based on the best-fit curve are shown in Table 6.8. An estimated maximum standard deviation of less than 0.0001 is reached for an observation window of 2100 handover related events.

Besides these two empirical analyses another theoretic approach can be used to estimate the observation window sizes. From the theory of performance evaluation techniques for the calculation of the bit error rate the following relation is well known:

$Window_{Event}$	100	250	500	750	1000	1500	2100
Max. STD	0.0664	0.0393	0.0174	0.0077	0.0034	0.00068	0.000097

Table 6.8: Standard deviation for different observation windows from the fitting curve

$$\sigma_{BER} = \sqrt{\frac{p(1-p)}{N_{bits}}} \tag{6.8}$$

with the standard deviation σ_{BER}, the bit error probability p and the number of bits N_{bits} that need to be transferred to assure the standard deviation. The equation relates the standard deviation, an error rate representing the channel quality and the number of observed events. These three components can be replaced by the standard deviation of the negative handover rate (HPI_{sum} values), the typical observed mean negative handover rate as error probability and the number of observed events represented by the observation window size. Thus, we can use the formula to estimate the observation window size (number of events) by rearranging 6.8 to:

$$N_{events} = \frac{p_{neg}(1-p_{neg})}{\sigma^2_{HPI}} \tag{6.9}$$

Now using the negative handover event ratio p_{neg} and the desired standard deviation of the HPI_{sum} values σ_{HPI} set to the desired value of 0.001. As negative handover rate we select a standard value from real networks of 1 %[2]. The resulting number of observation events N_{events} is 9900. Note that the results from this theory are very sensitive to the observed negative handover rate as for a negative handover rate of 2 % the needed amount of observation events rises to 19600 already. With the assumption that the number of negative events in a mobile communication network is around 1 %, the theory confirms the results from the first empirical analysis that roughly 10,000 handover related events have to be observed to allow a precise evaluation of the current handover performance. The conclusion from the analysis of the needed observation window sizes in this section is as follows: the assumption for the identification of the needed observation window size in this section is the objective to evaluate the handover performance with a granularity of 0.1 %. This objective originates from the network operator demand[3], to identify a handover performance in this granularity and to optimise the performance if an improve-

[2]This value was discussed in the SOCRATES project and quoted as around 1 % from the industry partners

[3]Again this demand was discussed in the SOCRATES project

ment of this granularity can be reached. This statement shows that an improvement of the handover performance in the order of 0.1 % is desirable. Nevertheless, the analysis in this section shows that the evaluation of the handover performance in this level of detail cannot serve as performance indicator for the optimisation algorithms. This is because only few cells in a real network manage more than 10,000 handover events a day. The observation window estimation based on the fitting curve, resulting in roughly 2,000 handover related events to allow the analysis of the handover performance in the order of 0.1 %, has to be considered as the weakest approach. This is because the extrapolation of the needed observation window sizes bases on a limited number of simulated window sizes (only up to 600 s) and the fitting is based on visual inspection. The two theoretical approaches both estimate a needed observation window size of 10,000 events. Summing up all approaches verify that several thousand events have to be observed, which leads to the conclusion that the optimisation algorithms can rely on a very detailed analysis of the handover performance if the aim for the optimisation is an adaptation to network condition changes in the order of hours. Thus, the next section targets the identification of a smaller observation window that serves the objective to improve the current handover performance by the optimisation of the handover configuration parameters.

6.7 Deduction of the Minimal Observation Window to Enable Optimisation of the Handover Performance

This section addresses the dimensioning of the observation window to allow an optimisation of the handover performance. The optimisation of the handover control parameters is based on the observation of the current handover performance in the network. The handover performance is represented by the HPIs which are influenced by the observation windows as introduced before. In the optimisation process the HPIs or HPI_{sum} of the current HOP will be compared to the equivalent observed values of another HOP. This means the performance of the two HOPs is observed for a certain duration (observation window) and the HOP with the better performance is selected. The result from the statistical analysis of the HPIs shows that the standard deviation of the HPI_{sum} values is higher for shorter observation windows. In the case of a comparison of the handover performance of two HOPs with similar performance the probability of a misinterpretation is higher. Hence, the optimisation of the handover control parameters could lead to an increase of negative handover events in the long-run. The aim of the following investigation is to quantify the probability of a misinterpretation of the han-

dover performance while comparing two HOPs subject to the observation window size. The assumption is that the probability should decrease for higher observation window sizes.

To calculate the probability that a HOP is identified as the better performing HOP we use the probability density function of the observed HPI_{sum} values in a HOP. Let X and Y be two random processes with the probability density functions $f_x(x)$ and $f_y(y)$ that generated by variables x and y. In order to calculate the probability that the value of an event x_i is larger than the value of an event y_i the distribution function $F_z(z)$ of the random process z with

$$z = x - y \tag{6.10}$$

needs to be calculated. In the case that $z > 0$, x is larger than y as well. The distribution function $F_z(z)$ can be calculated as:

$$F_z(z) = P\{x - y \leq z\} = \int_{y=-\infty}^{\infty} \int_{x=-\infty}^{z+y} f_{xy}(x, y) dx dy \tag{6.11}$$

and hence the probability density function $f_z(z)$ calculates as:

$$f_z(z) = \frac{dF_z(z)}{dz} = \int_{-\infty}^{\infty} f_{xy}(z + y, y) dy \tag{6.12}$$

If x and y are statistically independent, 6.12 reduces to:

$$f_z(z) = \int_{-\infty}^{\infty} f_x(z + y) f_y(y) dy = f_x(-z) * f_y(z) \tag{6.13}$$

which is the convolution of $f_x(-z)$ and $f_y(y)$. Finally, the probability that x is larger than y can be calculated from $f_z(z)$ as:

$$P\{x > y\} = P\{z > O\} = 1 - P\{z \leq O\} = 1 - \int_{z=-\infty}^{0} f_z(z) \tag{6.14}$$

To answer the question how probable it is that the better HOP (in the long-run) is identified in a comparison of the HPI_{sum} values an analysis using Equations 6.13 and 6.14 is conducted. The analysis is based on the same simulation results as used before and follows these steps:

1. Run a loop over all considered cells and observation window sizes (event based)
2. Identify the best HOP by the lowest mean of the HPI_{sum} values over the complete simulation time

3. Run a loop over all remaining HOPs considered in the analysis

4. Calculate the probability for a successful identification of the better HOP using Equations 6.13 and 6.14

In step 2 only the HPI_{sum} values starting from the simulation step in which the HPI_{sum} is calculated for the first time are considered. This means the amount of values used for the identification of the best HOP may differ for the individual observation window sizes. Especially for higher observation windows a lower amount of HPI_{sum} values is considered since the required number of considered events has to be reached to calculate the HPI_{sum} value. The amount of considered HOPs (step 3) for this analysis is reduced to avoid corruption of the analysis results, i.e. extreme settings of the HYS and TTT lead to a high amount of negative handover events. A comparison of the performance of such a HOP with the best HOP will always lead to a perfect identification of the better HOP. However, this result is irrelevant since a HOP with extreme handover control parameter settings will not be selected as handover operating point in a network. The selection of the considered HOPs is based on the results of the analysis of the selected HOPs for different weighting parameter settings as visualized in Figure 6.11 Sub-figure (c). The used subset of HYS values ranges from 0 dB to 5 dB and the subset of TTT values from 0.1 s to 1 s resulting in a total number of 42 considered HOPs. As probability density functions $f_x(x)$ and $f_y(y)$, which are required for the calculation of the probability for a successful identification of the better HOP (step 4), the histograms of the HPI_{sum} values with a granularity of 0.001 are used. The case that the values are identical is not assessed as a successful identification of the better HOP. A minimum set of 1,000 HPI_{sum} values is defined to perform the calculation of the probability to ensure significant results.
Figure 6.23 depicts the result of the analysis for six exemplary cells. The coloured bars give the minimum and maximum probability values that have been calculated for the individual observation window size. The black curve shows the development of the mean probability computed from all 42 performance comparisons (the performance of the best HOP is not compared with itself). The results prove that, as expected, the mean probability of the identification of the better HOP increases for higher observation window sizes. The reason behind this is the lower standard deviation of the HPI_{sum} values for higher observation windows. Moreover, a mean identification probability of above 90 % is reached for observation window sizes below 100 events in any case. This means that in contrast to the results of the analysis on the amount of handover related events, which are needed to identify the current handover performance in a network

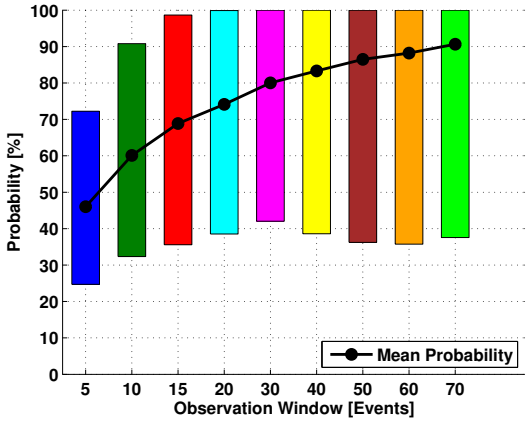

(a) Cell 15

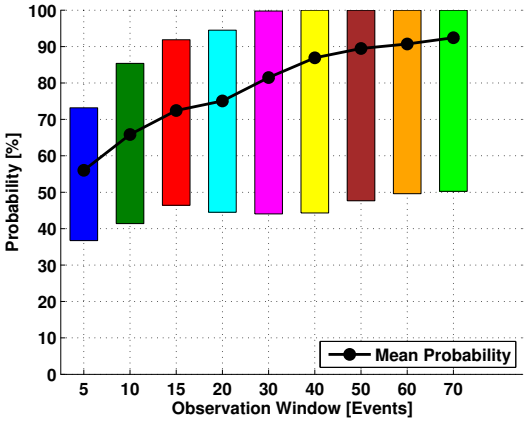

(b) Cell 16

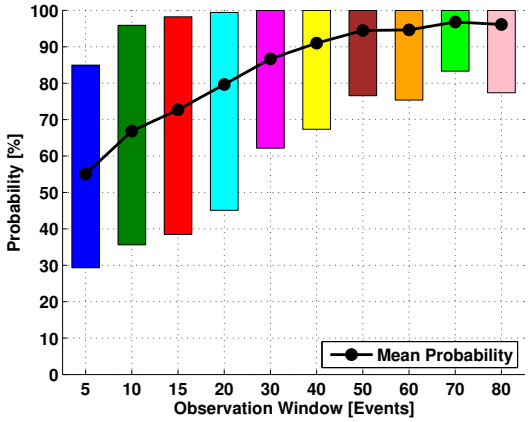

(c) Cell 31

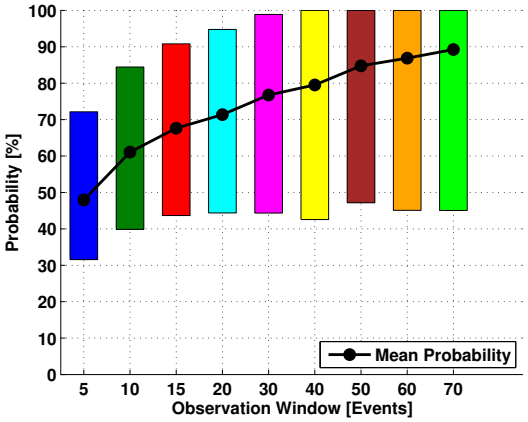

(d) Cell 34

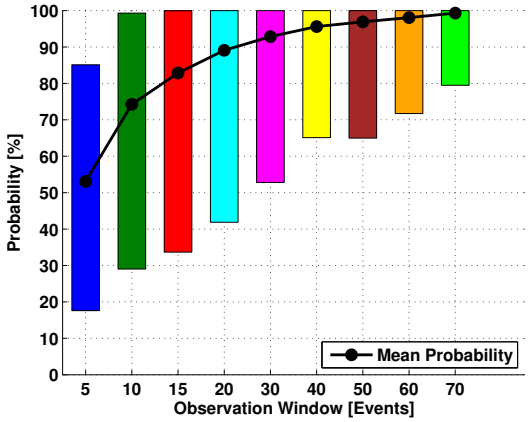

(e) Cell 134

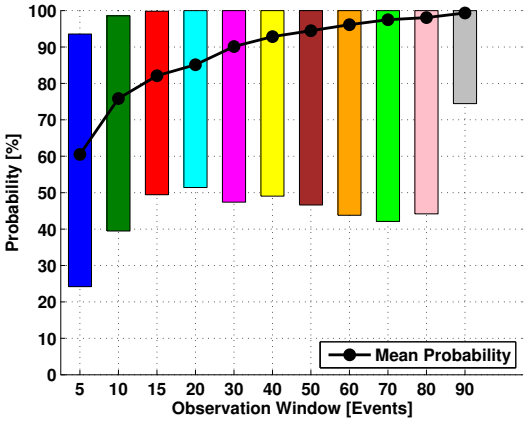

(f) Cell 136

Figure 6.23: Identification probability of the best HOP for different event domain observation windows

where more than 2,000 events need to be considered, a significantly lower amount of events is needed to compare the performance of different HOPs. This fact enables faster optimisation of the handover control parameters. The drawback is the shown minimum probability for the cells and observation windows which still lies below 40 % in the case of Figure 6.23(a). The assumption is that in these cases two HOPs with very similar handover performances exist which would complicate the identification of the better HOP. It might be possible that a differentiation between these HOPs is not necessary since the performance difference is negligible.

The mean identification probability of the best HOP aggregated over all 65 considered cells is given in Figure 6.24. Sub-figure 6.24(a) shows the results using the method based on the convolution of the histograms of the HPI_{sum} values as introduced before. The observation window based on 40 handover related events allows a mean identification of the better HOP in more than 90 % of the cases. The aprupt increase in the identification rate to almost 100 % by an observation window of 100 handover related events, is caused by the fact that only one of the 65 cells has enough handover events to allow this observation window size in the analysis. Hence, this result cannot be seen as reliable. Nevertheless, the analysis shows that a minimum window size of 40 events allows an identification of the better performing HOP with a high probability. Hence, an observation window of 40 events and higher windows will be considered for the evaluation of the handover performance for the optimisation algorithms.

The computation of the probability of the identification of the best HOP, which is based on the convolution of the probability density function in Equation 6.13, is only possible if the input variables are statistically independent. To check this we have to verify that the following condition is true:

$$P(x \cap y) = P(x) \cdot P(y) \tag{6.15}$$

The verification of the condition shows that the input variables (HPI_{sum} values from two HOPs in one cell) are statistically dependent. The reason behind this is that the users in the network travel the same route independent of the HOP selection in the cell. Dependent on the HOP selection in the cell the users change to a neighbour cell which results in a handover related event. However, the handover related event takes place when the user resides in the cell border area. Due to the fact that every user in the scenario moves with a certain speed towards a target location the handover related event will take place in a similar moment (simulation time) in most cases. At least the few negative handover events that are still present in the best performing HOP will

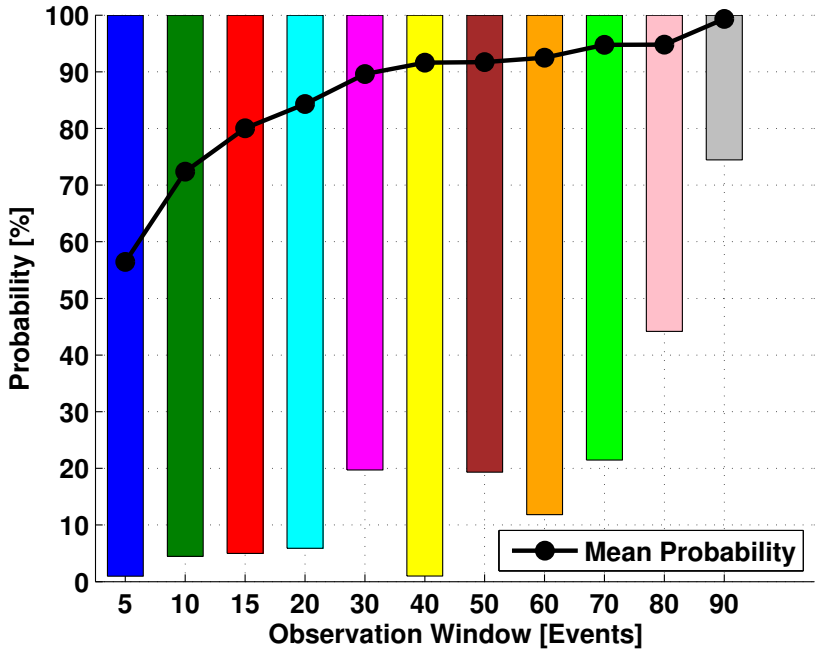

(a) Based on the Histograms of all HPI_{sum} values

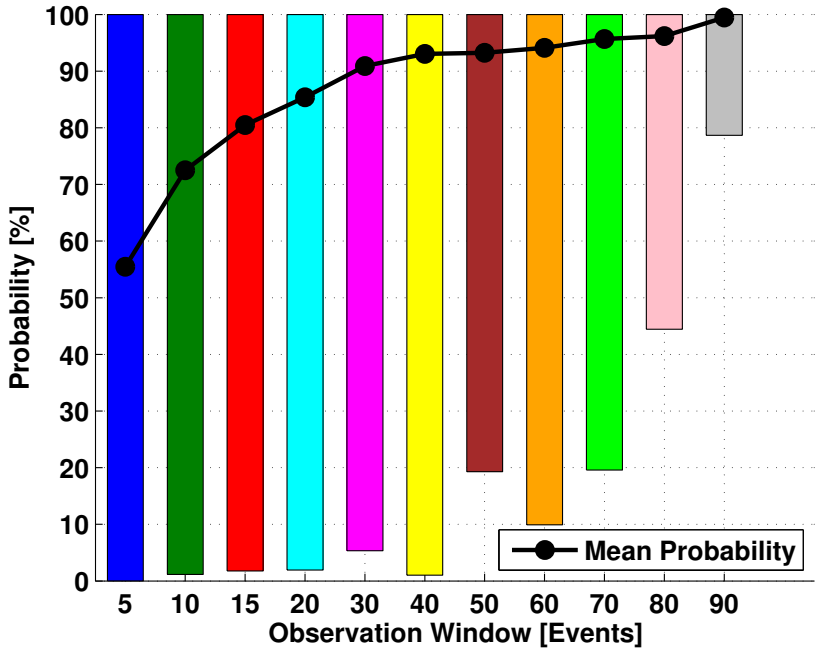

(b) Based on Comparison in the same Time Step

Figure 6.24: Mean identification probability of the best HOP for different event domain observation windows

show up in most of the other HOPs in similar moments. Hence, the HPI_{sum} values are per definition statistically dependent. But this is only true if the HPI_{sum} values for the two HOPs are generated for the same observation time, i.e. the same user activities in the network. If the handover performance of a HOP is observed for some time and compared to the performance of a HOP observed afterwards, the variables will be statistically independent. Hence, the results of the analysis are valid for this case. We will come back to this fact later when introducing the handover optimisation algorithms.

For the case that the evaluation of the handover performance is based on the same time span for different HOPs the HPI_{sum} values are not statistically independent. To check the impact of the statistical dependence on the probability of a successful identification of the better HOP, we run a second analysis. This time the HPI_{sum} values of the best HOP are only compared to the HPI_{sum} values of the other HOPs in the same simulation time step. Thus, the observation window for different HOPs is similar since the same user movement and related cell changes are observed in both cases. Nevertheless, the observed handover related events are not exactly the same since different handover control parameter settings influence the amount of handovers and the negative handover rate. The mean identification probability of the best HOP for this analysis is given in Figure 6.24(b). A comparison with Figure 6.24(a) reveals that the identification probability is very similar in both cases. In the second case the identification probability is slightly higher due to the same observation phase that influences the HPI_{sum} values in a similar way. This eases the identification of the best HOP. Anyway the difference between the methods is insignificant.

A conspicuous behaviour of the identification probability is that the minimum identification probability sometimes decreases for larger observation windows whereas the general trend of an increasing identification rate is still proven by the increasing mean rate. An extreme example for this is visualized in Figure 6.25 where the minimum identification probability drops from about 52 % to 45 %. To clarify this behaviour the course of the HPI_{sum} values for the comparison of one HOP to the best HOP is visualized in Figure 6.26. For simplification the shown results are taken from the comparison using the statistically dependent values since it is easier to follow the results in a diagram. We selected the largest identification probability drop from an observation window of 20 events to a window of 30 events. Subfigure 6.26(a) shows the course of the HPI_{sum} values for the two HOPs. In the green areas the identification of the best HOP is successful since the corresponding HPI_{sum} values are lower than the values of the comparative HOP. In the areas marked red it is the other way around and the identification fails. In the orange

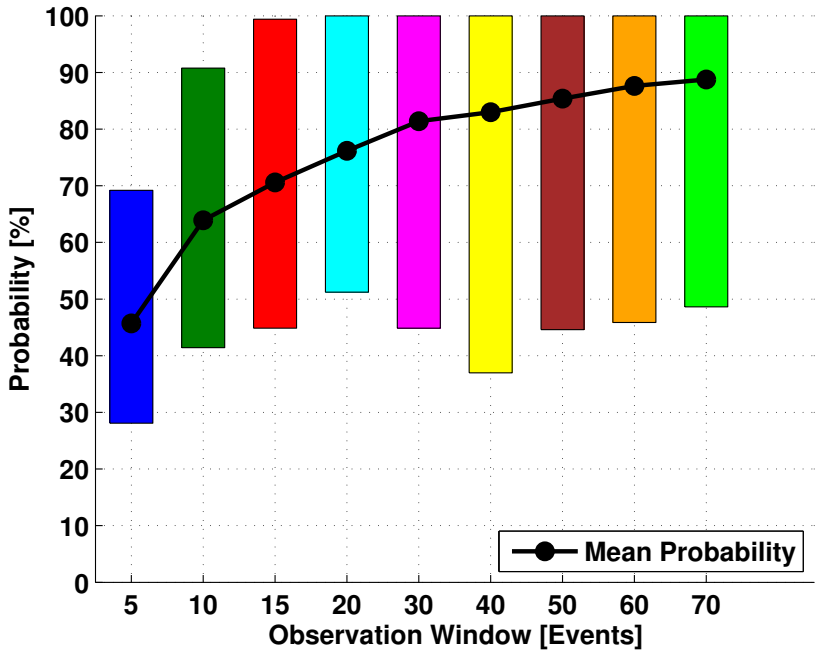

Figure 6.25: Identification probability of the best HOP for different event domain observation windows in cell 34

areas the values are identical leading to an unsuccessful identification as well. Hence, the identification probability of the best HOP is about 57 %. To classify this low identification rate, it is important to understand that the performance of the compared HOPs is similar if the identification rate is low. Hence, the consequence for the optimisation of the handover performance is minor if the better of two very similar HOPs cannot be identified.

For an observation window of 30 events the identification probability drops by 10 % to about 47 % for the comparison of the same two HOPs (Figure 6.26(b)). A closer look at the course of the HPI_{sum} values reveals that two reasons are behind it. Firstly, the larger observation window leads to a time shift in the availability of values for both HOPs since a larger number of handover related events has to be observed. In the case of an observation window of 20 events the identification of the best HOP was successful in the time span that misses in the second case. Secondly, in the simulation time around 300 to 350 seconds, where the identification was successful as well, it is unsuccessful for a larger window. The reason for this is the opposed trend in the HPI_{sum} values for the two HOPs. While the values go upwards for the best HOP they decrease for the comparative HOP. In the case of a smaller observation window the identification is still successful for a short time frame. In the second case the negative trend for the

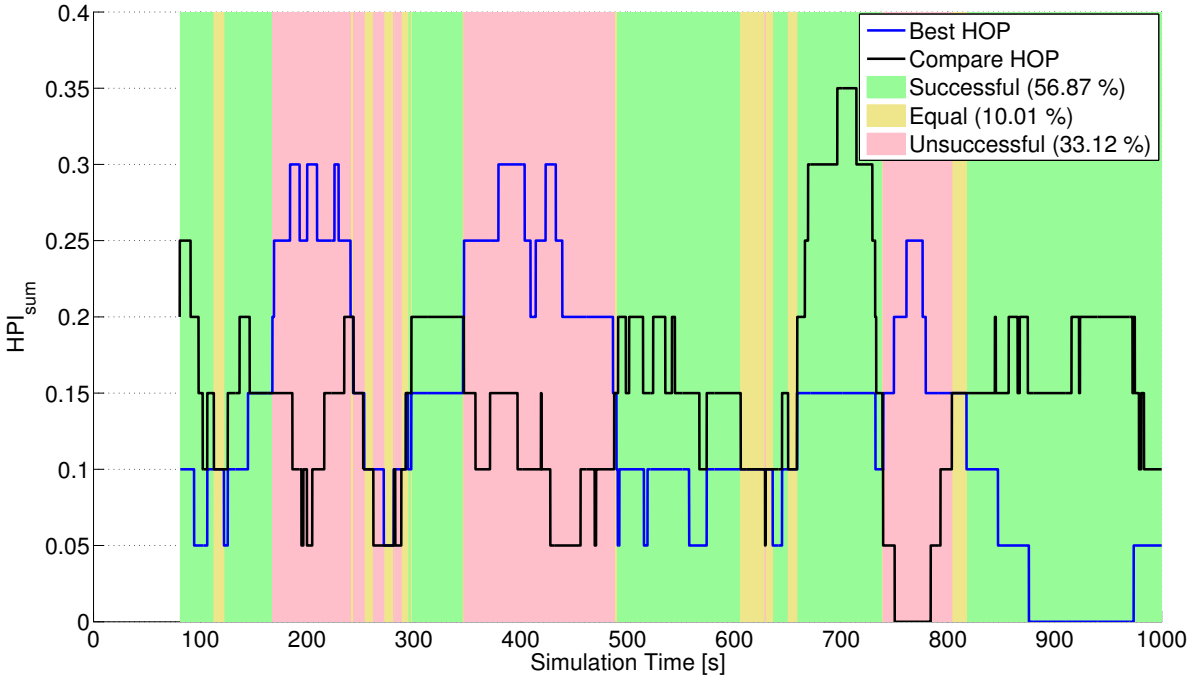

(a) Observation Window based on 20 Events

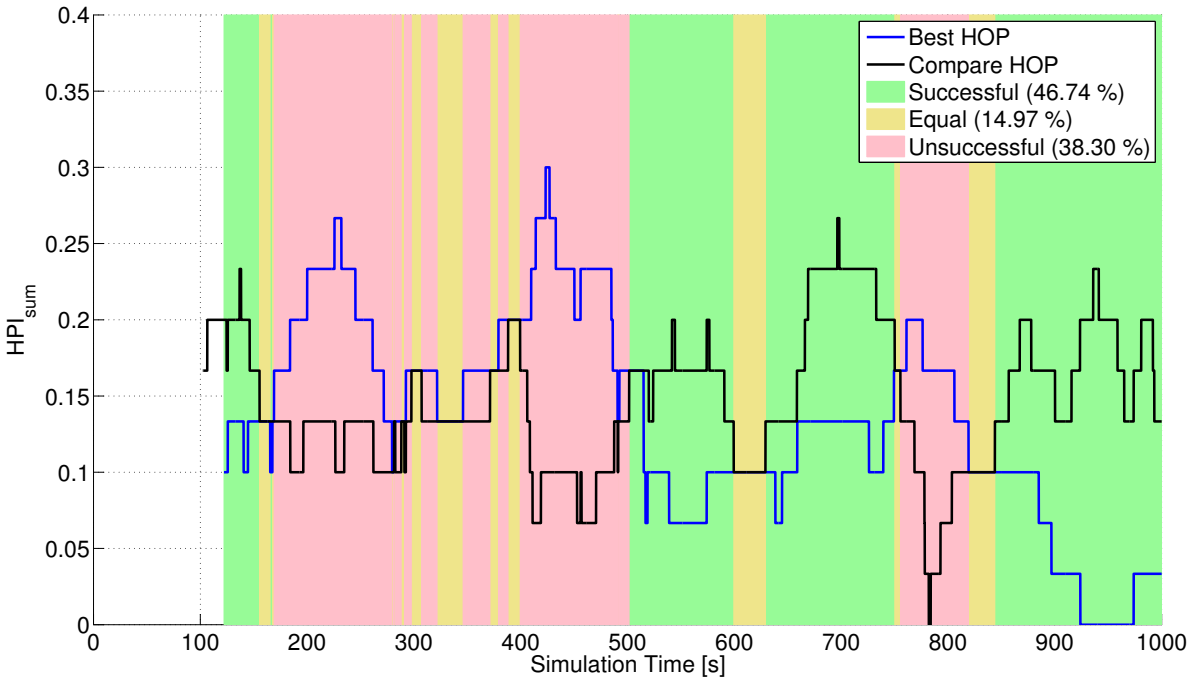

(b) Observation Window based on 30 Events

Figure 6.26: HPI_{Sum} values and result of the comparison of two HOPs in cell 34

best HOP and the positive trend for the comparative HOP influence the HPI_{sum} values for a longer time due to the longer observation window and hence the identification is unsuccessful for the complete period. This clarifies that the temporal sequence of the handover related events and especially the sequence of negative handover events have a large impact on the identification probability of a better performing HOP for relatively short observation windows. As Figure 6.24 points out, the impact of this effect on the identification probability is decreased for larger observation window as the minimum identification probability rises for larger windows.

A conspicuous behaviour of the identification probability is that in some cases especially for the calculations which are based on statistically dependent values the identification probability is close to zero. An example for this case is given in Figure 6.27 for a comparison of two HOPs in cell 29. The graph shows that the identification is successful in about 10 % of the cases. In the majority of the cases the HPI_{sum} values are equal and hence an identification of the better HOP is impossible. This effect is a drawback for the calculation of the HPI_{sum} values based on an equal amount of handover related events. In particular for small observation windows the probability of identical HPI_{sum} values in different HOPs, beyond that if based on the same time span (same user mobility in

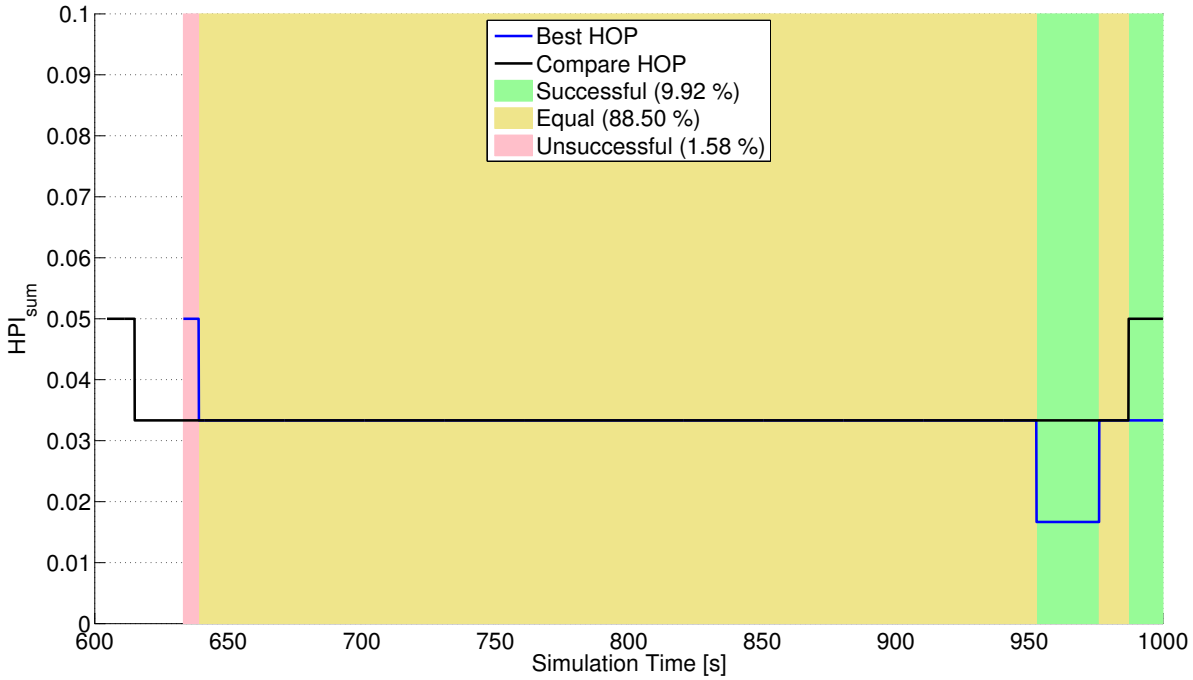

Figure 6.27: HPI_{Sum} values and result of the comparison of two HOPs in cell 29 (observation window based on 60 events)

the network), is increased. In the aforementioned case, the identification probability falls to below 10 %. Nevertheless, these effects can only be observed in a few cases and the general trend of an increasing identification probability for larger observation windows is unharmed.

A final important question is the performance degradation in the network in the case of an unsuccessful identification of the best HOP, i.e. how many additional negative handover events happen in the network with sub-optimal handover control parameter settings. Table 6.9 shows the mean, minimum and maximum performance degradation for different observation windows. In this evaluation all comparative HOPs with an identification rate of below 90 % have been regarded. Hence, the number of HOPs considered decrease for larger observation window sizes since the identification probability increases. For an observation window of 40 events defined as minimum window for the further optimisation algorithms the mean performance degradation is approximately around 0.7 %. The maximum degradation around 4 % is still quite high and would lead to an unacceptable increase in negative handover events in the network. The minimum performance degradation is negative for observation windows between five and 80 events. The reason for this is that the best HOP is not identified by the mean of the HPI_{sum} values for every cell.

For the evaluation of the performance degradation the total number of negative handover related events in the complete simulation time has been considered. In some cases the sequence of the handover related events lead to a lower mean handover performance

$Window_{Event}$	5	10	15	20	30	40
Mean Performance Degradation [%]	2,43	1,90	1,50	1,19	0,85	0,66
Minimum Performance Degradation [%]	-0,49	-0,49	-0,40	-0,43	-0,52	-0,43
Maximum Performance Degradation [%]	15,97	10,00	8,68	7,74	4,58	3,99
$Window_{Event}$	50	60	70	80	90	100
Mean Performance Degradation [%]	0,50	0,48	0,38	0,38	1,15	1,15
Minimum Performance Degradation [%]	-0,43	-0,43	-0,23	-0,09	1,15	1,15
Maximum Performance Degradation [%]	3,49	3,49	3,05	1,15	1,15	1,15

Table 6.9: Mean performance degradation for different event domain observation windows

for a HOP with a larger total number of negative handover events. This can happen for example if a series of negative handover events is followed by a series of successful handover events in a short time span. The outcome of this is that the negative handover events are represented by the HPI_{sum} values for a shorter time frame and hence the comparison of the mean handover performance with a better HOP fails. For an observation window of 50 events the mean degradation is approximately around 0.5 %, i.e. that one additional handover event of 200 handover events is negative. This degradation is in an acceptable order. The mean degradation constantly decreases up to an observation window of 80 events. The results for larger windows can be neglected since they base on one comparison result only since merely one cell shows this amount of events in every HOP and only in one comparison an identification rate of below 90 % has been identified.

6.8 Conclusions

The following conclusions on the evaluation of the handover performance can be drawn from the examinations in this chapter:

1. To evaluate the handover performance stable network conditions have to prevail, i.e. significant changes in the network configuration that impact the cell borders influence the handover performance. Major network changes necessitate to restart the evaluation phase.

2. The HPIs show opposing trends for higher or lower handover control parameters. This means the optimisation of the handover performance will always be a weighting up of the ping-pong handover ratio against the failure event ratio. The consequence for the optimisation algorithms is that the network operators need to specify a policy on the trade off between the negative handover events. The optimisation algorithms need to guarantee the impact of the operator policy on the optimisation goal and the sensitivity of policy changes on the optimisation result has to be transparent for the operators.

3. The analysis of the HPI characteristics shows that the observation time for the handover performance evaluation increases for HOPs with a better performance. This means it should be possible to evaluate a poor handover performance faster than to identify the better of two good performing HOPs. Thus, the optimisation algorithms should allow fast performance improvement in the case of a poor starting HOP selection.

4. The introduction of the weighted sum of the HPIs as target function for the optimisation allows to steer the optimisation goal according to the operator policy. The simulation results show that a HOP selection according to the target function leads to less ping-pong or failure events in the network subject to the settings of the weighting parameters. Nevertheless, simulations in different simulation environments show that the sensitivity of the parameter changes depends on the simulation environment. In the more realistic Hanover scenario the "optimal" HOP selection of the individual cells is spread in a larger area of the optimisation space. The conclusion is that in real networks the individual situation in the cells requires a cell specific handover configuration.

5. The comparison of the simulation results from the Hanover scenario and the 3GPP-Scenario reveals that a larger range of handover control parameters is selected as optimal handover operating points in the case of the more realistic simulation assumptions. The conclusion from this is that in reality the individual cell situation subject to the environment of the cell needs a special optimisation of the handover control parameter settings. Thus, local, cell-wise optimisation has to be performed.

6. The results of the load dependent simulations demonstrate the impact of the network load on the handover optimisation goal. In consequence the optimisation of the handover parameters has to be possible within the time span of similar network load. Optimisation cycles of several hours will not permit optimal handover performance in networks with high load fluctuation. The adaptation speed of the handover optimisation algorithms on load changes is an important assessment criterion.

7. The identification of an adequate observation window proves that the observation window has to be selected in the event domain. The dependence of the handover related events on the current HOP and load situation in the network makes it impossible to select an observation window in the time domain. The reliability of the HPIs for time domain evaluations complicates the optimisation of the handover performance. Event domain evaluations showed a significant higher robustness.

8. The analysis of the optimal event domain observation window size educed that 2,000 to 10,000 handover related events have to be observed to allow an accurate handover performance analysis. The conclusion from this is, in consideration of the reliability of the estimation approaches that have been used, that several thou-

sand handover related events have to be observed to allow a detailed analysis of the handover performance. Compared to the typical amount of handover events in cells in real networks these number will not allow a fast optimisation of the handover performance since only few cells located close to highways show more than 10,000 handover related events a day. Thus, an accurate evaluation of the current handover performance cannot be the basis for the handover optimisation algorithms.

9. A deeper analysis of the needed observation window sizes to identify a better performing HOP in a direct performance comparison showed that significant fewer events have to be considered. In the simulation scenarios 40 events allowed an identification rate of more than 90 % already. Thus, the optimisation algorithms will evaluate fewer events and compare the observed performance to the statistics of other HOPs.

Chapter 7

Handover Optimisation Algorithms

The handover optimisation algorithms presented in this chapter use measurements to identify the best handover control parameter settings in the cells. The open question is which measurement information is useful for the optimisation of the handover parameters. This question is closely connected to the question if it is possible to identify the best moment for a handover decision. To illustrate the complexity of identifying the best moment for a handover decision, the following example is given.

In real networks the shadow fading creates a patchwork of best server areas that, in combination with user mobility, leads to frequent best server changes for the UEs. A user moving in this patchwork reports best server changes to the network and waits for the handover decision. The complication in this particular case is that the network does not know where the user will move to and how the service quality from the different cells will be in this area. Any decision could be wrong as the following example indicates. Let us assume that a small cell serves an indoor area as well as a part of the side-walk and street in front of the building, in which the cell is located. If a user passes the building with high speed, it is clear that the user should not be handed over to the small cell. The risk for a radio-link failure or handover failure is too high since the coverage area of the small cell is too small. If the user walks on the side-walk, a handover might become necessary in case the user speed is low or because the user walks up and down in front of the building. Avoiding the handover could lead to a radio-link or handover failure.

In the special case that a user approaches the small cell serving area with high speed (e.g. driving in a car), stopping in front of the building or driving into the front yard of the building, the user needs to be handed over to the small cell timely even though the individual user speed is high. This demonstrates that the user speed and size of the best server area are not sufficient indicators to justify a handover. The time a user stays in a best server area is dependent on the user speed and the destination of the moving user.

Furthermore, shadow fading caused by buildings or other obstacles has an impact on the handover behaviour and thus, on the optimisation of the control parameters settings. If a user passes a building or turns at a traffic light, the signal strength of the connected cell might drop significantly in a short time period. In this case a handover needs to be triggered immediately even for users with a low speed. Nevertheless, the user speed is an important parameter since the signal quality of the cells changes faster for high speed users, thus the serving cell changes have to be triggered in time.
The following measurement information and parameters are identified as potential candidates to support the optimisation of the handover control parameters:

- Handover Performance Indicators
- User Speed
- Network Load
- User Location
- Signal Strength Maps

The HPIs are the most important measurements for the optimisation of the handover control parameters since they reflect the current handover performance in the cell. In Chapter 6 the HPIs have been discussed intensively. The user speed is accounted for in a user speed class, i.e. high speed, medium speed and low speed. Still, a user classified as high speed user can show a huge variety in the instantaneous speed, e.g. a UE located in a car stands still in front of a traffic light or moves with 50 $\frac{km}{h}$ on the street. Due to the fact that the difference in mobility of vehicular, pedestrian and indoor users is severe, a separate optimisation of the handover parameters for the speed classes (mobility types) could be beneficial. As the results of Section 6.4 showed the network load impacts the handover performance in that sense that less failure events are observed if the network load decreases. An adaptation of the control parameters leads to fewer negative handover events in this case. On the other hand increasing load leads to a higher amount of failure events in the network. Thus, significant load changes require a reconfiguration of the handover parameters, i.e. the adaptation speed to network load changes is important.
The first three measurements and parameters are used by the optimisation algorithms to optimize the handover control parameters. The user location and signal strength maps enable the analysis of the surrounding of the UE. This means that individual handover decisions based on the user situation become possible. The drawback of this concept is

that the accuracy of the user location identification is dependent on the hardware in the UE and the environment, i.e. the identification of an indoor user location is more difficult since the buildings block the line-of-sight to the satellites. The concept of detailed signal strength maps stored in the cells and permanently updated by UE measurements is promising [Neuland11] [Johansson12] [TUBS16], but currently the accuracy of the maps is limited. Moreover, the computation time of the user location and the signal strength maps for an instant decision on the handover moment is too high. Hence, the user location and signal strength maps are not used for the optimisation in this work. For future investigations these information might permit user-wise handover decisions.
In the following two handover optimisation algorithms are presented. Section 7.1 describes the neighbouring HOP performance based handover optimisation algorithm. The user measurement report based handover optimisation algorithm is described in Section 7.2.

7.1 Neighbouring HOP Performance Handover Optimisation Algorithm

The Neighbouring HOP Performance Handover Optimization Algorithm (NHP-Opt) has mainly been developed by the author of this dissertation in the SOCRATES project [SOCRATES08]. Parts of the following algorithm description are taken from paper [Jansen11] and from an internal project deliverable [Jansen10a]. The simulation results in the SOCRATES project are based on a simulation scenario, which has been developed in the project and contains consortium confidential information. Thus, and for comparability reasons with new solutions developed in this dissertation, the results presented in this work base on the simulation scenarios described in Section 5.4. The first optimisation algorithm developed in the project monitors the HPIs separately and derives the adaptation steps for the handover control parameters [Jansen10b]. A drawback of this algorithm is that the adaptation proposals from the HPIs might be contradictory and hence no optimisation is possible in these cases. Further advancements of the NHP-Opt can be found in [Balan11a] and [Balan11b].
The NHP-Opt is executed locally in every cell in the network. The current handover performance of a cell is determined by the weighted sum of the three HPIs introduced as the target function in equation 6.1 in Section 6.3. This means the handover related events are monitored for a certain time span. As the examinations in Section 6.6 showed the evaluation of the current handover performance should be defined in the event domain.

The optimisation speed is dependent on the frequency of handover events in the cells and thus, on the number of users located in the cell edge area of the cells.
The basic idea of the algorithm is to simplify the optimisation problem from a parallel or simultaneous optimisation of two handover control parameters to a combined optimisation. This is achieved by reducing the range of allowed HOPs to a subset lying on a diagonal line in the handover parameter operating space. Figure 7.1 illustrates an example for the limitation of the optimisation space.
This limitation allows an ordering of the allowed HOPs. The current configuration gets two possible neighbouring HOPs that can be selected as new handover control parameter

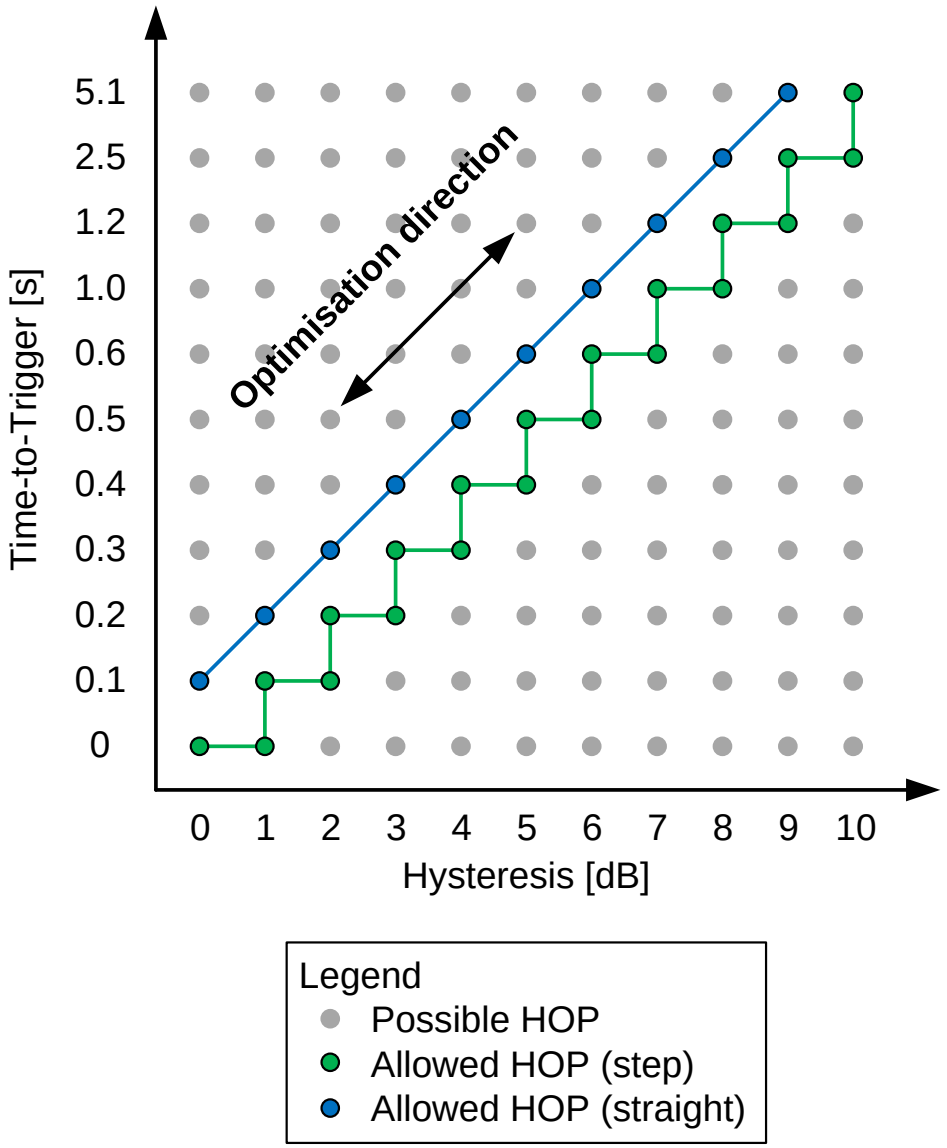

Figure 7.1: Limitation of the allowed handover operating points

configurations. Thus, it is possible to change the HOP in one of the two optimisation directions if the observed handover performance does not fulfil the requirements of the network operator. For example, the neighbouring HOP towards lower HYS and TTT values can be selected if the HPI_{fail} or the radio-link failure ratio HPI_{rlf} is too high. In the case that the ping-pong handover ratio HPI_{pp} is too high the neighbouring HOP in the opposite direction can be selected. This is because the analysis of the HPIs in Section 6.2 showed that the probability for better performance in the corresponding optimisation directions is large. The drawback of this limited set of HOPs is that it cannot be guaranteed that the best HOP for the given weighting parameters will be found by the optimisation algorithm.

However, the controllability and observability studies in [Jansen10b] and the analysis of the handover performance using the target function in Section 6.3 showed that very small HYS and TTT values lead to very high ping-pong handover ratios up to almost 100 % and HOPs with very high HYS and TTT values lead to a failure event ratio of 100 %. Medium handover control parameter values or the combination of one high and one low value show the best performance. This means that every diagonal line in the handover operating space originating at small HYS and TTT values and ending in the area of high HYS and TTT values crosses an area of better handover performance. The analysis of the impact of the weighting parameters on the selection of the HOP in Section 6.3 showed that the area of better handover performance is shifted, but nevertheless, the area lies between the two extreme cases. An optimisation along the reduced space of allowed HOPs will henceforth improve the handover performance compared to a random (experienced-based) HOP selection. It might become necessary to shift the diagonal line if the resulting handover performance is still unacceptable.

Figure 7.1 shows two alternatives for the reduced optimisation space of allowed HOPs, the step and the straight version. The performance of the two options differs in many aspects. The first difference is the optimisation speed. The straight line of allowed HOPs covers a smaller number of HOPs and hence the identification of a better operating point is faster. The drawback of this implementation is that less HOPs can be selected and the probability of a performance degradation in comparison to a solution that covers all HOPs increases. The step version contains more HOPs but the optimisation speed is lower. Moreover, a certain probability exists that the performance of two neighbouring HOPs is very similar and the selection of the optimisation direction is complicated. The result could be an oscillation between two neighbouring HOPs.

As mentioned before, the NHP-Opt evaluates the current handover performance based

on the target function in equation 6.1. The importance of the individual HPIs can be influenced by the weighting parameters. The impact of the weighting parameters on the optimisation result has been analysed in Section 6.3. Figure 7.2 presents a flowchart of the algorithm that will be detailed in the following.

Before the optimisation algorithm is initiated, all cells in the network have to select an allowed HOP as starting condition. The starting HOP does not influence the optimisation result in the long run but it may influence the adaptation speed in the beginning of the simulation. For HOPs with very low or very high HYS and TTT values the optimisation algorithm may need quite a number of optimisation steps before a good handover performance is reached. Especially in real networks the temporary degradation of the handover performance could lead to reduced trustworthiness in SON algorithms. Hence, the starting HOPs should be selected in an area of good performance based on network experience.

In addition to the starting HOPs the initial optimisation direction has to be selected for all cells. The optimisation direction is switched, if the optimisation algorithms experiences worse handover performance in the current configuration compared to the last HOP. Worse handover performance is detected by a higher HPI_{sum} value. The selection of a starting optimisation direction will not influence the optimisation capability of the algorithm in the long-run but can influence the performance of the algorithm in the starting phase. This is the case if the handover performance is worse in the neighbouring HOP in the initial optimisation direction and better in the opposite direction.

In every time step the handover related statistics are collected. The optimisation is carried out in fixed optimisation intervals as shown in Figure 6.1. These intervals are defined as a fixed number of handover related events. Once the handover performance statistics contain this number of events the HPI_{sum} is calculated from the HPIs. If the HPI_{sum} is equal to zero, no optimisation is needed since the HPIs are all equal to zero as well and no negative handover events have been observed. If the HPI_{sum} is not equal to zero, the handover performance of the current HOP is compared to the performance of an adjacent HOP in the predefined optimisation direction. Thus, the handover control parameters are adapted to the adjacent HOP settings and another observation phase is started. Once the observation results (HPI_{sum} values) from the two HOPs are available, the better performing HOP is selected and the next HOP in the optimisation direction of the better performing HOP is selected as new HOP to be analysed.

During initialization, the HOPs of all the eNBs in the scenario are set to the same value. Subsequently, each eNB will change the current HOP individually, based on the

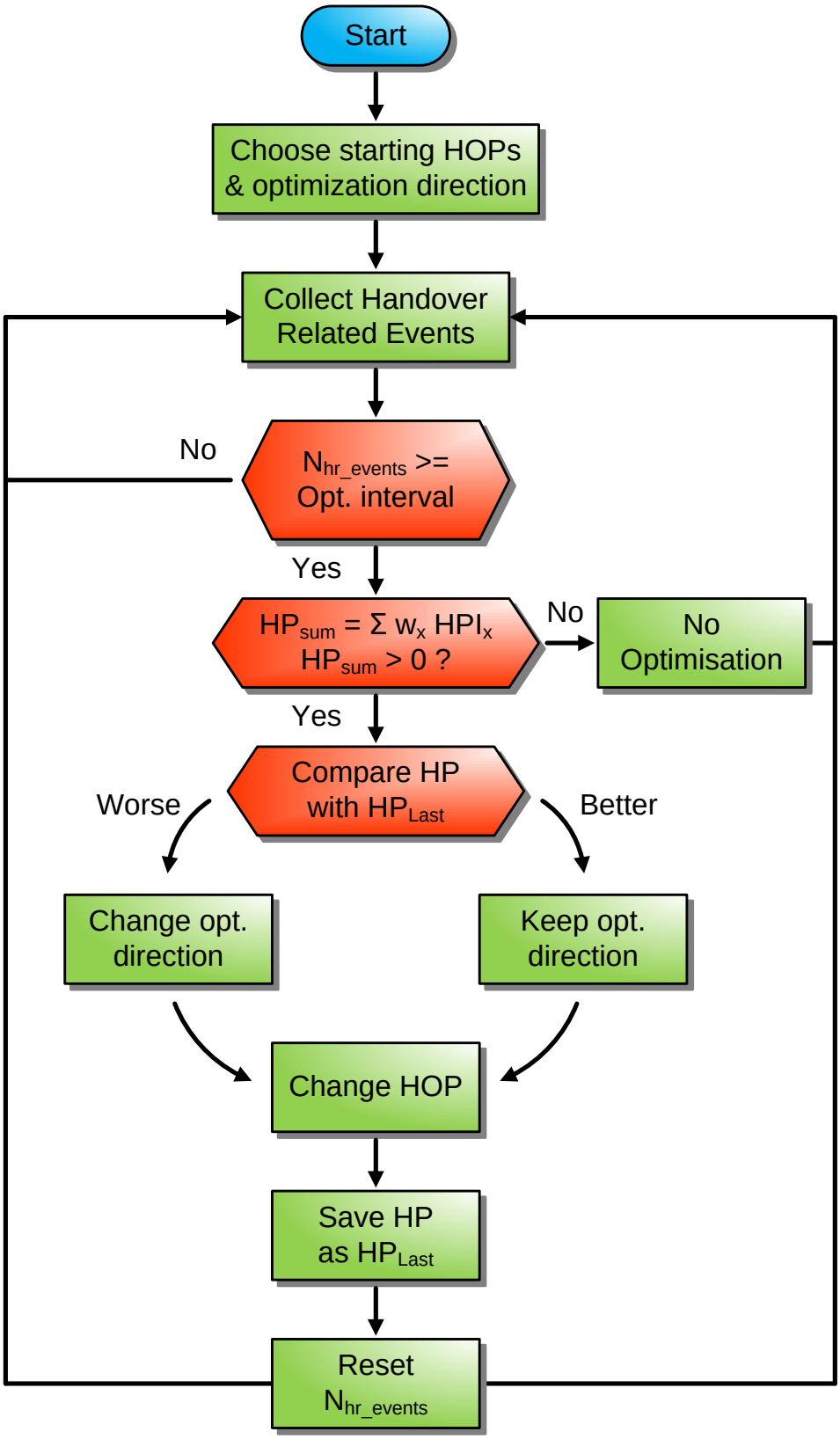

Figure 7.2: Flowchart of the NHP-Opt algorithm

observed cell performance. The diagonal on which the optimisation will be carried out, is dependent on the initial HOP setting, since this diagonal has to pass through this HOP. Thus, the selection of the same starting HOP assures that the same diagonals are used in every cell in the network. For very extreme or inappropriate initial HOP settings, the algorithm may perform sub-optimally since the absolute minimum might be impossible to reach and a local minimum will be achieved instead.
If the performance of the current HOP is worse than the performance of the previous HOP, the optimisation direction is switched and a new HOP in this direction is chosen. If the performance of the current HOP is better, a new HOP is chosen in the current optimisation direction. The HOPs can be found by going up and down the allowed HOPs as shown in Figure 7.1. Finally, the HPI_{sum} value of the last HOP and the handover optimisation direction are saved since they are needed for the next optimisation decision. There is no direct relationship between the HOP settings or changes of neighbouring eNBs (group behaviour or alignment), i.e. the optimisation activities of a cell are not harmonised with the activities of adjacent cells.
The decision to use the HPI_{sum} as the input parameter for this algorithm, in opposite to base the optimisation on the single HPI values on their own, has two advantages:

- The HPI_{sum} offers a more complete view on the network performance. Since the three HPIs are closely related, certain compromises must be made in order to improve the overall handover performance. For instance, a HOP setting that minimizes the radio-link failure ratio will most probably increase the ping-pong handover ratio.

- The weights used for calculating the HPI_{sum} are a direct translation of the operator policy, i.e. the optimisation goal of the operator. Hence, this approach enables the operator to influence the optimisation goal. The operator can adapt the weights of the HPI_{sum} (or their relative value to each other) to control the resulting handover performance.

The evaluation of the performance of the NHP-Opt is based on system-level simulations in different simulation scenarios. The results are discussed in the following sections.

7.1.1 Performance Evaluation in the Hanover Scenario

The simulation parameters for the system-level simulations in the Hanover scenario are given in Table 7.1. The remaining scenario parameters are listed in Table 5.2 in Section

Parameter	Value	Description
Simulation Scenario	Hanover	-
Simulation Time	3000 s	Repetition of User Mobility[5]
Simulation Step Size	100 ms	-
Interference Model	Cell Load	Real Cell Load (See equation 5.5)
HPI_{sum} weighting parameters	S1 and S2	Two Sets considered
Inactive Cell Load	10 %	Load of Cells Without Users
Minimum Cell Load	10 %	If User Cell Load is Smaller
Load Multiplication Factor	1.5	-
Minimum Number of Users	10 Users per Cell	To be Considered for Evaluation
Considered Cells	65 Cells	Full-fill the Requirements[6]

Table 7.1: Simulation parameters for the Hanover scenario

5.4.1. The duration of the simulations is set to 3,000 s to allow the evaluation of the algorithm in the long-run. The discussion on the network requirements in Section 6.1 showed that a successful optimisation (evaluation of the handover performance) can only be achieved in "stable" network conditions. This means the load fluctuation and network configuration changes need to be small in the optimisation phase. Thus, the performance improvement in 3000 s simulation time should be significant to enable the adaptation of the handover control parameters to varying network conditions.

The real cell load caused by the users in the network is taken into account for the calculation of the interference from neighbouring cells. The minimum cell load of active and inactive cells is set to 10 %, i.e. the minimum interference in the case of load dependent SINR calculation from a cell is 10 %. Two sets of weighting parameters for the calculation of the HPI_{sum} are considered for the performance evaluation. Weighting parameter set one (S1) defines $w_{pp} = w_{fail} = w_{rlf} = 1$. The second weighting parameter

[5]The user mobility traces in this scenario have a length of 1000 s. For longer simulations the user mobility is repeated and the optimisation algorithm is continued with the latest cell parameter settings from the earlier run.

[6]The requirement for a cell to be considered in the performance evaluation is that at least ten UEs are connected to the cell in any time step during the simulation. Cells in the outlying area are simulated as interference sources but not considered for the evaluation of the handover optimisation algorithm.

set (S2) is $w_{pp} = 1$ and $w_{fail} = w_{rlf} = 3$. The load multiplication factor of 1.5 assures a load situation in the network without cell overload. At least 10 users have to be connected to a cell simultaneously so that the cell is considered for the performance evaluation.

The development of the HPI-values and the handover control parameters of cell 34 in one simulation run is depicted in Figure 7.3. As starting HOP the HYS is set to 0 dB and the TTT to 0 s in all cells. Due to the fact that the selected starting HOP is the smallest possible HOP the initial optimisation direction is upward. The first handover control parameters that will be adapted by the optimisation algorithm is the HYS parameter. Hence, the allowed HOPs in the optimisation are described by the stair function in Figure 7.1. This simulation with extreme starting conditions is conducted to evaluate the optimisation speed of the algorithm. An observation window size of 40 events has been chosen based on the earlier analysis of the minimum observation window size. Weighting parameter set S2 is used for the calculation of the HPI_{sum}.

The plot starts with a simulation time of 38.3 s shown on the x-axis which is the time when 40 handover related events have been observed in cell 34. The optimisation algorithm selects a new HOP in the current optimisation direction, i.e. the HOP with a HYS of 1 dB and a TTT of 0 s. The y-axis for the handover control parameters is given

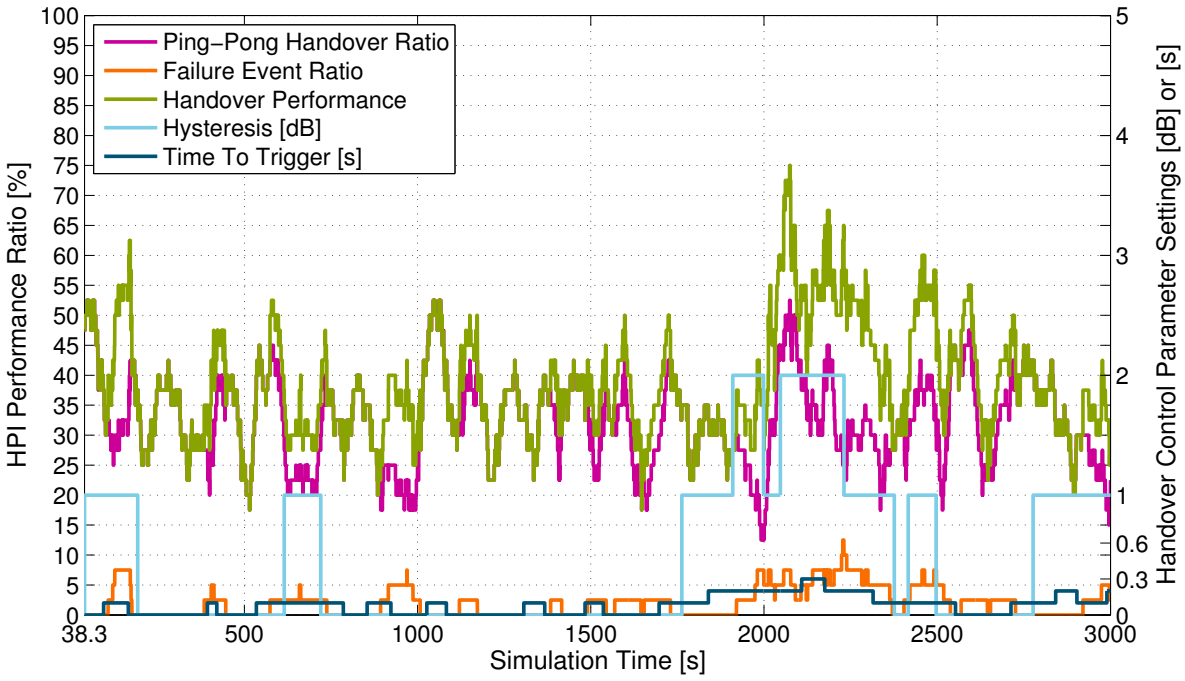

Figure 7.3: HPI-performance and control parameter changes in cell 34 (HOP[0,0])

on the right side of the figure. The handover performance frequently fluctuates between values of 20 % and 75 % in the simulation run. The optimisation of the handover control parameters does not improve the performance in this example cell. Moreover, the starting HOP is reached several times in the optimisation phase.

The reasons for this behaviour of the NHP-Opt are manifold. Figure 7.4 shows the mean handover performance in all HOPs for cell 34 for weighting parameter set S2. All HOPs with low HYS and TTT settings lying on the stair function beginning at the starting HOP show a similar mean handover performance ratio in this simulation. This means the identification of a best HOP is difficult in this case. In addition the NHP-Opt tends to identify local minimum handover performance ratios as best handover performance. This is caused by the limitation of the handover optimisation algorithm to compare the current handover performance only to neighbouring HOPs. As discussed before this limitation prevents jumps in the individual HPIs. Nevertheless, the probability to overcome an area of HOPs with worse performance to reach an area of better performance is small. Furthermore, the best performing HOP on the stair function, i.e. the HOP with a HYS of 4 dB and a TTT of 0.3 s for cell 34, shows a similar mean handover performance as many other Low_{HOPs} on the stair function. The short observation window size and the similar performance of several HOPs lead to the small performance gain depicted in

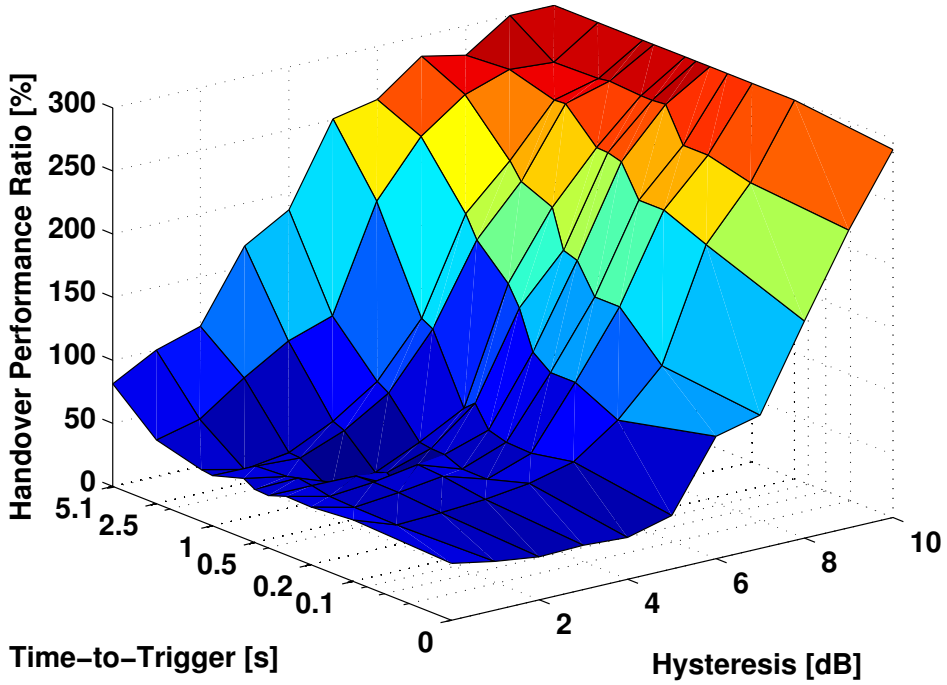

Figure 7.4: Mean handover performance (HPI_{sum}) in cell 34 ($w_{pp} = 1, w_{fail} = w_{rlf} = 3$)

Figure 7.3.

The development of the HPI-values and the handover control parameters in another simulation run is shown in Figure 7.5. A different starting HOP with a HYS of 8 dB and a TTT of 1 s is selected for this run. The first impact of the starting HOP with a higher HYS and TTT value is that fewer handover related events are observed in this simulation run. The starting point of the simulation time, as shown in Figure 7.5, is 456.1 s, meaning that 40 handover related events have been observed in this time period. Due to the lower amount of observed handover related events, only six optimisation steps and control parameter changes are executed. In the earlier simulation with lower HYS and TTT values 36 optimisation steps were executed. The optimisation speed is slowed down by the selection of the starting HOP. Moreover, the handover control parameters are increased twice in the optimisation phase, which is caused by the similar performance of the compared HOPs. Nevertheless, both compared HOPs show an overall bad performance and increasing the handover control parameters hinders a quick performance improvement. This results in a failure event ratio of more than 40 % at the end of the simulation. Again the optimisation speed is low but the handover performance is improved by the optimisation algorithm compared to the starting condition.

Figure 7.6 illustrates the HPI-value and handover control parameter progress for a sim-

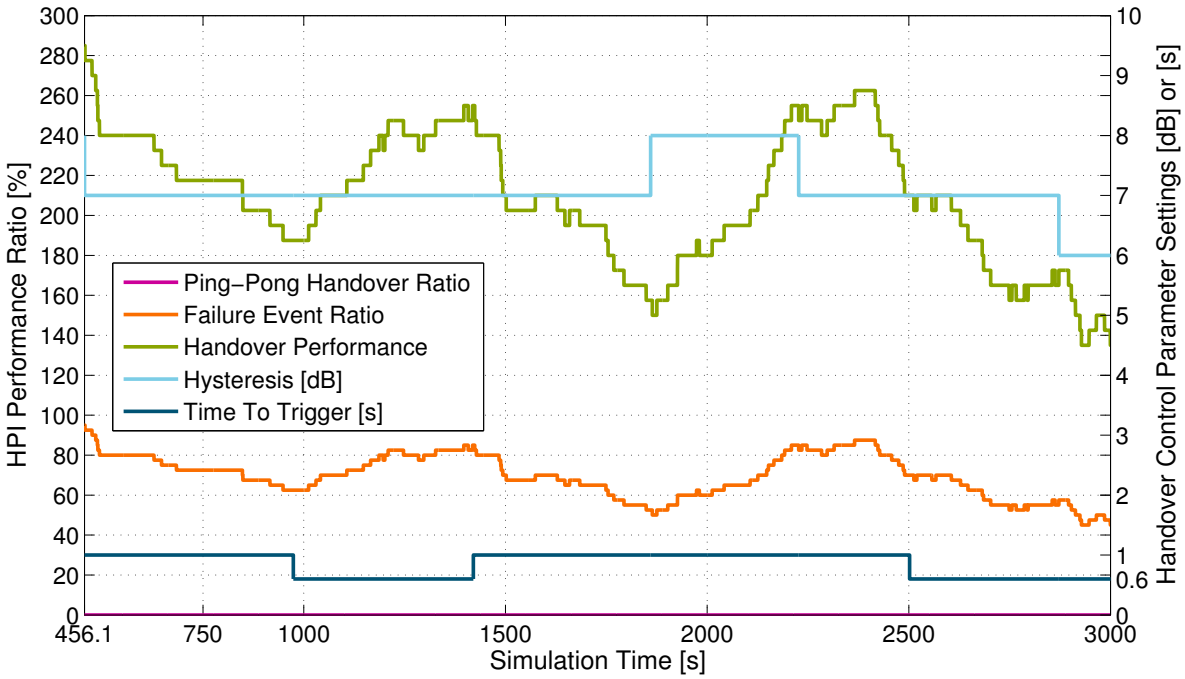

Figure 7.5: HPI-performance and control parameter changes in cell 34 (HOP[8,1])

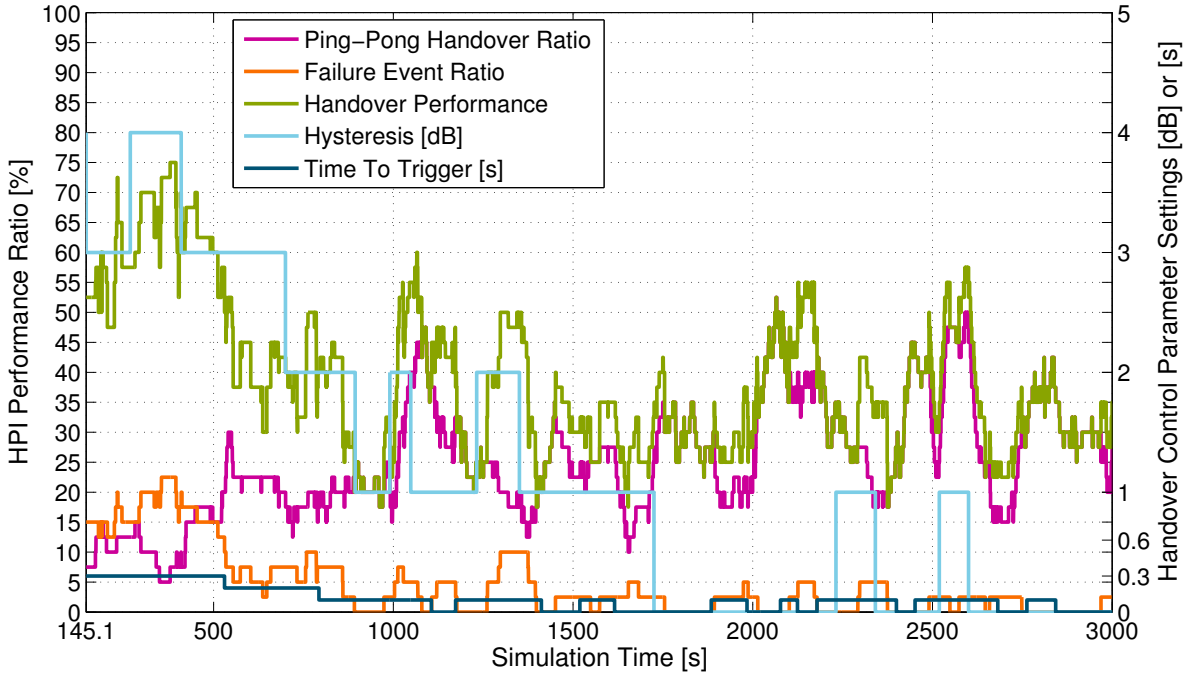

Figure 7.6: HPI-performance and control parameter changes in cell 34 (HOP[4,0.3])

ulation run with a starting HOP composed of a HYS of 4 dB and a TTT of 0.3 s. This starting HOP shows a good handover performance compared to the other HOPs on the stair function. For the same reason as discussed before, i.e. the constitution of the mean handover performance caused by the weighting parameter settings shown in Figure 7.4, the optimisation algorithm drives the handover control parameters to low values. Nevertheless, the failure event ratio decreases to values close to zero which is the objective for the selected weighting parameter settings. Therefore, the optimisation target is reached in this example.

The statistics of different simulation runs for all 65 cells are listed in Table 7.2. The table contains the result of six simulation runs with three sets of starting HOPs and the two weighting parameter sets S1 and S2. The observation window is set to 40 handover related events in all simulation runs. HPI_{fail_event} Start and HPI_{pp} Start show the HPI statistics of the starting HOP. HPI_{fail_event} Opt. and HPI_{pp} Opt. give the average performance of the network with running optimisation algorithm. The development of the handover performance in the last 1000 s of the simulation is given by HPI_{fail_event} Opt_{L1000} and HPI_{pp} Opt_{L1000}. The best HOP lying on the stair function of allowed HOPs is identified by the lowest mean HPI_{sum} value over the complete simulation time. The performance of this HOP is represented by HPI_{fail_event} $Best_{Stair}$

$N_{hr\_events} = 40$	Starting HOP					
	HYS 0 dB TTT 0 s		HYS 8 dB TTT 1 s		HYS 4 dB TTT 0.3 s	
HPI_{fail_event} Start	0.29 %	0.29 %	84.93 %	84.93 %	10.14 %	10.14 %
HPI_{pp} Start	42.97 %	42.97 %	0 %	0 %	7.90 %	7.90 %
HPI_{fail_event} Opt.	1.82 %	1.54 %	64.08 %	64.05 %	7.74 %	6.99 %
HPI_{pp} Opt.	30.80 %	33.33 %	0.09 %	0.09 %	11.02 %	13.86 %
HPI_{fail_event} Opt_{L1000}	2.52 %	2 %	52.41 %	52.38 %	7 %	6.30 %
HPI_{pp} Opt_{L1000}	27.45 %	31.09 %	0.25 %	0.22 %	11.13 %	15.23 %
HPI_{fail_event} $Best_{Stair}$	6.68 %	2.43 %	6.68 %	2.43 %	6.68 %	2.43 %
HPI_{pp} $Best_{Stair}$	6.55 %	14.60 %	6.55 %	14.60 %	6.55 %	14.60 %
HPI_{fail_event} Best	5.88 %	2.47 %	5.88 %	2.47 %	5.88 %	2.47 %
HPI_{pp} Best	4.32 %	9.81 %	4.32 %	9.81 %	4.32 %	9.81 %
Weighting Parameters	S1 (1 1)	S2 (1 3)	S1 (1 1)	S2 (1 3)	S1 (1 1)	S2 (1 3)
$Time_{Best\_Stair\_HOP}$	4.19 %	8.65 %	0.36 %	0.13 %	17.59 %	16.75 %
$Time_{Best\_Stair\_L1000}$	6.09 %	9.32 %	1.09 %	0.40 %	17.33 %	17.31 %
$Time_{Best\_HOP}$	1.9 %	3.32 %	0 %	0 %	5.68 %	6.94 %
$Time_{Best\_HOP\_L1000}$	2.23 %	3.43 %	0 %	0 %	4.46 %	8.11 %

Table 7.2: Performance of the neighbouring HOP performance optimisation algorithm for an event domain observation window of 40 events

and HPI_{pp} $Best_{Stair}$. This best performing HOP identification procedure does not automatically lead to the HOP with the lowest amount of negative handover events. The reason for this is that as long as no new handover related events are observed in a cell the last handover performance observation is saved as current performance. Consequentially, the chronology of the handover related events influences the evaluation of the handover performance. HPI_{fail_event} Best and HPI_{pp} Best show the handover performance statistics of the best HOP in the complete set of possible HOPs.

The first simulation run (column 1) starts with a HYS of 0 dB and a TTT of 0 s. Weight-

ing parameter set S1 is used in this simulation. The starting HOP shows a high ping-pong handover ratio of 42.97 % and a small failure events ratio of 0.29 %. According to the weighting parameter settings, the negative handover ratio (the sum of the ping-pong handover ratio and the failure event ratio) should decrease in the optimisation and the failure event ratio and ping-pong handover ratio should approximate. The HPI ratios for the optimized case show that the ping-pong ratio and the negative handover ratio decrease. In the last 1,000 s of the simulation the ping-pong handover ratio is further improved and the total ratio of negative handover events still decreases. However, as discussed for the example in cell 34 the difference to the best performing stair function HOP is still significant in the end of the simulation. Changing the weighting parameters to S2, slows down the improvement of the ping-pong handover ratio by the optimisation algorithm. As a higher weighting parameter value for the failure events aims at lower failure event ratios in the network the optimisation result proves this impact on the optimisation goal, but the performance at the end of the simulation is still sub-optimal.

The results for the starting HOP with a HYS of 8 dB and a TTT of 1 s show a very high failure event ratio in the starting HOP. The reduction of failure events is similar for both weighting parameter sets. The handover performance in the last 1,000 s of the simulation still shows a failure event ratio of more than 50 %. The example of cell 34 using the same starting HOP showed a similar (slow) optimisation result and only a few optimisation steps in the simulation time. The reason for this is that the reduced number of handover related events for high HYS and TTT values decelerates the optimisation process.

In the simulation runs with a starting HOP with a HYS of 4 dB and a TTT of 0.3 s the performance of the starting HOP is significantly better compared to the earlier two starting HOPs. The NHP-Opt fails to optimize the handover performance for weighting parameter set S1. As explained before the optimisation target for this weighting parameter set is the smallest negative handover event ratio, i.e. the sum of the failure event and ping-pong handover ratio. A comparison of the negative handover event ratio in the starting HOP (10.14 % + 7.90 % = 18.04 %) and the same ratio for the complete simulation time in the optimized case (7.74 % + 11.02 % = 18.76 %) shows that the overall performance is worse using the NHP-Opt. The performance increases for the last 1000 s (Negative Handover Ratio: 18.13 %) but fails to reach the performance of the starting HOP. The failure event performance in the last 1000 s simulation time is similar to the failure event performance in the best stair HOP. The ping-pong handover ratio is still more than 4.5 % higher in the optimized case. Changing the weighting parameter set to

S2 leads to better failure event performance in the end of the simulation. Nevertheless, the difference to the best possible failure event performance is still significant.

The last four rows in Table 7.2 give the statistics on the time the cells in the simulation runs use the best stair HOP or best overall HOP. The numbers prove that the optimisation algorithm increases the probability for better handover performance in the network and that medium HYS and TTT values for the starting HOP improve the optimisation speed. Nevertheless, the identification of the best performing HOP fails in most of the cases. It should be noted that the algorithm design, i.e. the continuous switching to a neighbouring HOP, limits the identification rate of the best HOP to roughly 50 %. Further improvements of the algorithm by colleagues in the SOCRATES project in [Balan11b] and [Balan11a] introduce an abort criterion to stop the fluctuation of the HOP in the long-run. The problem is that other criterions to continue the optimisation have to be defined as well in this case. Nevertheless, the optimisation by the NHP-Opt needs an abort criterion to reach a stable state in the network.

Table 7.3 shows the simulation results for the same set of 6 simulation runs with an observation window size of 50 events. The impact of the larger observation window on the optimisation result is depending on the selection of the starting HOP. For the starting HOP with a HYS of 0 dB and a TTT of 0 s the time the cells use the best stair HOP increases. This is caused by the fact that the HPI_{sum} values are more reliable for longer observation windows, i.e. the handover performance evaluation is more reliable. The optimisation runs with a starting HOP with a HYS of 8 dB and a TTT of 1 s show a worse selection rate for the best performing HOPs. The lower amount of handover related events for high HYS and TTT values in combination with a longer observation window size, avoids faster handover performance improvements. The selection of a starting HOP with a HYS of 4 dB and a TTT of 0.3 s further increases the identification rate of the best performing HOP and stair HOP for weighting parameter set S1. In this case the reliability of the HPI_{sum} values benefits the handover optimisation decisions compared to a smaller observation window. For weighting parameter set S2 a lower identification rate can be observed compared to the observation window of 40 events. This starting HOP is less optimal for this weighting parameter set and the longer observation window slows down the optimisation for weighting parameter set S2.

The outcome of the handover performance optimisation for an observation window of 60 handover related events is listed in Table 7.4. The selection of a starting HOP with a HYS of 0 dB and a TTT of 0 s leads to a decreasing selection rate of the best performing stair HOP compared to an observation window of 50 events. This is caused by both, the

$N_{hr\_events} = 50$	Starting HOP					
	HYS 0 dB TTT 0 s		HYS 8 dB TTT 1 s		HYS 4 dB TTT 0.3 s	
HPI_{fail_event} Start	0.29 %	0.29 %	84.93 %	84.93 %	10.14 %	10.14 %
HPI_{pp} Start	42.97 %	42.97 %	0 %	0 %	7.90 %	7.90 %
HPI_{fail_event} Opt.	1.96 %	1.19 %	67.18 %	67.14 %	7.98 %	7.23 %
HPI_{pp} Opt.	31.40 %	34.22 %	0.06 %	0.06 %	11.29 %	13.20 %
HPI_{fail_event} Opt_{L1000}	2.71 %	1.52 %	55.44 %	55.34 %	7.33 %	6.50 %
HPI_{pp} Opt_{L1000}	28.15 %	32.21 %	0.16 %	0.16 %	11.58 %	14.37 %
HPI_{fail_event} $Best_{Stair}$	6.61 %	2.38 %	6.61 %	2.38 %	6.61 %	2.38 %
HPI_{pp} $Best_{Stair}$	7.43 %	15.77 %	7.43 %	15.77 %	7.43 %	15.77 %
HPI_{fail_event} Best	5.92 %	2.35 %	5.92 %	2.35 %	5.92 %	2.35 %
HPI_{pp} Best	4.72 %	10.55 %	4.72 %	10.55 %	4.72 %	10.55 %
Weighting Parameters	S1 (1 1)	S2 (1 3)	S1 (1 1)	S2 (1 3)	S1 (1 1)	S2 (1 3)
$Time_{Best\_Stair\_HOP}$	7.26 %	10.01 %	0 %	0 %	19.73 %	15.82 %
$Time_{Best\_Stair\_L1000}$	8.79 %	11.30 %	0 %	0 %	23.31 %	17.09 %
$Time_{Best\_HOP}$	2.2 %	4.25 %	0 %	0 %	5.52 %	5.37 %
$Time_{Best\_HOP\_L1000}$	2.71 %	5.58 %	0 %	0 %	5.64 %	5.96 %

Table 7.3: Performance of the neighbouring HOP performance optimisation algorithm for an event domain observation window of 50 events

longer optimisation cycle and the slower adaptation of the handover control parameters. The simulation runs with a starting HOP with a HYS of 8 dB and a TTT of 1 s lack a significant optimisation of the handover performance due to the small number of handover related events and the long optimisation cycle. The implication of this behaviour is that the NHP-Opt is unsuitable to optimize the handover control parameters quickly if the starting HOP shows a low number of handover related events compared to the allowed HOPs in the optimisation. In the case that a starting HOP with a HYS of 4 dB and a TTT of 0.3 s is chosen the identification rate of the best stair performing HOP negligibly

$N_{hr\_events} = 60$	Starting HOP					
	HYS 0 dB TTT 0 s		HYS 8 dB TTT 1 s		HYS 4 dB TTT 0.3 s	
HPI_{fail_event} Start	0.29 %	0.29 %	84.93 %	84.93 %	10.14 %	10.14 %
HPI_{pp} Start	42.97 %	42.97 %	0 %	0 %	7.90 %	7.90 %
HPI_{fail_event} Opt.	1.75 %	1.06 %	71.08 %	71.08 %	7.79 %	7.03 %
HPI_{pp} Opt.	32.45 %	35.15 %	0 %	0 %	11.22 %	13.11 %
HPI_{fail_event} Opt_{L1000}	2.37 %	1.25 %	60.53 %	60.53 %	7.24 %	6.01 %
HPI_{pp} Opt_{L1000}	29.37 %	33.66 %	0 %	0 %	11.98 %	15.38 %
HPI_{fail_event} $Best_{Stair}$	6.53 %	2.35 %	6.53 %	2.35 %	6.53 %	2.35 %
HPI_{pp} $Best_{Stair}$	7.59 %	15.94 %	7.59 %	15.94 %	7.59 %	15.94 %
HPI_{fail_event} Best	5.76 %	2.42 %	5.76 %	2.42 %	5.76 %	2.42 %
HPI_{pp} Best	5.45 %	10.89 %	5.45 %	10.89 %	5.45 %	10.89 %
Weighting Parameters	S1 (1 1)	S2 (1 3)	S1 (1 1)	S2 (1 3)	S1 (1 1)	S2 (1 3)
$Time_{Best\_Stair\_HOP}$	6.20 %	8.01 %	0 %	0 %	20.73 %	14.82 %
$Time_{Best\_Stair\_L1000}$	7.89 %	7.08 %	0 %	0 %	23.61 %	18.74 %
$Time_{Best\_HOP}$	2.64 %	3.44 %	0 %	0 %	3.37 %	3.17 %
$Time_{Best\_HOP\_L1000}$	3.08 %	3.74 %	0 %	0 %	3.20 %	4.51 %

Table 7.4: Performance of the neighbouring HOP performance optimisation algorithm for an event domain observation window of 60 events

increases compared to an observation window of 50 handover related events. The fact that the starting HOP shows better handover performance compared to the other starting HOPs combined with the slower optimisation and the higher reliability of the HPI values favours the slightly better simulation result. Nevertheless, these characteristics of the NHP-Opt with longer observation windows limit the optimisation speed. In the case that sudden and severe changes in the network necessitate a faster adaptation of the handover control parameters the optimisation by the algorithm might fail.

7.1.2 Conclusion on the Applicability of the NHP-Opt

The results of the system-level simulations show that the NHP-Opt optimizes the handover performance in the LTE network. The handover performance is improved by the algorithm compared to the starting condition independent of the starting HOP configuration and the observation window size. Nevertheless, the selection of the starting HOP configuration and the observation window size has an impact on the optimisation result as the final handover performance significantly differs in the individual simulation runs. Moreover, the simulation runs with different weighting parameter settings proved that the handover performance in the network can be controlled and managed by the weighting parameters. Thus, the network operator can influence the optimisation objective according to his operator policy.

However, the simulation results prove that the optimisation speed of the NHP-Opt is limited. The reason for this is that the handover control parameter optimisation is carried out step wise, i.e. the current HOP of a cell is only adapted to a neighbouring HOP in the optimisation space. The fact that neighbouring HOPs tend to show similar handover performance increases the probability for fluctuations in the handover control parameter adaptation in areas of sub-optimal handover performance in the optimisation space. This leads to further deceleration of the handover performance optimisation. Especially with a view to the increasing complexity of future mobile communication networks in terms of energy saving, femto-cell and spectrum adaptation functions the adaptation speed to new network conditions is very important. In addition the simulation results reveal that local minima in the optimisation space handicap the identification of the best performing HOP.

The consequence of these problems is that the identification rate of the best performing HOP using the NHP-Opt is low in all simulation runs. Above all the NHP-Opt lacks the ability to find the best HOP in the complete set of handover control parameters by the reduction of the allowed HOPs for the optimisation algorithm. Furthermore, the definition of an abort criterion to terminate the optimisation phase and the introduction of an initiation criterion for the optimisation turns out to be difficult. Neither the identification of similar handover performance in neighbouring HOPs nor the stable handover performance in the selected HOP allow the interpretation that the best performing HOP has been identified. Thus, it is desirable to find an optimisation algorithm with faster adaptation ability of the handover control parameters and a higher identification probability of the best performing HOP in the cells.

7.2 Handover Performance Prediction Optimisation Algorithm

The Handover Performance Prediction Optimization Algorithm (HP-Pred-Opt) follows the concept of the prediction of the handover performance for a set of potential handover control parameters (e.g. all specified HOPs). To predict the handover performance, the handover procedure is virtually executed for every specified HOP and the handover related events, i.e. the handover failure events and ping-pong handover events, are predicted and stored for every HOP. As the handover procedure is based on the UE RSRP measurements, immediate reporting of the RSRP measurements to the entity that conducts the handover performance prediction is necessary. For the definition of considered handover control parameter sets in this dissertation (See Section 3.2 for details) this translates to 121 handover procedure simulations in the case that a UE detects a stronger cell. To predict the handover related events an estimation method for the SINR is required, since the detection of handover or radio-link failures bases on the signal quality. The optimisation algorithm is split in two parts as shown in Figure 7.7.

The first part is the measurement based prediction of the handover related events visualized on the left side of the figure. This handover performance prediction report generation process can be executed in the eNB or the UE. In both cases measurements, system performance indicators and control parameter settings have to be transferred to the entity that generates the prediction report. The report generation is started by the A6-Event introduced in Section 3.1.2. It should be noted that all offset parameters defined for the event A6 are set to zero. By this means it is assured that the handover related events can be predicted for a HYS of 0 dB and a TTT of 0 s. Immediate reporting of the signal strength development of the neighbouring cells is necessary in the case that a neighbour becomes better than the serving cell to predict the handover behaviour of the UE in this (lowest) HOP.

The A6-Event starts the simulation of the handover procedure for every considered HOP. Simulation of the handover procedure means that for every HOP the point in time for the handover decision is calculated based on the development of the RSRP measurements from the neighbouring cells. If the handover decision is made in a HOP, the UE virtually changes the connected cell after a pre-defined handover execution time. Consecutively, further handover decisions in the new connected cell are predicted as well. This enables the identification of ping-pong handovers to the original SeNB. If the estimated SINR falls below a pre-defined threshold, i.e. the minimum SINR, a radio-link failure or in the

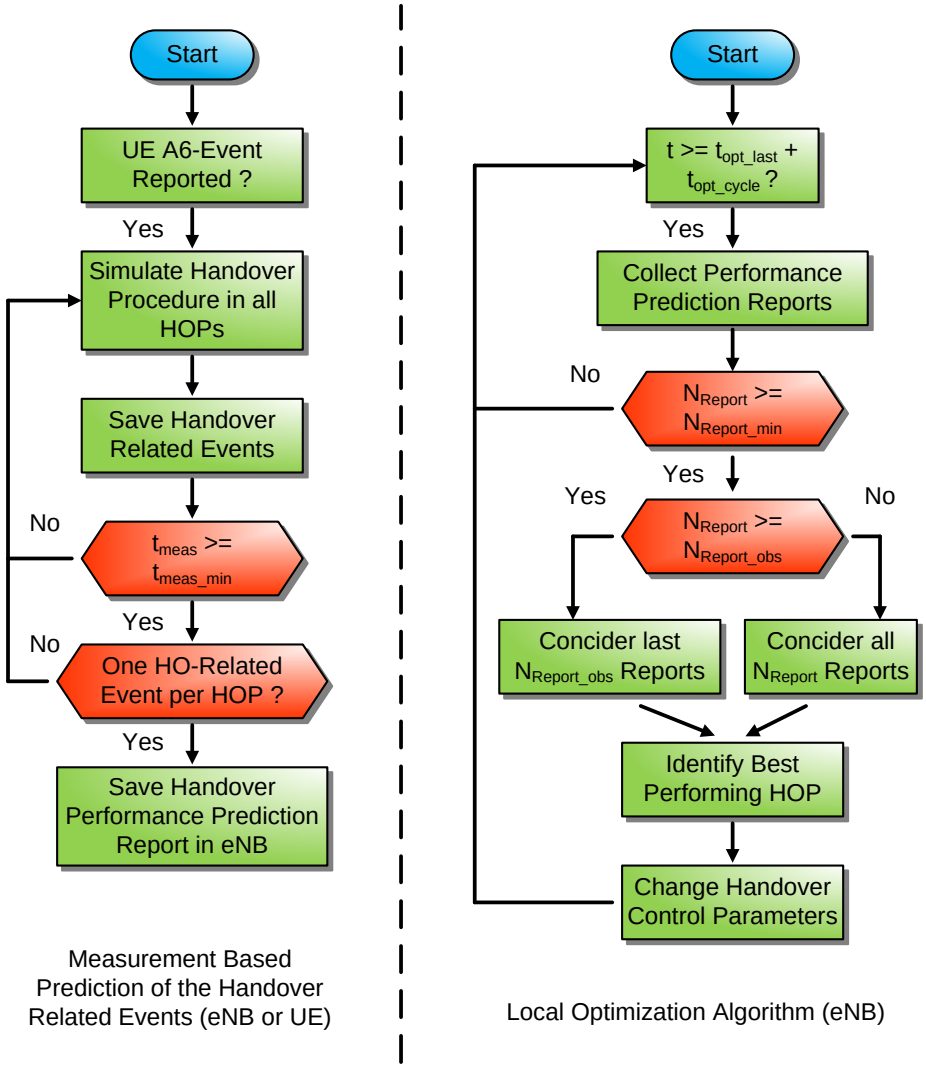

Figure 7.7: Flowchart of the handover performance prediction optimisation algorithm

case of an ongoing handover process a handover failure is reported for this HOP. The simulated handover related events are stored per HOP in the simulation process.

The pre-defined threshold t_{meas_min} defines the minimum measurement time for the development of the RSRPs. The handover procedure in every HOP is simulated at least for the time span t_{meas_min} as well. If the simulation time is larger than this threshold, the number of handover related events in the individual simulated HOPs is checked. In the case that at least one handover related event occurred in each HOP the simulation of the handover procedure is terminated and the predicted handover related events in every HOP are reported to the SeNB in a handover performance prediction report. Besides the handover related events, about which the report holds information, the predicted

mean SINR the UE would encounter if the corresponding HOP would be selected. The steps of the simulated handover procedure and the necessary additional information to perform the prediction of the handover related events are shown in Figure 7.8. The SINR estimator is the central entity in the handover procedure simulation process. In

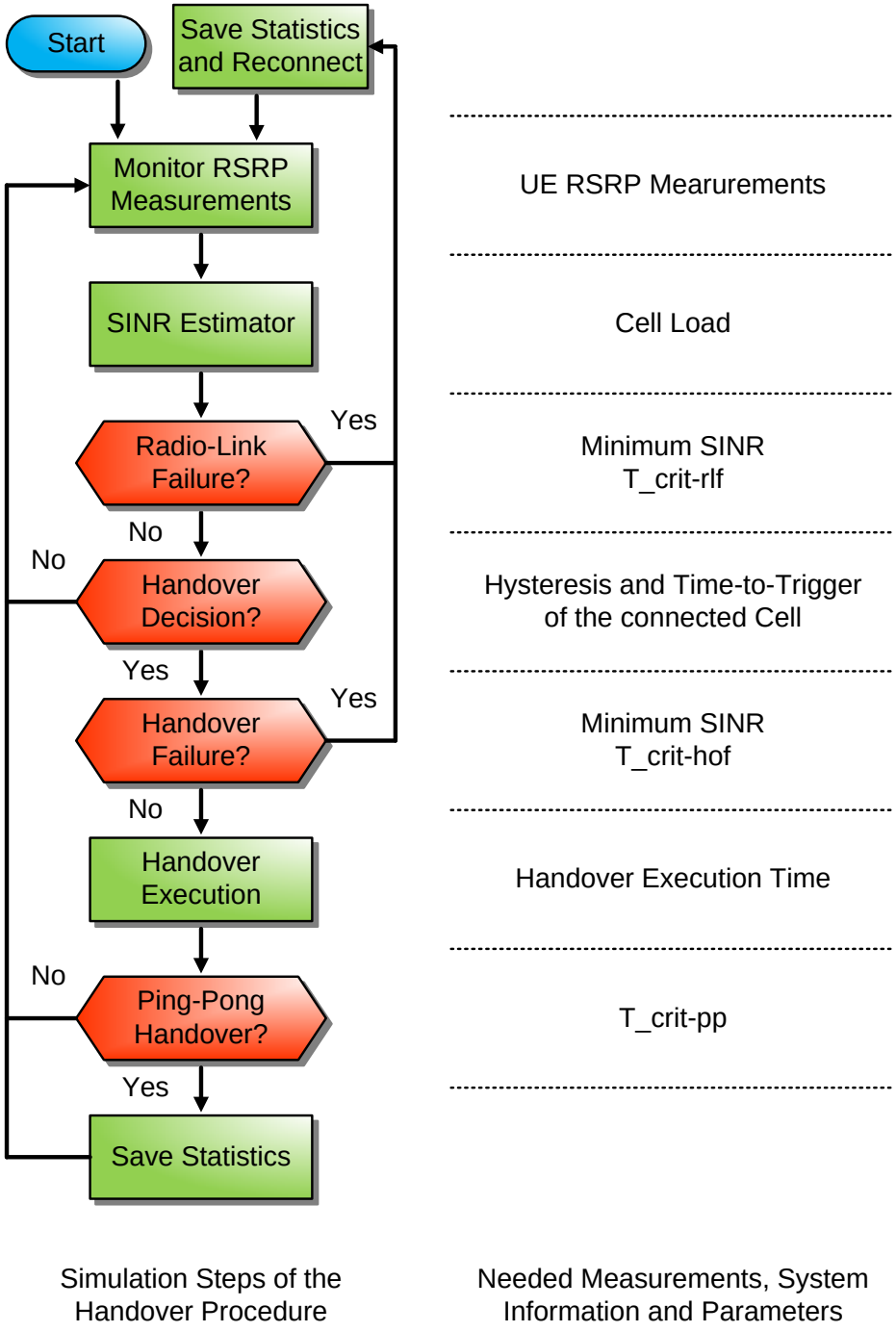

Figure 7.8: Flowchart of the simulated handover procedure and the needed information

addition to the RSRP measurements, monitored by the UE, the SINR estimator uses the cell load information from the network exchanged via the load reporting between the cells as introduced in Section 3.4. The SINR is calculated using Equation 5.5 taking account of the current load situation in the network. The detection of the radio-link and handover failures is based on the estimated SINRs. The handover decision is taken subject to the handover control parameters HYS and TTT. If the UE virtually changed the connected cell in the simulation already, the handover control parameters of the virtually connected cell (one of the possible (neighbouring) target cells for the handover) are needed to simulate the handover events. Thus, an exchange of the handover configuration between the cells is necessary. The remaining simulation parameters as the minimum SINR condition or the time span $T_{crit-pp}$ are the same parameters used in the system simulation for the detection of the handover related events.

The second part of the optimisation algorithm is dedicated to the analysis of the handover performance prediction reports as shown on the right side of Figure 7.7. The optimisation is carried out in pre-defined optimisation cycles. In an optimisation action the handover performance prediction reports are analysed by each cell. N_{Report_min} defines the minimum number of reports required before an optimisation is initiated. This minimum number of reports has a major impact on the optimisation speed of the algorithm since a low value (e.g. ten reports) will allow a fast adaptation of the handover control parameters. By contrast, the probability that ten reports represent the handover performance of all HOPs is low. Hence, the quality of the optimisation decision is affected by the minimum number of considered reports as well. N_{Report_obs} specifies the observation window, i.e. the number of reports that is usually considered to optimize the handover performance in a cell. If more reports than N_{Report_obs} are available, only the latest N_{Report_obs} are considered for the optimisation. This is to enable a fast adaptation to changing network conditions. In any other case all available reports are considered.

The identification of the best HOP is based on the same HPIs and the weighted sum of the HPIs (Equation 6.1) as for the NHP-Opt. To evaluate the handover performance in all HOPs, the predicted handover related events from the reports are used to calculate the predicted HPIs. The HOP with the lowest HPI_{sum} value is identified as the best performing HOP for the cell. The handover control parameters are adapted to the best performing HOP in each cell at the end of the optimisation action. Due to the fact that the handover related events are predicted for every HOP based on the same user movement, the HP-Pred-Opt allows the identification of the HOP with the fewest amount of negative handover events as well. This is beneficial for the optimisation since

HOPs with a higher total amount of negative handovers which qualify as the "best performing" HOP due to a significantly higher total amount of handover events, can be identified as sub-optimal handover configuration.

7.2.1 Performance Evaluation in the Hanover Scenario

The simulation parameters for the system-level simulations in the Hanover scenario are given in Table 7.5. The remaining scenario parameters are listed in Table 5.2 in Section 5.4.1. The duration of the simulations is set to 1,000 s. Weighting parameter set one (S1) ($w_{pp} = w_{fail} = w_{rlf} = 1$) is considered for the calculation of the HPI_{sum}. The minimum measurement duration t_{meas_min} is set to 30 s, i.e. the handover related events are predicted at least for 30 s after a neighbouring cell becomes stronger than the serving cell of a user. The first optimisation of the handover control parameters is initiated when ten handover performance prediction reports are available (N_{Report_min}). From that point in time all available prediction reports are used for the optimisation until 40 reports are available (N_{Report_obs}). During the further optimisation procedure the latest 40 reports are considered. The optimisation actions are taken every 10 s, which is the selected optimisation cycle. The remaining simulation parameters and assumptions are the same as in the simulations for the NHP-Opt. The performance evaluation is split in two parts: the first part concentrates on the optimisation of the handover performance of one cell in the network. The second part investigates the simultaneous optimisation of all cells in the network.

Optimisation of the Handover Performance of Cell 31

As a first step in the evaluation of the performance of the HP-Pred-Opt the algorithm is used to optimize the handover performance of cell 31. This cell is selected since the most handover events are observed in this cell. For comparison, the NHP-Opt is executed with the same objective. To evaluate the performance with fixed handover control parameter settings, 121 system-level simulations for all HOPs considered for the optimisation (See Section 3.2) are executed. In these simulations the handover control parameter settings were set to a HYS of 4 dB and a TTT of 0.3 s for all cells except cell 31. This means the handover performance for one fixed HOP in all cells and all HOPs considered by the optimisation algorithms in cell 31 has been simulated. The result of this evaluation is that cell 31 shows the best handover performance for a HYS of 2 dB and a TTT of 0 s. The handover performance with activated optimisation for cell 31, using the NHP-Opt

Parameter	Value	Description
Simulation Scenario	Hanover	-
Simulation Time	1,000 s	-
Simulation Step Size	100 ms	-
Interference Model	Cell Load	Real Cell Load (See equation 5.5)
HPI_{sum} weighting parameters	S1	-
Inactive Cell Load	10 %	Load of Cells Without Users
Minimum Cell Load	10 %	If User Cell Load is Smaller
Load Multiplication Factor	1.5	-
Minimum Number of Users	10 Users per Cell	To be Considered for Evaluation
Considered Cells	65 Cells	Full-fill the Requirements[7]
t_{meas_min}	30 s	-
N_{Report_min}	10	-
N_{Report_obs}	40	-
Optimisation Cycle	10 s	-

Table 7.5: Simulation parameters for the Hanover scenario

or the HP-Pred-Opt respectively, is compared to two sets of fixed handover parameter settings: the best performing HOP and the starting HOP.
The development of the HPI_{sum} values for the two optimisation algorithms and the two sets of fixed handover parameter settings is depicted in Figure 7.9. Figure 7.9(a) shows the results for a starting HOP with a HYS of 4 dB and a TTT of 0.3 s and Figure 7.9(b) is dedicated to a starting HOP with a HYS of 8 dB and a TTT of 1 s. The mean performance over the complete simulation time is given in the legend of the figures. In the case that a starting HOP with a HYS of 4 dB and a TTT of 0.3 s is selected both optimisation algorithms improve the handover performance compared to the fixed starting HOP settings as the mean performance indicates. The HP-Pred-Opt performs slightly better than the NHP-Opt which is caused by the larger optimisation space, i.e. the complete

[7]The requirement for a cell to be considered in the performance evaluation is that at least ten UEs are connected to the cell in any time step during the simulation. Cells in the outlying area are simulated as interference sources but not considered for the evaluation of the handover optimisation algorithm.

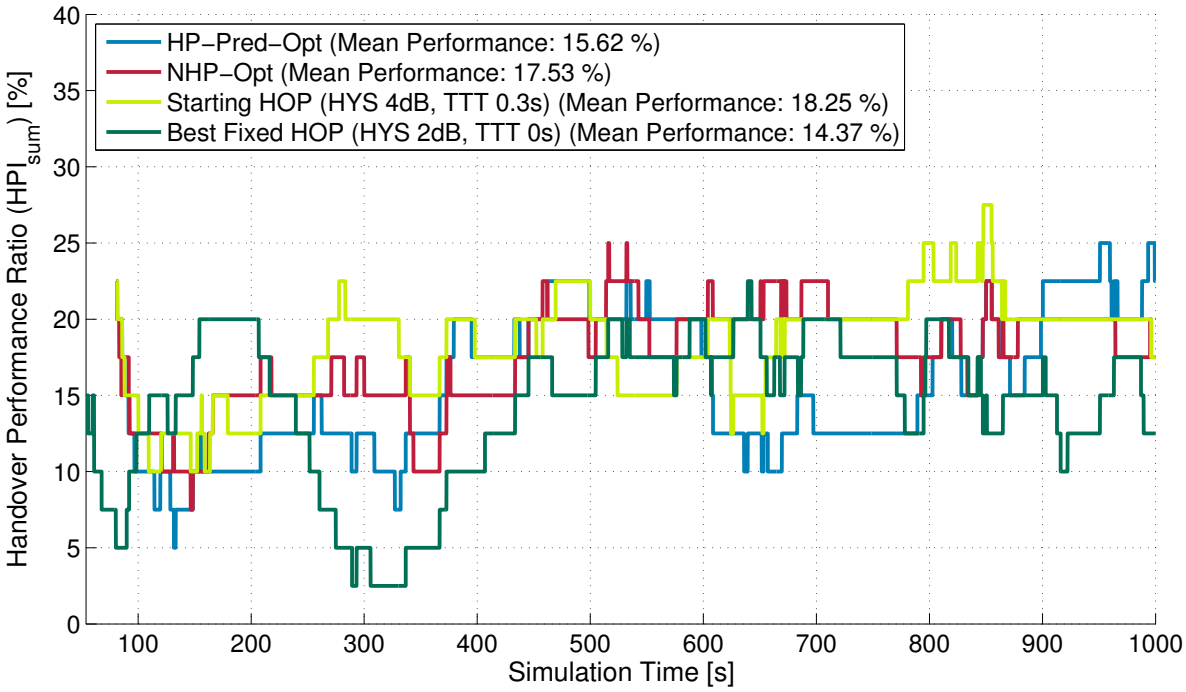

(a) Starting HOP (HYS 4dB, TTT 0.3s)

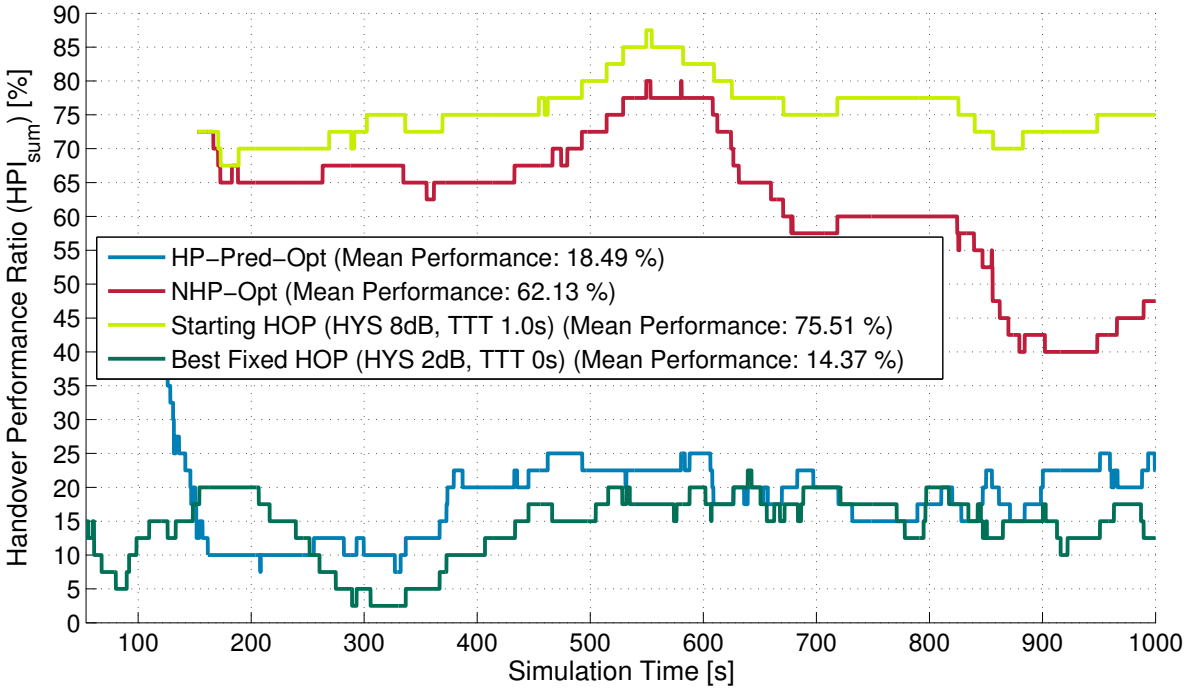

(b) Starting HOP (HYS 8dB, TTT 1s)

Figure 7.9: Comparison of the development of the handover performance of cell 31 for the two optimisation algorithms, the starting HOP and the best fixed performing HOP

set of HOPs, that are considered by the HP-Pred-Opt. Nevertheless, the fixed HOP with a HYS of 2 dB and a TTT of 0 s outperforms the two optimisation algorithms. However, the optimisation result of the HP-Pred-Opt is close to the performance of the best fixed handover parameter settings, which shows that the optimisation of the handover performance is successful.

Figure 7.9(b) shows the result of the optimisation algorithms using a starting HOP with a HYS of 8 dB and a TTT of 1 s. As the analysis in Section 7.1 already showed, the NHP-Opt slowly improves the handover performance compared to the starting HOP performance but fails to significantly reduce the negative handover events in cell 31. The HP-Pred-Opt almost instantly improves the handover performance to values similar to the performance of the best fixed HOP. The reason behind is that the handover performance prediction reports allow larger performance optimisation in one optimisation step since the handover performance is predicted for the complete optimisation space. Hence, the HP-Pred-Opt is robust against suboptimal starting HOP selection.

The development of the handover performance of cell 31 for a starting HOP with a HYS of 0 dB and a TTT of 0 s is illustrated in Figure 7.10(a). Similar to the observation for a starting HOP with a HYS of 4 dB and a TTT of 0.3 s both optimisation algorithms improve the handover performance of cell 31. In this case the NHP-Opt performs slightly better than the HP-Pred-Opt. In contrast to the observations on the performance of the NHP-Opt, where all cells were optimized at the same time (Table 7.2), the starting HOP lacks a significantly higher mean handover performance ratio compared to the simulation with a starting HOP with a HYS of 4 dB and a TTT of 0.3 s. The reason for this is visualized in Figure 7.10(b). The mean handover performance over the complete simulation time of 1,000 s for all HOPs is shown in this figure. A large amount of HOPs ranging from HYS values of 0 - 5 db and TTT values of 0 - 1 s lead to a similar mean handover performance in cell 31. Thus, the starting HOP with a HYS of 0 dB and a TTT of 0 s lies in the area of good handover performance, as the starting HOP with a HYS of 4 dB and a TTT of 0.3 s. This starting condition is beneficial for the NHP-Opt and leads to the successful performance improvement by this algorithm.

In the investigations on the characteristics of the HPIs (Section 6.2) the area with low HYS and TTT settings was dominated by high ping-pong handover ratios leading to high HPI_{sum} values (Figure 6.6). In that case the handover control parameters were changed to the same fixed values in all cells in the network. Compared to the handover performance observations in the case that only the handover control parameters of cell 31 are changed, the increase in negative handover events caused by additional

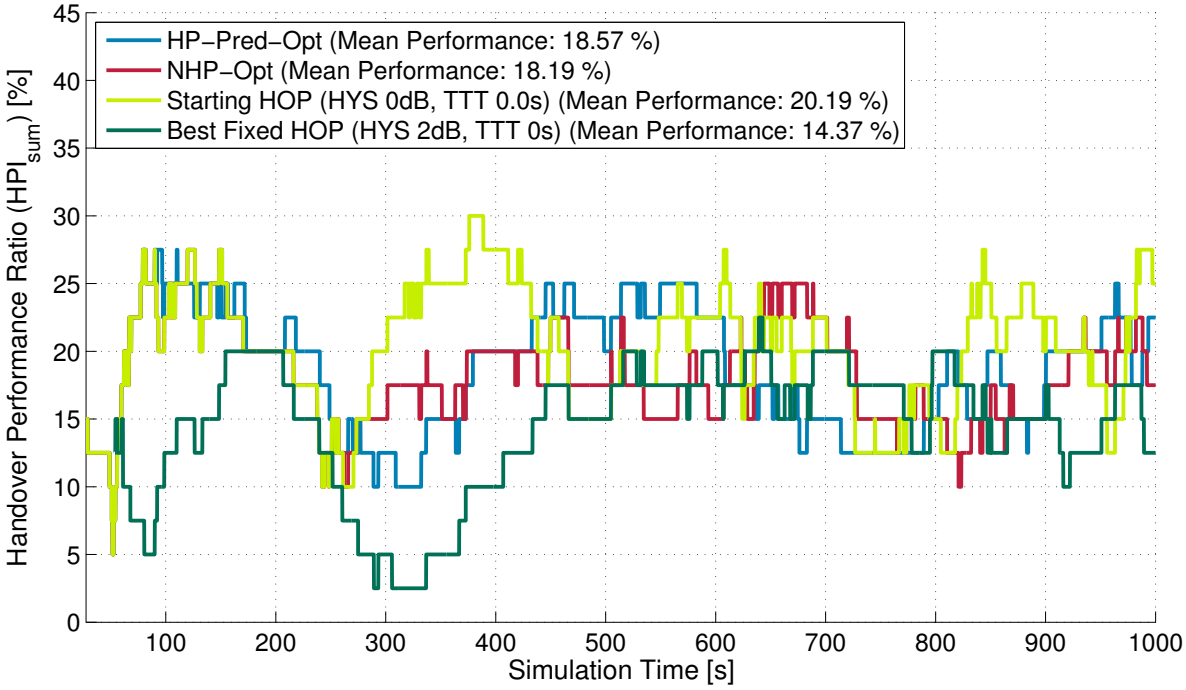

(a) Starting HOP (HYS 0dB, TTT 0s)

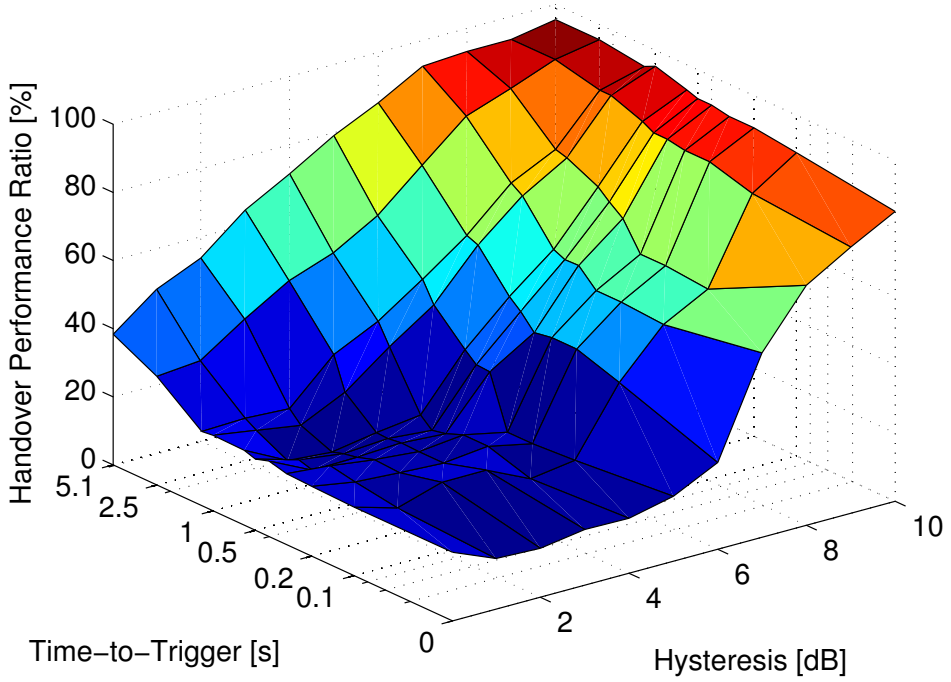

(b) Mean Handover Performance (HPI_{sum}) in Cell 31 ($w_{pp} = w_{fail} = w_{rlf} = 1$)

Figure 7.10: Comparison of the development of the handover performance of cell 31 for one HOP and the mean performance in all considered HOPs

ping-pong handovers is missing. The increase in negative handover events can only be observed if low handover control parameters are selected in the cell to optimise (cell 31) and the neighbouring cells. This makes clear that the interaction of the handover control parameters selection of neighbouring cells is important for the optimisation of the handover performance in the network. In other words, the HOP selection of a cell influences the own handover performance and might impact the handover performance of neighbouring cells as well.

This insight leads to another assessment criterion for the evaluation of the performance of the optimisation algorithms, which is the influence of the optimisation activities in one cell on the handover performance of the neighbouring cells. The best server map in Figure 7.11 illustrates the coverage area of cell 31 and the neighbouring cells. Cells 23, 25, 27, 32, 33 and 138 are taken into account for the analysis on the impact on the neighbouring cells. Figure 7.12 depicts the development of the mean handover performance of cell 31 and the six neighbouring cells. In the simulation results shown in

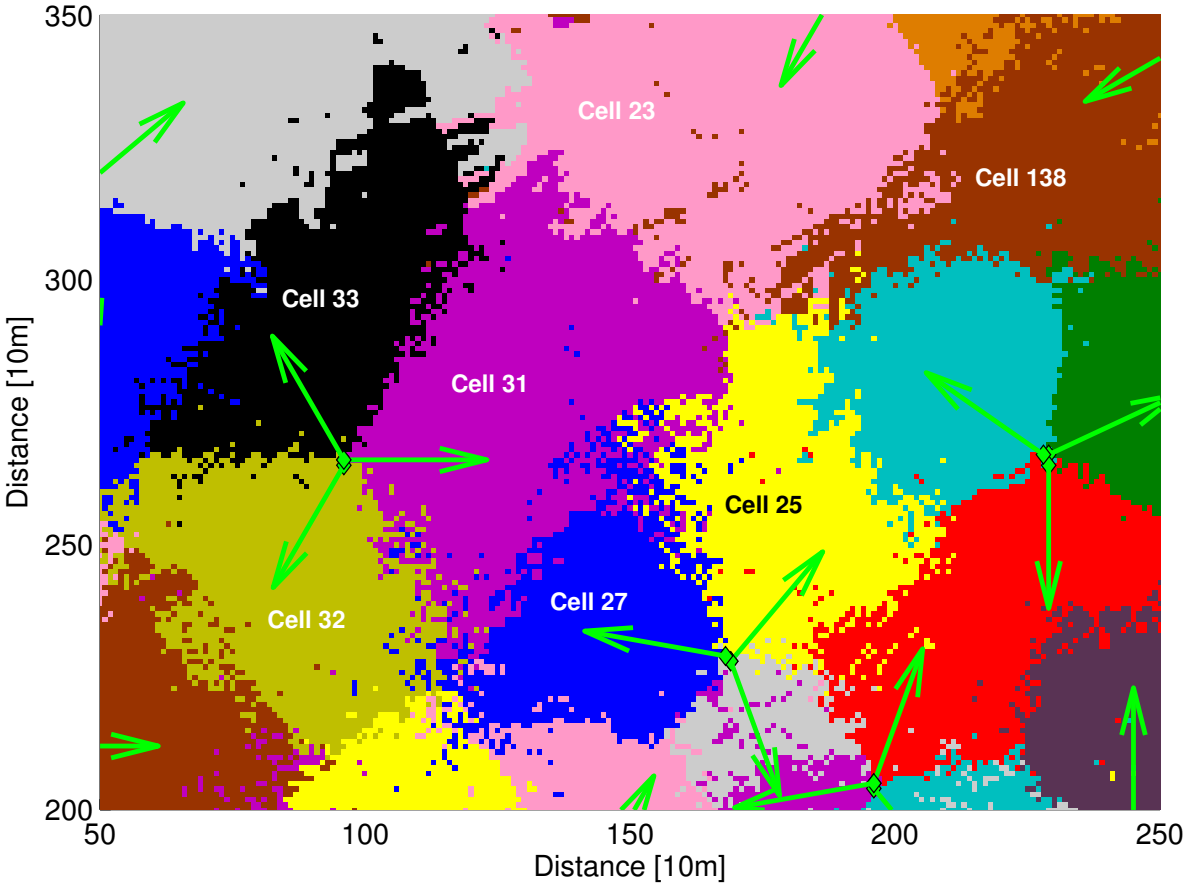

Figure 7.11: Best server map of cell 31 and the neighbouring cells

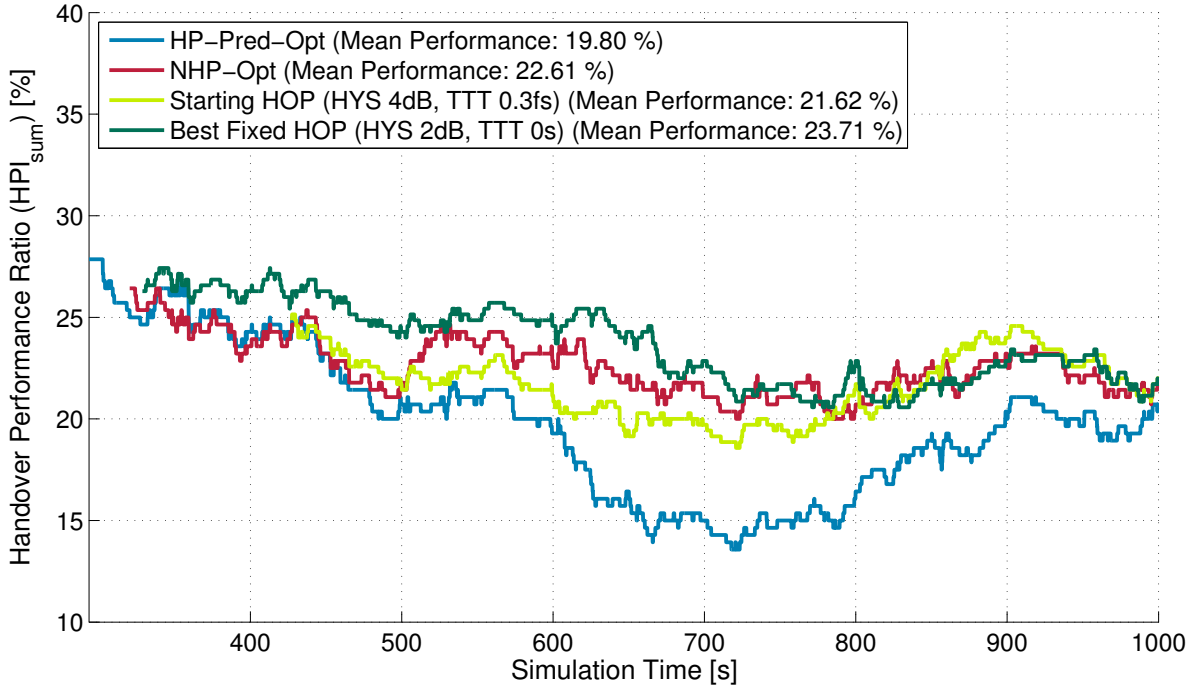

(a) Starting HOP (HYS 4dB, TTT 0.3s)

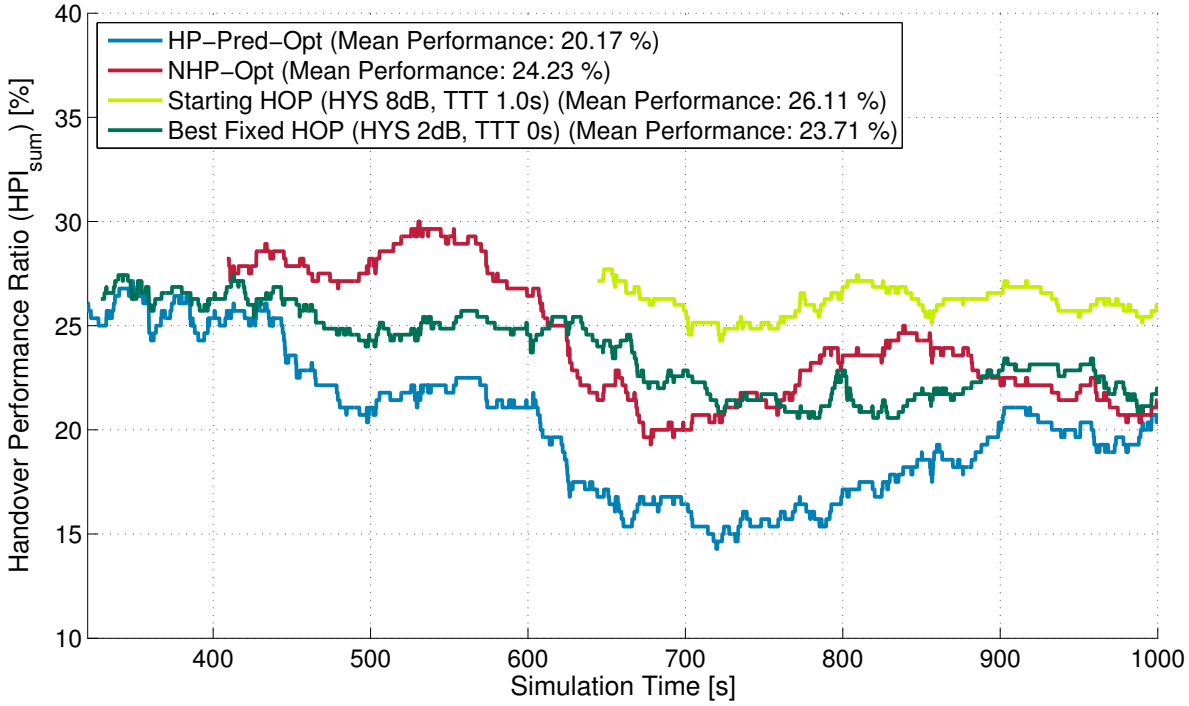

(b) Starting HOP (HYS 8dB, TTT 1s)

Figure 7.12: Comparison of the development of the mean handover performance of cell 31 and its neighbouring cells for the two optimisation algorithms, the starting HOP and the best performing HOP

Figure 7.12(a) a starting HOP with a HYS of 4 dB and a TTT of 0.3 s is selected for the two optimisation algorithms. The HOPs of the neighbouring cells remain unchanged for the complete simulation time. In the case that cell 31 uses the best performing HOP for the own handover performance (HYS 2 dB, TTT 0 s), additional negative handover events are generated in the neighbouring cells. This leads to the worst mean handover performance for fixed handover parameter settings using the best HOP for cell 31. The problem using this HOP in cell 31 is that a TTT of 0 s leads to a higher number of ping-pong handovers in the neighbouring cells.

The NHP-Opt and the starting HOP show a similar mean performance of the seven cells but the optimisation fails to improve the handover performance. The best mean handover performance is observed in the case that the HP-Pred-Opt is used to optimize the handover performance. Regardless of the result that clearly confirms the best mean performance for the HP-Pred-Opt, the optimisation algorithm does not comprehend the impact of the own optimisation activities on the neighbouring cells. The fact that other HOPs than the best performing HOP in cell 31 temporarily show better handover performance as well as the ability of the HP-Pred-Opt to quickly identify and switch to these HOPs leads to the better performance result for cell 31 and the neighbouring cells. Moreover, these temporary better HOPs in cell 31 have higher HYS and TTT values that minimizes the impact on the neighbouring cells. However, this cannot be guaranteed for all cells in a network. The trend for a higher number of negative handover events for low handover control parameters even in the own cells increases the probability that the HP-Pred-Opt improves the handover performance, but with respect to the impact on the neighbouring cells, the optimisation might fail.

The mean handover performance of cell 31 and the neighbouring cells using a starting HOP with a HYS of 8 dB and a TTT of 1 s is illustrated in Figure 7.12(b). Again the HP-Pred-Opt shows the best performance of the four considered cases. The bad performance of the starting HOP and the limited ability of the NHP-Opt to quickly improve the handover performance favour the second best mean performance of the best performing HOP of cell 31 (HYS 2 dB, TTT 0 s). The lower impact on the handover performance of the neighbouring cells in the case that higher handover control handover parameters are selected, causes the NHP-Opt to perform similar to the best performing HOP in cell 31 after 600 s simulation time. This is the point in time where the high number of failure events starts to be compensated by the NHP-Opt and the disturbance on the neighbouring cells is still very low. If only the handover performance of cell 31 is considered (Figure 7.9(b)), the NHP-Opt fails to reach the performance level of the

best performing HOP in cell 31.

Another important aspect for the achievement of the optimisation goal is the identification and adaptation of the handover parameters to load fluctuations in the network. The results in Section 6.4 disclosed that the handover performance can benefit from load specific handover control parameter settings. To evaluate the performance of the optimisation algorithms in the context of load fluctuations, a simulation run with an abrupt rise of the network load is executed. In the beginning of the simulation the cell load in all cells is set to a value of 20 %. At a simulation time of 500 s the cell load suddenly increases to 90 %, which causes a significant increase in the inter-cell interference. Figure 7.13 shows the result of the simulation run and compares the performance of the two optimisation algorithms and the same fixed handover parameter settings considered before. The HP-Pred-Opt clearly outperforms the NHP-Opt and the fixed HOP settings in cell 31 as it is able to quickly adapt to new network conditions. After 500 s simulation time up to 700 s the handover performance ratio decreases in the case that the HP-Pred-Opt is used. This is similar to the behaviour of the starting HOP and the NHP-Opt. Once the new prediction reports originated from the new network condition take the majority

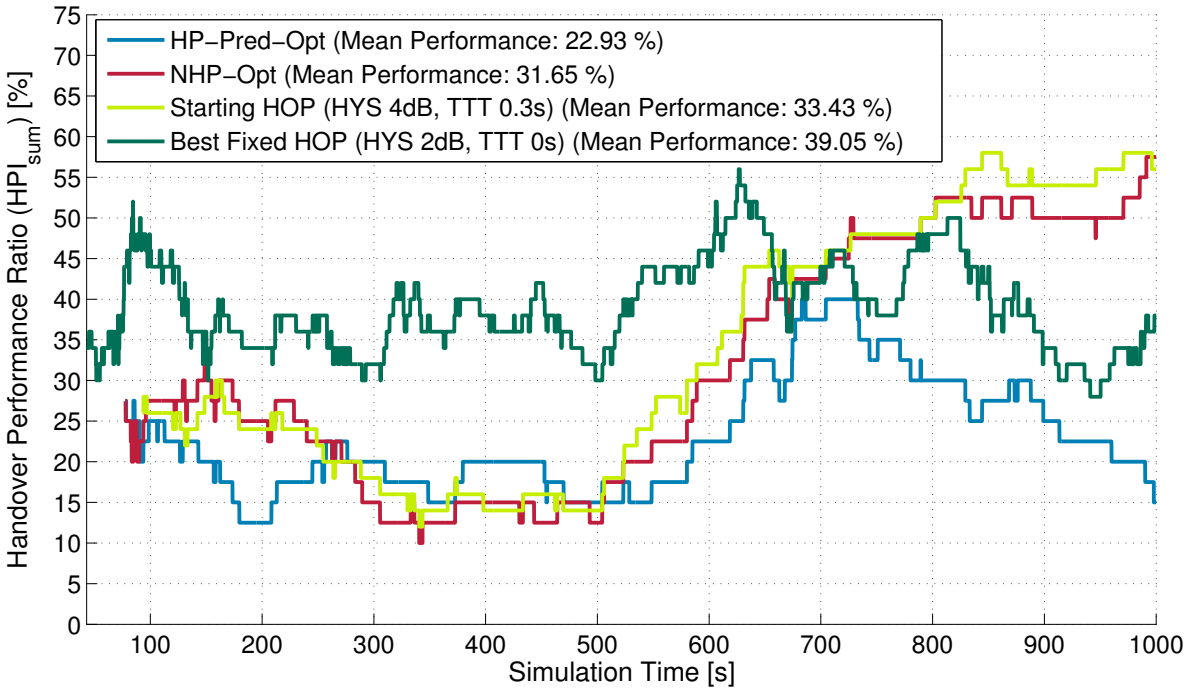

Figure 7.13: Comparison of the development of the handover performance of cell 31 in the case of an abrupt load change from 20 % to 90 % network load at a simulation time of 500 s for the two optimisation algorithms, the starting HOP and the best performing HOP

$N_{hr\_events} = 40$	Neighbour Cell HOP Selection						
HYS	0 dB	1 dB	2 dB	3 dB	4 dB	5 dB	6 dB
TTT	0 s	0.1 s	0.1 s	0.2 s	0.3 dB	0.4 s	0.5 s
HPI_{fail_event}	10.68 %	10.78 %	9.12 %	10.25 %	10.45	8.14 %	8.50 %
HPI_{pp}	30.96 %	29.34 %	23.36 %	12.70 %	8.64 %	1.26 %	0 %
N_{fail_events}	39	36	25	25	23	13	13
N_{pp}	113	98	64	31	19	2	0
N_{succ}	326	298	249	219	197	146	140

Table 7.6: Influence of HOP changes in neighbouring cells on the handover performance of cell 31

of the 40 prediction reports considered for the optimisation the HP-Pred-Opt improves the handover performance. This shows that the HP-Pred-Opt allows fast adaptation to changing network conditions.

As the optimisation activities of cell 31 and hence, the changes in the handover control parameters influence the handover performance of the neighbouring cells, HOP changes in the neighbouring cells influence the handover performance of cell 31 as well. Table 7.6 shows the handover performance of cell 31 with a fixed HOP configuration of a HYS of 4 dB and a TTT of 0.3 s. In seven simulation runs the HOPs of the neighbouring cells 23, 25, 27, 32, 33 and 138 are switched to other fixed settings for a simulation time of 1,000 s. The result of the simulations shows that the failure event ratio is more robust to HOP changes in the neighbouring cells. Nevertheless, the total number of failure events in cell 31 varies from 13 to 39 events for the different simulation runs, whereas the ping-pong handover ratio varies from almost 30 % to 0 % without any changes in the handover control parameters of cell 31. The total amount of events varies from zero to 119 events. These results highlight that the assessment of the impact of the own optimisation activities on the handover performance is challenging.

Simultaneous Optimisation of the Handover Performance in all Cells

The second step in the evaluation of the performance of the HP-Pred-Opt is dedicated to the simultaneous optimisation of the handover performance of all cells. Figure 7.14 shows the development of the handover performance of cell 31 in the case that all cells in the

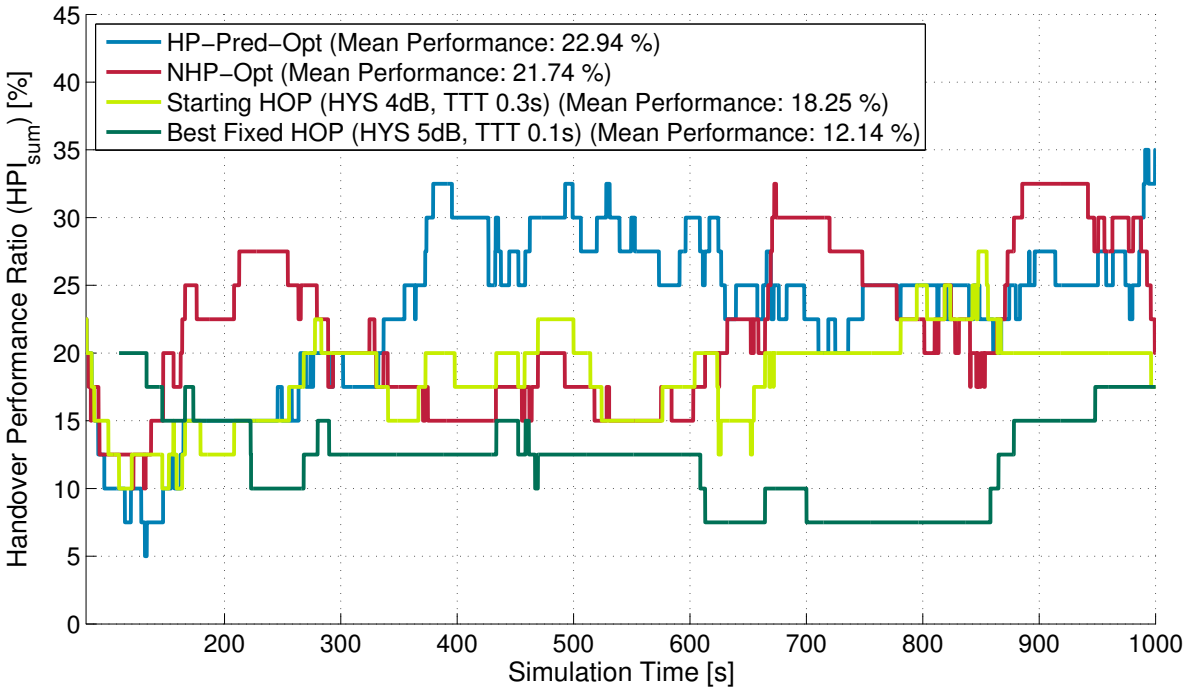

(a) Starting HOP (HYS 4dB, TTT 0.3s)

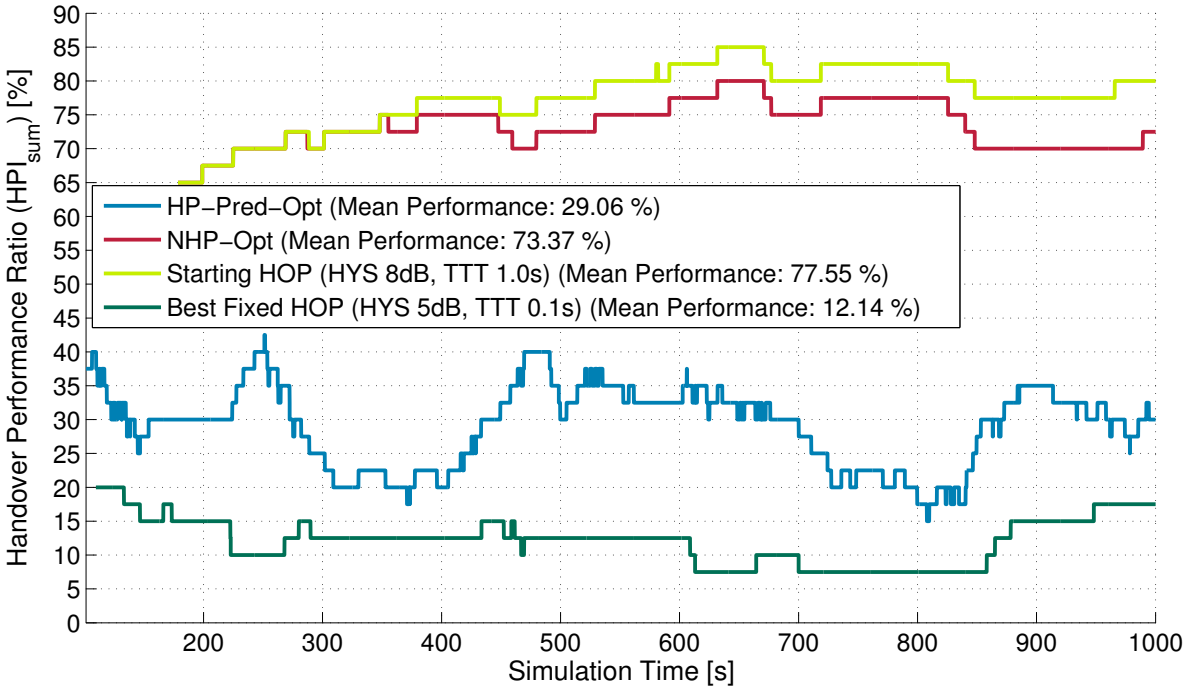

(b) Starting HOP (HYS 8dB, TTT 1s)

Figure 7.14: Comparison of the development of the handover performance of cell 31 for the two optimisation algorithms, the starting HOP and the best performing HOP

network are optimized simultaneously. The results visualized in Figure 7.14(a) base on a simulation with a starting HOP with a HYS of 4 dB and a TTT of 0.3 s. The optimisation algorithms fail to improve the handover performance compared to the performance of fixed starting HOP settings in all cells. The reason for this is that the optimisation instances in the cells aim to improve the cell handover performance only, and neglect the impact of the optimisation actions on the neighbouring cells. Some of the handover performance prediction reports, used by the HP-Pred-Opt to identify the optimal HOP, show negative handover events independent of the HOP selection of the cell the reports are generated for. This shows that handover control parameter adaptation cannot solve the optimisation problem regarding the handover performance of one individual cell. In the case that a suboptimal starting HOP is selected (Figure 7.14(b)) the HP-Pred-Opt still outperforms the NHP-Opt and the starting HOP performance. Nevertheless, a far more optimal solution exists as the best performing fixed HOP selection (HYS 5 dB, TTT 0.1 s) in all cells shows.

The performance of the HP-Pred-Opt can be improved by the identification of the HOP with the smallest total amount of negative handover events. In this case the HPI_{sum} is replaced as the target function by the smallest amount of negative handover events. This is possible due to the handover performance prediction reports, that allow the analysis of the amount of handover related events based on the same user mobility. This means the prediction reports contain information about the potential network experience and handover behaviour in all HOPs. The identification of the HOP with the smallest amount of negative handover events has the additional advantage, that HOPs with a huge amount of successful handover events are not preferred to HOPs with less signalling traffic and fewer negative handover events. Figure 7.15 shows the result of a simulation run with the new target function. The performance of the HP-Pred-Opt is slightly improved but the missing consideration of the impact on neighbouring cells still avoids a good optimisation result. The evaluation of the handover performance improvement for other cells leads to similar results.

The optimisation results for the simultaneous optimisation of the handover performance of all cells presented in this section so far, all base on the prediction of the handover performance of all possible HOPs in the SeNB (the cell the UE is connected to when the A6-Event occurs) and the current handover control parameter settings in the neighbouring cells (See Figure 7.8). This means every cell aims to optimise the own handover performance to the current network condition and the handover configuration in the adjacent cells. The fact that all cells optimise their own parameters at the same time

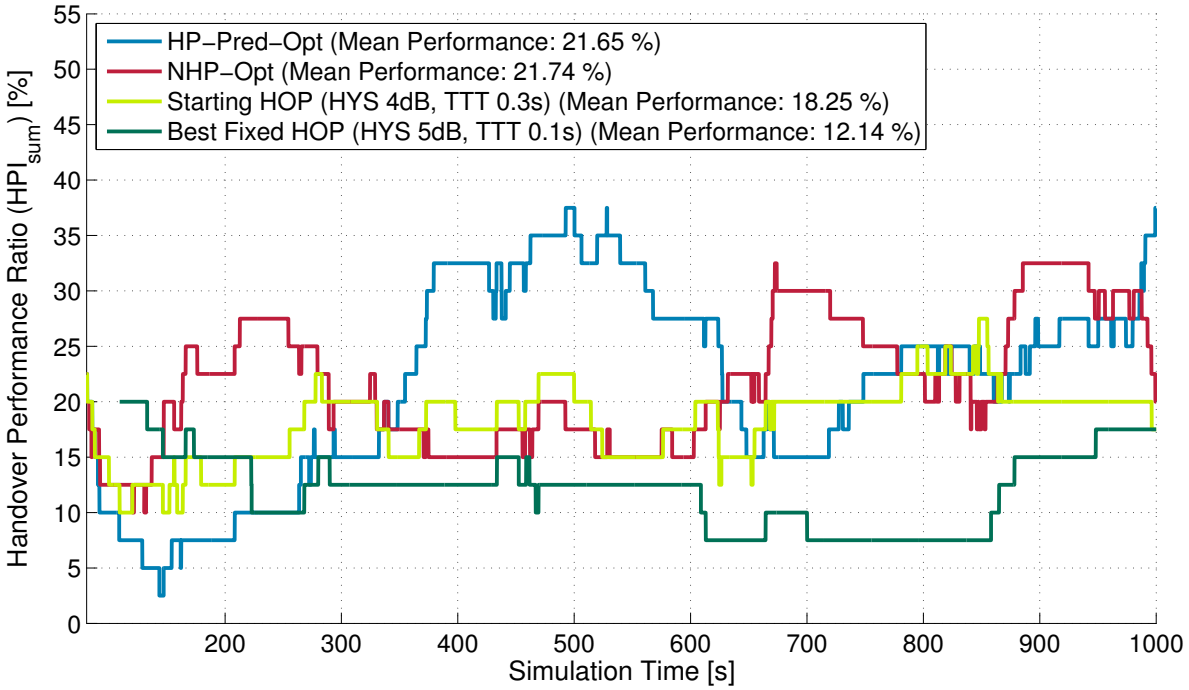

Figure 7.15: Comparison of the development of the handover performance of cell 31 for the two optimisation algorithms, the starting HOP and the best performing HOP. The HP-Pred-Opt is based on the smallest total amount of negative handover events.

interferes with the aim to optimise to the adjacent cell handover configuration. At the time a new configuration is selected in a cell the adjacent cells might have switched to another configuration already. This effect and the disregard of the impact on the handover performance of the adjacent cells lead to the sub-optimal handover performance at the end of the simulation.

To compensate the missing information on the impact on the adjacent cells two approaches appear reasonable: firstly, the impact on the adjacent cells has to be evaluated separately, which means that if a cell changes the handover configuration the change in handover performance in the adjacent cells has to be evaluated and reported back to the optimised cell. Secondly, the anticipated impact on the adjacent cells has to be included in the prediction of the handover performance to allow an impact sensitive optimisation of the handover configuration. The first solution has a major impact on the optimisation cycle since it prohibits the simultaneous optimisation of all cells and adds evaluation time for the impact on the adjacent cells to the optimisation cycle. Hence, the optimisation speed and the ability to quickly adapt to new network conditions would suffer from this solution. The second solution requires a quick and reliable estimation

of the impact on the adjacent cells.

To estimate the impact on the handover performance of the adjacent cells, the regarded handover configuration of the TeNB in the simulation of the handover procedure is adjusted. So far, the current handover control parameter settings of the TeNB of the handover are used to simulate the handover procedure. Figure 7.16 shows the development of the handover performance of cell 31 for the case that the same handover control parameter settings are assumed in the SeNB and the TeNB for the prediction of the handover performance in every HOP. Still the prediction of the handover performance lacks the information of the impact on the adjacent cells. Nevertheless, the prediction reports include a notion on the handover performance in a HOP if the adjacent cells would select the same HOP as well. This excludes HOPs with an improved performance for a single cell but significant negative impact on the handover performance in the network from the favoured HOPs. As Figure 7.16 verifies, the HP-Pred-Opt based on prediction reports for equal HOP settings in the SeNB and TeNB now outperforms the

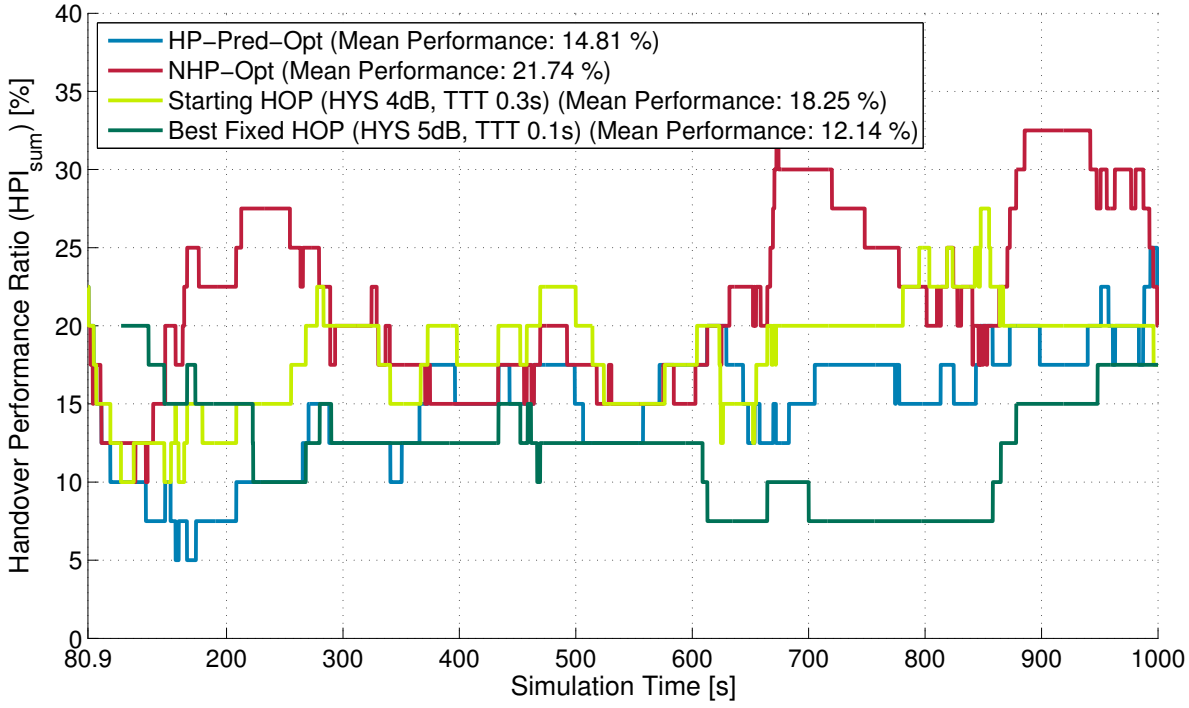

Figure 7.16: Comparison of the development of the handover performance of cell 31 for the two optimisation algorithms, the starting HOP and the best performing HOP. The HP-Pred-Opt is based on the smallest total amount of negative handover events. Equal HOP settings are considered for the generation of the prediction reports.

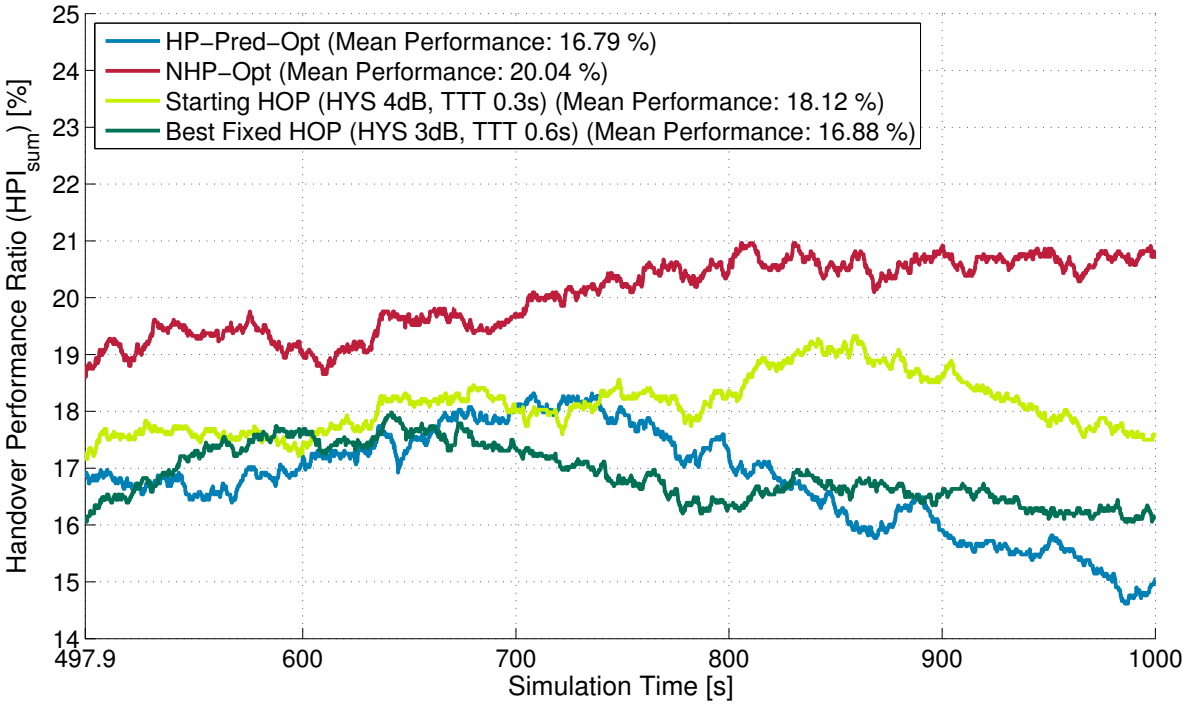

Figure 7.17: Comparison of the development of the mean handover performance of 52 cells for the two optimisation algorithms, the starting HOP and the best performing HOP. The HP-Pred-Opt is based on the smallest total amount of negative handover events. Equal HOP settings are considered for the generation of the prediction reports.

handover performance using the NHP-Opt and the starting HOP in cell 31.

More important than the performance improvement in one cell is the development of the handover performance in the complete network. Figure 7.17 shows the development of the mean handover performance in the 52 cells with the biggest handover activity in the network. The HP-Pred-Opt shows the best mean handover performance in the network compared to the NHP-Opt, the starting HOP and the most optimal fixed HOP setting in the complete network. This proves that the networks benefits from cell individual optimisation of the handover control parameters. The 52 cells have been selected since more than 40 handover related events are observed in the first 500 s of the simulation. That is why the plot starts after 497.9 s.

7.2.2 Conclusion on the Applicability of the HP-Pred-Opt

The evaluation of the HP-Pred-Opt for the optimisation of the handover performance of a single cell shows that the algorithm optimizes the handover performance and reaches

a performance close to the optimal fixed HOP selection in the cell. The HP-Pred-Opt is robust against starting HOP selection in the cell to optimize and quickly improves the handover performance. The simulation results demonstrate that optimal performance in a single cell does not automatically lead to the best possible performance in the network. The impact of optimisation actions on the neighbouring cells limits the total gain in handover performance. If the handover performance of the cell to optimize and the neighbouring cell is evaluated, the HP-Pred-Opt by far shows the best mean handover performance. Nevertheless, the reason for this more optimal performance is not a characteristic of the HP-Pred-Opt, since the optimisation algorithms neglects the impact on the neighbouring cells as well. The evaluation of the performance improvement in an environment with an abrupt load increase, the HP-Pred-Opt shows the ability to quickly adapt to changing network conditions. In sum up, the HP-Pred-Opt significantly and quickly improves the handover performance of a single cell and quickly adapts to network condition changes.

In the case of a simultaneous optimisation of the handover performance in all cells in the network, the HP-Pred-Opt fails to identify a global optimal solution for the handover configuration if the handover control parameter settings of the TeNBs are considered for the handover procedure simulation. The reason for this is that the HP-Pred-Opt neglects the impact on the handover performance of the neighbouring cells, hence it generates negative handover events in surrounding cells. These negative handover events cannot be avoided by the optimisation of the handover control parameters of the neighbouring cells since the negative handover events are observed in every HOP in the prediction reports. Nevertheless, the HP-Pred-Opt quickly improves the handover performance in the case that a suboptimal starting configuration is selected. If the target function is replaced by the objective to identify the HOP with the smallest amount of negative handover events in the cell, the HP-Pred-Opt leads to a slightly worse performance than the starting HOP, which is a good performing global HOP selection already.

If the same HOPs are assumed for the prediction of the handover performance for every HOP, the HP-Pred-Opt reaches a better handover performance level than the best performing fixed HOP setting in all cells in the network. The concept of basing the optimisation decisions on the handover performance prediction reports combines several advantages: the evaluation of the handover performance bases on the same events, the performance in all considered HOPs is analysed at the same time and the prediction reports allow to conclude on the impact of neighbour HOP selection on the own handover performance.

Chapter 8

Summary, Conclusion and Outlook

In this dissertation we prove that *an adaptation of the handover configuration to changes in the interference condition in the network (load variation) is highly beneficial.* The consequence of this finding is that *self-optimisation (SON) of the handover configuration in the order of tens of minutes to allow an adaptation to load condition changes over a day is the design target for the handover optimisation algorithms.* A *missing adaptation to the daily load condition changes leads to additional negative handover events of up to 11 %.* In LTE system-level simulations with different fixed load conditions in all cells, varying from 10 % cell load (resource utilisation) to 100 % in steps of 10 %, we analysed the best handover configuration for every cell. Under the assumption that every cell selects the best handover configuration for every load condition, the total negative handover event rate varies from about 0.4 % (10 % cell load) to roughly 15 % (100 % cell load). The reason for the performance difference is that in low load conditions the handover can be initiated at a time the user deeply entered the cell coverage area of a potential handover target cell already. Due to the low load condition (resulting in a low interference condition as well), the signal quality allows the user to keep up the communication with the serving cell. If the adaptation to the current load condition in the network is neglected, e.g. the optimal handover configuration for a fixed load condition of 70 % is applied in all other conditions as well, the performance degradation in other load conditions varies from roughly 3 % to about 11 % additional negative handover events. If the optimal handover configuration for a load condition of 100 % is applied, the performance degradation varies from roughly 2 % to almost 11 % additional negative handover events. These results prove that it is highly beneficial to adapt the handover configuration to the network load condition. Due to the fact that the load conditions in a mobile network often show strong variations over a day, the consequence for the development of handover optimisation algorithms is an adaptation ability to load

condition changes in the order of tens of minutes.

In a comparison of the "best" handover configuration selection, derived from system-level simulations, in a homogeneous 3GPP simulation scenario and a detailed, realistic Hanover simulation scenario we prove that *only realistic modelling of the user mobility and signal propagation discovers a handover performance improvement by cell individual handover configuration selection.* Depending on the optimisation target function definition up to *81 % of the cells in the 3GPP simulation scenario select the same handover configuration whereas only about 26 % of the cells select the same handover configuration in the Hanover scenario.* In system-level simulations we evaluate the influence of the simulation scenario on the handover configuration selection of the cells. The handover performance for all considered handover configurations is simulated and the best configuration per cell is identified. In this analysis we show that in typical 3GPP simulation scenarios based on hexagonal network layout and random walk user mobility, most cells in the scenario select the same or similar handover configuration. This is caused by the regular network grid and the random user mobility that leads to random cell border crossing positions in the simulations. The conclusion from the simulation results in this scenario could be that the cell-individual adaptation of the handover configuration is not necessary. In a more realistic simulation scenarios based on ray-optical pathloss predictions and three user mobility types, i.e. vehicular mobility on roads, pedestrian mobility on sideways and indoor mobility in different building levels, the cells select significantly more different handover configurations. These results prove that the selection of the simulation scenario is important to assess handover optimisation approaches.

We prove that *the observation cycle for the evaluation of the current handover performance has to be defined in the event domain and an exact evaluation of the handover performance discards as the basis for the optimisation decisions.* The handover performance observation cycle, which is the time the current handover performance is observed to conclude on the optimisation need, mainly impacts the ability to adapt to load condition changes in the network as too long observation cycles slow down the optimisation speed. The investigations in this dissertation verify that the observation cycle has to be defined in the event domain. This means the Handover Performance Indicators need to be based on the same amount of handover related events. The option *to base the observation cycle on a fixed time span (time domain definition), which is the state of the art definition in current research, proved to significantly degrade the comparability of handover performance observation results.* Assuming the objective to analyse the handover performance with an accuracy of 0.1 %, which is an important performance

difference for the network operators, we show that several thousand handover related events have to be observed to conclude on the current handover performance. An optimistic estimate leads to 2000 handover related events, two other approaches identify at least 10,000 events as needed observation cycle. Due to the fact that only few cells in a network see more than 10,000 handover events a day and the objective to adapt to load condition changes in the network, *the exact identification of the handover performance fails as basis for the handover optimisation.*

In the case of a direct comparison of the handover performance of two handover configuration sets, we prove that *an observation cycle of 40 handover related events allows an identification rate of more than 90 % of the better performing configuration.* These results show that *an adaptation to temporary network conditions is possible based on the performance comparison of different handover configurations.* Nevertheless, it depends on the amount of observed handover events in a cell how fast the adaptation to new network conditions can be.

We develop a novel handover optimisation algorithm that optimises the handover performance on the basis of a step-wise comparison of the handover performance in two handover configuration sets in this dissertation. *The algorithm, named Neighbouring HOP Performance Handover Optimization Algorithm (NHP-Opt), reliably optimises the handover performance in the cells.* The drawback of the solution is *the step-wise optimisation, which requires a number of observation cycles to improve the performance.* Moreover, the algorithm tends to identify local minima in the optimisation space as the best handover configuration since the risk to significantly degrade the handover performance disallows large handover configuration changes. We prove that *the NHP-Opt fails to quickly adapt to load condition changes, which leads to the conclusion that the optimisation concept disqualifies for the needs for future mobile communication networks.*

In this dissertation we prove that *the Handover Performance Prediction Optimization Algorithm (HP-Pred-Opt) by far outperforms state-of-the-art handover optimisation concepts. The basic idea of the HP-Pred-Opt is to predict the handover performance of a cell for all specified HOPs on the bases of handover performance prediction reports from the UEs.* Model predictive control algorithms have been used in other research areas before. The application in the area of handover optimisation allows an evaluation of the complete optimisation space, which has not been possible with state-of-the-art handover optimisation algorithms. In combination with the observation interval of 40 handover related events, identified as reliable observation cycle in this dissertation, *the prediction reports allow a direct identification of the "best" estimated handover performance and*

hence a quick adaptation of the handover configuration. To predict the handover events, the handover procedure is virtually executed for all handover configurations based on the signal strength measurements of the UE. The key role for a successful performance prediction plays the prediction of the signal quality, which uses the load information from the load reporting between the cells. Signal quality prediction models have been used in the area of optimisation of the scheduling decision before. Based on the performance prediction the optimisation algorithm selects the "optimal" HOP, i.e. the HOP with the best predicted handover performance. The simulation results show that the HP-Pred-Opt quickly optimises the handover performance of the network independent of the starting handover condition and reliably reaches performance levels close to or even better than the best performing fixed handover configuration. Fixed configuration refers to the case that all cells in the network select the same handover configuration for the complete simulation. The fact that the prediction reports allow the comparison of the HOPs for the same user movement, i.e. the exact same path selection for all HOPs, increases the probability to identify the better performing HOP. In system simulations with varying load condition, the algorithm proves to quickly adapt to the new situation. Moreover, the prediction reports even allow the identification of sub-optimal HOP selection in adjacent cells.

Outlook

Future research activities in the area of handover optimisation need to focus on the mutual interaction of handover configuration changes in adjacent cells. The simulation results in this dissertation prove that handover configuration changes in cells influence the handover performance of adjacent cells. The concept to predict the handover performance for all handover configuration sets allows to estimate the mutual interaction of handover configuration changes. Though the complexity of an optimisation including the mutual interaction significantly increases. One of the key questions for future research is how this information can be used to further optimise the handover performance in the network. Especially in the case that the handover configuration is optimised per cell-pair, the mutual interaction could be used for a simultaneous optimisation of both handover configurations.

Beyond that the user speed classes should be regarded by future optimisation concepts. The problem here is that the amount of observed handover events per user speed class is significantly lower as for the complete cell. Thus, a successive optimisation scheme

that adapts the global handover configuration first and modifies the speed class offsets in a second step, is imaginable. Recent research activities focus on the classification of the users not only in speed classes but moreover in mobility behaviour types [Sas14]. To combine classification results with the Handover Performance Prediction Optimization Algorithm (HP-Pred-Opt) opens up new possibilities for a quick and reliable handover optimisation.

For the implementation of the prediction report based optimisation algorithm, developed in this dissertation, in live networks the accuracy of the signal quality prediction is crucial. Recent research in the area of scheduling gain prediction models on the basis of the cell load information of adjacent cells show a good agreement with detailed scheduling simulations [Hasselbach12]. The implementation of these models along with the prediction based handover optimisation concept provides the opportunity to solve the handover problems in future mobile communication networks.

Appendix A

Applicability of State-of-the-Art Optimisation Methods to the Handover Optimisation Problem

In this dissertation the meaning and chances of handover optimisation in infrastructure communication networks has been elaborated and based on a detailed analysis of the HPIs a handover performance prediction based optimisation algorithm has been developed and suggested to solve the handover optimisation problem. Nevertheless many optimisation methods are used in engineering sciences in recent years. In this chapter the applicability of state-of-the art optimisation methods on the handover optimisation problem is evaluated based on the findings in this dissertation.

Heuristics

It is worth discussing whether heuristics can be seen as optimisation methods in general. However, the simplicity and easy implementation of heuristics makes them an interesting and important group of problem solving methods [Gigerenzer99]. One application area in computer sciences are virus scanners that use heuristics for the identification of viruses. Heuristics qualify as optimisation methods in the case that limited knowledge and limited time are available and nevertheless an action with a high probability of success is needed. Heuristics base on experiences with a system, thumb rules and educated guesses which are of course not the most promising indicators for system configuration changes but show an acceptable reliability for many practical problems.
An application area for heuristics in handover optimisation is the replacement of human optimisers that currently tune the handover parameter settings in mobile communication

networks. The experiences of the human optimisers and simple rules like - lower TTT and HYS values lead to fewer failure events - can be used as rule sets. Nevertheless, the success of a heuristics based optimisation of the handover parameters is questionable. The results of the analysis in this dissertation show that the best optimisation action is dependant on the individual cell and its environment. Moreover the load in the network influences the handover performance in the HOPs. Simple global heuristics with easy rule sets would most probably fail to significantly improve the handover performance in changing network conditions and individual cell situations. Similar to the conclusion on the applicability of the NHP-Opt a heuristic incorporates a high risk of performance degradation and lack the flexibility to adapt to changing system conditions.

Simulated Annealing

Simulated annealing is an iterative optimisation method derived from the cooling process of e.g. glowing metal that is used in the case that the optimisation space is too large to allow trial and error of all states or simple mathematical calculations [Kirkpatrick83]. A slow cooling process allows the atoms to form stable crystals which leads to a low-energy state close to the optimum. Similar to this process simulated annealing searches for a global optimum in the optimisation space by slowly decreasing the "temperature" of the process. In contrast to simple heuristics that aim to find a local optimum by comparing the neighbouring states to the current state simulated annealing allows selecting a neighbour with worse performance to escape a local optimum. This way the probability to find the global optimum is increased. The temperature defines the performance difference that is accepted to select a neighbour state with worse performance. Nevertheless the algorithm prefers neighbouring states with better performance. Once the temperature cooled down to zero the algorithm terminates and delivers with a high probability the optimum state.

As elaborated in this dissertation the key in handover optimisation lies in a quick identification of a better performing HOP and a low risk for performance degradation. Moreover mobile communication systems underlie a permanent performance change caused by network condition changes like the network load and user mobility. Simulated annealing is per definition an optimisation method that evaluates many states in the optimisation space to increase the probability to find the global optimum with a high risk for temporary performance degradation. This contradicts the aim for a low probability of handover performance degradation. Furthermore the evaluation of a single state

in the optimisation space takes the observation time as described in this dissertation which slows down the optimisation speed. To sum up simulated annealing evaluates many states in a large optimisation space with a high risk for temporary performance degradation but handover optimisation needs an optimisation algorithm that derives a better state with high probability and only a few state changes and a very low risk of performance degradation.

Fuzzy Logic

Fuzzy logic is a theory that allows the consideration of linguistic variables like “small“, “very“, “a bit“ or “high“ in mathematical models [Klir95]. In contrast to boolean logic in which the variables take values of “0“ or “1“ the linguistic variables in fuzzy logic take values from a defined range. The exact values for the variables are determined in the fuzzy logic optimisation process and not pre-defined. In addition to the fuzzy variables high-level rule sets similar to the rules discussed for the heuristics are defined and in tables or matrices the interrelation between the optimisation state (observations), fuzzy variables and high-level rules is expressed. The aim of the fuzzy logic optimisation is to interpret and learn the mathematical meaning of the linguistic variables.

Fuzzy logic optimisation algorithms have been addressed to the handover optimisation problem by the research community [Luengo14]. Starting from an initial HOP selection - as for the optimisation algorithms developed in this dissertation - the performance of the initial HOP is evaluated. For the selection of the next HOP the high-level rule sets like - lower TTT and HYS values lead to fewer failure events - are used to determine the optimisation direction and the fuzzy variables give the optimisation step size. In the optimisation process the step sizes and hence the interpretation of the fuzzy variables is adapted according to the system observations. The simulation results in [Luengo14] show that the fuzzy logic optimisation performs slightly better but still similar to the performance of the NHP-Opt developed in the SOCRATES project. The reason is that the evaluation of the best optimisation direction from high-level rule sets fails in the handover optimisation space. As evaluated in this dissertation dependant on the individual cell situation and the network conditions large or small optimisation steps in completely different optimisation direction are needed to increase the system performance.

Reinforcement Learning/Q-Learning

Reinforcement learning is a machine learning technique that bases on rewards for actions of a software agent in the environment (optimisation space) [Sutton98]. The environment is described by a Markov decision process that describes the states of the system and the possible action from a state to other states. The rewards for the actions of the software agent are granted after the new state is reached and evaluated. The agent learns about the quality of its actions by the rewards. The advantage of reinforcement learning is that these techniques do not need any detailed information on the Markov process and target large Markov decision processes.
For the handover optimisation problem reinforcement learning has been evaluated in [Luengo14] as well. The challenge in using reinforcement learning for handover optimisation is the definition of the possible states of the system. As evaluated in this dissertation the individual handover configurations of the the cells influence the handover performance of the neighbouring cells. Therefore a handover configuration change in a neighbouring cell leads to a new state for the cell to optimise. Moreover network condition changes significantly influence the handover performance and hence leads to new states in the Markov process. Already the classification of different states is challenging since the number of considered neighbouring cells, the handover configuration in these cells and the significance of a network condition change influences the Markov state. If a cell has e.g. 5 neighbouring cells and the load in one of these cells increases by 5 % a new Markov state could be reached. However, reinforcement learning needs several experiences with decisions from one Markov state to a following state to learn about the optimisation action. For handover optimisation this means that only a limited set of Markov states can be considered to allow for high optimisation speed. As for fuzzy logic optimisation the risk of significant performance degradation in the optimisation process is present with reinforcement learning as well.

Game Theory

Game theory can be defined as “the study of mathematical models of conflict and cooperation between intelligent rational decision-makers“ [Myerson91]. A well known problem that serves as a standard example for a game addressed by game theory is the prisoners dilemma. Two members of a criminal group have been arrested and are questioned in separate rooms without any chance to communicate with each other. The accuser has

no chance to convict any of the two of all crimes they committed in the case that the two cooperate and reveal no information and hence both will serve only one year in prison. If both prisoners admit the crimes they both serve in prison for 2 years. But if one of the two prisoners admits the crimes and betrays the other prisoner the betrayer is set free and the other prisoner will serve in prison for 3 years. From the point of view of any of the two prisoners the logical choice is to betray the other prisoner since in that case he will be free or in prison for only 2 years if the other betrays as well. Nevertheless the optimal global solution would be if both prisoners remain silent since in total only 2 years in prison (one per prisoner) would be declared. This example depicts the application area of game theory since the best decision for an individual leads to a suboptimal global solution. The interdependency between the individual decisions is important to find the global optimum.
The findings in this dissertation on the handover optimisation problem show a huge overlap with the application area of game theory. The optimal solution for an individual cell (HOP selection) proved to lead to a suboptimal global handover performance. Hence, the consideration of the interdependencies between the individual cell handover configurations is crucial to identify the global optimum performance. In cooperation with the HP-Pred-Opt developed in this dissertation that delivers the performance prediction for the individual HOPs the handover performance could further be improved by global optimisation with a game theory approach.

Conclusion

To sum up the key for successful handover optimisation lies in a fast and reliable performance evaluation of the HOPs in the optimisation space. The suggested HP-Pred-Opt that uses performance predictions to allow actions with a high probability of better performance proved to outperform any other optimisation solution addressed to the problem of handover optimisation so far. Nevertheless, the HP-Pred-Opt does not guarantee a global performance optimum since it is only designed to avoid performance degradation in neighbouring cells but does not search for the global optimum handover configuration. Thus a combination of a predictive optimisation algorithm with game theory techniques seems a promising research field for the future.

Appendix B

The Handover Performance Indicator Handover Failure

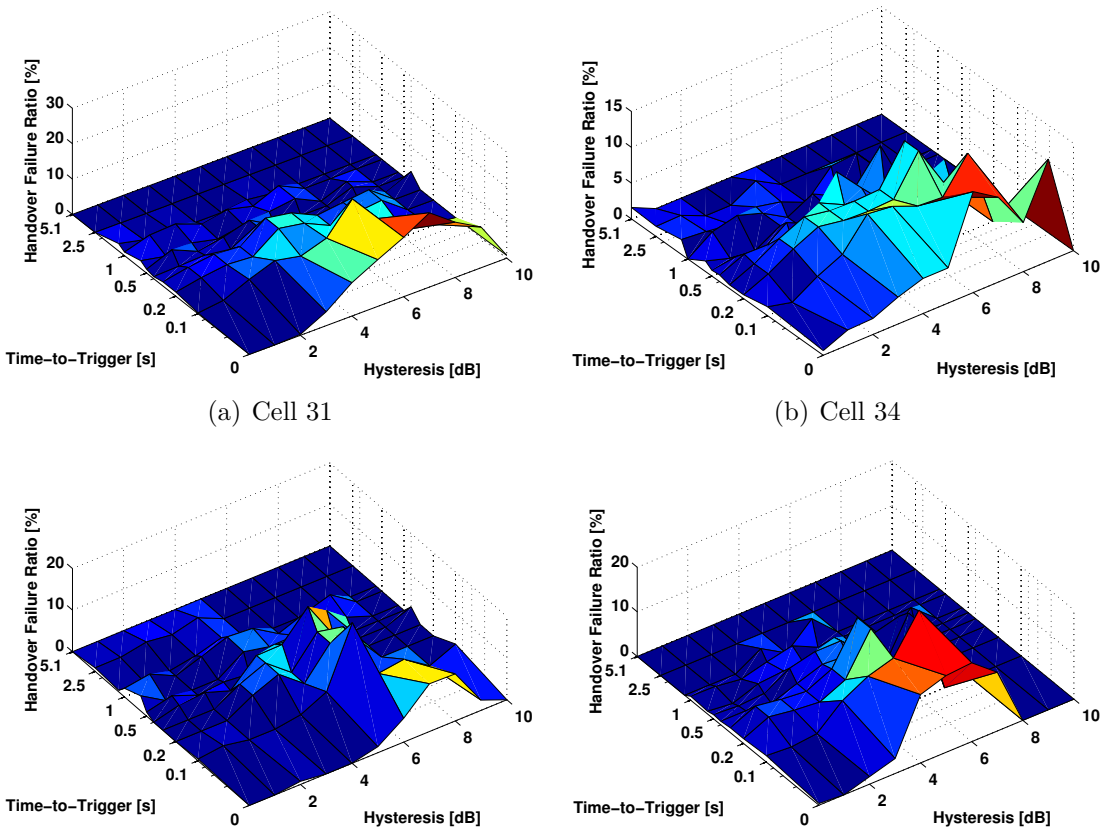

(a) Cell 31

(b) Cell 34

(c) Cell 36

(d) Cell 90

Figure B.1: Comparison of handover failure ratios in the HOP-plane for different cells (Simulation Time: 1000 s)

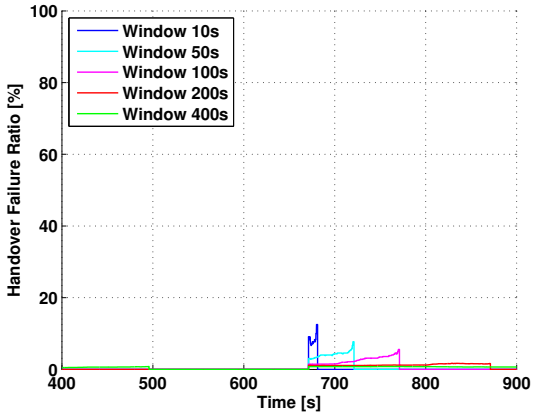

(a) HYS 1 dB, TTT 0.1 s

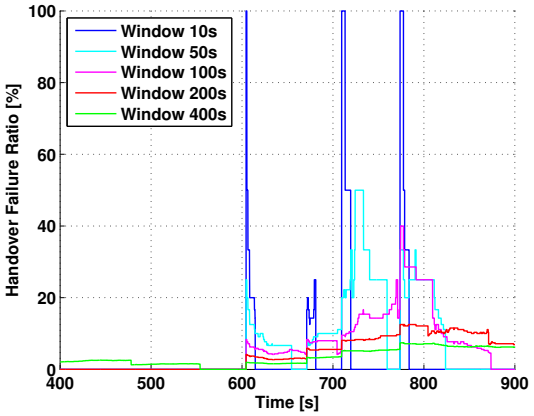

(b) HYS 3 dB, TTT 0.1 s

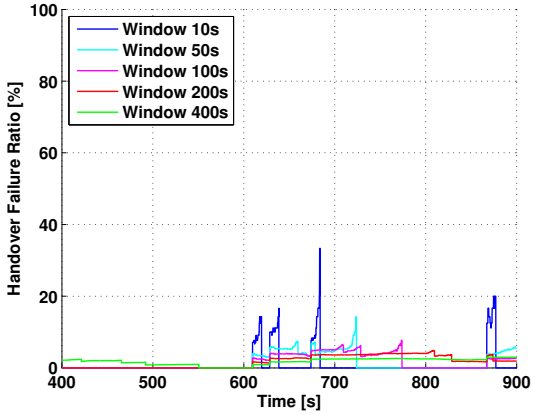

(c) HYS 1 dB, TTT 0.3 s

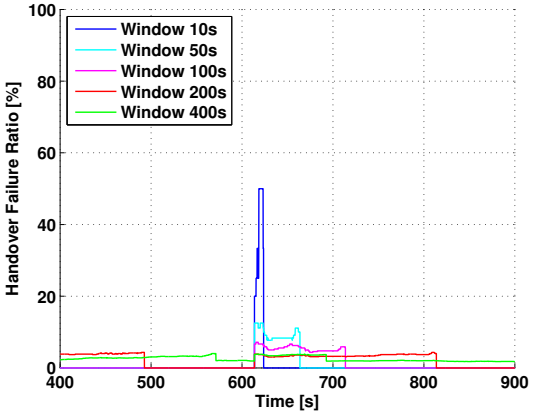

(d) HYS 3 dB, TTT 0.3 s

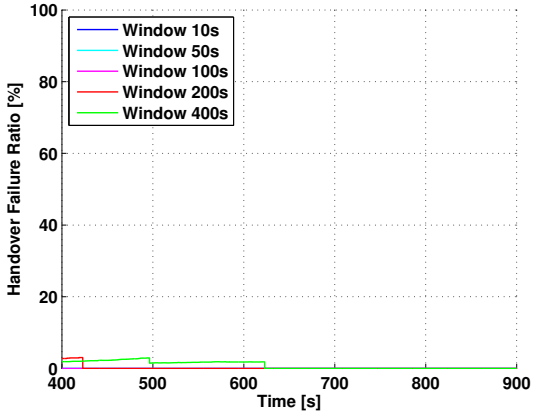

(e) HYS 3 dB, TTT 1.0 s

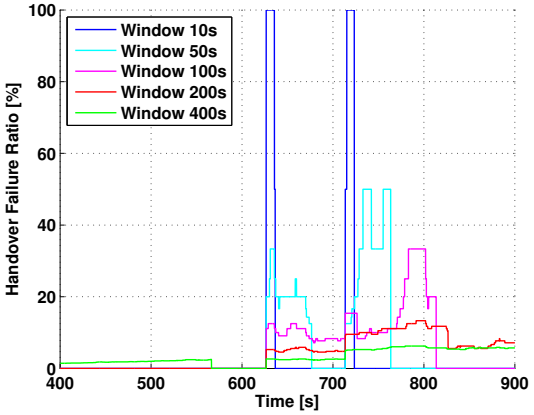

(f) HYS 6 dB, TTT 1.0 s

Figure B.2: The handover failure performance of cell 31 for different HOPs and observation window sizes

Appendix C

Impact of the Target Function Weighting Factors on the Identification of the "best" Handover Operating Point and the Observed Handover Performance

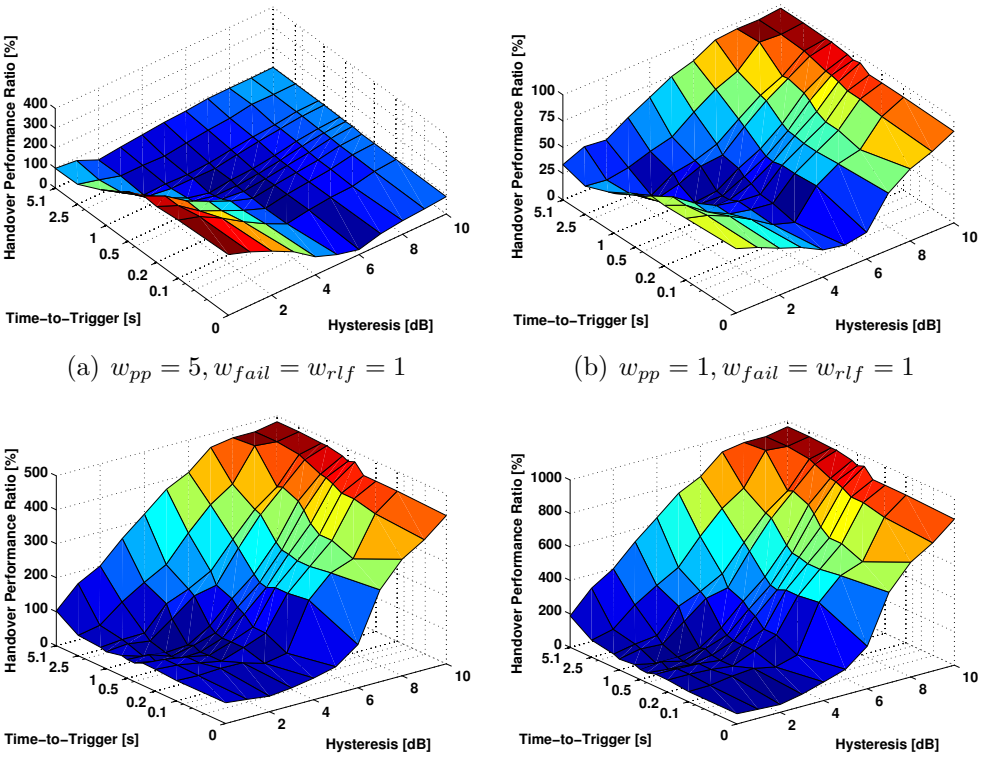

(a) $w_{pp} = 5, w_{fail} = w_{rlf} = 1$

(b) $w_{pp} = 1, w_{fail} = w_{rlf} = 1$

(c) $w_{pp} = 1, w_{fail} = w_{rlf} = 5$

(d) $w_{pp} = 1, w_{fail} = w_{rlf} = 10$

Figure C.1: Impact of the HPI_{sum} weighting factors on the evaluation of the HOP performance of cell 31 (simulation time: 1000 s)

Parameter	Set 1	Set 2	Set 3	Set 4	Set 5	Set 6	Set 7
w_{pp}	10	5	3	1	1	1	1
w_{fail}	1	1	1	1	3	5	10
w_{rlf}	1	1	1	1	3	5	10
HYS	3 dB	3 dB	2 dB	2 dB	2 dB	2 dB	1 dB
TTT	1.2 s	1.2 s	1.2 s	1.2 s	1.2 s	1.2 s	1 s
HPI_{pp}	0 %	0 %	3.98 %	3.98 %	3.98 %	3.98 %	16.28 %
HPI_{fail}	1.62 %	1.62 %	0 %	0 %	0 %	0 %	0 %
HPI_{rlf}	14.89 %	14.89 %	3.17 %	3.17 %	3.17 %	3.17 %	1.76 %
HPI_{sum}	16.51	16.51	15.11	7.15	13.48	19.81	33.84

Table C.1: Performance of the best HOP in cell 31 subject to different weighting parameter settings

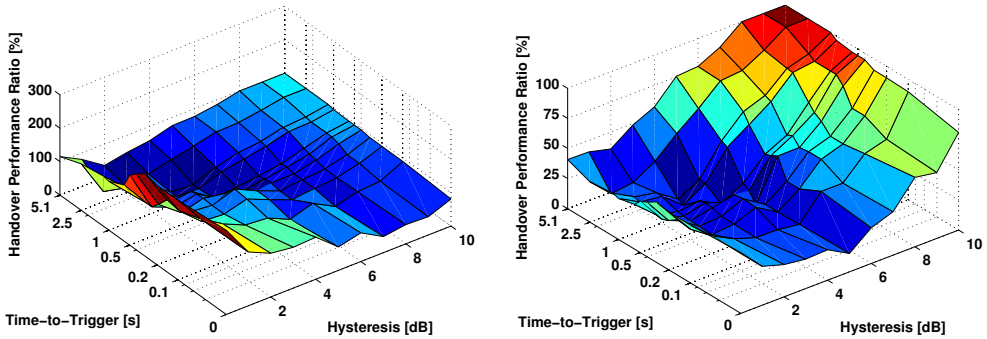

(a) $w_{pp} = 5, w_{fail} = w_{rlf} = 1$ (b) $w_{pp} = 1, w_{fail} = w_{rlf} = 1$

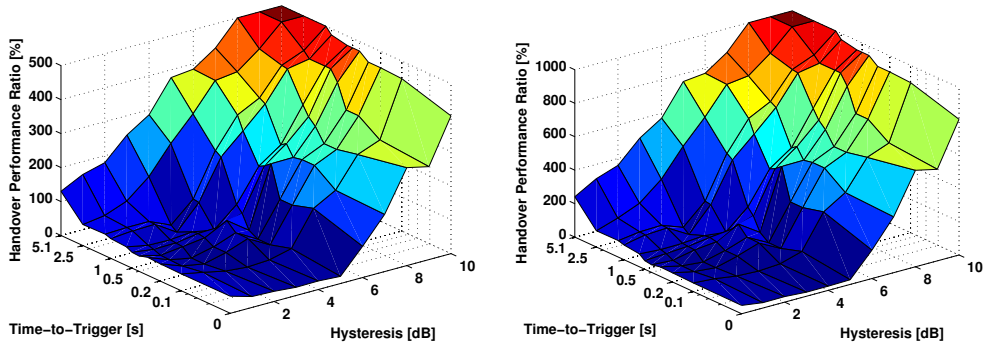

(c) $w_{pp} = 1, w_{fail} = w_{rlf} = 5$ (d) $w_{pp} = 1, w_{fail} = w_{rlf} = 10$

Figure C.2: Impact of the HPI_{sum} weighting factors on the evaluation of the HOP performance of cell 36 (simulation time: 1000 s)

Parameter	Set 1	Set 2	Set 3	Set 4	Set 5	Set 6	Set 7
w_{pp}	10	5	3	1	1	1	1
w_{fail}	1	1	1	1	3	5	10
w_{rlf}	1	1	1	1	3	5	10
HYS	5 dB	5 dB	5 dB	4 dB	4 dB	4 dB	4 dB
TTT	0.1 s	0.1 s	0.1 s	0.1 s	0.1 s	0.1 s	0.1 s
HPI_{pp}	0 %	0 %	0 %	2.16 %	2.16 %	2.16 %	2.16 %
HPI_{fail}	0 %	0 %	0 %	0 %	0 %	0 %	0 %
HPI_{rlf}	6.13 %	6.13 %	6.13 %	0 %	0 %	0 %	0 %
HPI_{sum}	6.13	6.13	6.13	2.16	2.16	2.16	2.16

Table C.2: Performance of the best HOP in cell 36 subject to different weighting parameter settings

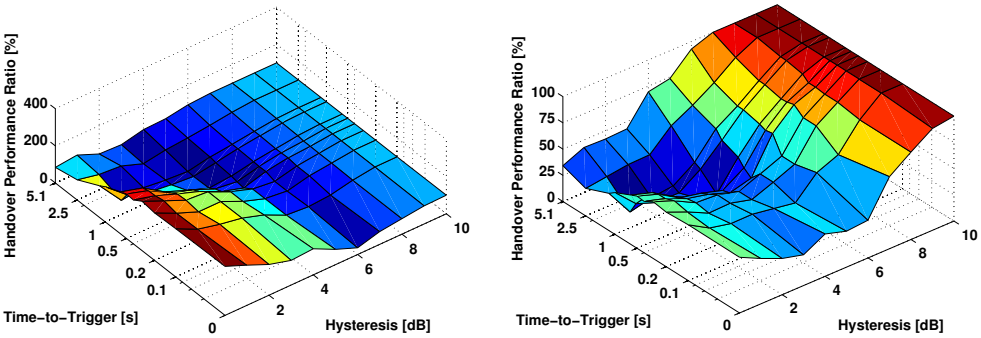

(a) $w_{pp} = 5, w_{fail} = w_{rlf} = 1$ (b) $w_{pp} = 1, w_{fail} = w_{rlf} = 1$

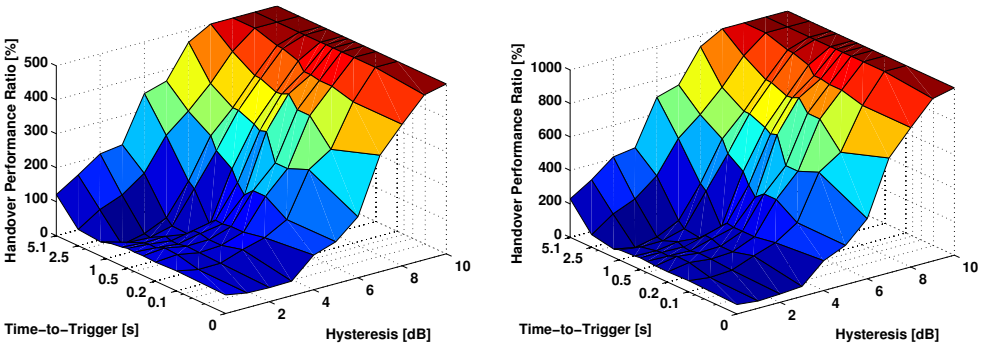

(c) $w_{pp} = 1, w_{fail} = w_{rlf} = 5$ (d) $w_{pp} = 1, w_{fail} = w_{rlf} = 10$

Figure C.3: Impact of the HPI_{sum} weighting factors on the evaluation of the HOP performance of cell 90 (simulation time: 1000 s)

Parameter	Set 1	Set 2	Set 3	Set 4	Set 5	Set 6	Set 7
w_{pp}	10	5	3	1	1	1	1
w_{fail}	1	1	1	1	3	5	10
w_{rlf}	1	1	1	1	3	5	10
HYS	4 dB	4 dB	1 dB	1 dB	1 dB	2 dB	0 dB
TTT	1 s	1 s	1 s	1 s	1 s	1 s	1.2 s
HPI_{pp}	0 %	0 %	4.83 %	4.83 %	4.83 %	9.44 %	29.22 %
HPI_{fail}	2.73 %	2.73 %	2.41 %	2.41 %	2.41 %	0 %	0 %
HPI_{rlf}	24.40 %	24.40 %	2.49 %	2.49 %	2.49 %	3.49 %	0 %
HPI_{sum}	27.13	27.13	19.39	9.73	19.53	26.89	29.22

Table C.3: Performance of the best HOP in cell 90 subject to different weighting parameter settings

Appendix D

Performance of the HPIs and HOP Selection for Changing Cell Load

	Cell Load									
	10%	20%	30%	40%	50%	60%	70%	80%	90%	100%
Optimised	0.05	0.26	0.49	1.03	0.98	1.25	2.09	2.75	3.26	3.43
Optimised (Load 70%)	6.11	6.09	5.85	5.15	3.92	2.87	2.09	1.85	1.66	1.37
Performance Degradation	6.06	5.83	5.36	4.12	2.94	1.62	0	-0.90	-1.60	-2.06
Optimised	0.05	0.26	0.49	1.03	0.98	1.25	2.09	2.75	3.26	3.43
Optimised (Load 100%)	10.24	10.38	9.77	9.14	7.82	6.70	5.92	4.70	4.04	3.43
Performance Degradation	10.19	10.12	9.28	8.11	6.84	5.45	3.83	1.95	0.78	0

Table D.1: Mean ping-pong handover ratio (HPI_{pp}) as a function of the cell load. Optimised performance to the current cell load, optimised for a fixed cell load and the performance degradation.

	Cell Load									
	10%	20%	30%	40%	50%	60%	70%	80%	90%	100%
Optimised	0.17	0.40	1.23	1.59	3.54	4.42	4.15	5.87	6.79	8.67
Optimised (Load 70%)	0.31	0.98	1.46	1.79	2.58	3.18	4.15	6.80	10.74	15.97
Performance Degradation	0.14	0.58	0.23	0.20	-0.96	-1.24	0	0.93	3.95	7.30
Optimised	0.17	0.40	1.23	1.59	3.54	4.42	4.15	5.87	6.79	8.67
Optimised (Load 100%)	0.64	1.11	1.84	2.30	3.14	3.78	4.80	5.95	7.09	8.67
Performance Degradation	0.47	0.71	0.61	0.71	-0.40	-0.64	0.65	0.08	0.30	0

Table D.2: Mean radio link failure ratio (HPI_{rlf}) as a function of the cell load. Optimised performance to the current cell load, optimised for a fixed cell load and the performance degradation.

	Cell Load									
	10%	20%	30%	40%	50%	60%	70%	80%	90%	100%
Optimised	0	0.10	0.49	0.57	1.08	1.68	1.10	2.45	2.68	2.87
Optimised (Load 70%)	0.35	0.50	1.87	1.03	3.46	4.66	1.10	7.30	8.93	8.78
Performance Degradation	0.35	0.40	1.38	0.46	2.38	2.98	0	4.85	6.25	5.91
Optimised	0	0.10	0.49	0.57	1.08	1.68	1.10	2.45	2.68	2.87
Optimised (Load 100%)	0.22	0.26	1.06	1.15	2.89	3.82	1.48	4.48	3.80	2.87
Performance Degradation	0.22	0.16	0.57	0.58	1.81	2.14	0.38	2.03	1.12	0

Table D.3: Mean handover failure ratio (HPI_{rlf}) as a function of the cell load. Optimised performance to the current cell load, optimised for a fixed cell load and the performance degradation.

Own Publications

[Amirijoo08] Amirijoo, M.; Litjens, R.; Spaey, K.; Doettling, M.; Jansen, T.; Scully, N. and Tuerke, U., 'Use Cases, Requirements and Assessment Criteria for Future Self-Organising Radio Access Networks', in *SELF-ORGANIZING SYSTEMS*, vol. 5343, pp. 275–280, Springer Berlin Heidelberg, Vienna, 2008, ISBN 978-3-540-92156-1, ISSN 0302-9743.

[Balan09] Balan, I.; Moerman, I.; Jansen, T.; Scully, N.; Turk, J. and Mills, A., 'SOCRATES Deliverable D3.1B - Self-optimisation of stand-alone functionalities: Handover parameter optimisation', Tech. rep., SOCRATES Consortium, 2009.

[Balan11a] Balan, I.; Jansen, T.; Sas, B.; Moerman, I. and Kürner, T., 'Enhanced weighted performance based handover optimization in LTE', in *Future Network & Mobile Summit*, pp. 1–9, IEEE, Warsaw, 2011, URL http://ieeexplore.ieee.org/xpls/abs_all.jsp?arnumber=6095252.

[Balan11b] Balan, I.; Sas, B.; Jansen, T.; Moerman, I.; Spaey, K. and Demeester, P., 'An enhanced weighted performance-based handover parameter optimization algorithm for LTE networks', *EURASIP Journal on Wireless Communications and Networking*, vol. 2011, no. 1, pp. 1–11, 2011, ISSN 1687-1499, URL http://jwcn.eurasipjournals.com/content/2011/1/98.

[Jansen09] Jansen, T.; Amirijoo, M.; Türke, U.; Jorguseski, L.; Zetterberg, K.; Nascimento, R.; Schmelz, L.C.; Turk, J. and Balan, I., 'Embedding multiple self-organisation functionalities in future radio access networks', in *69th IEEE Vehicular Technology Conference (VTC-Spring)*, pp. 1–5, IEEE, Barcelona, 2009, ISBN 9781424425174, ISSN 15502252.

[Jansen10a] Jansen, T.; Balan, I.; Stefanski, S. and Scully, N., 'SOCRATES Deliverable D3.2 - Self-optimisation methods for multiple (interacting) functionalities

in wireless access networks: Handover parameter optimisation', Tech. rep., SOCRATES Consortium, 2010.

[Jansen10b] Jansen, T.; Balan, I.; Turk, J.; Moerman, I. and Kurner, T., 'Handover Parameter Optimization in LTE Self-Organizing Networks', in *72nd Vehicular Technology Conference (VTC-Fall)*, pp. 1–5, IEEE, Ottawa, Canada, Sep. 2010, ISBN 978-1-4244-3573-9, ISSN 1090-3038, URL http://ieeexplore.ieee.org/lpdocs/epic03/wrapper.htm?arnumber=5594245.

[Jansen10c] Jansen, T.; Nuckelt, J.; Schlegel, P.; Kürner, T. and Reimers, U., 'Untersuchung zur Eignung von LTE-Netzen für die Übertragung von Rundfunk', Tech. rep., 2010, URL http://www.die-medienanstalten.de/index.php?id=81&iID=40233.

[Jansen11] Jansen, T.; Balan, I.; Stefanski, S.; Moerman, I. and Kürner, T., 'Weighted performance based handover parameter optimization in LTE', in *73rd Vehicular Technology Conference (VTC-Spring)*, pp. 1–5, IEEE, Budapest, Hungary, 2011, ISBN 9781424483310, ISSN 15502252.

[Jansen12] Jansen, T.; Türke, U.; Mueller, C.M. and Werthmann, T., 'The IC 1004 Urban Hannover Scenario - 3D Pathloss Predictions and realistic traffic and mobility patterns', in *5th IC 1004 Management Committee Meeting, TD(12)05059*, pp. 1–6, Bristol, UK, 2012.

[Kürner11] Kürner, T.; Amirijoo, M.; Balan, I.; Berg, H.V.D.; Eisenblätter, A.; Jansen, T.; Jorguseski, L.; Litjens, R.; Linnell, O.; Lobinger, A.; Neuland, M.; Phillipson, F.; Schmelz, L.C.; Sas, B.; Scully, N.; Spaey, K.; Stefanski, S.; Turk, J.; Türke, U. and Zetterberg, K., 'SOCRATES Deliverable D5.9 - Final Report on Self-Organisation and its Implications in Wireless Access Networks', Tech. Rep. 135, SOCRATES Consortium, 2011.

[Lobinger10] Lobinger, A.; Stefanski, S.; Jansen, T. and Balan, I., 'Load Balancing in Downlink LTE Self-Optimizing Networks', in *71st IEEE Vehicular Technology Conference (VTC-Spring 2010)*, pp. 1–5, IEEE, Taipei, 2010, ISBN 978-1-4244-2518-1, URL http://ieeexplore.ieee.org/lpdocs/epic03/wrapper.htm?arnumber=5493656.

[Nuckelt13] Nuckelt, J.; Rose, D.M.; Jansen, T. and Kürner, T., 'On the Use of OpenStreetMap Data for V2X Channel Modeling in Urban Scenarios', in *7th*

European Conference on Antennas and Propagation (EuCAP), pp. 3984 – 3988, IEEE, Gothenburg, 2013.

[Rose11] Rose, D.M.; Jansen, T. and Kurner, T., 'Modeling of Femto Cells - Simulation of Interference and Handovers in LTE Networks', in *73rd Vehicular Technology Conference (VTC-Spring)*, pp. 1–5, IEEE, Budapest, May 2011, ISBN 978-1-4244-8332-7, ISSN 1550-2252, URL http://ieeexplore.ieee.org/lpdocs/epic03/wrapper.htm?arnumber=5956421.

[Rose12] Rose, D.M.; Baumgarten, J.; Jansen, T. and Kürner, T., 'How a Real City Fits into a Hexagonal World', in *Geoinformatik 2012 - Mobilität und Umwelt*, pp. 1–8, Braunschweig, 2012.

[Rose13a] Rose, D.M.; Jansen, T.; Hahn, S. and Kürner, T., 'Impact of realistic indoor mobility modelling in the context of propagation modelling on the user and network experience', in *7th European Conference on Antennas and Propagation (EuCAP)*, pp. 3979 – 3983, IEEE, Gothenburg, 2013.

[Rose13b] Rose, D.M.; Jansen, T.; Werthmann, T.; Türke, U. and Kürner, T., 'The IC 1004 Urban Hannover Scenario - 3D Pathloss Predictions and Realistic Traffic and Mobility Patterns', in *8th IC 1004 Management Committee Meeting, TD(13)08054*, pp. 1–12, Ghent, Belgium, 2013.

[Scully09] Scully, N.; Turk, J.; Litjens, R.; Türke, U.; Amirijoo, M.; Jansen, T. and Schmelz, L.C., 'SOCRATES Deliverable D2.6 - Review of use cases and framework II', Tech. Rep. 28, SOCRATES Consortium, Dec. 2009.

Other Publications

[3GPP10] 3GPP, 'TS 36.814 Evolved Universal Terrestrial Radio Access (E-UTRA); Further advancements for E-UTRA physical layer aspects (Release 9): V 9.0.0', Tech. rep., 3rd Generation Partnership Project, 2010, URL http://www.3gpp.org/DynaReport/36814.htm.

[3GPP11] 3GPP, 'TR 36.902 Evolved Universal Terrestrial Radio Access Network (E-UTRAN); Self-configuring and self-optimizing network (SON) use cases and solutions (Release 9): V 9.3.1', Tech. rep., 3rd Generation Partnership Project, 2011.

[3GPP12a] 3GPP, 'TS 36.214 Evolved Universal Terrestrial Radio Access (E-UTRA); Physical layer; Measurements (Release 11): V11.1.0', Tech. rep., 3rd Generation Partnership Project, 2012, URL http://www.3gpp.org/DynaReport/36214.htm.

[3GPP12b] 3GPP, 'TS 36.314 Evolved Universal Terrestrial Radio Access (E-UTRA); Layer 2 - Measurements (Release 11): V 11.1.0', Tech. rep., 3rd Generation Partnership Project, 2012, URL http://www.3gpp.org/DynaReport/36314.htm.

[3GPP12c] 3GPP, 'TS 36.942 Evolved Universal Terrestrial Radio Access (E-UTRA); Radio Frequency (RF) system scenarios (Release 11): V 11.0.0', Tech. rep., 3rd Generation Partnership Project, 2012.

[3GPP13a] 3GPP, 'TS 36.300 Evolved Universal Terrestrial Radio Access (E-UTRA) and Evolved Universal Terrestrial Radio Access Network (E-UTRAN): Overall description, Stage 2 (Release 11): V 11.5.0', Tech. rep., 3rd Generation Partnership Project, 2013, URL http://www.3gpp.org/DynaReport/36300.htm.

[3GPP13b] 3GPP, 'TS 36.331 Evolved Universal Terrestrial Radio Access (E-UTRA); Radio Resource Control (RRC); Protocol specification (Release 11): V 11.3.0', Tech. rep., 3rd Generation Partnership Project, 2013, URL http://www.3gpp.org/DynaReport/36331.htm.

[3GPP14a] 3GPP, 'TS 36.104 Evolved Universal Terrestrial Radio Access (E-UTRA); Base Station (BS) radio transmission and reception (Release 12): V 12.4.0', Tech. rep., 3rd Generation Partnership Project, Jun. 2014, URL http://www.3gpp.org/dynareport/36104.htm.

[3GPP14b] 3GPP, 'TS 36.133 Evolved Universal Terrestrial Radio Access (E-UTRA); Requirements for support of radio resource management (Release 11): V 11.8.0', Tech. rep., 3rd Generation Partnership Project, 2014, URL http://www.3gpp.org/DynaReport/36133.htm.

[3GPP14c] 3GPP, 'TS 36.211 Evolved Universal Terrestrial Radio Access (E-UTRA); Physical channels and modulation (Release 12): V 12.3.0', Tech. rep., 3rd Generation Partnership Project, Sep. 2014, URL http://www.3gpp.org/dynareport/36211.htm.

[3GPP14d] 3GPP, 'TS 36.212 Evolved Universal Terrestrial Radio Access (E-UTRA); Multiplexing and channel coding (Release 12): V 12.2.0', Tech. rep., 3rd Generation Partnership Project, Sep. 2014, URL http://www.3gpp.org/dynareport/36212.htm.

[3GPP14e] 3GPP, 'TS 36.213 Evolved Universal Terrestrial Radio Access (E-UTRA); Physical layer procedures (Release 12): V 12.3.1', Tech. rep., 3rd Generation Partnership Project, Sep. 2014, URL http://www.3gpp.org/dynareport/36213.htm.

[3GPP14f] 3GPP, 'TS 36.306 Evolved Universal Terrestrial Radio Access (E-UTRA); User Equipment (UE) radio access capabilities (Release 12): V12.2.0', Tech. rep., 3rd Generation Partnership Project, Sep. 2014, URL http://www.3gpp.org/dynareport/36306.htm.

[3GPP14g] 3GPP, 'TS 36.423 Evolved Universal Terrestrial Radio Access Network (E-UTRAN); X2 application protocol (X2AP) (Release 12): V 12.1.0', Tech. rep., 3rd Generation Partnership Project, 2014, URL http://www.3gpp.org/DynaReport/36423.htm.

[Awada11] Awada, A.; Wegmann, B.; Rose, D.; Viering, I. and Klein, A., 'Towards self-organizing mobility robustness optimization in inter-RAT scenario', in *73rd Vehicular Technology Conference (VTC-Spring)*, pp. 1 – 5, IEEE, Budapest, Hungary, 2011, ISBN 9781424483310, ISSN 15502252.

[Awada13] Awada, A.; Wegmann, B.; Viering, I. and Klein, A., 'A SON-based algorithm for the optimization of inter-RAT handover parameters', *IEEE Transactions on Vehicular Technology*, vol. 62, no. 5, pp. 1906–1923, 2013, ISSN 00189545.

[Awada14] Awada, A., *Inter-RAT Mobility Robustness Optimization in Self-Organizing Networks*, Ph.D. thesis, Technische Universität Darmstadt, 2014.

[Baumgarten12] Baumgarten, J.; Chee, K.L.; Hecker, A.; Kürner, T.; Braun, M. and Zahn, P., 'Performance of Prediction Models in Suburban/Rural Residential Areas at 860, 2300 and 3500 MHz', in *6th European Conference on Antennas and Propagation (EuCAP)*, pp. 1412–1416, IEEE, Prague, Czech Republic, 2012.

[Behrisch11] Behrisch, M.; Bieker, L.; Erdmann, J. and Krajzewicz, D., 'SUMO - Simulation of Urban MObility - an Overview', in *Proceedings of the 3rd International Conference on Advances in System Simulation (SIMUL 2011)*, pp. 63–68, 2011, ISBN 9781612081694.

[Beletchi13] Beletchi, A.; Huang, F.; Zhuang, H. and Zhang, J., 'Mobility Self-Optimization in LTE Networks based on Adaptive Control Theory', in *Globecom Workshops (GC Wkshps)*, pp. 87–92, IEEE, Atlanta, USA, 2013, ISBN 9781479928514.

[Bergman12] Bergman, P.; Moe, J. and Gunnarsson, F., 'Self-optimizing handover oscillation mitigation - Algorithms and field evaluations', in *9th International Symposium on Wireless Communication Systems (ISWCS)*, pp. 31–35, IEEE, Paris, France, Aug. 2012, ISBN 978-1-4673-0762-8, URL http://ieeexplore.ieee.org/lpdocs/epic03/wrapper.htm?arnumber=6328324.

[Buenestado13] Buenestado, V.; Ruiz-Aviles, J.M.; Toril, M. and Luna-Ramirez, S., 'Mobility Robustness Optimization in Enterprise LTE Femtocells', in *77th Vehicular Technology Conference (VTC Spring)*, pp. 1–5, IEEE, Dresden, Germany, Jun. 2013, ISBN 978-1-4673-6337-2, URL http://ieeexplore.ieee.org/lpdocs/epic03/wrapper.htm?arnumber=6692637.

[Deygout66] Deygout, J., 'Multiple knife-edge diffraction of microwaves', *IEEE Transactions on Antennas and Propagation*, vol. 14, 1966, ISSN 0018-926X.

[Dimou09] Dimou, K.; Wang, M.; Yang, Y.; Kazmi, M.; Larmo, A.; Pettersson, J.; Muller, W. and Timner, Y., 'Handover within 3GPP LTE: Design Principles and Performance', in *70th Vehicular Technology Conference (VTC-Fall)*, pp. 1–5, IEEE, Anchorage, USA, Sep. 2009, ISBN 978-1-4244-2514-3, URL http://ieeexplore.ieee.org/lpdocs/epic03/wrapper.htm?arnumber=5378909.

[DLR14] DLR, 'SUMO Homepage', 2014, URL http://sumo-sim.org/.

[E308] E3, 'End-to-End Efficiency', 2008, URL https://ict-e3.eu/.

[e.V.14] e.V., F., 'OpenStreetMap - Deutschland', 2014, URL www.openstreetmap.de.

[Ewe11] Ewe, L. and Bakker, H., 'Base station distributed handover optimization in LTE self-organizing networks', in *22nd International Symposium on Personal, Indoor and Mobile Radio Communications (PIMRC)*, 1, pp. 243–247, IEEE, Toronto, Canada, Sep. 2011, ISBN 978-1-4577-1348-4, URL http://ieeexplore.ieee.org/lpdocs/epic03/wrapper.htm?arnumber=6139958.

[Ferreira02] Ferreira, L.; M.Correia, L.; Serrador, A.; Carvalho, G.; Fledderus, E. and Perera, R., 'MOMENTUM Deliverable D1.3 - UMTS Deployment and Mobility Scenarios', Tech. rep., Oct. 2002.

[Flanagan02] Flanagan, J. and Novosad, T., 'WCDMA network cost function minimization for soft handover optimization with variable user load', in *56th Vehicular Technology Conference (VTC-Fall)*, vol. 4, pp. 2224

– 2228 vol.4, IEEE, Vancouver, Canada, 2002, ISBN 0-7803-7467-3, ISSN 1090-3038.

[GANDALF05] GANDALF, 'Project Achievements: Monitoring and self-tuning of RRM parameters in a multi-system network', 2005, URL http://www.celticplus.eu/pub/Project-leaflets/Webquality/Final/gandalf_final_lq.pdf.

[Gigerenzer99] Gigerenzer, G.; Todd, P.M. and Group, A.R., *Simple Heuristics That Make Us Smart*, Oxford University Press, 1999, ISBN 0-19-512156-2.

[GPRA11] GPRA and TNS Emnid, 'GPRA-Vertrauensindex Q3/2011: Verbraucher verlieren Vertrauen in die deutsche Wirtschaft', Tech. rep., Gesellschaft Public Relations Agenturen, 2011, URL http://www.gpra.de/news-media/vertrauensindex/.

[Hahn14] Hahn, S.; Rose, D.M. and Kürner, T., 'Automated Modelling of Realistic Indoor Walls in the Context of Small Cell Propagation', in *8th European Conference on Antennas and Propagation (EuCAP)*, pp. 2116–2120, IEEE, The Hague, The Netherlands, 2014.

[Hasselbach12] Hasselbach, P.P., *Capacity Optimization for Self-organizing Networks: Analysis and Algorithms*, Ph.D. thesis, Technische Universität Darmstadt, 2012.

[Holma09] Holma, H. and Toskala, A., *LTE for UMTS: OFDMA and SC-FDMA based radio access*, Wiley, 2009, ISBN 9780470994016, URL http://books.google.com/books?id=AHr43Lh-roQC&pgis=1.

[Holma11] Holma, H. and Toskala, A., *LTE for UMTS: Evolution to LTE-Advanced: Second Edition*, 2011, ISBN 9780470660003.

[Johansson12] Johansson, J.; Hapsari, W.; Kelley, S. and Bodog, G., 'Minimization of drive tests in 3GPP release 11', *IEEE Communications Magazine*, vol. 50, pp. 36–43, 2012, ISSN 01636804.

[Khan14] Khan, M.S.I.; Rahman, M.; Raahemifar, K.; Mišić, J. and Mišić, V.B., 'Self-Optimizing Control Parameters for Minimizing Ping-Pong

Handover in Long Term Evolution (LTE)', in *27th Biennial Symposium on Communications (QBSC)*, pp. 118–122, IEEE, Kingston, Canada, 2014, ISBN 9781479939725.

[Kirkpatrick83] Kirkpatrick, S.; Gelatt Jr., C.D. and Vecchi, M.P., 'Optimization by Simulated Annealing', *Science*, vol. 220, pp. 671–680, 1983, ISSN 00368075, URL http://www.jstor.org/stable/1690046.

[Kitagawa11] Kitagawa, K.; Komine, T.; Yamamoto, T. and Konishi, S., 'A handover optimization algorithm with mobility robustness for LTE systems', in *22nd International Symposium on Personal, Indoor and Mobile Radio Communications (PIMRC)*, pp. 1647 – 1651, IEEE, Toronto, Canada, 2011.

[Klir95] Klir, G.J. and Yuan, B., *Fuzzy Sets and Fuzzy Logic: Theory and Applications*, Prentice Hall, 1995, ISBN 0131011715.

[Krajzewicz12] Krajzewicz, D.; Erdmann, J.; Behrisch, M. and Bieker, L., 'Recent Development and Applications of {SUMO - Simulation of Urban MObility}', *International Journal On Advances in Systems and Measurements*, vol. 5, pp. 128–138, 2012, ISSN 1942-261x, URL http://elib.dlr.de/80483/.

[Kreher10] Kreher, R. and Gaenger, K., *LTE Signaling, Troubleshooting, and Optimization*, 2010, ISBN 9780470689004.

[Kürner99] Kürner, T., 'A run-time efficient 3D propagation model for urban areas including vegetation and terrain effects', in *49th IEEE Vehicular Technology Conference (VTC-Spring 1999)*, vol. 1, pp. 782–786, Houston, Texas, 1999, ISBN 0-7803-5565-2, ISSN 1090-3038.

[Kürner02] Kürner, T. and Meier, A., 'Prediction of outdoor and outdoor-to-indoor coverage in urban areas at 1.8 Ghz', *IEEE Journal on Selected Areas in Communications*, vol. 20, pp. 496–506, 2002, ISSN 07338716.

[Kürner10] Kürner, T. and Schack, M., '3D ray-tracing embedded into an integrated simulator for car-to-X communications', in *Symposium Digest*

- *20th URSI International Symposium on Electromagnetic Theory (EMTS 2010)*, pp. 880–882, 2010, ISBN 9781424451531.

[Kürner12] Kürner, T. and Lostanlen, Y., 'Propagation Models for Wireless Network Planning', in G. De la Roche; A.A. Glazunov and B. Allen, editors, *LTE-Advanced and Next Generation Wireless Networks: Channel Modelling and Propagation*, pp. 317–347, Wiley, 2012.

[Lee10] Lee, Y.; Shin, B.; Lim, J. and Hong, D., 'Effects of time-to-trigger parameter on handover performance in SON-based LTE systems', in *16th Asia-Pacific Conference on Communications (APCC)*, pp. 492–496, IEEE, Auckland, New Zealand, 2010, ISBN 9781424481293.

[Legg10] Legg, P.; Hui, G. and Johansson, J., 'A Simulation Study of LTE Intra-Frequency Handover Performance', in *72nd Vehicular Technology Conference (VTC-Fall)*, pp. 1–5, IEEE, Ottawa, Canada, Sep. 2010, ISBN 978-1-4244-3573-9, URL http://ieeexplore.ieee.org/lpdocs/epic03/wrapper.htm?arnumber=5594477.

[Lostanlen12] Lostanlen, Y. and Kürner, T., 'Ray Tracing Modeling', in G. De la Roche; A.A. Glazunov and B. Allen, editors, *LTE-Advanced and Next Generation Wireless Networks: Channel Modelling and Propagation*, pp. 271–291, Wiley, 2012.

[Lüders01] Lüders, C., *Mobilfunksysteme*, Vogel, 1 edn., 2001.

[Luengo14] Luengo, P.M.n., *Optimization of Mobility Parameters using Fuzzy Logic and Reinforcement Learning in Self-Organizing Networks*, Ph.D. thesis, Universidad de Málaga, 2014.

[MOMENTUM01] MOMENTUM, 'FP5 Models and Simulations for Network Planning and Control of UMTS project, IST-2000-28088', 2001.

[Monserrat07] Monserrat, J.; Fraile, R. and Rubio, L., 'Application of alternating projection method to ensure feasibility of shadowing cross-correlation models', *Electronics Letters*, vol. 43, no. 13, pp. 724 – 725, 2007.

[Monserrat08] Monserrat, J.; Fraile, R.; Calabuig, D. and Cardona, N., 'Complete Shadowing Modeling and its Effect on System Level Performance

Evaluation', in *67th Vehicular Technology Conference (VTC-Spring)*, pp. 294 – 298, IEEE, 2008.

[Mwanje12] Mwanje, S.S.; Zia, N. and Mitschele-Thiel, A., 'Self-organized handover parameter configuration for LTE', in *9th International Symposium on Wireless Communication Systems (ISWCS)*, pp. 26–30, IEEE, Paris, France, 2012, ISBN 9781467307604, ISSN 21540217.

[Mwanje14] Mwanje, S.S. and Mitschele-Thiel, A., 'Distributed Cooperative Q-Learning for Mobility-Sensitive handover Optimization in LTE SON', in *Symposium on Computers and Communication (ISCC)*, pp. 1 – 6, IEEE, Madeira, Portugal, 2014.

[Myerson91] Myerson, R.B., *Game Theory: Analysis of Conflict*, Harvard University Press, 1991, ISBN 0674341163.

[Neuland11] Neuland, M.; Kürner, T. and Amirijoo, M., 'Influence of Different Factors on X-Map Estimation in LTE', in *73rd Vehicular Technology Conference (VTC-Spring)*, pp. 1–5, IEEE, Budapest, 2011, URL http://ieeexplore.ieee.org/iel5/5954014/5956103/05956332.pdf?arnumber=5956332.

[NGMN08] NGMN, 'NGMN Use Cases related to Self Organising Network, Overall Description', Tech. rep., NGMN Alliance, 2008, URL http://www.ngmn.org/uploads/media/NGMN_Use_Cases_related_to_Self_Organising_Network__Overall_Description.pdf.

[Office14] Office, E.C., 'Documentation Database', 2014, URL http://www.ecodocdb.dk.

[OSM14a] OSM, 'OpenStreetMap Project', 2014, URL www.openstreetmap.org.

[OSM14b] OSM, 'OpenStreetMap Wiki', 2014, URL wiki.openstreetmap.org/wiki/Main_Page.

[Rose12a] Rose, D.M. and Kürner, T., 'Outdoor-to-indoor propagation - Accurate measuring and modelling of indoor environments at 900 and

1800 MHz', in *6th European Conference on Antennas and Propagation (EuCAP)*, pp. 1440–1444, IEEE, Prague, Czech Republic, 2012, ISBN 9781457709180.

[Rose12b] Rose, D.M. and Kürner, T., 'Stochastic Models of User and Load Distribution. GreenNets Deliverable D3.2 - Power Consumption and CO2 Footprint Reduction in Mobile Networks by Advanced Automated Network Management Approaches', Tech. rep., GreenNets Consortium, Nov. 2012.

[Rose14] Rose, D.M.; Hahn, S. and Kürner, T., 'Automated Modelling of Realistic Multi-Storey Buildings and the Impact of Windows on Small Cell Propagation', in *8th European Conference on Antennas and Propagation (EuCAP)*, pp. 3468–3472, IEEE, The Hague, The Netherlands, 2014.

[Sas14] Sas, B.; Spaey, K. and Blondia, C., 'Classifying Users Based on Their Mobility Behaviour in LTE Networks', in *10th International Conference on Wireless and Mobile Communications (ICWMC)*, pp. 198 – 205, IARIA, Seville, 2014.

[Schack12] Schack, M., *Integrated Simulation of Communication Applications in Vehicular Environments*, Ph.D. thesis, Technische Universität Braunschweig, 2012.

[Schröder08] Schröder, A.; Lundqvist, H. and Nunzi, G., 'Distributed self-optimization of handover for the long term evolution', in *Self-Organizing Systems, 3rd International Workshop (IWSOS)*, vol. 5343 LNCS, pp. 281–286, Springer-Verlag Berlin Heidelberg, Vienna, Austria, 2008, ISBN 3540921567, ISSN 03029743.

[Scully08] Scully, N.; Thiel, S.; Litjens, R.; Jorguseski, L.; Nascimento, R.; Linnell, O.; Zetterberg, K.; Amirijoo, M.; Blondia, C.; Spaey, K.; Moerman, I.; Balan, I.; Kürner, T.; Hecker, A.; Jansen, T.; Oszmianski, J. and Schmelz, L.C., 'SOCRATES Deliverable D2.1 - Use Cases for Self-Organising Networks', Tech. Rep. 71, SOCRATES Consortium, 2008.

[SEMAFOUR12] SEMAFOUR, 'FP7 Self-Management for Unified Heterogeneous Radio Access Networks project, INFSO-ICT-316384', 2012, URL http://www.fp7-semafour.eu.

[SOCRATES08] SOCRATES, 'FP7 Self-Optimisation & self-ConfiguRATion in wirelEss networkS project, INFSO-ICT-216284', 2008, URL http://www.fp7-socrates.eu/.

[Song09] Song, Q.; Wen, Z.; Wang, X.; Guo, L. and Yu, R., 'Time-Adaptive Vertical Handoff Triggering Methods for Heterogeneous Systems', in *Advanced Parallel Processing Technologies, 8th International Symposium (APPT)*, pp. 302 – 312, Springer-Verlag Berlin Heidelberg, Rapperswil, Switzerland, 2009.

[Statista14] Statista, 'Number of apps available in leading app stores as of July 2014', 2014, URL www.statista.com.

[Stuart08] Stuart, A.; Ord, K. and Arnold, S., *Kendall's Advanced Theory of Statistics, Classical Inference and the Linear Model*, Wiley, 6 edn., 2008.

[Sutton98] Sutton, R.S. and Barto, A.G., *Reinforcement Learning: An Introduction*, vol. 9, The MIT Press, 1998, ISBN 9780262193986.

[Tseng10] Tseng, S.M. and Tseng, W.Z., 'Drop rate optimization by tuning time to trigger for WCDMA systems', in *2nd International Conference on Ubiquitous and Future Networks (ICUFN)*, pp. 233–236, IEEE, Jeju Island, Korea (South), 2010, ISBN 9781424480883.

[TUBS16] TUBS, 'X-Map App für Android - Empfangsqualität in Mobilfunknetzen räumlich erfassen', 2016, URL www.ifn.ing.tu-bs.de/xmap/.

[Viering11] Viering, I.; Wegmann, B.; Lobinger, A.; Awada, A. and Martikainen, H., 'Mobility robustness optimization beyond Doppler effect and WSS assumption', in *8th International Symposium on Wireless Communication Systems (ISWCS)*, November, pp. 186 – 191, IEEE, Aachen, Germany, 2011, URL http://ieeexplore.ieee.org/xpls/abs_all.jsp?arnumber=6125335.

[Watanabe13] Watanabe, Y.; Sugahara, H.; Matsunaga, Y. and Hamabe, K., 'Inter-eNB Coordination-Free Algorithm for Mobility Robustness Optimization in LTE HetNet', in *77th Vehicular Technology Conference (VTC Spring)*, pp. 1–5, IEEE, Dresden, Germany, Jun. 2013, ISBN 978-1-4673-6337-2, URL http://ieeexplore.ieee.org/lpdocs/epic03/wrapper.htm?arnumber=6692597.

[Werner07] Werner, C.; Voigt, J.; Khattak, S. and Fettweis, G., 'Handover parameter optimization in WCDMA using fuzzy controlling', in *International Symposium on Personal, Indoor and Mobile Radio Communications (PIMRC)*, pp. 1 – 5, IEEE, Athens, Greece, 2007, ISBN 1424411440.

[Zetterberg13] Zetterberg, K.; Ramachandra, P.; Gunnarsson, F.; Amirijoo, M.; Wager, S. and Dudda, T., 'On Heterogeneous Networks Mobility Robustness', in *77th Vehicular Technology Conference (VTC Spring)*, pp. 1–5, Ieee, Dresden, Germany, Jun. 2013, ISBN 978-1-4673-6337-2, URL http://ieeexplore.ieee.org/lpdocs/epic03/wrapper.htm?arnumber=6692658.

Student Theses

[Baumgarten11] Baumgarten, J., *Repeater - Möglichkeit zur Verbesserung des Load Balancing in LTE?*, Diplomarbeit, Technische Universität Braunschweig, Institut für Nachrichtentechnik, 2011, dipl. 11/026.

[Hahn12] Hahn, S., *Entwicklung von dreidimensionalen Gebäudeinnenmodellen auf Basis realer Geodaten und Implementierung eines realistischen Indoor Mobilitätsmodells*, Masterarbeit, Technische Universität Braunschweig, Institut für Nachrichtentechnik, 2012, dipl. 12/015.

[Jansen08] Jansen, T., *Entwicklung eines Szenarios für die Car-to-Car-Kommunikation zur Verifikation von Wellenausbreitungseffekten*, Diplomarbeit, Technische Universität Braunschweig, Institut für Nachrichtentechnik, 2008, dipl. 08/018.

[Sulak12] Sulak, J., *Integration eines Fahrradfahrer- und Fußgänger-Mobilitätsmodells in einen LTE-Simulator*, Masterarbeit, Technische Universität Braunschweig, Institut für Nachrichtentechnik, 2012, dipl. 12/014.